

**Workshop on  
Dynamics in  
Viscous Liquids III**

**Accademia Nazionale dei Lincei  
Centro Linceo «Beniamino Segre»**

**Rome**

**March 30 – April 2, 2011**

**Abstract Booklet**



# International Workshop on Dynamics in Viscous Liquids III

Accademia Nazionale dei Lincei  
Centro Linceo Interdisciplinare “Beniamino Segre”

Rome, Palazzina dell’Auditorio  
Via della Lungara, 230

March 30 – April 2, 2011

## Programme

Organization

Giorgio Parisi, Thomas Voigtmann, and Emanuela Zaccarelli



# Contents

<b>1 Useful Information</b>	<b>7</b>
<b>2 Programme</b>	<b>11</b>
<b>3 Abstracts</b>	<b>21</b>
3.1 Talks . . . . .	21
3.2 Posters A . . . . .	73
3.3 Posters B . . . . .	119
<b>4 Author Index</b>	<b>161</b>



## Introduction

It is our pleasure to welcome you in Rome to the 3rd International Workshop on Dynamics in Viscous Liquids. After the first such meeting in Munich (2004, organized by Andreas Meyer and Thomas Voigtmann) and a second incarnation in Mainz (2006, organized by Jürgen Horbach and Wolfgang Paul), this is the third workshop following its peculiar “no invited talks” rule.

This workshop series brings together the leading experts on theoretical and experimental advances in the field of viscous liquid dynamics – from glass-forming liquids, viscous metallic or oxide melts, and polymers to dense colloidal suspensions and other soft-matter model systems.

Our aim is that the oral presentations at the workshop reflect the latest developments in the field, and stimulate fruitful debate. At the same time, the workshop shall also provide a platform especially for young researchers working in this field. Hence, the workshop’s programme is completely determined by a programme committee that bases its decision on the one-page abstracts submitted by all contributing participants. These are the abstracts collected in this booklet. We, the organizers, wish to thank the committee for spending its time and for a very stimulating meeting with many in-depth discussions. Having received close to 150 submissions, all of which carefully read and judged by the committee members, a tough selection of only 50 talks (i.e. roughly one third) had to be made. We think that the final program outlined here proves the excellent job done by the committee.

The workshop takes place in the fascinating venues of the Accademia dei Lincei – the oldest scientific academy in the world, dating back to the time of Galileo Galilei, who was among the first members. We

are grateful to the Accademia and to the Centro Interdisciplinare Beniamino Segre and in particular its Director Prof. Tito Orlandi for their generous support; we would also like to thank the staff of the Accademia, especially Mariella Masciangelo, Daniela Volpato, and Daniele Evangelista for their help. This means that we are able to host the workshop in the headquarters of a prestigious academy, in midst of one of Rome’s liveliest quarters, Trastevere, with the historic center and the Vatican state being nearby. We will also have the chance to visit next door’s Villa Farnesina with its renowned renaissance frescoes (located inside the Accademia dei Lincei).

We cordially thank the German-Dutch collaborative research center “SFB Transregio TR6 – Physics of Colloidal Suspensions under External Fields” for providing substantial financial support funded through the German Science Foundation (Deutsche Forschungsgemeinschaft, DFG); in particular we thank the spokesperson, Prof. Hartmut Löwen, for offering his support from very early on. Special thanks go to Brigitte Schumann, secretary of the SFB TR6 for taking care of numerous administrative matters and for her generous commitment which involved coming all the way from Düsseldorf to Rome. Our warmest thanks also go for her invaluable help in local support to Raffaella Mazzearelli.

We hope that this workshop will, as its two predecessors, prove to be a stimulating, entertaining, and productive meeting for all of us. We wish you all a pleasant stay in Rome,

*Giorgio Parisi*  
*Thomas Voigtmann*  
*Emanuela Zaccarelli*



# 1 Useful Information

## Programme Committee

Kurt Binder	Universität Mainz, Germany
Giulio Biroli	CEA Saclay, France
Leticia Cugliandolo	Paris, France
Mark Ediger	University of Wisconsin, U.S.A.
Stefan Egelhaaf	Universität Düsseldorf, Germany
Daan Frenkel	Cambridge University, U.K.
Matthias Fuchs	Universität Konstanz, Germany
Georg Maret	Universität Konstanz, Germany
Giorgio Parisi	Università di Roma “La Sapienza”, Italy
Srikanth Sastry	Jawaharlal Nehru Centre Bangalore, India
Francesco Sciortino	Università di Roma “La Sapienza”, Italy

## Organization

Emanuela Zaccarelli	Consiglio Nazionale delle Ricerche, Istituto dei Sistemi Complessi and Dipartimento di Fisica, Università di Roma “La Sapienza”, Italy
Thomas Voigtmann	Institut für Materialphysik im Weltraum, DLR, Köln and Zukunftskolleg, Universität Konstanz, Germany

## Conference Secretary

Raffaella Mazzarelli  
Brigitte Schumann

## Conference Office

Accademia dei Lincei  
Palazzina dell’Auditorio  
Via della Lungara 230  
Roma  
Italy  
e-mail: office@viscous-liquids.de

## Funding



German-Dutch Collaborative Research Center SFB TR6  
Physics of Colloidal Dispersions in External Fields  
funded through Deutsche Forschungsgemeinschaft (DFG)

## Useful Addresses

The workshop location right next to Villa Farnesina is just north of Trastevere, where you can find numerous shops and restaurants. The map indicates just a few (selected from the Gambero Rosso and other guides), from up-market (\*\*) to more basic.

The conference dinner takes place in the restaurant “Al Pompiere” [26].

### Restaurants

- 1 Antico Arco\*\*, piazzale Aurelio 7  
mediterranean based on Roman tradition
- 2 Asinocotto\*\*, via dei Vascellari 48  
mediterranean/international
- 3 Enoteca Ferrara\*\*, piazza Trilussa 41  
international with Roman touch
- 4 Paris\*\*, piazza San Calisto 7a  
traditional Roman
- 5 Il Sanlorenzo\*\*, via dei Chiavari 4  
sea-food/slow-food cuisine
- 6 Sora Lella\*\*, via di Ponte Quattro Capi 16  
Roman trattoria
- 7 Cecco Er Carettiere\*, via Benedetta 10/11  
traditional Trastevere location
- 8 A' Ciaramira\*, via Natale del Grande 41  
fish & seafood
- 9 Dar Cordaro\*, piazzale Portuense 4  
traditional Roman trattoria
- 10 Crudo\*, via degli Specchi 6  
(raw) fish
- 11 Il Drappo\*, vicolo del Malpasso 9  
Sardinian
- 12 Glass Hostaria\*, vicolo del Cinque 58  
regional, seafood, stylish place
- 13 Da Giggetto\*, Via del Portico d'Ottavia 21  
well-known place in the Roman ghetto
- 14 Le Mani in Pasta\*, via dei Genovesi 37  
Italian pasta, small authentic restaurant
- 15 Osteria della Gensola\*, piazza della Gensola 15  
regional Italian, fish
- 16 Rivadestra\*, via della Penitenza 7  
north-Italian and Neapolitan influences
- 17 L'Antica Trattoria da Gildo, via della Scala 31/a  
traditional Roman
- 18 Bir & fud, via Benedetta 23  
beer and food, pizza, fried specialities
- 19 Cave Canem, piazza San Calisto 11  
regional, simple style
- 20 La Frascetta, via San Francesco a Ripa 134  
Italian, pizza
- 21 Ivo a Trastevere, via San Francesco a Ripa 158  
pizza and Roman
- 22 Osteria Rugantino, via della Lungaretta 54  
standard Roman restaurant
- 23 Sette Ocche in Altalena, via dei Salumi 36  
Italian food, pizza
- 24 Sora Margherita, piazza delle Cinque Scole 30  
simple Roman-jewish trattoria
- 25 Trattoria degli Amici, piazza di Sant'Egidio 5  
simple trattoria
- 26 Al Pompiere\*, Via di Santa Maria de' Calderari 38  
conference dinner
- 27 Jaipur, via San Francesco a Ripa 56  
Indian
- 28 Thien Kim, via Giulia 201  
Vietnamese

### Wine & Cocktail Bars

- A Ma che siete venuti a fa', via Benedetta 25  
large selection of beer & liquor, no food
- B Freni e Frizioni, via del Politeama 4/6  
cocktail bar
- C La Mescita/Enoteca Ferrara, piazza Trilussa 41  
wine bar
- D Enoteca Trastevere, via della Lungaretta 86  
wine bar, some smaller food dishes

### Take-Away

- I Planet Kebab, via Natale Del Grande 17  
one of the best kebab places in the area
- II Sisini, via San Francesco a Ripa 137  
pizza take-away
- III Alberto Pica, via della Seggiola 12  
large selection of ice creams

### Culture & Night Life

- a Big Mama, vicolo di San Francesco a Ripa 18  
music/jazz club
- b Lettere Cafe, via San Francesco a Ripa 100  
coffee, food, and books; live music/poetry



map data: [openstreetmap.org](https://openstreetmap.org)



## 2 Programme

	Wed 30/03	Thu 31/03	Fri 01/04	Sat 02/04
08:00–08:45	Registration			
08:45–09:00	Opening			
09:00–10:20	W. Kob	M. Laurati	P. Keim	A. S. Keys
	C. Dasgupta	J. Horbach	C. Dalle-Ferrier	G. Tarjus
	M. Mosayebi	J.M. Brader	S. Lang	H. Tanaka
	C. Cammarota	M. Siebenbürger	D. Coslovich	E. Sanz
10:20–10:50	coffee			
10:50–12:10	G. Szamel	F. Weysser	S. Buzzaccaro	C. A. Angell
	K. Miyazaki	Ch. J. Harrer	B. Ruzicka	F. Mallamace
	R. Schilling	P. Chaudhuri	J. R. Gomez-Solano	
	F. Zamponi	R. Besseling	C. P. Royall	
12:10–14:00	lunch			Guided Tour 12:00–13:00
14:00–15:20	J. C. Dyre	Poster 13:45–15:20	Poster 13:45–15:20	
	A. Meyer			
	P. Gallo			
	J. Wuttke			
15:20–15:50	coffee			
15:50–17:10	K. Kroy	A. Heuer	L. Berthier	
	N. Gnan	P. Verrocchio	M. Sperl	
	M. Medina-Noyola	M. Tarzia	H. Jacquin	
	D. Villamaina	S. Franz	P. Charbonneau	
	break			
17:30–18:10		F. Sausset	G. Monaco	
		F. Cardinaux	A. Arbe	
19:00–	Conference Dinner			

**Wednesday, March 30****08:00 Registration****08:45 Welcome Note***G. Parisi, E. Zaccarelli, and Th. Voigtmann***Session 1**, Chair: Hartmut Löwen**09:00 W. Kob**, Université Montpellier 2*Static and Dynamic Length Scales in Glass-Forming Liquids***09:20 C. Dasgupta**, Indian Institute of Science, Bangalore*Growing length scales and their relation to growing time scales in glass-forming liquids***09:40 M. Mosayebi**, ETH Zürich*A static correlation length diverging at the glass transition***10:00 C. Cammarota**, CEA, Saclay*A phase-separation perspective on dynamic heterogeneities in glass-forming liquids***10:20 Coffee break****Session 2**, Chair: Wolfgang Götze**10:50 G. Szamel**, Colorado State University*Dynamic glass transition: mode-coupling theory, replica approach and emergence of rigidity***11:10 K. Miyazaki**, University of Tsukuba*Is the Mode-Coupling Theory a Mean Field Description of the Glass Transition?***11:30 R. Schilling**, Universität Mainz*Mean-field limit of mode-coupling theory***11:50 F. Zamponi**, CNRS, Paris*Quantum glass transition and superfluidity of hard spheres***12:10 Lunch****Session 3**, Chair: Kia Ngai**14:00 J. C. Dyre**, Roskilde University*Isomorphs in liquid phase diagrams and their consequences for viscous dynamics***14:20 A. Meyer**, Deutsches Zentrum für Luft- und Raumfahrt, Köln*Relation of properties of mass transport with melt structure in multicomponent viscous metals***14:40 P. Gallo**, Università Roma Tre*Slow dynamics and fragile-to-strong transition in confined water and in aqueous solutions.***15:00 J. Wuttke**, Forschungszentrum Jülich*Supercooled water dynamics near the resolution limit of neutron backscattering***15:20 Coffee break****Session 4**, Chair: Andrea Puglisi**15:50 K. Kroy**, Universität Leipzig*Hot Brownian Motion: When Big Beads Beat Bittie Beads***16:10 N. Gnan**, Università di Roma "La Sapienza"*Predicting The Effective Temperature of a Glass***16:30 M. Medina-Noyola**, Universidad Autónoma de San Luis Potosí*Incomplete Equilibration of Dense Hard-Sphere Fluids***16:50 D. Villamaina**, Università di Roma "La Sapienza"*Ratchet effect in an aging glass*

## Thursday, March 31

**Session 5**, Chair: Frank Scheffold

- 09:00** **M. Laurati**, Universität Düsseldorf  
*Dynamics of Supercooled Colloidal Dispersions under Flow: A Study of Transient Regimes*
- 09:20** **J. Horbach**, Deutsches Zentrum für Luft- und Raumfahrt, Köln  
*The relaxation of stresses in a glassforming soft-sphere mixture after the switch-off of shear*
- 09:40** **J.M. Brader**, University of Fribourg  
*Nonlinear response of dense colloidal suspensions under oscillatory shear*
- 10:00** **M. Siebenbürger**, Helmholtz-Zentrum für Materialien und Energie Berlin  
*Startup experiments of concentrated suspensions*

**10:20** **Coffee break**

**Session 6**, Chair: Stefan Egelhaaf

- 10:50** **F. Weysser**, Universität Konstanz  
*A mixture of binary hard discs at the glass transition under shear*
- 11:10** **Ch. J. Harrer**, Universität Konstanz  
*Active and Nonlinear Microrheology*
- 11:30** **P. Chaudhuri**, Université Claude Bernard Lyon 1  
*Flow of soft jammed materials – linking global flow to local properties*
- 11:50** **R. Besseling**, University of Edinburgh  
*Shear banding and flow-concentration coupling in colloidal glasses*

**12:10** **Lunch**

**13:45** **Poster Session A**

**15:20** **Coffee break**

**Session 7**, Chair: Srikanth Sastry

- 15:50** **A. Heuer**, Universität Münster  
*Facilitation effects in supercooled liquids as a key ingredient for the dynamics*
- 16:10** **P. Verrocchio**, Università di Trento  
*Cooperatively rearranging regions and their interfaces close to the glass transition*
- 16:30** **M. Tarzia**, Université Pierre et Marie Curie, Paris  
*First steps towards a renormalization group approach for glasses*
- 16:50** **S. Franz**, CNRS and Université Paris-Sud  
*Field Theory of Fluctuations in Glasses*

**17:10** **Break**

**Session 8**, Chair: Juan Colmenero

- 17:30** **F. Sausset**, Université Paris Sud  
*Characterizing order in amorphous systems*
- 17:50** **F. Cardinaux**, University of Fribourg  
*Heterogeneous dynamics in dense monodisperse emulsions*

**Friday, April 1**

**Session 9**, Chair: Thomas Voigtmann

- 09:00** **P. Keim**, University of Konstanz  
*Dynamics and local order in a 2D colloidal glass former*
- 09:20** **C. Dalle-Ferrier**, Universität Düsseldorf  
*Glass-like dynamics of colloids in modulated potentials*
- 09:40** **S. Lang**, Universität Erlangen-Nürnberg  
*Glass transition in confined geometry: A mode-coupling theory*
- 10:00** **D. Coslovich**, Université Montpellier II  
*Slow dynamics in cluster crystals and cluster glasses*

**10:20** **Coffe break**

**Session 10**, Chair: Emanuela Zaccarelli

- 10:50** **S. Buzzaccaro**, Politecnico di Milano  
*Highly nonlinear dynamics in a slowly sedimenting colloidal gel*
- 11:10** **B. Ruzicka**, Università di Roma “La Sapienza”  
*Phase Separation and Equilibrium gels in a colloidal clay*
- 11:30** **J. R. Gomez-Solano**, CNRS, Lyon  
*Nonequilibrium fluctuations of a Brownian particle in a quenched gelatin droplet*
- 11:50** **C. P. Royall**, University of Bristol  
*Faceted polyhedral colloidal ‘rocks’: low-dimensional slow networks*

**12:10** **Lunch**

**13:45** **Poster Session B**

**15:20** **Coffee break**

**Session 11**, Chair: Giulio Biroli

- 15:50** **L. Berthier**, Université Montpellier 2  
*Six ‘critical’ packing fractions for disordered hard sphere systems*
- 16:10** **M. Sperl**, Deutsches Zentrum für Luft- und Raumfahrt, Köln  
*Glass Transition in Driven Granular Matter*
- 16:30** **H. Jacquin**, Université Paris Diderot – Paris 7  
*Microscopic many-body theory of the jamming transition*
- 16:50** **P. Charbonneau**, Duke University  
*Structural Correlations in Jammed and Glass-Forming Hard Sphere Fluids*

**17:10** **Break**

**Session 12**, Chair: Ulrich Buchenau

- 17:30** **G. Monaco**, European Synchrotron Radiation Facility, Grenoble  
*Macroscopic, mesoscopic and microscopic regimes for the dynamical properties of disordered systems*
- 17:50** **A. Arbe**, Centro de Física de Materiales, San Sebastián  
*Nanophase Separation and Anomalous Dynamics in Comb-like Polymers*
- 19:00** **Conference Dinner** (Ristorante Al Pompiere, via di Santa Maria de’ Calderari 38)

**Saturday, April 2**

**Session 13**, Chair: Francesco Sciortino

- 09:00** **A. S. Keys**, University of California Berkeley  
*Computer simulation study of structure and dynamics of elementary excitations in model glass forming liquids*
- 09:20** **G. Tarjus**, Université Pierre et Marie Curie, Paris  
*The role of attractive forces in visquous liquids and its consequence for theories of the glass transition*
- 09:40** **H. Tanaka**, University of Tokyo  
*Structural signature of slow dynamics in supercooled liquids: Critical-like glassy structural ordering*
- 10:00** **E. Sanz**, University of Edinburgh  
*Crystallization Mechanism of Hard Sphere Glasses*
- 10:20** **Coffee break**

**Session 14**, Chair: Giorgio Parisi

- 10:50** **C. A. Angell**, Arizona State University  
*An evaluation of the “ideal glassformer” concept, using van der Waals ellipsoids in the Gay-Berne model*
- 11:10** **F. Mallamace**, Università di Messina  
*The dynamic crossover temperature is as important as the glass transition temperature: Evidence from liquid transport coefficients*
- 11:30** **Closing Remarks**, G. Parisi
- 12:00** **Guided Tour to Villa Farnesina**

## List of Poster Contributions

- A1 C. A. Angell**, Arizona State University  
*Decoupling of viscosity from diffusive mobility in a molecular liquid, caused by isothermal introduction of 2nm structural inhomogeneities*
- A2 A. Furukawa**, University of Tokyo  
*Mesoscopic natures of the anomalous viscous transport and viscoelasticity in supercooled liquids*
- A3 H. E. Castillo**, Ohio University  
*Dynamical heterogeneity in structural glasses and correlated fluctuations of the time variables*
- A4 L. Yelash**, Universität Mainz  
*Atomistic molecular dynamics simulations of polybutadiene at graphite: Slowing down in confined melt vs. bulk*
- A5 J. S. Hansen**, Roskilde University  
*Viscous properties of water*
- A6 H. Morhenn**, Technische Universität München  
*Short time dynamics of a medium length polyethylene melt*
- A7 M. Bernabei**, Donostia International Physics Center  
*From caging to Rouse dynamics in polymer melts with intramolecular barriers: a critical test of the Mode Coupling Theory.*
- A8 M. Hofmann**, University Bayreuth  
*Glassy and polymer dynamics in confining geometry as revealed by NMR*
- A9 M. Z. Slimani**, Donostia International Physics Center  
*Heterogeneities of segmental dynamics in lamellar phases of diblock copolymers*
- A10 J. K Basu**, Indian Institute of Science, Bangalore  
*Unusual dynamics of polymer grafted nanoparticles*
- A11 A. Grzybowski**, Silesian University  
*Specific volume and activation volume scalings in viscous systems*
- A12 K. Kaminski**, University of Silesia  
*Identification of the molecular origin of secondary relaxation process which is commonly observed in the whole family of the saccharides.*
- A13 M. Romanini**, Universitat Politècnica de Catalunya  
*Removal of hydrogen-bond-induced clusters in m-fluoroaniline by mixing with aromatic compounds: emergence of genuine Johari-Goldstein relaxation*
- A14 P. Włodarczyk**, University of Silesia  
*Identification the origins of non-JG secondary modes. Conformational interconversion as JG secondary mode.*
- A15 T. Scopigno**, Università di Roma “La Sapienza”  
*Visualizing Coherent Acoustic Phonons in Disordered Materials*
- A16 B. Jakobsen**, Roskilde University  
*Temperature-independent decoupling between the characteristic time scales of five independent linear response functions*
- A17 D. Gundermann**, Roskilde University  
*Experimental connection between density scaling and the Prigogine-Defay ratio of a glass-forming liquid*
- A18 K. Niss**, Roskilde University  
*Dynamic thermal expansivity of a molecular liquid near the glass transition*
- A19 L. Bøhling**, Roskilde University  
*Investigation of infinite frequency shear and bulk moduli on strongly correlating liquids*
- A20 N. P. Bailey**, Roskilde University  
*Perturbation theory approach to determining the effective inverse power-law exponent for strongly correlating liquids.*

- A21 T. S. Ingebrigtsen**, Roskilde University  
*NVU dynamics: Replacing Newton's 2nd law with Newton's 1st law*
- A22 T. B. Schrøder**, Roskilde University  
*Theory of isomorphs: applications to generalized Lennard-Jones liquids*
- A23 U. Buchenau**, Forschungszentrum Jülich  
*Relation between the shear fluctuation spectrum and the dielectric fluctuation spectrum in highly viscous liquids*
- A25 J. Papini**, Roskilde University  
*Cooling by Heating - new phenomenon establishes subtle thermomechanical coupling*
- A26 M. A. Ramos**, Universidad Autónoma de Madrid  
*Thermodynamic and kinetic properties of glass-forming monoalcohols*
- A27 G. Diezemann**, Universität Mainz  
*The Kovacs effect: New insights from the Gaussian trap model*
- A28 C. Rehwald**, Universität Münster  
*Identification of coupling processes in supercooled liquids*
- A29 L. Leuzzi**, Università di Roma "La Sapienza"  
*Dynamic and thermodynamic properties underlying secondary processes in a mean-field exactly solvable model glass*
- A30 T. Rizzo**, Università di Roma "La Sapienza"  
*On the Decay Exponents of Mode Coupling Theory*
- A31 M. Pica Ciamarra**, Università di Napoli Federico II  
*Geometrical approach to the glass transition*
- A32 M. Schmiedeberg**, Universität Düsseldorf  
*Mapping the slowdown of the dynamics of soft spheres onto hard sphere behavior*
- A33 R. Zargar**, University of Amsterdam  
*Direct measurement of the free energy of hard sphere glasses*
- A34 I. Elyukhina**, South Ural State University  
*Analysis of oscillating-cup technique for measurement of density and non-Newtonian properties*
- A35 V.I. Lad'yanov**, Ural Branch of Russian Academy of Sciences  
*On the viscosity and the crystallization processes of the Co-(Fe, Cr)-Si-B amorphizing melts*
- A36 L.V. Kamaeva**, Ural Branch of Russian Academy of Sciences  
*The use of the temperature and concentration dependences of viscosity for the study of structure of Me(Fe,Ni,Co)-P melts*
- A37 S. G. Menshikova**, Udmurt State University  
*On viscosity and relaxation processes of the glass-forming AL-TM-REM melts*
- A38 S. Wei**, Universität des Saarlandes  
*Chemical disordering of crystals and its relation to liquid-liquid transitions in strong liquids*
- A39 Z. Evenson**, Universität des Saarlandes  
*Equilibrium viscosity, enthalpy recovery and free volume relaxation in a  $Zr_{44}Ti_{11}Ni_{10}Cu_{10}Be_{25}$  bulk metallic glass*
- A40 S. Jabbari-Farouji**, CNRS and Université Paris-Sud  
*Isotropic-nematic transition of charged disks*
- A41 S. Sharifi**, University of Sistan and Baluchestan  
*Nanoscale structural characterization and relaxation of the oil-in-water nanoemulsion with Hydrophobically End-Capped Poly (ethylene oxide)*
- A42 S. Sharifi**, University of Sistan and Baluchestan  
*The effect of depletion interaction on relaxation and structure of nanoemulsion*

- A43 E. Del Gado**, ETH Zurich  
*Non-linear response of dipolar colloidal gels to external fields*
- A44 R. Messina**, Universität Düsseldorf  
*Ultra-fast quenching of binary colloidal suspensions in external magnetic fields*
- A45 P. E. Ramírez-González**, Universidad Autónoma de San Luis Potosí  
*Theoretical study of aging and instantaneous quenches in attractive Yukawa systems*
- B1 A. Heuer**, Universität Münster  
*Non-linear response in glass-forming systems: Computer simulations*
- B2 D. Winter**, Universität Mainz  
*Non-linear single-particle-response of glassforming systems to external fields*
- B3 N. Koumakis**, IESL Heraklion  
*Yielding of colloidal glasses and gels*
- B4 O. Herbst**, Deutsches Zentrum für Luft- und Raumfahrt, Köln  
*Brownian dynamics simulation of extensional shear flow in dense colloidal hard-sphere systems at the glass transition*
- B5 S. Papenkort**, Universität Konstanz and Zukunftskolleg der Universität Konstanz  
*Lattice-Boltzmann Simulation of Non-Newtonian Liquids*
- B6 T. Divoux**, Université de Lyon  
*Transient fluidization processes leads to quantitative predictions for the Herschel–Bulkley model in Simple Yield Stress Fluids*
- B7 M. Hussainov**, University of Tartu  
*Technique for Experimental Studying of Elongational Behavior of High Reactivity Viscoelastic Liquids: Application to Alkoxide-Based Sol-Gel Precursors.*
- B8 J. Chattoraj**, Université Paris Est – Laboratoire Navier  
*Avalanche size in sheared amorphous solids at low temperature*
- B9 C. Barentin**, Université de Lyon  
*Confined diffusion of probes in a colloidal suspension*
- B10 C. L. Klix**, University of Konstanz  
*Elastic Properties of Glasses*
- B11 A. Lederer**, Universität Mainz  
*Suppression of multiple scattering effects in colloidal model systems*
- B12 V. Nosenko**, Max-Planck-Institut für extraterrestrische Physik Garching  
*Shear Melting and Shear Flows in a 2D Complex (Dusty) Plasma*
- B13 A. Bronsch**, Freiberg University of Mining and Technology  
*Particle influence on the viscosity measurements of molten slags*
- B14 A. Jacob**, TU Bergakademie Freiberg  
*Determination of physical chemical properties of molten slags using molecular dynamics simulation*
- B17 D. Truzzolillo**, IESL Heraklion  
*Star-linear polymer mixtures: a subtle balance between depletion and osmotic shrinkage*
- B18 F. Scheffold**, University of Fribourg  
*Dynamics and elasticity of highly compressed microgel phases*
- B19 P. Bacova**, University of the Basque Country (UPV/EHU)  
*Dynamics of branch points in star polymers by computer simulations*
- B20 R. Juárez-Maldonado**, Universidad Autónoma de Zacatecas  
*Effects of polydispersity on dynamic arrest properties of model colloidal systems*
- B21 N. Gnan**, Università di Roma “La Sapienza”  
*Colloidal Effective Interactions: the Role of Attraction in the Solvent*

- B22 F. Sciortino**, Università di Roma “La Sapienza”  
*How do Self-Assembling Polymers and Gels Age Compared to Glasses?*
- B23 M. Isobe**, Nagoya Institute of Technology  
*Study of Transient Nuclei near Freezing*
- B24 V.A. Martinez**, University of Edinburgh  
*Dynamical Signature at the Freezing Transition*
- B25 B. Seoane**, Universidad Complutense de Madrid  
*Effective potential study of hard-spheres crystallization*
- B26 C. Valeriani**, University of Edinburgh  
*The Crystallization of Hard-Sphere Glasses*
- B27 H. J. Schöpe**, Universität Mainz  
*Crystallization and vitrification of a hard sphere like colloidal model system*
- B28 M. Camargo**, Universität Düsseldorf  
*Equilibrium dynamics of binary cluster crystals*
- B29 S. Sastry**, Centre for Advanced Scientific Research Bengaluru  
*Free Volume Distributions in Hard Sphere Fluid and Jammed Configurations*
- B30 A. Puglisi**, CNR-ISC Rome, Italy  
*Spontaneous rotation and slow “breathing” in a vertically vibrated dense granular monolayer*
- B31 G. Gradenigo**, Università di Roma “La Sapienza”  
*Growing time and length scales in the dissipative dynamics of a granular fluid*
- B34 I. Buttinoni**, Stuttgart University  
*A New Species of Active Brownian Particles*
- B35 H. H. Wensink**, Universität Düsseldorf  
*Zero Reynolds number turbulent flow in active liquid crystals*
- B36 P. Papadopoulos**, University of Leipzig  
*Interplay of macroscopic and microscopic viscoelastic properties in spider silk*
- B37 C. Maggi**, Università di Roma “La Sapienza”  
*Effective Interactions between Colloids Suspended in a Bacterial Bath*
- B39 C. Scholz**, Universität Stuttgart  
*Flow and Transport Properties of Microstructured Porous Media*
- B40 F. Höfling**, Max-Planck-Institut für Metallforschung Stuttgart  
*Lorentz-like power-law decay of velocity anti-correlations in a supercooled liquid*
- B41 M. Spanner**, Universität Erlangen-Nürnberg  
*Aspects of subdiffusive transport in the Lorentz Model*
- B42 J. Kurzidim**, Technische Universität Wien  
*Dynamic arrest of colloids in porous environments: disentangling crowding and confinement*
- B43 S. Schnyder**, Deutsches Zentrum für Luft- und Raumfahrt, Köln  
*Influence of Matrix Dynamics on Anomalous Diffusion in Strongly Heterogeneous Binary Mixtures*
- B44 W. Schirmacher**, Universität Mainz  
*Anomalous diffusion and long-time tails in quenched-disordered systems*
- B45 A. Sarracino**, Università di Roma “La Sapienza”  
*On anomalous diffusion and fluctuation-dissipation relations*



## **3 Abstracts**

### **3.1 Talks**

## Static and Dynamic Length Scales in Glass-Forming Liquids

Walter Kob,<sup>1,\*</sup> Sándalo Roldán-Vargas,<sup>1,2</sup> and Ludovic Berthier<sup>1</sup>

<sup>1</sup>*Laboratoire des Colloïdes, Verres et Nanomatériaux,  
UMR CNRS 5587, Université Montpellier 2, 34095 Montpellier, France*

<sup>2</sup>*Departamento de Física Aplicada, Grupo de Física de Fluidos y Biocoloides,  
Universidad de Granada, 18071 Granada, Spain*

More than forty years ago Adam and Gibbs put forward the idea that the relaxation dynamics of glass-forming liquids is closely related to the existence of “cooperatively relaxing regions” (CRR), i.e. that particles can move only if they do so in a collective manner [1]. Within this theory it is found that the size of the CRRs increases with decreasing temperature, thus giving a first example of a dynamical length scale that grows upon cooling. However, even today we do not have a clear picture on the nature of these mobile/immobile domains, *if* they really are the relevant entities for the relaxation of the system. Although a few years ago new theoretical results showed that certain types of susceptibilities can give some approximate information on the size of the relaxing domain [2], the interpretation of the experimental data has turned out to be highly nontrivial [3].

Inspired by the Adam-Gibbs theory, the so-called “random first order theory” (RFOT) proposes that glass-forming systems should have an increasing *static* length scale [4]. This scale is supposed to be related to the size of the local minima in the free energy landscape of the system and is given by an interplay between the number of states that are locally available (i.e. the local entropy) and the surface tension of the interface between these domains/mosaic tiles. Although the existence of these tiles is from a theoretical point of view attractive, there is so far only little *direct* evidence that these domains really exist. A notable exception is the study of Biroli *et al.* who, using computer simulation of spherically confined systems, have recently presented results that seem to be compatible with the presence of mosaic tiles [5]. Support for the existence of growing dynamical and static length scales comes also from analytical results that predict that a dynamic length should diverge at the mode-coupling temperature  $T_c$ , whereas the static one

at the Kauzmann temperature  $T_K$  [6]. However, these results have been obtained for mean-field like models and therefore their relevance for finite dimensional systems is not known.

The system we study is a binary mixture of elastic soft spheres. The liquid is equilibrated using periodic boundary conditions in all three directions. Subsequently we freeze all the particles that are within a slice that is perpendicular to the  $z$ -axis. Particles outside this slice are considered to be fluid like particles and they now move in a space that is confined by two rough walls. Thus this setup allows us to study the point-to-set correlation with high accuracy.

In Fig. 1 we show a superposition of snapshots of the system. Thus this graph allows us to obtain an idea on the structure of the density field of the particles which is generated by the rough wall. In this talk we will discuss how the structural and dynamical properties of the system depend on  $z$ . We find that there is a growing static length scale that is related to the increasing importance of multi-point correlation functions. Furthermore we find that also the length scale characterizing the dynamic properties increases at high and intermediate temperatures. Surprisingly we find that this scale starts to *decrease* again around the mode-coupling temperature of the system. Our results give evidence for the existence of *two* relaxation mechanisms, the relevance of each changes with temperature. Thus this result seems to be in qualitative agreement with the prediction of RFOT [7]. Finally we show how these results affect also the relaxation dynamics of system as studied in computer simulations of small systems with periodic boundary conditions in all three dimensions.

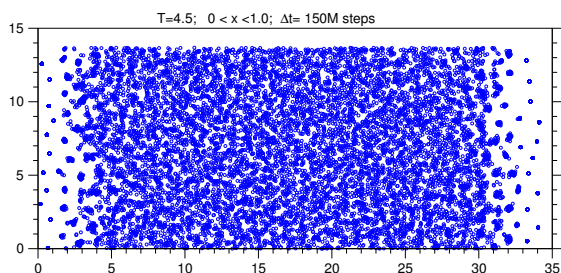


FIG. 1. Superposition of snapshots of the system at  $T = 4.5$ . The frozen walls are between  $0 \leq z \leq 1.4$ . Only the particles with  $0 \leq x \leq 1.0$  are shown. Consecutive snapshots are spaced by  $2.55 \cdot 10^7$  time units.

\* Corresponding author: walter.kob@univ-montp2.fr

- [1] G. Adam and J.H. Gibbs, *J. Chem. Phys.* **43**, 139 (1965).
- [2] L. Berthier *et al.*, *Science* **310**, 1797 (2005).
- [3] C. Dalle-Ferrier *et al.*, *Phys. Rev. E* **76**, 041510 (2007).
- [4] X.Y. Xia and P.G. Wolynes, *Proc. Natl. Acad. Sci.* **97**, 2990 (2000).
- [5] G. Biroli *et al.*, *Nat. Phys.* **4**, 771 (2008).
- [6] S. Franz and A. Montanari, *J. Phys. A: Math. Gen.* **40**, F251 (2007).
- [7] J.D. Stevenson, J. Schmalian, and P.G. Wolynes, *Nat. Phys.* **2**, 268 (2006).

## Growing length scales and their relation to growing time scales in glass-forming liquids

Smarajit Karmakar,<sup>1</sup> Chandan Dasgupta,<sup>2,\*</sup> and Srikanth Sastry<sup>3</sup>

<sup>1</sup>*Department of Chemical Physics, The Weizmann Institute of Science, Rehovot 76100, Israel*

<sup>2</sup>*Department of Physics, Indian Institute of Science, Bangalore-560012, India*

<sup>3</sup>*Jawaharlal Nehru Centre for Advanced Scientific Research, Bangalore-560064, India*

The notion of a growing length scale of “cooperatively rearranging regions” is often invoked to explain the enormous increase in the viscosity and relaxation time of a liquid upon supercooling. Recent studies of dynamic heterogeneity (spatial heterogeneity in the local dynamics) provide fresh impetus in this direction. Using molecular dynamics simulations and finite-size scaling for a realistic glass-forming liquid, we establish [1] that the growth of dynamic heterogeneity with decreasing temperature is indeed governed by a growing dynamic length scale. We also perform an extensive computational study [2] of a four-point, time-dependent structure factor, defined from spatial correlations of mobility, for the same liquid for system sizes extending up to 351232 particles. Our estimates for the dynamic correlation length and susceptibility are consistent with the results from our previous finite size scaling analysis [1]. We find [3] scaling exponents that are inconsistent with predictions from inhomogeneous mode coupling theory [4] and a recent simulation confirmation [5] of these predictions.

Our study [1] of the dependence of the simultaneously growing time scale of the long-time  $\alpha$ -relaxation on system size does not exhibit the same scaling behavior as the dynamic heterogeneity: this time scale is instead determined, for all studied system sizes and temperatures, by the configurational entropy, in accordance with the Adam-Gibbs relation. The validity of the “random first-order transition” theory [6], that provides a rationalization of the Adam-Gibbs relation, is investigated by exploring [7] the relation between the  $\alpha$ -relaxation time and the configurational entropy in two and four dimensions. Our preliminary results indicate that the Adam-Gibbs relation is surprisingly “universal” in the sense that it is obeyed in all dimensions.

We also investigate [8] the dependence of the time scale of the short-time  $\beta$ -relaxation on temperature and system size. At low temperatures, the  $\beta$ -relaxation time, defined [5] as the time at which the logarithmic derivative of the mean-square displacement with respect to time reaches its minimum value, exhibits a strong dependence on the system size. A finite-size scaling analysis of this dependence on the system size reveals the existence of a length scale that grows as the temperature is reduced. Surprisingly, the temperature dependence of this length scale

is found to be identical to that of the length scale that governs the growth of dynamic heterogeneity at the  $\alpha$ -relaxation time scale. This result shows that the dynamics of glass-forming liquids is governed by a growing length scale even in the short-time “caging” regime, and suggests a close connection between the short-time dynamics and dynamic heterogeneity at time scales of the order of the  $\alpha$ -relaxation time.

In the “energy landscape” description of glassy dynamics, the short-time behavior is expected to be closely related to the properties of the potential energy minima (“inherent structures”) explored by the system. To investigate this relation, we use the eigenvalues and eigenvectors of the Hessian matrix evaluated at the inherent structures in a harmonic analysis [9] to calculate the dynamic behavior at short times. Preliminary results indicate the presence of a characteristic time scale in the short-time dynamics that tracks the frequency of the “Boson peak” in the density of normal modes. The dependence of this time scale on temperature and system size suggests the presence of a characteristic length scale. Detailed results for this length scale and its relation to the length scale of dynamic heterogeneity at the  $\alpha$ -relaxation time scale will be available in the near future.

A part of the work described here was carried out by P. Bhuyan, S. Sengupta and S. Banerjee.

\* Corresponding author: cdgupta@physics.iisc.ernet.in

- [1] S. Karmakar, C. Dasgupta, and S. Sastry, *Proc. Nat. Acad. Sci (USA)* **106**, 3675 (2009).
- [2] S. Karmakar, C. Dasgupta, and S. Sastry, *Phys. Rev. Lett.* **105**, 015701 (2010).
- [3] S. Karmakar, C. Dasgupta, and S. Sastry, *Phys. Rev. Lett.* **105**, 019801 (2010).
- [4] G. Biroli, J.-P. Bouchaud, K. Miyazaki, and D. R. Reichman, *Phys. Rev. Lett.* **97**, 195701 (2006).
- [5] Richard S. L. Stein and H. C. Andersen, *Phys. Rev. Lett.* **101**, 267802 (2008).
- [6] V. Lubchenko and P. G. Wolynes, *Annu. Rev. Phys. Chem.* **58**, 235 (2007).
- [7] S. Sengupta, S. Karmakar, S. Sastry and C. Dasgupta, manuscript in preparation.
- [8] S. Karmakar, C. Dasgupta, and S. Sastry, manuscript in preparation.
- [9] P. Bhuyan, S. Banerjee, S. Karmakar, C. Dasgupta and S. Sastry, work in progress.

## A static correlation length diverging at the glass transition

Majid Mosayebi,<sup>1,\*</sup> Emanuela Del Gado,<sup>2</sup> Patrick Ilg,<sup>1</sup> and Hans Christian Öttinger<sup>1</sup>

<sup>1</sup>ETH Zürich, Department of Materials, Polymer Physics, CH-8093 Zürich, Switzerland

<sup>2</sup>ETH Zürich, Department of Civil Engineering,  
Microstructure and Rheology, CH-8093, Zürich, Switzerland

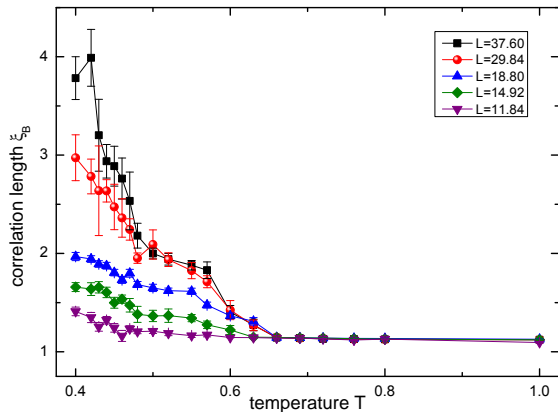


FIG. 1. Static correlation length  $\xi_B$  as function of temperature for different system sizes. Results are for a binary Lennard-Jones mixture, which is an established model for fragile glass formers [6]. Figure taken from [5].

Is there a static, structural origin of the dramatic slowing down of dynamics in supercooled liquids? A few recent findings [1] give novel indications of a growing static correlation length, as several theories had indeed assumed. Here we give evidence of a clear structural signature of the glass transition from computer simulations, in terms of a static correlation length which shows characteristic finite-size scaling known from critical phenomena.

Following a nonequilibrium thermodynamic theory of glasses [2], here we use small, static deformations to perturb the inherent structures – that are local minima of the underlying potential energy landscape – of supercooled liquids approaching the glass transition. By comparing inherent structures before and after applying the deformation, we can extract a non-affine displacement field [3]. We define a static correlation length from the size of correlated regions in the non-affine displacement field by successive coarse graining [4]. Figure 1 shows the correlation length  $\xi_B$  as a function of temperature. In the high temperature liquid phase we observe a low value of  $\xi_B$  of the order of the particles diameter  $\sigma$ . In the supercooled regime, however, the static correlation length  $\xi_B$  increases considerably, indicating the onset of the glassy dynamics and the approach towards the glass transition [5].

We also observe in Fig. 1 a systematic system-size dependence of  $\xi_B(T)$  in the supercooled regime. Such a significant increase of  $\xi_B$  with system size is reminiscence of critical phenomena where the correlation length  $\xi$  associated with the order parameter characterizing the transition diverges at the critical temperature  $T_c$  as  $\xi \sim (T - T_c)^{-\nu}$ . If the increase of  $\xi_B$  upon

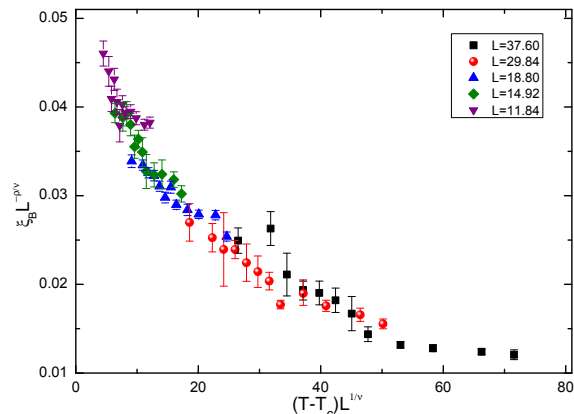


FIG. 2. Data collapse after proper scaling of the axes, according to finite-size scaling hypothesis. The estimated values of critical exponents are  $\rho \approx 0.9 \pm 0.1$ , and  $\nu \approx 0.65 \pm 0.1$ , if we identify the critical temperature  $T_c$  with the Kauzmann temperature. Figure taken from [5].

lowering the temperature is indeed due to a diverging static correlation length  $\xi$  underlying the glass transition, then  $\xi_B$  should diverge as well, and in the infinite system  $\xi_B(T) \sim (T - T_c)^{-\rho}$ . In Fig. 2 the data collapse is shown after performing the finite-size scaling analysis. Our numerical results are consistent with random first order theory [1], predicting a divergence with a critical exponent  $\nu = 2/3$  at the Kauzmann temperature, where the extrapolated configurational entropy vanishes.

Our study has been performed at constant density, where our estimate of the critical temperature  $T_c$  extracted from  $\xi_B$  is apparently below the lowest temperature at which we have been able to equilibrate the system. However, the true critical point would not necessarily be located at the density chosen here and only a systematic investigation in the  $(T, P)$ -plane will shed further light on its existence, nature, and location.

\* Corresponding author: mosayebi@mat.ethz.ch

- [1] V. Lubchenko, P. G. Wolynes, *Annu. Rev. Phys. Chem.* **58**, 235 (2007).
- [2] H. C. Öttinger, *Phys. Rev. E* **74**, 095501 (2006).
- [3] E. Del Gado, P. Ilg, M. Kröger, H. C. Öttinger, *Phys. Rev. Lett.* **101**, 095501 (2008).
- [4] F. Leonforte, A. Tanguy, J. P. Wittmer, J.-L. Barrat, *Phys. Rev. Lett.* **97**, 055501 (2006).
- [5] M. Mosayebi, E. Del Gado, P. Ilg, H. C. Öttinger, *Phys. Rev. Lett.* **104**, 205704 (2010).
- [6] W. Kob, H. C. Andersen, *Phys. Rev. E* **51**, 4626 (1995).

# A phase-separation perspective on dynamic heterogeneities in glass-forming liquids

C. Cammarota,<sup>1,\*</sup> A. Cavagna,<sup>2</sup> I. Giardina,<sup>2</sup> G. Gradenigo,<sup>3</sup> T. S. Grigera,<sup>4</sup> G. Parisi,<sup>5</sup> and P. Verrocchio<sup>6</sup>

<sup>1</sup>*IPhT, CEA Saclay, France*

<sup>2</sup>*Centre for Statistical Mechanics and Complexity (SMC), CNR-INFN.*

<sup>3</sup>*CNR-ISC and Dipartimento di Fisica, Università Sapienza*

<sup>4</sup>*INIFTA and Departamento de Física, Universidad Nacional de La Plata, and CCT La Plata*

<sup>5</sup>*Dipartimento di Fisica, Sapienza Università di Roma*

<sup>6</sup>*Dipartimento di Fisica, Università di Trento*

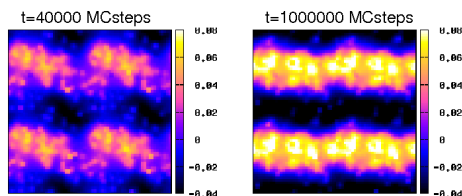


FIG. 1. Fluctuations of the overlap field for the constrained dynamics with  $\hat{Q} = 0.25$ .  $\tau_\alpha = 40000$  MC steps.

The conspicuous lack of a growing correlation length, contrasting with the very steep increase of the relaxation time, has been a puzzle in the physics of structural glasses for quite a long time. The first breakthrough has been the discovery of dynamic heterogeneities and the detection of a growing dynamical correlation length  $\xi_d$  [1]. Dynamic heterogeneities show up as regions with very different mobility of the particles during a time lag comparable to the  $\alpha$  relaxation time,  $\tau_\alpha$ . Pure thermodynamics is involved in the definition of a completely different correlation length,  $\xi_s$ , discovered more recently: the Point to Set length [2]. This length is naturally determined in the Random First Order Theory by the balance between the amorphous surface tension cost and the configurational entropy gain of any rearrangement [3]. An important issue is the unification of the dynamic and the thermodynamic frameworks, so as the understanding of the interplay between the two correlation lengths.

Although the static-dynamic connection is clear in mean field systems and in some more realistic systems [4], we are quite far from a unifying picture in real glass-formers. We face this problem studying dynamic heterogeneities in a glass-forming liquid with constrained global overlap. This approach shows that the surface tension, which is a crucial ingredient of the thermodynamic framework, also plays a key role in the formation of dynamic heterogeneities.

Dynamic heterogeneities usually show a time-dependent size  $\xi(t)$  with a maximum  $\xi(\tau_\alpha) = \xi_d$ . Beyond  $\tau_\alpha$  the system loses the memory of its initial configuration, i.e. the mobility becomes large everywhere, and there is no signal showing spatial heterogeneity in the dynamics. The large time behaviour of a dynamics in which the system cannot entirely lose memory of its initial configuration would be completely different. We have implemented this dynamics by imposing a lower bound  $\hat{Q}$  on the overlap  $Q(t)$ . This quantity

measures the similarity between an equilibrium initial configuration taken as a reference configuration, and the configuration at  $t$ . In the unconstrained dynamics  $Q(t \gg \tau_\alpha)$  is 0. The constrained dynamics shows the same behaviour of the unconstrained one at short time  $t$ , including the growth of the dynamic heterogeneities. Yet, at large  $t$  things necessarily change as we reject all the particle movements which do not fulfill the constraint  $Q(t) \geq \hat{Q}$ . Two alternative hypotheses are possible for the large time behaviour of the constrained system. Heterogeneities, just grown during the unperturbed short time regime, may shrink back towards a large time configuration in which particles with low and high mobility are spread across all the system. A second possibility is that heterogeneities merge letting  $\xi(t)$  grow beyond  $\xi_d$  and driving the system towards a phase separated highly correlated state. The first scenario would be incompatible with the existence of a surface tension cost of any rearrangements. On the contrary, the second picture is the expected one in presence of a non-zero surface tension. In this case a merging of the rearranged regions would be preferable since the system pays a smaller global interface cost.

Inspection of the constrained dynamics at large  $t$  gives evidence for phase separation of the system into high and low mobility regions, the picture naturally expected in presence of a non-zero surface tension. The enlarging of the dynamic heterogeneities is less marked when the temperature is higher. This is consistent with the idea that the surface tension decays at high temperature [5]. Moreover we find that the decrease of the global energy is compatible with the coarsening process in systems undergoing phase separation [6]. Finally fluctuations of the order parameter around the value  $\hat{Q}$  reveal the outline of an effective thermodynamic potential [7] which shows evidence of the Maxwell construction, i.e. the landmark of phase separation.

\* Corresponding author: chiara.cammarota@cea.fr

- [1] Annu. Rev. Phys. Chem. **51**, 99 (2000); Phys. Rev. Lett. **82**, 5064 (1999); J. Non-Cryst. Sol. **307**, 215 (2002).
- [2] J. Chem. Phys. **121**, 7347 (2004); Nat. Phys. **4**, 771 (2008).
- [3] Phys. Rev. A **40**, 1045 (1989).
- [4] Math. Theor. **40**, F251 (2007).
- [5] J. Stat. Mech. L12002 (2009); J. Chem. Phys. **131**, 194901 (2009).
- [6] Adv. Phys. **43**, 357 (1994).
- [7] Physica A **261**, 317 (1998).

# Dynamic glass transition: mode-coupling theory, replica approach and emergence of rigidity

Grzegorz Szamel\*

*Department of Chemistry, Colorado State University, Fort Collins, CO 80523, USA*

We first clarify the relation between the ergodicity breaking transition predicted by mode-coupling theory and the so-called dynamic transition predicted by the static replica approach [1]. Following Franz and Parisi [2], we consider a system of particles in a metastable state characterized by non-trivial correlations with a quenched configuration. The assumption that in a metastable state particle currents vanish is shown to lead to an expression for the replica off-diagonal direct correlation function in terms of a non-trivial part of the replica off-diagonal static four-point correlation function. A factorization approximation for this four-point function results in an approximate closure for the replica off-diagonal direct correlation function. The replica off-diagonal Ornstein-Zernicke equation combined with this closure coincides with the equation for the non-ergodicity parameter derived using the mode-coupling theory.

Second, we identify Goldstone modes of the amorphous solid that appears at the dynamic transition and derive a formal expression for its shear modulus. This expression is complementary to the formula used by Yoshino and Mezard [3]. To calculate the modulus we combine our formal expression with the above described version of the replica approach which is consistent with the mode-coupling theory.

We gratefully acknowledge the support of NSF Grant CHE 0909676.

\* Corresponding author: grzegorz.szamel@colostate.edu

- [1] G. Szamel, *Europhys. Lett.* **91**, 56004 (2010).
- [2] S. Franz and G. Parisi, *Phys. Rev. Lett.* **79**, 2486 (1997).
- [3] H. Yoshino and M. Mezard, *Phys. Rev. Lett.* **105**, 015504 (2010).

# Is the Mode-Coupling Theory a Mean Field Description of the Glass Transition?

Kunimasa Miyazaki,<sup>1,\*</sup> Atsushi Ikeda,<sup>1</sup> Patrick Charbonneau,<sup>2</sup> and J. A. van Meel<sup>3</sup>

<sup>1</sup>*Institute of Physics, University of Tsukuba, Tennodai 1-1-1, Tsukuba 305-8571, Japan*

<sup>2</sup>*Department of Chemistry, Duke University, Durham, North Carolina, 27708, USA*

<sup>3</sup>*FOM Institute for Atomic and Molecular Physics, Science Park 113, 1098 XG Amsterdam, The Netherlands*

Mode-Coupling Theory (MCT) is conjectured to be a mean field description of dynamics of supercooled liquids. It is said to be the “mean-field” in two senses; (i) MCT is a “Landau theory” of the glass transition in a sense that it can make a robust and universal prediction on critical dynamics near the nonergodic transition points  $T_{mct}$  [1], such as dynamic scaling at the beta regime, although it is “polluted” by heterogeneous fluctuations in finite dimensional systems. (ii) MCT is said to be a dynamic counterpart of the replica theory for liquids, a mean field thermodynamic theory of the glass transition [2]. The liquid replica theory predicts a dynamic transition temperature  $T_d$  followed by the thermodynamic glass transition at a lower temperature  $T_K$ . Inspired by the facts that these two transition points exist for some mean-field models of the spin glasses and their dynamics are described by equations which are mathematically equivalent with MCT,  $T_d$  of the replica theory is often identified with MCT’s the nonergodic transition point  $T_{mct}$ . However, the  $T_d$ - $T_{mct}$  equivalence has never been proved or disproved, partially because many uncontrolled approximations of liquid theories employed to calculate these temperatures blur the generic equivalence or difference of the two theories.

In this presentation, we discuss the glassy dynamics of one-component hard-sphere fluids in spatial dimensions higher than 3 in order to clarify the status of MCT as the mean field theory [3, 4]. Our results are two-fold; (i) If MCT is really a mean-field theory, one expects that the time/temperature range over which the MCT-like critical properties are observed is wider in higher dimensions. A MD simulation for hard sphere system in four dimension is performed. We demonstrate that the violation of the Stokes-Einstein relation is suppressed and thus dynamic heterogeneities are reduced in  $4d$ . Furthermore, comparison of MCT with simulation results for the density correlation functions  $F_s(k, t)$  shows that the density range where MCT works is wider and fitting works better than lower-dimensional systems. As a byproduct, we also find that the nucleation rate is suppressed even for the monodisperse system and the  $4d$  hard sphere fluid is one of the cleanest glass formers.

(ii) Systems in higher dimensions are ideal systems to compare the replica theory and MCT because many approximations which were employed in lower dimensions are lifted because the static correlations become insensitive to approximations as dimensions increases and can be computed analytically at infinite  $d$  limit.

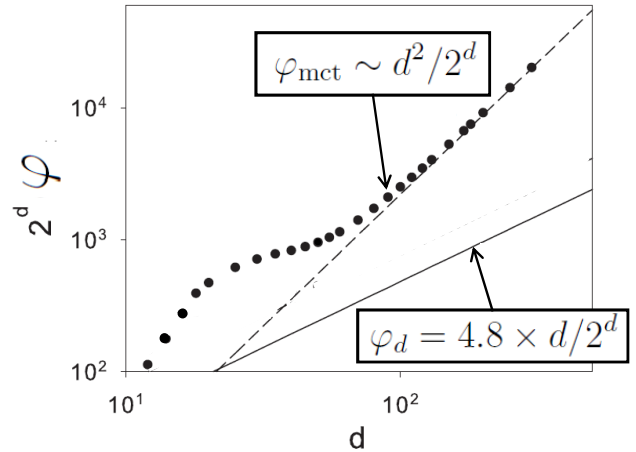


FIG. 1.  $\varphi_{mct}$  (Filled circles) and  $\varphi_d$  (solid line) as a function of  $d$ .

We compute the nonergodic transition density  $\varphi_{mct}$  and its replica-theory counterpart  $\varphi_d$  (instead of temperatures) for hard sphere fluids as well as the nonergodic parameter  $F_s(k, t = \infty)$  for arbitrary dimensions  $d \geq 3$ . We find that, for  $d = 3$  and  $4$ , MCT’s predictions agree better with simulation results than the replica theory. But MCT falters in higher dimensions. In the  $d \rightarrow \infty$  limit,  $\varphi_{mct}$  behaves as  $d^2/2^d$ , whereas the replica theory predicts  $\varphi_d \sim d/2^d$  (see Fig.1) [2, 5]. We argue that the discrepancy is due to the failure of MCT. MCT predicts pathological negative values in the real space representation of  $F_s(k, \infty)$  (the van Hove function) which is generically a non-negative quantity. These results raise more questions than answers on the mean-field picture of the structural glass transition and call for reconsideration or revision of MCT.

A. I. is supported by the JSPS and K. M. by KAKENHI No. 2154016 and Priority Areas “Soft Matter Physics”.

\* Corresponding author: kunimasa@sakura.cc.tsukuba.ac.jp

- [1] A. Andreatov, G. Biroli, and J.-P. Bouchaud, EPL **88**, 16001 (2009).
- [2] G. Parisi and F. Zamponi, Rev. Mod. Phys. **82**, 789 (2010).
- [3] P. Charbonneau, A. Ikeda, J. A. van Meel, and K. Miyazaki, Phys. Rev. E **81**, 040501(R) (2010).
- [4] A. Ikeda and K. Miyazaki, Phys. Rev. Lett. **104**, 255704 (2010).
- [5] B. Schmid and R. Schilling, Phys. Rev. E **81**, 041502 (2010).

## Mean-field limit of mode-coupling theory

Rolf Schilling\* and Bernhard Schmid

*Institut für Physik, Johannes Gutenberg-Universität, Staudinger Weg 7, 55099 Mainz, Germany*

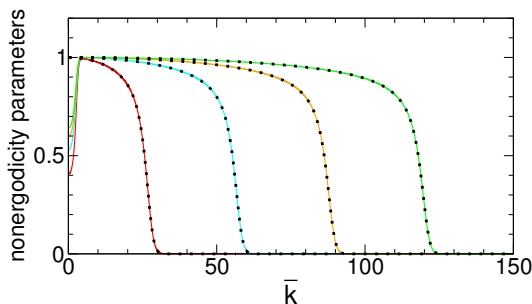


FIG. 1.  $k$ -dependence of the critical collective (solid line) and self (dotted line) nonergodicity parameters on the scale  $\bar{k} = k\sigma/\sqrt{d}$  for  $d = 200, 400, 600$  and  $800$  (from left to right).

In the last two and a half decades the understanding of the structural glass transition has made significant progress due to mode-coupling theory (MCT) [1] and replica theory [2]. Whereas replica theory is a microscopic approach to a static glass transition at e.g. a packing fraction  $\varphi_K$ , MCT provides an equation of motion for the intermediate scattering function  $S(k, t)$ , or its self part  $S^{(s)}(k, t)$  of a liquid. It predicts a dynamic glass transition from an ergodic to a nonergodic phase. Since MCT involves the factorization of the memory kernel (a four-point correlator) into a product of two-point correlators, it has been interpreted as a mean-field theory (MFT) [3]. For systems in thermal equilibrium MFT becomes exact, e.g. in the limit of spatial dimensions  $d \rightarrow \infty$  or for infinite range interactions. This has motivated us to investigate MCT for a liquid of hard hyperspheres with diameter  $\sigma$  for  $d \rightarrow \infty$ .

First, we have calculated numerically the critical collective and self nonergodicity parameters (NEP)  $f_c(k; d)$  and  $f_c^{(s)}(k; d)$ , respectively, up to  $d = 800$  [4]. The result is shown in Figure 1.

Figure 1 clearly shows the non-Gaussian  $k$ -dependence. Three different  $k$ -scales exist. In the limit  $d \rightarrow \infty$  both NEP differ on a scale  $k \sim d^{1/2}$ , become identical for  $k \sim d$  where they converge to one, and they vary from one to zero on a scale  $k \sim d^{3/2}$ .

Based on these results we have been able to prove analytically that the critical packing fraction is given by  $\varphi_c(d) \sim d^2 2^{-d}$  [4]. Figure 2 demonstrates that the numerical result approaches this  $d$ -dependence for  $d > 100$ . These results have also been found by an independent numerical approach [5].

Replica theory yields  $\varphi_K(d) \sim d \ln(d/2) 2^{-d}$  [6] which is below  $\varphi_c(d)$ . Because  $\varphi_K(d)$  has to be above  $\varphi_c(d)$  both results are inconsistent.

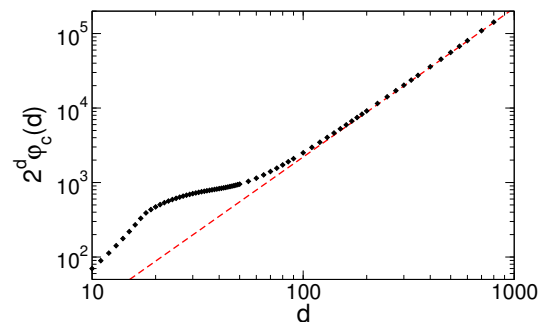


FIG. 2.  $d$  dependence of the critical packing fraction  $\varphi_c(d)$  on a log-log representation. Symbols denote the numerical result and the dashed line represents the analytical result.

The authors of Ref. [5] also reported negative dips in the long-time limit  $G_{c,\infty}^{(s)}(r; d)$  of the self part of the van Hove function. We have found that these dips are absent not only for  $G_{c,\infty}^{(s)}(r; d)$  but also for the corresponding collective quantity  $G_{c,\infty}(r; d)$  for  $d \rightarrow \infty$ . In that limit both quantities become Gaussian on a scale  $rd/\sigma = O(1)$ .

The fact that  $G_{c,\infty}^{(s)}(r; d)$  and  $G_{c,\infty}(r; d)$  are non-negative for  $d \rightarrow \infty$ , as it should be, does not necessarily imply that MCT becomes exact in the mean-field limit  $d \rightarrow \infty$ . For instance, if it would turn out that e.g. the quadratic pre-exponential factor of  $\varphi_c(d)$  contradicts more general features, one would have to conclude that MCT does not become exact for  $d \rightarrow \infty$ . Consequently MCT would not be a MFT, at least in the conventional sense. It is interesting to note that applying the MCT strategy to a lattice  $\phi^4$ -model with interaction range  $N$  yields an ergodic-nonergodic transition at a finite temperature, whereas it can be shown that the Newtonian dynamics of this model becomes nonergodic in the limit  $N \rightarrow \infty$  for all finite temperatures [7]. Accordingly, MCT for the mean-field  $\phi^4$ -model is not exact.

\* Corresponding author: rolf.schilling@uni-mainz.de

- [1] W. Götze, *Complex Dynamics of Glass-Forming Liquids - A Mode-Coupling Theory*, (Oxford University Press, Oxford, 2009)
- [2] M. Mézard and G. Parisi, Phys. Rev. Lett. **82**, 747 (1999)
- [3] G. Biroli and J.-P. Bouchaud, Europhys. Lett. **67**, 21 (2004)
- [4] B. Schmid and R. Schilling, Phys. Rev. E **81**, 041502 (2010)
- [5] A. Ikeda and K. Miyazaki, Phys. Rev. Lett. **104**, 255704 (2010)
- [6] G. Parisi and F. Zamponi, J. Stat. Mech.: Theory Exp (2006) P03017
- [7] W. Kob and R. Schilling, J. Phys.: Condens. Matter **3**, 9195 (1991)

## Quantum glass transition and superfluidity of hard spheres

Laura Foini,<sup>1,2</sup> Guilhem Semerjian,<sup>1</sup> and Francesco Zamponi<sup>1,\*</sup>

<sup>1</sup>*LPTENS, CNRS UMR 8549, associée à l'UPMC Paris 06, 24 Rue Lhomond, 75005 Paris, France*

<sup>2</sup>*SISSA and INFN, Sezione di Trieste, via Bonomea 265, I-34136 Trieste, Italy*

A consistent theory of the glass transition is the so-called Random First Order Transition (RFOT) theory, which includes Mode-Coupling Theory (MCT) and replica theory for the description of dynamics and thermodynamics respectively. Its extension to quantum systems has been initiated long time ago by studying the quantum version of the  $p$ -spin glasses and related models [1–3]. The main result of these studies is that the high temperature RFOT-like glass transition is turned into a first order transition between the liquid and the glass at very low temperature. However, the picture provided by these studies is not complete, since all the models that have been studied are in the glass phase at low enough  $T$  in absence of quantum fluctuations. The possibility of studying the glass transition at low  $T$  as a function of another control parameter (e.g. the density  $\rho$ ) adds an important ingredient to the discussion, which is entropy. In fact, the models studied in [1–3] have a non-extensively degenerate ground state, hence their entropy at  $T = 0$  vanishes. Conversely, lattice glass models might have a finite entropy even at  $T = 0$  (think for instance to hard spheres) and in this case the glass transition is completely driven by entropy.

In a recent paper, Markland et al. [4] developed a quantum extension of MCT, and they applied their theory to the description of quantum hard spheres. Their most interesting result is the prediction of a re-entrance in density of the glass transition line upon increasing quantum fluctuations. This means that one can glassify a liquid of hard spheres around, say, 50% packing fraction, by increasing the thermal wavelength of the particles). This phenomenon is extremely counterintuitive: one would expect that the quantum nature of particles would promote, through tunnelling, the exploration of the phase space, therefore inhibiting the dynamical arrest.

I will present a study of the quantum version of a mean field model of glass-former, the Biroli-Mézard model [5], which has a glass transition at  $T = 0$  as a function of  $\rho$ , driven by entropy. It is a realistic model of interacting bosons, which can be quantized adding an hopping term and therefore allowing for a superfluid phase. We investigated the phase diagram of the model by means of the cavity method, and we showed that the phase diagram is quite rich, displaying superfluid, normal liquid, and glass phases, separated by different phase transitions. We obtained two main results: *i*) at low enough temperature the glass transition line is re-entrant as a function of quantum fluctuations, as found in [4], and *ii*) the standard RFOT glass transition is replaced by a first order superfluid-glass transition at zero temperature, accompanied by

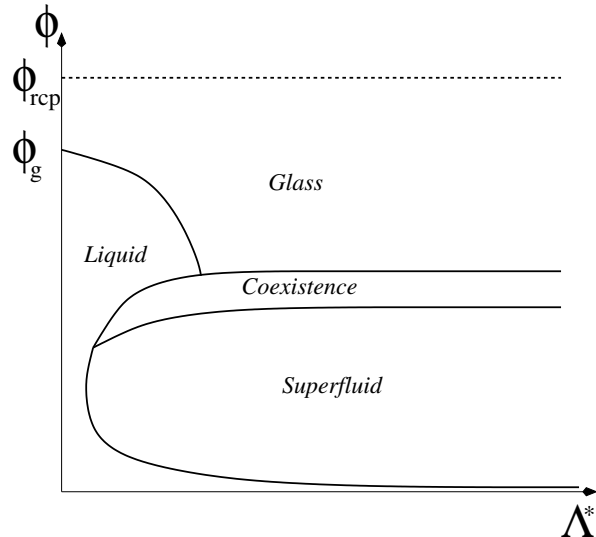


FIG. 1. Phase diagram of quantum hard spheres in presence of exchange, deduced from Ref. [4] and this work.  $\phi$  is the packing fraction, and  $\Lambda^*$  is the thermal wavelength of the particles. The glass transition is re-entrant. The superfluid transition can be first or second order; in the former case it is accompanied by phase coexistence. Note that at very low temperature  $\Lambda^*$  is large, therefore one always has a first order transition between the superfluid and a non-superfluid glass.

phase coexistence between the two phases, while at the same time the glass transition completely disappears.

Our results show that for models with such a complex phase space in the classical limit, introducing quantum fluctuations has a dramatically singular effect, changing completely the nature of the transition between the liquid and the glass phases. Moreover, the first order superfluid-glass transition is accompanied by a jump in density, implying that there exists an interval of densities where the two phases would coexist in a finite dimensional version of the model. One would therefore obtain a simultaneous presence of superfluid and glassy ordering, which however would not give rise to a true superglass phase since they would be phase separated.

\* Corresponding author: francesco.zamponi@lpt.ens.fr

- [1] Y. Y. Goldschmidt, Phys. Rev. B **41**, 4858 (1990).
- [2] G. Biroli and L. F. Cugliandolo, Phys. Rev. B **64**, 014206 (2001).
- [3] H. Westfahl, J. Schmalian, and P. G. Wolynes, Phys. Rev. B **68**, 134203 (2003).
- [4] T. E. Markland, J. A. Morrone, B. J. Berne, K. Miyazaki, E. Rabani, and D. R. Reichman, Nature Physics **7**, 134 (2010).
- [5] G. Biroli and M. Mézard, Phys. Rev. Lett. **88**, 025501 (2001).

## Isomorphs in liquid phase diagrams and their consequences for viscous dynamics

Jeppe C. Dyre,\* Nicoletta Gnan, Nicholas P. Bailey, Ulf R. Pedersen, and Thomas B. Schröder

*DNRF Center “Glass and Time”, Roskilde University, Denmark*

This paper presents a new concept in the statistical physics of condensed matter, “isomorphs” [1]; these are curves in a classical mechanical system’s phase diagram with the property that several quantities are invariant along them. It was previously shown that van der Waals type liquids and metallic liquids have strong virial/potential energy correlations in their  $NVT$  thermal equilibrium fluctuations [2]. Such “strongly correlating” liquids have isomorphs to a good approximation, and liquids that have isomorphs are strongly correlating (Appendix A of [1]). This paper discusses the consequences of the existence of isomorphs for viscous liquid dynamics. The overall picture is that strongly correlating liquids have simpler physics than liquids in general, i.e., van der Waals liquids and metallic liquids are simpler than hydrogen-bonding, covalent, or strongly ionic liquids.

To define an isomorph we first recall that for any microscopic configuration  $(\mathbf{r}_1, \dots, \mathbf{r}_N)$  of a thermodynamic state point with density  $\rho$ , the reduced coordinates are defined by  $\tilde{\mathbf{r}}_i \equiv \rho^{1/3} \mathbf{r}_i$ . Two state points (1) and (2) with temperatures  $T_1$  and  $T_2$  and densities  $\rho_1$  and  $\rho_2$  are said to be *isomorphic* [1] if, whenever two of their microscopic configurations  $(\mathbf{r}_1^{(1)}, \dots, \mathbf{r}_N^{(1)})$  and  $(\mathbf{r}_1^{(2)}, \dots, \mathbf{r}_N^{(2)})$  have identical reduced coordinates, they have proportional configurational  $NVT$  Boltzmann probability factors:

$$e^{-U(\mathbf{r}_1^{(1)}, \dots, \mathbf{r}_N^{(1)})/k_B T_1} = C_{12} e^{-U(\mathbf{r}_1^{(2)}, \dots, \mathbf{r}_N^{(2)})/k_B T_2}. \quad (1)$$

The constant  $C_{12}$  depends only on the state points (1) and (2), not on the microscopic configurations. *Isomorphic curves* in the state diagram are defined as curves for which any two state points are isomorphic. The property of being isomorphic defines a mathematical equivalence relation on the set of state points and isomorphs are the corresponding equivalence classes. The proportionality of Boltzmann factors implies identical statics and dynamics at isomorphic state points, as well as of configurational entropy and other thermodynamic quantities [1].

The property of having isomorphs is generally approximate – only inverse-power law liquids have exact isomorphs. Thus Eq. (1) should be read as obeyed to a good approximation for the physically relevant configurations, i.e., those that do not have *a priori* negligible canonical probabilities [1]. An important class of model liquids having isomorphs to a good approximation are the Lennard-Jones and similar systems [2].

As detailed in Ref. 1 the existence of isomorphs has consequences for liquids in general. Several quantities are invariant along an isomorph, for instance the configurational entropy  $S_c$  and the relaxation time, as well as, e.g., the radial distribution function(s)  $g(r)$ . Thus theories linking reduced-unit transport coefficients to  $S_c$  like Rosenfeld’s excess entropy scaling and/ or  $g(r)$  find a natural framework in the isomorph concept [1]. Interestingly, the known exceptions from various more or less empirical rules seem all to relate to liquids that are not strongly correlating [1]. Other observations that find a natural explanation by isomorphs include [1]: phenomenological melting rules, Young and Andersen’s approximate scaling principle, the two-order parameter maps of Debenedetti and collaborators. – This paper, however, focuses on insights into viscous liquid dynamics that come from considering isomorph properties and invariants. The following topics are dealt with [1, 3, 4] :

1. *Density scaling*
2. *Isochronal superposition*
3. *Frequency-dependent thermoviscoelastic response functions*
4. *The Prigogine-Defay ratio: Strongly correlating liquids as approximate single-parameter liquids*
5. *Cause of the relaxation time’s non-Arrhenius temperature dependence: The isomorph filter*
6. *Fictive temperature variations following a temperature jump*

The centre for viscous liquid dynamics “Glass and Time” is sponsored by the Danish National Research Foundation (DNRF).

\* Corresponding author: dyre@ruc.dk

- [1] N. Gnan, T. B. Schröder, U. R. Pedersen, N. P. Bailey, and J. C. Dyre, *J. Chem. Phys.* **131**, 234504 (2009).
- [2] U. R. Pedersen, N. P. Bailey, T. B. Schröder, and J. C. Dyre, *Phys. Rev. Lett.* **100**, 015701 (2008); N. P. Bailey, U. R. Pedersen, N. Gnan, T. B. Schröder, and J. C. Dyre, *J. Chem. Phys.* **129**, 184507, *ibid* 184508 (2008); T. B. Schröder, N. P. Bailey, U. R. Pedersen, N. Gnan, and J. C. Dyre, *J. Chem. Phys.* **131**, 234503 (2009); U. R. Pedersen, T. B. Schröder, and J. C. Dyre, *Phys. Rev. Lett.* **105**, 157801 (2010).
- [3] K. L. Ngai, R. Casalini, S. Capaccioli, M. Paluch, and C. M. Roland, *J. Phys. Chem. B* **109**, 17356 (2005).
- [4] N. Gnan, C. Maggi, T. B. Schröder, and J. C. Dyre, *Phys. Rev. Lett.* **104**, 125902 (2010).

## Relation of properties of mass transport with melt structure in multicomponent viscous metals

Andreas Meyer,\* Jürgen Horbach, and Thomas Voigtmann

*Institut für Materialphysik im Weltraum, Deutsches Zentrum für Luft- und Raumfahrt (DLR), 51170 Köln, Germany*

Diffusion and viscosity are important material parameters to characterize multicomponent metallic alloys. Little is known to date about the microscopic dynamics determining these transport processes. For a certain class of densely-packed metals, the dynamics seems to be qualitatively well described by a hard-sphere (HS) model, even though one might expect that electronic contributions to the interactions should manifest themselves in some form. In fact, it remains to discover how chemical-ordering effects influence atomistic transport, and what is the role played by the individual components of the alloy. More generally, the question that arises in this context is how a given static structure of a melt relates to its transport properties. Here, we address this structure–dynamics relationship by a combination of innovative neutron scattering experiments with the mode-coupling theory for dense liquids.

We study a binary metallic melt system Zr-Ni as a realistic example. The mode-coupling theory of the glass transition (MCT) by Götze et al. accurately describes the qualitative effects of mass transport in dense fluids. It is approximative and has well-known deficiencies in the low- $T$  regime around  $T_g$ . MCT predicts the dynamics from the statics, and can deal with arbitrary  $N$ -component mixtures. It requires as input the  $N \times N$  symmetric matrix of partial static structure factors  $S(q)$  for a large range of wave numbers  $q$  (several times the main peak position) [1].

To determine the full set of partial static structure factors in Zr-Ni, we prepared different samples (approximately 1.5 g in mass), containing  $^{60}\text{Ni}$ ,  $^{58}\text{Ni}$  and natural Ni, for two different compositions. To avoid reactions of the chemically highly reactive melts with the sample environment, we employed containerless processing within a high-purity He atmosphere by electromagnetic levitation (EML) and, recently, also electrostatic levitation. The static structure factor was then determined by neutron scattering at the high-intensity two-axis diffractometer D20 of the ILL [2]. The variation of scattering lengths owing to the different Ni isotopes allows then to extract  $S(q)$  from three independent measurements. For later comparison of the dynamical behavior with the MCT calculation, Ni-self diffusion has been measured using quasielastic neutron scattering at the time-of-flight spectrometer TOFTOF of the FRM II, again in combination with EML for sample processing. At small wave vectors, the scattering signal is dominated by the incoherent Ni contribution. The low- $q$  behavior of the relaxation times of the incoherent intermediate scattering function thus allows to extract  $D_{\text{Ni}}$  on an absolute scale,

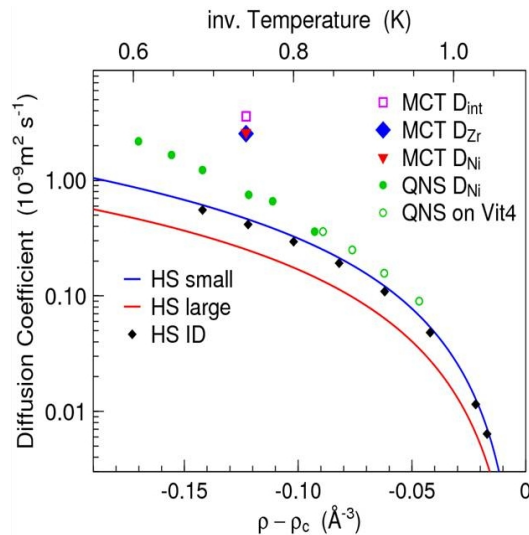


FIG. 1. Diffusion coefficients in binary Zr-Ni obtained from quasielastic neutron scattering (QNS) and calculated within MCT using partial  $S(q)$  as input. Results for a hard sphere (HS) mixture with equal particle size disparity is shown for comparison.

as demonstrated recently also for pure Ni [3].

Our MCT calculations predict that on the Zr rich side Zr and Ni diffusion proceeds with almost equal rates, and thus is more strongly coupled than one would expect from the analogy with a binary hard-sphere mixture (Fig. 1), where only the difference in covalent radii between the two elements is accounted for, but no chemical-ordering effects. How this is changed as a function of composition is currently under investigation. Recent molecular dynamics simulations using Zr-Ni model potentials indicate that subtle features in the static structure factor at  $q$  values below the structure factor maximum, where chemical short range ordering becomes visible, indeed are related to the coupling of diffusive dynamics of the Zr and Ni atoms. How this in turn relates to viscous flow is addressed by simulation and measurements of viscosity on oscillating freely-suspended droplets.

It is a pleasure to thank Dirk Holland-Moritz, Florian Kargl, Fan Yang and Phillip Kuhn for their collaboration.

\* Corresponding author: andreas.meyer@dlr.de

- [1] Th. Voigtmann, A. Meyer, D. Holland-Moritz, S. Stüber, T. Hansen, T. Unruh, EPL **82**, 66001 (2008).
- [2] D. Holland-Moritz, S. Stüber, H. Hartmann, T. Unruh, T. Hansen, A. Meyer, Phys. Rev. B **79**, 064204 (2009).
- [3] A. Meyer, S. Stüber, D. Holland-Moritz, O. Heinen, T. Unruh, Phys. Rev. B **77**, 092201 (2008).

## Slow dynamics and fragile-to-strong transition in confined water and in aqueous solutions.

Paola Gallo\*

*Dipartimento di Fisica, Università Roma Tre,  
Via della Vasca Navale 84, I-00146 Rome, Italy*

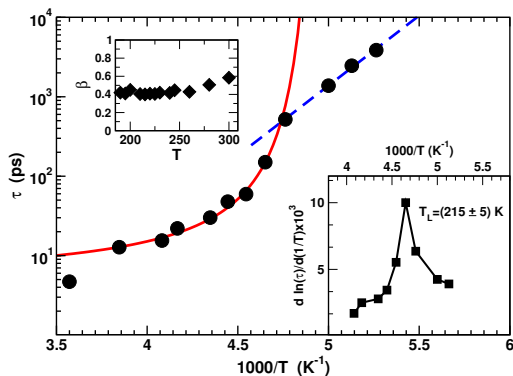


FIG. 1. Main frame: Arrhenius plot of the relaxation time of free water in MCM-41  $\tau$  as a function of  $1000/T$ . At high temperature, below 300 K, the points are fitted with the Vogel-Fulcher-Tamman formula (bold line)  $\tau = \tau_0^{VFT} \exp\left[\frac{BT_0}{T-T_0}\right]$  where  $B$  is the fragility parameter and  $T_0$  is an ideal glass transition temperature located below the experimental glass transition temperature  $T_g$ . The parameters extracted from the fit are  $B = 0.25$  and  $T_0 = 200$  K. At low temperature the fit is done with the Arrhenius function (long dashed line)  $\tau = \tau_0^A \exp[E_A/k_B T]$  where  $E_A$  is the activation energy. We find from our data an activation energy of  $E_A = 34$  kJ/mol. Lower inset: inverse temperature derivative of the logarithm of  $\tau$ . Upper inset:  $\beta$  values.

In the past years several theoretical and experimental studies have led to a picture according to which the anomalous properties of water might be due to the presence of a liquid-liquid phase transition in the supercooled region possibly terminating in a liquid-liquid critical point. On the other hand water also shows upon supercooling a behaviour typical of a glass former approaching the Mode Coupling Theory (MCT) crossover temperature,  $T_C$ . Above  $T_C$  the dynamics of water is that typical of a fragile glass former and below  $T_C$  hopping processes mutate the behaviour of the liquid from fragile to that of a strong glass former.

I will show molecular dynamics simulations results of deeply supercooled water confined in a cylindrical pore of MCM-41 silica material [1, 2]. The dynamics is divided in that of free water (water in the center of the pore) and bound water (water close to the hydrophilic surface). A fragile to strong (FS) dynamic transition at  $T=215$  K is located for free water, see fig.1, analogous to what found in experiments on water in MCM-41 [3] and in simulation of the bulk [4]. The maximum found in the specific heat at the FS transition suggests that also for our system this tran-

sition is related to the crossing of the Widom line, indicating the presence a low density and high density liquid-liquid coexistence.

I will show that an FS transition can be also found in solvophobic solutions of Jagla water-like particles “mutatis mutandis” [6]. Also this transition is connected with the liquid-liquid critical point phenomenon. Therefore in water the Widom line appears to be the switching line for hopping.

In the last part of the presentation I will analyze the analogies between confined water and water in two aqueous solutions of disaccharides: maltose and trehalose. An MCT behaviour for free water is found in both solutions. Similar to water in MCM41, bound water does not follow MCT. Our analysis gives evidence that the main differences between the two disaccharides solutions occur in the dynamic behaviour of hydration water molecules, which have for trehalose a better affinity with that of water close to protein surface. Hence trehalose, with respect to maltose, would be able to slow down more consistently the hydration water dynamics and to create a dynamical environment more similar to that which is needed to maintain functional conformation of proteins.

All these studies point out that experiments and simulations in confined water and in solutions are extremely relevant for the comprehension of low temperature bulk properties, supporting the idea of a unified scenario for supercooled water encompassing dynamics and thermodynamics.

I wish to thank for the fruitful interactions the colleagues that have collaborated with me in the topics covered by this presentation: M. Rovere and S.-H. Chen for water in MCM-41, D. Corradini, S.V. Buldyrev and H.E. Stanley for the solutions of water and hard spheres and A. Magno for the aqueous solution of water and disaccharides.

\* Corresponding author: gallop@fis.uniroma3.it

- [1] P. Gallo, M. Rovere and S.-H. Chen, J. Phys. Chem. Lett. **1**, 729 (2010).
- [2] P. Gallo, M. Rovere and S.-H. Chen, J. Phys.: Condens. Matter **28**, 284102 (2010).
- [3] L. Liu, S.-H. Chen, A. Faraone, C.-W. Yen and C.-Y. Mou, Phys. Rev. Lett. **95**, 117802 (2005).
- [4] L. Xu, P. Kumar, S. V. Buldyrev, S.-H. Chen, P. H. Poole, F. Sciortino and H. E. Stanley, Proc. Natl. Acad. Sci. U.S.A. **102**, 16558 (2005).
- [5] P. Gallo, A. Magno and M. Rovere, in preparation (2010).
- [6] D. Corradini, S. Buldyrev, P. Gallo and H. E. Stanley, Phys. Rev. E **81**, 061504 (2010).

## Supercooled water dynamics near the resolution limit of neutron backscattering

Joachim Wuttke\*

Forschungszentrum Jülich, Jülich Centre for Neutron Science at FRM II,  
Lichtenbergstraße 1, 85747 Garching, Germany

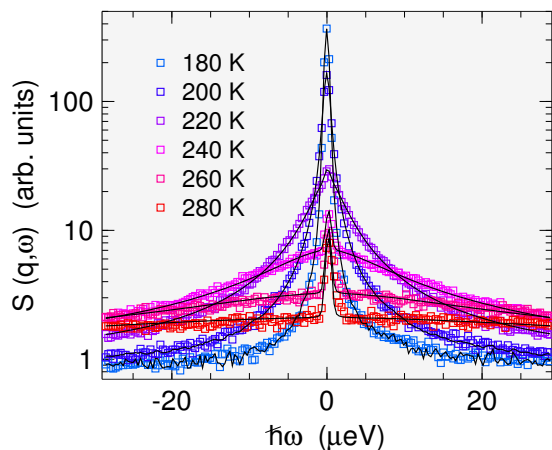


FIG. 1. Spectra of LiCl:7H<sub>2</sub>O for a wide temperature range, fitted by a KWW function, plus an elastic line to account for container scattering [5].

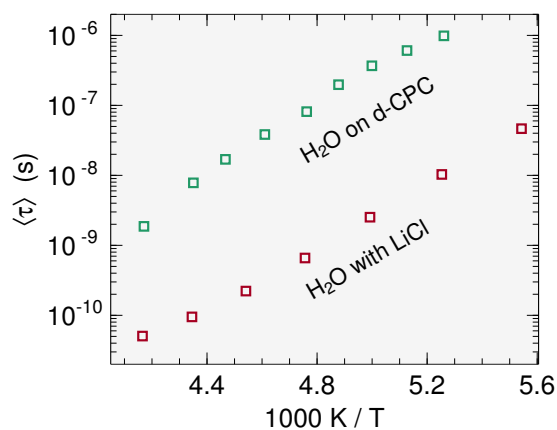


FIG. 2. Mean relaxation time of water on a deuterated protein (d-CPC) and in a salty solution [5].

Slow relaxation processes can be studied with unprecedented sensitivity at the new backscattering spectrometer SPHERES [1], which offers a signal-to-noise ratio of more than 1500:1.

An important topic, addressed by several user groups, is the dynamics of supercooled water. While bulk water inevitably crystallises, unlimited supercooling is possible in protein hydration water [2,3], in water confined to cracks and pores [4], and in certain salt solutions [5]. In a large variety of systems, low-temperature spectra can be described by an elastic delta line plus a quasielastic component approximated by a Kohlrausch-Williams-Watts function (Fig. 1).

Taking into account asymptotic degeneracies (elastic versus inelastic amplitude and inelastic amplitude versus relaxation time), and approximating the stretching exponent as temperature independent, the fits require an impressively low number of free parameters. If however the degeneracies are overlooked there is a high risk of producing artifacts. Specifically, we have argued [2] that a kink in  $\log \tau$  vs  $1/T$  observed in previous neutron backscattering experiments and attributed to a strong-to-fragile crossover [6] is an artifact from underdetermined fitting.

Comparing different systems, relaxation times are found to follow almost the same temperature dependence though absolute values differ by orders of magnitude (Fig. 2). This is clearly in contradiction with the idea that water in confined geometry is a proxy for bulk water, allowing investigations of the latter in the deeply supercooled state that is otherwise inaccessible because of crystallisation. Though the present experiments do not cover microscopic time scales, by extrapolating Fig. 2 it is obvious that the microscopic dynamics of water is substantially different in protein powder and in bulk solution. Furthermore, between 190 and 240 K, there is no kink, no cross-over, no critical point whatsoever in Fig. 2: the Widom line of supercooled bulk water [7] leaves no trace in the long-time dynamics of modified or confined water.

On the other hand, the results of Fig. 2 look perfectly consistent with a mode-coupling scenario: different microscopic dynamic can lead to similar, universal long-time behavior. I hope this will motivate theorists to address the microscopic dynamics of supercooled water in confined geometries in mode-coupling terms.

\* Corresponding author: j.wuttke@fz-juelich.de

- [1] [http://www.jcms.info/jcms\\_spheres](http://www.jcms.info/jcms_spheres)
- [2] W. Doster, S. Busch, A. M. Gaspar, M.-S. Appavou, J. Wuttke, H. Scheer, Phys. Rev. Lett. **104**, 098101 (2010).
- [3] F.-X. Gallat, M. Weik, J. Wuttke, to be published.
- [4] H.N. Bordallo, L.P. Aldridge, J. Wuttke, K. Fernando, W.K. Bertram, L. C. Pardo, Eur. Phys. J. Special Topics **189**, 197 (2010).
- [5] J. Wuttke, to be published.
- [6] S.-H. Chen, L. Liu, E. Fratini, P. Baglione, A. Faraone, E. Mamontov, Proc. Natl. Acad. Sci. USA **103**, 9012 (2006).
- [7] P. H. Poole, F. Sciortino, U. Essmann, H. E. Stanley, Nature **360**, 324 (1992).

## Hot Brownian Motion: When Big Beads Beat Bittie Beads

Klaus Kroy,<sup>1,\*</sup> Daniel Rings,<sup>1</sup> Dipanjan Charkaborty,<sup>1</sup> Markus Selmke,<sup>2</sup> and Frank Cichos<sup>2</sup>

<sup>1</sup>*Institut für Theoretische Physik, Universität Leipzig, Postfach 100920, 04009 Leipzig, Germany*

<sup>2</sup>*Institut für Experimentelle Physik 1, Universität Leipzig, Linnéstraße 5, 04103 Leipzig, Germany*

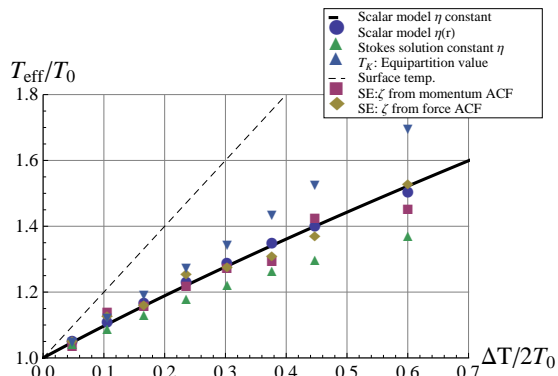


FIG. 1. (*Unpublished results.*) Preliminary data for the effective temperature  $T_{\text{HBM}}$  *i)* as predicted by the theory of hot Brownian motion (circles) and if the full temperature dependent function  $\eta(T)$  is replaced by a constant viscosity in our scalar model (line) and in the Stokes solution (upright triangles) and *ii)* from molecular dynamics simulations of a Lennard–Jones system using three different ways of extracting an effective temperature.

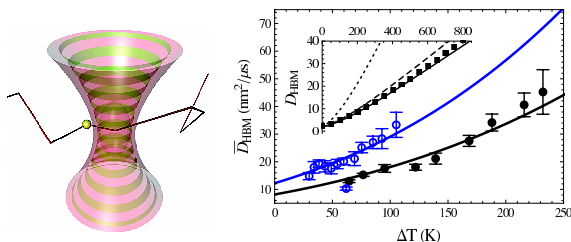


FIG. 2. *Left (quoted from Ref. [1]):* A nanoparticle diffusing through a laser focus. *Right (quoted from Ref. [2]):* The effective diffusion coefficient  $D_{\text{HBM}}(\Delta T)$  of hot gold nano-particles traversing a laser focus in water as a function of the temperature increase  $\Delta T$  at the particle surface with respect to the solvent at infinity (considerable overheating is possible [3]). Symbols represent our experimental data (open/closed for  $R = 40/60$  nm), the solid lines our analytical predictions. (For solvent and focus parameters and the error bars see Ref. [2]; the notation  $\bar{D}$  indicates that the theoretical predictions account for the inhomogeneous laser intensity in the focus.) The inset compares exact theoretical results for  $D_{\text{HBM}}(\Delta T)$  according to numerical predictions obtained with a differential shell method (squares) to two analytical approximations of increasing sophistication (dashed/solid), and the naive identification of the effective parameters of hot Brownian motion with the conditions at the particle surface (dotted).

While the isothermal Brownian motion of small particles in simple liquids is very well understood, little is known about the motion of particles that are considerably hotter than the ambient solvent. However, situations in which this occurs are abundant in the context of modern single-molecule techniques and nano-

technological and biomedical applications, for example, when a metal nanoparticle is trapped or tracked by (or simply diffusing through) a laser focus or deliberately heated during laser surgery.

We are studying this new phenomenon of non-equilibrium Brownian dynamics that we baptized “hot Brownian motion” (HBM) [2] by molecular dynamics simulations of a Lennard–Jones fluid (Fig. 1), analytically by fluctuating hydrodynamics (Fig. 2, lines), and by experiments with gold nanoparticles diffusing in a laser focus (Fig. 2, symbols with error bars). One of the main aims is to establish, via judicious coarse graining a practical effective Langevin description for heated nanoparticles in a simple solvent with a temperature-dependent viscosity. To derive the appropriate generalized Markovian Langevin equation we calculate the pertinent effective temperature and viscosity parameters  $T_{\text{HBM}}$  and  $\eta_{\text{HBM}}$  that map the problem onto that of a nanoparticle undergoing ordinary isothermal Brownian motion. The analytical results for the effective fluctuation-dissipation and Stokes-Einstein relations compare favorably with results from our molecular dynamics simulations and with measurements of laser-heated gold nano-particles as exemplified in Figs. 1 and 2. A particularly amusing finding is that, due to the non-monotonic Mie absorption coefficient of the nanoparticles, the diffusion coefficient can have a non-monotonic size dependence, including parameter regions where large particles diffuse substantially faster than small ones.

We are currently exploring the scope of our effective description of hot Brownian motion, and whether it can be extended to situations involving external potentials, interacting particles, shorter times (where memory effects come into play), and situations involving rotational Brownian motion, which is characterized by its own effective temperature and viscosity parameters, different from those for translational motion. Most importantly, we try to see whether the concept of  $T_{\text{HBM}}$  can be extended to account for the apparent “equipartition” temperature (triangles pointing downward in Fig. 1) given by the mean-square velocity, which turns out to be different from  $T_{\text{HBM}}$ .

*Acknowledgement:* DFG support via FOR 877.

\* Corresponding author: kroy@itp.uni-leipzig.de

- [1] R. Radünz, D. Rings, K. Kroy, and F. Cichos, J. Phys. Chem. A **113**, 1674 (2009).
- [2] D. Rings, R. Schachoff, M. Selmke, F. Cichos, and K. Kroy, Phys. Rev. Lett. **105**, 90604 (2010).
- [3] S. Merabia, S. Shenogin, L. Joly, P. Keblinski, and J.-L. Barrat, Proc. Natl. Acad. Sci. (USA) **106**, 15113 (2009)

## Predicting The Effective Temperature of a Glass

Nicoletta Gnan,<sup>1,\*</sup> Claudio Maggi,<sup>1</sup> Thomas B. Schröder,<sup>2</sup> and Jeppe C. Dyre<sup>2</sup>

<sup>1</sup>Dipartimento di Fisica, Università di Roma “La Sapienza”, I-00185, Roma, Italy

<sup>2</sup>DNRF Center “Glass and Time”, IMFUFA, Dept. of Sciences, Roskilde University, P.O. Box 260, DK-4000 Roskilde, Denmark

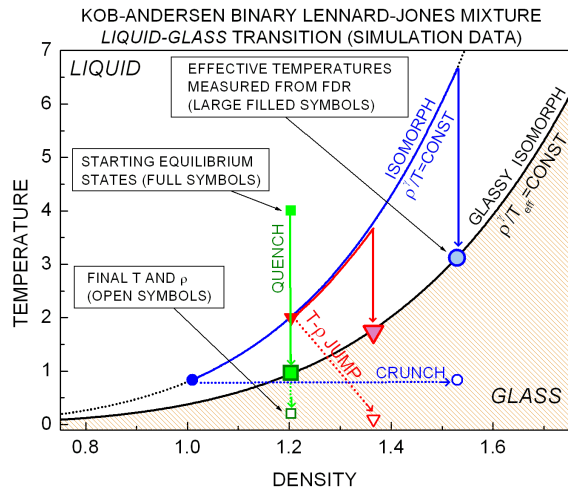


FIG. 1. Patterns followed by the KABLJ liquid in different off-equilibrium density and/or temperature jumps. Consider for example the case of a crunch (horizontal dotted line), where the system is densified at constant temperature. This transformation is equivalent to a quench (right-most vertical line) from an isomorph state point having the final density of the crunch. Thus the  $T_{\text{eff}}$  (filled circle) is identical for these transformations.

Condensed matter is frequently found in out-of-equilibrium states. For example, in systems like supercooled liquids, dense colloids, spin systems, etc., the (off-equilibrium) glassy state occurs naturally after cooling or compression from a state of thermal equilibrium. In these cases an *effective temperature* ( $T_{\text{eff}}$ ) can be introduced for describing the non-equilibrium properties of the glass [2].

In this work [3] we show the existence of a special class of liquids for which the aging behavior is simpler than other liquids. Only for these liquids, named “strongly correlating liquids” (SCLs) [4], the effective temperature calculated from the violation of the fluctuation-dissipation theorem (FDT) depends only on the final density (Fig. 1). Moreover for such liquids data from a single quench simulation provides enough information to predict the effective temperature of any glass produced by jumping from an equilibrium state (Fig. 2). Finally we find that the equation identifying the dynamic glass transition curve in the  $(T, \rho)$  plane defined by the effective temperature is an isomorph, i.e. a curve along which microscopic configurations of state points have proportional canonical probabilities [5].

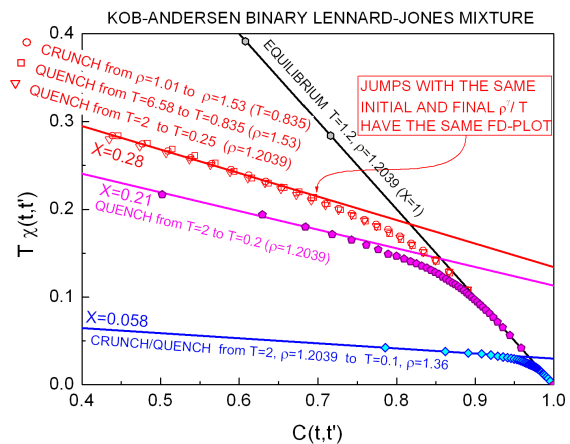


FIG. 2. Response vs. correlation function for several density/temperature jumps for the KABLJ system. The crunch ( $\circ$ ) overlaps very well with the quench ( $\square$ ) that takes the system from an initial state isomorph to the one of the crunch to the same final state. Note also the good superposition of the additional quench ( $\nabla$ ) that takes the system from a state isomorph to the initial state of ( $\circ$ ) to a state isomorph to the final one of ( $\circ$ ). Full lines have slopes predicted from the density scaling relation for  $T_{\text{eff}}$ , adjusted only by a vertical shift to fit the data.

We show that the effective temperature of an SCL naturally follows the density scaling relation  $\rho^\gamma/T_{\text{eff}} = \text{const}$ . These predictions are validated by simulations of the Kob-Andersen binary Lennard-Jones liquid and shown not to apply for the non-strongly correlating monatomic Lennard-Jones Gaussian liquid.

The center for viscous liquid dynamics *Glass and Time* is sponsored by the Danish National Research Foundation (DNRF).

\* Corresponding author: nicoletta.gnan@roma1.infn.it

- [1] R. Di Leonardo, L. Angelani, G. Parisi, and G. Ruocco, *Phys. Rev. Lett.* **84**, 6054 (2000).
- [2] A. Crisanti and R. Ritort, *J. Phys. A* **36**, R181 (2003).
- [3] N. Gnan, C. Maggi *et al.*, *Phys. Rev. Lett.* **104**, 125902 (2010).
- [4] U. R. Pedersen *et al.*, *Phys. Rev. Lett.* **100**, 015701 (2008); N. P. Bailey *et al.*, *J. Chem. Phys.* **129**, 184507 and 184508 (2008).
- [5] N. Gnan, T. B. Schröder, U. R. Pedersen, N. P. Bailey, and J. C. Dyre, *J. Chem. Phys.* **131**, 234504 (2009).
- [6] F. Sciortino and P. Tartaglia, *Phys. Rev. Lett.* **86**, 107 (2001).

## Incomplete Equilibration of Dense Hard-Sphere Fluids

M. Medina-Noyola,<sup>1,\*</sup> Pedro E. Ramírez-González,<sup>1</sup> Luis E. Sánchez-Díaz,<sup>1</sup>  
G. Pérez-Ángel,<sup>2</sup> Rigoberto Juárez-Maldonado,<sup>3</sup> and Alejandro Vizcarra-Rendón<sup>3</sup>

<sup>1</sup>*Instituto de Física “Manuel Sandoval Vallarta”, Universidad Autónoma de San Luis Potosí,  
Álvaro Obregón 64, 78000 San Luis Potosí, SLP, México*

<sup>2</sup>*Departamento de Física Aplicada CINVESTAV-IPN,  
Unidad Mérida Apartado Postal 73 Cordemex 97310. Mérida, Yuc., Mexico*

<sup>3</sup>*Unidad Académica de Física, Universidad Autónoma de Zacatecas,  
Paseo la Bufa y Calzada Solidaridad, 98600, Zacatecas, Zac., Mexico*

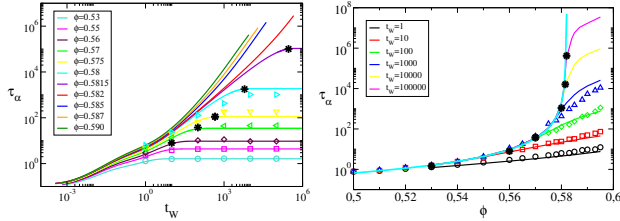


FIG. 1.  $\alpha$ -relaxation time  $\tau_\alpha(k; \phi, t_w)$  of a hard-sphere system (a) as a function of  $t_w$  at fixed volume fraction  $\phi$  and (b) as a function of  $\phi$  at fixed  $t_w$ , according to the NE-SCGLE theory (solid lines) and to the MD simulations (symbols). The asterisks in (a) highlight the points  $(t_w^{eq}(\phi), \tau_\alpha^{eq}(k; \phi))$ , whereas the asterisks in (b) indicate the predicted crossover volume fraction  $\phi^{(c)}(t_w)$  corresponding to the various waiting times.

The self-consistent generalized Langevin equation (SCGLE) theory of colloid dynamics and dynamic arrest [1] has recently been extended [2] to describe the irreversible evolution of the static structure factor and of the intermediate scattering function of a liquid in response to changes in the macroscopic control parameters such as the temperature or density. Here we present the application of the resulting non-equilibrium theory (“NE-SCGLE”) to the description of the slow dynamics of incompletely equilibrated glass-forming liquids.

For this, we consider the spontaneous isochoric equilibration of a hard-sphere fluid after it was prepared in a non-equilibrium state with the desired volume fraction  $\phi$  but with a prescribed *non-equilibrium* static structure factor  $S_0(k; \phi)$ , different from the equilibrium structure factor  $S_{eq}(k; \phi)$ . The predicted evolution of the  $\alpha$ -relaxation time  $\tau_\alpha(k; \phi, t_w)$  and of the long-time self-diffusion coefficient  $D_L(\phi, t_w)$  as a function of the evolution time  $t_w$  is then calculated for an array of volume fractions, and the results for  $\tau_\alpha$  are illustrated in Fig.1(a). These plots indicate that  $\tau_\alpha(k; \phi, t_w)$  reaches its equilibrium value  $\tau_\alpha^{eq}(k; \phi)$  only after an *equilibration* waiting time  $t_w^{eq}(\phi)$ , always longer than  $\tau_\alpha^{eq}(k; \phi)$  itself, and that both characteristic times increase strongly with  $\phi$ .

On the other hand, for a given waiting time the plot of  $\tau_\alpha(k; \phi, t_w)$  as a function of  $\phi$  exhibits two regimes corresponding to samples that have fully equilibrated within this waiting time ( $\phi < \phi^{(c)}(t_w)$ ) and to samples for which equilibration is not yet complete

( $\phi > \phi^{(c)}(t_w)$ ) (Fig. 1(b)). The crossover volume fraction  $\phi^{(c)}(t_w)$  first increases rather fast with  $t_w$ , but then saturates asymptotically to the dynamic arrest volume fraction  $\phi^{(a)}$  predicted by the equilibrium SCGLE theory [1].

In this presentation we also show that this two-regime scenario is also observed in the results of the corresponding molecular dynamics (MD) simulation experiment [3] (represented by the symbols in the figure). These simulations determine, in particular, the volume fraction dependence of the *equilibrium*  $\alpha$ -relaxation time  $\tau_\alpha^{eq}(k; \phi)$  within the window  $0 \leq \phi \leq \phi^{(c)}(t_w^{max})$ , where  $t_w^{max}$  is the maximum waiting time achieved in the simulation experiment (in our case  $t_w^{max} = 10^5$ , yielding  $\phi^{(c)}(t_w^{max}) \approx 0.58$ ). The corresponding results can be fitted with the *full numerical solution* of the *equilibrium* SCGLE theory, adapted to Newtonian liquids (Eqs. (1), (2), and (5-8) of Ref [1] with  $D^0 = \sqrt{\pi}/16\phi$ , and with  $k_c = 8.4823$  adjusted to fit these equilibrium data). According to this fit (cyan solid line in Fig. 1(b)),  $\tau_\alpha^{eq}(k; \phi)$  diverges at  $\phi^{(a)} \approx 0.582$ . We discuss the possible implications of these theoretical predictions, regarding a possible alternative interpretation of the experimental results of Brambilla et al. [4].

Finally, in this presentation we show that a similar scenario is predicted to occur in soft-sphere systems when the  $\alpha$ -relaxation time  $\tau_\alpha(k)$  and the long-time self-diffusion coefficient  $D_L$  are plotted as a function of the pressure or of the inverse temperature [5].

This work was supported by the Consejo Nacional de Ciencia y Tecnología (CONACYT, México), through grant No. 84076 and CB-2006-C01-60064, and by Fondo Mixto CONACyT-SLP through grant FMSLP-2008-C02-107543.

\* Corresponding author: medina@ifisica.uaslp.mx

- [1] R. Juárez-Maldonado *et al.*, Phys. Rev. E **76**, 062502 (2007).
- [2] P. Ramírez-González and M. Medina-Noyola, J. Phys.: Condens. Matter **21** (2009) 504103; *ibid.* arXiv:1011.4023v1 [cond-mat.soft]; *ibid.* arXiv:1011.4025v1 [cond-mat.soft].
- [3] G. Pérez-Ángel *et al.*, arXiv:1011.4030v1 [cond-mat.soft].
- [4] G. Brambilla *et al.* Phys. Rev. Lett. **102** (2009) 085703.
- [5] P. Ramírez-González and M. Medina-Noyola, manuscript in preparation.

## Ratchet effect in an aging glass

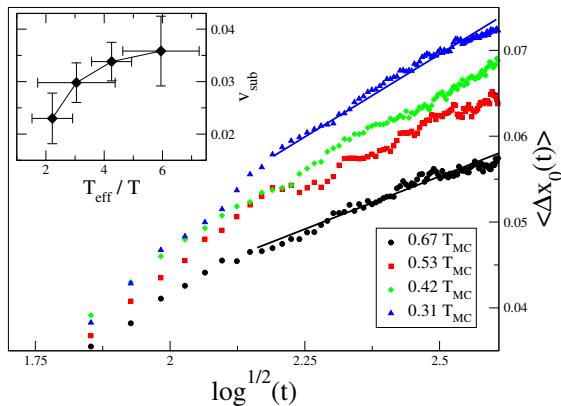
Dario Villamaina,<sup>1,\*</sup> Giacomo Gradenigo,<sup>1</sup> Alessandro Sarracino,<sup>1</sup> Tomas S. Grigera,<sup>2</sup> and Andrea Puglisi<sup>1</sup><sup>1</sup> CNR-ISC and Dipartimento di Fisica, Università di Roma “La Sapienza”, p.le A. Moro 2, 00185, Roma, Italy<sup>2</sup> Instituto de Investigaciones Fisicoquímicas Teóricas y Aplicadas (INIFTA), La Plata, Argentina

FIG. 1. (Color online) Main: Asymmetric intruder drift for different quench temperatures; linear fits yield sublinear velocities. Inset:  $v_{sub}$  versus  $T_{eff}/T$ .

In an irreversible environment, thermal fluctuations can be rectified in order to produce a directed current. After a few fundamental examples of historical and conceptual value, in the last twenty years a huge amount of devices and models—usually known as Brownian ratchets or motors—have been proposed. The necessary condition to obtain a ratchet is the simultaneous breaking of space and time-reversal symmetries. The time-reversal symmetry breaking is customarily obtained by coupling the system with reservoirs at two different temperatures: an asymmetric intruder in such a multi-temperature environment displays an average drift.

The present work, inspired from the latter scenarios with a continuous flow of energy in a non-thermalized medium, shows a study of the ratchet phenomenon in the aging dynamics of fragile glass-formers. In such a system the ratchet is formed by the asymmetric interaction of a single particle, the intruder, with all the other particles of the system. The two temperatures necessary to have an out-of-equilibrium environment are represented by the quench temperature  $T$  and the effective temperature  $T_{eff}$  of the still non-equilibrated modes of the aging glass former. In order to observe a directed motion we quenched the system well below its mode coupling temperature,  $T_{MC}$ , where the equilibration time exceeds the simulation time and an effective temperature  $T_{eff}$  can be defined and measured from the violation of the equilibrium fluctuation-dissipation relation. In this situation a net average drift is observed, see fig. 1, steady on a

logarithmic time-scale:

$$\langle \delta x(t) \rangle \sim \log^{1/2}(t) \quad (1)$$

The *subvelocity* of the intruder, defined as  $d\langle \delta x(t) \rangle/d\tau$  with  $\tau = \log^{1/2}(t)$ , grows when the ratio  $T_{eff}/T$  is increased, namely when the quench temperature is lowered: this corresponds to the general behavior of thermal ratchets in contact with two thermal reservoir.

The results of a similar experiment are presented also for an *asymmetric* version of the Sinai model, which describes the diffusion of an intruder through a random correlated potential. Its long-time dynamics is ruled by activated events and is characterized by a logarithmic time-scale: for this reasons it appears to be a well fitted candidate to reproduce the previous experiment in a more controlled setup. The numerical study of the *asymmetric* Sinai model shows a behavior in striking similarity with those of Fig. 1 for the glass-former model: a drift, still growing on a logarithmic time-scale, is observed only when both time reversal and spatial symmetry are broken. The comparison between the two models studied suggests that the non-equilibrium drift is mainly ruled by activated events and that the observed phenomenon is quite general and does not depend on the specific model.

In conclusion, through numerical simulations in different models and different choices of the quench temperature, always chosen in the deep slowly relaxing regime, we have given evidences of the existence of a “glassy ratchet” phenomenon. The drift velocity slowly decays in time and can be appreciably different from zero for at least three orders of magnitude in time. The overall intensity of the drift, measured in terms of a “sub-velocity”, is monotonically increasing with the distance from equilibrium, i.e. with the ratio  $T_{eff}/T$ . This observation supports the idea of regarding the ratchet drift as a “non-equilibrium thermometer”: it can be used as a device capable to say how far is a system from equilibrium. Recent theoretical and experimental advances in the study of functionalized or “patchy” particles [2] promise an experimental verification of our hypothesis in the near future.

The work of GG, AS, DV and AP is supported by the “Granular-Chaos” project, funded by Italian MIUR under the grant number RBID08Z9JE. TSG was partially supported by ANPCyT (Argentina).

\* Corresponding author: dario.villamaina@roma1.infn.it

[1] G. Gradenigo, A. Sarracino, D. Villamaina, T. S. Grigera and A. Puglisi, arXiv:1007.2090 (submitted to J. Stat. Phys)

[2] E. Bianchi, J. Largo, P. Tartaglia, E. Zaccarelli, F. Sciortino, PRL, **97**, 168301 (2006)

# Dynamics of Supercooled Colloidal Dispersions under Flow: A Study of Transient Regimes

M. Laurati,<sup>1,\*</sup> K. Mutch,<sup>1</sup> N. Koumakis,<sup>2</sup> G. Petekidis,<sup>2</sup> and S. U. Egelhaaf<sup>1</sup>

<sup>1</sup>*Soft Matter Laboratory, IPKM, Heinrich-Heine Universität Düsseldorf, Universitätstr. 1, 40225 Düsseldorf, Germany*

<sup>2</sup>*IESL-FORTH, Heraklion, Greece*

In the non-linear regime, application of shear to glassy and super-cooled colloidal dispersions induces yielding and flow. Under steady shear flow, the dynamics of these systems show an acceleration of the cage escape dynamics, with a structural relaxation time only controlled by the shear rate  $\dot{\gamma}$  [1, 2]. We recently started to investigate the regime which intercurrs between application of steady shear to a supercooled colloidal dispersion and the onset of steady flow. In rheology such a transient regime can be monitored in constant rate experiments. The stress evolution in these tests shows the appearance of an overshoot at intermediate strains before a steady stress value is achieved under flow (figure 1a, inset). The dynamics of such systems can be followed by confocal microscopy even during application of shear [1]. This data can then be analyzed as a function of waiting time  $t_w$ , i.e. at different times after switching on the shear field. At short times after shear application, the dynamics are characterized by super-diffusive behavior associated to cage-disruption, before at longer waiting times normal diffusion is established. This is clearly seen in the mean-squared displacements (MSD, figure 1a). Similar results were obtained by molecular dynamics (MD) simulations [3] and MCT calculations [3]. By combining experiments, MD simulations and a recent extension of mode-coupling theory (MCT) describing supercooled liquids and glasses under shear, we established, for a dense colloidal liquid and one shear rate, a clear connection between such dynamical behavior and the stress-overshoot observed in the stress-strain curves [3]. This study was recently extended, experimentally and by means of simulations, in order to investigate the influence of volume fraction and shear rate on these findings.

Furthermore, when the shear field keeping the system under flow is suddenly removed, glassy systems relax the accumulated stress. Such stress relaxation can be followed in rheological tests as a function of time (figure 1b, inset): For dense colloidal fluids stress is completely relaxed on a time scale comparable to the inverse shear rate. However, well inside the glass state and for Peclet numbers  $Pe < 1$ , the stress apparently does not fully relax to zero (figure 1b, inset). This suggests the existence of a frozen-in stress distinguishing the glass from the fluid state. The dynamics of the system during stress relaxation exhibits also a complex behavior: At short times after switching-off the shear field, a sub-diffusive regime is observed before the onset of long-time diffusion (figure 1b). At longer waiting times, the cage localizing particles starts to reform and eventually the equilibrium dynamics are re-

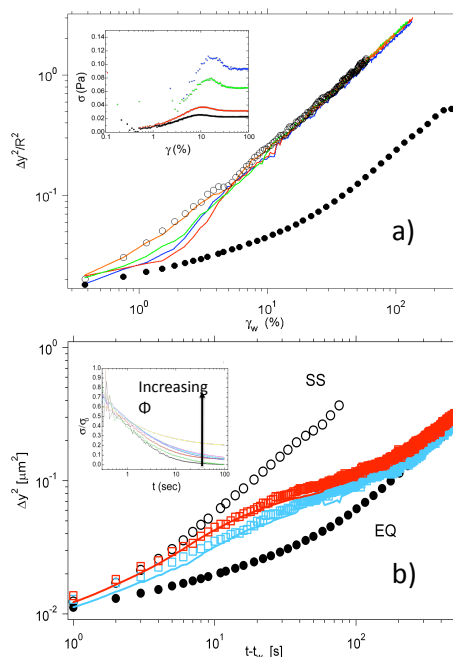


FIG. 1. a) Non-affine mean-squared displacements (MSD) of colloidal particles (radius  $R = 768$  nm) in the vorticity direction ( $y$ ) for a dense colloidal fluid (volume fraction  $\phi = 0.56$ ) sheared with  $Pe = 0.076$  at waiting times  $t_w = 0$  s (red), 4 s (blue), 30 s (green), 100 s (yellow). (●) Equilibrium MSD, (○) steady-state MSD under shear as determined by confocal microscopy. Inset: Step rate rheology experiments on a sample of smaller particles ( $R = 256$  nm), but same volume fraction and  $Pe = 0.076$  (black) and larger  $Pe$  values (bottom to top). b) MSDs for the same sample after cessation of shear flow, at  $t_w = 0$  s (red), 4 s (blue). Inset: Stress relaxation experiments on a sample of smaller particles ( $R = 256$  nm) and same  $Pe$ , for  $\phi = 0.56$  (black) and larger values (bottom to top).

covered. MCT calculations quantitatively reproduce the dynamical behavior (figure 1b) and qualitatively show agreement with rheological results (not shown).

We acknowledge support from DFG through the SFB TR6 network and the FOR1394 Research Unit.

\* Corresponding author: marco.laurati@uni-duesseldorf.de

- [1] R. Besseling, E.R. Weeks, A.B. Schofield and W.C.K. Poon, *Phys. Rev. Lett.* **99**, 028301 (2007).
- [2] F. Varnik, *J. Chem. Phys.* **125**, 164514, (2006).
- [3] J. Zausch, J. Horbach, M. Laurati, S.U. Egelhaaf, J.M. Brader, Th. Voigtmann and M. Fuchs, *J. Phys.: Condens. Matter* **20**, 404210 (2008).

## The relaxation of stresses in a glassforming soft-sphere mixture after the switch-off of shear

Jürgen Horbach<sup>1,\*</sup> and Jochen Zausch<sup>2</sup>

<sup>1</sup>*Institut für Materialphysik im Weltraum, Deutsches Zentrum für Luft- und Raumfahrt (DLR), 51170 Köln, Germany*

<sup>2</sup>*Institut für Physik, Johannes Gutenberg-Universität Mainz, Staudinger Weg 7, 55099 Mainz*

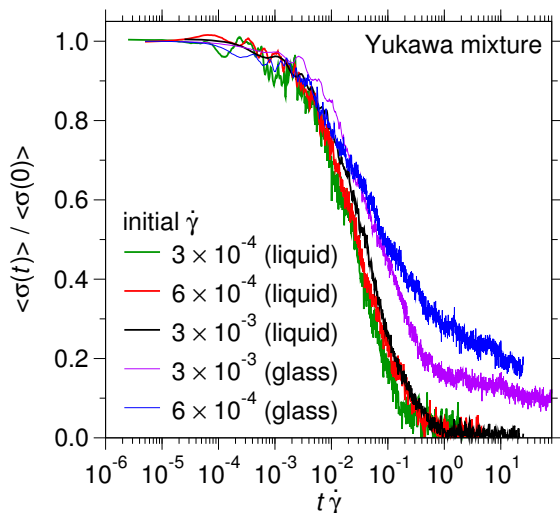


FIG. 1. Shear stress  $\langle \sigma(t) \rangle / \langle \sigma(0) \rangle$  as a function of  $t\dot{\gamma}$  after switching off shear in the steady state of a binary Yukawa mixture at the indicated shear rate  $\dot{\gamma}$ . The liquid and the glass state correspond to the temperatures  $T = 0.14$  and  $T = 0.05$ , respectively [2].

The rheological behavior of soft-glassy materials as well as of metallic glasses is of great technological importance and provides a rich phenomenology. If shear flow is imposed on a glassforming fluid at a constant shear rate  $\dot{\gamma}$ , a constant steady-state stress  $\sigma$  is built up that strongly affects relaxation processes in the fluid. An ubiquitous phenomenon is known as shear thinning, i.e. a decrease of the effective shear viscosity  $\eta_{\text{eff}} = \sigma / \dot{\gamma}$  with increasing  $\dot{\gamma}$ . Whereas for  $\dot{\gamma} \rightarrow 0$  the effective shear viscosity  $\eta_{\text{eff}}$  approaches the equilibrium shear viscosity  $\eta$ , in glassforming fluids  $\eta_{\text{eff}}$  can be orders of magnitude smaller than  $\eta$ .

To reveal non-linear phenomena such as shear thinning, it is crucial to understand the transition of a glassforming fluid from its quiescent state towards the final steady state flow [1] and, as recently shown [2], the relaxation of shear stress  $\sigma$  after switching off shear. In this contribution, we show that for the latter switch-off case the decay is qualitatively different above and below the glass transition temperature of the corresponding unsheared system.

To this end, molecular dynamics computer simulation of a binary AB mixture under shear were per-

formed. The particles interact via Yukawa potentials,  $V_{\alpha\beta}(r) = \varepsilon_{\alpha\beta} d_{\alpha\beta} \exp[-\kappa(r - d_{\alpha\beta})] / r$ , with  $r$  the distance between particles of type  $\alpha$  and  $\beta$  ( $\alpha, \beta = A, B$ ). The “particle diameters” are set to  $d_{AB} = 1.1 d_{AA}$ ,  $d_{BB} = 1.2 d_{AA}$ , the energy parameters to  $\varepsilon_{AB} = 1.4 \varepsilon_{AA}$ ,  $\varepsilon_{BB} = 2.0 \varepsilon_{AA}$ , and the screening parameter to  $\kappa_{AA} = \kappa_{BB} = \kappa_{AB} = 6/d_{AA}$ . For the masses,  $m_A = m_B = 1.0$  is chosen. The potentials are truncated at  $r_c^{\alpha\beta}$ , given by  $V_{\alpha\beta}(r_c^{\alpha\beta}) = 10^{-7} \varepsilon_{AA}$ .

The simulations were done for a 50:50 mixture of  $N = 2N_A = 2N_B = 1600$  particles, placed in a cubic simulation box of linear size  $L = 13.3 d_{AA}$  (corresponding to a density of  $\rho = 0.675 m_A / d_{AA}^3$ ). For the sheared system, we chose the  $x$  direction as the direction of shear and the  $y$  and  $z$  direction as the gradient and vorticity direction, respectively. Shear was imposed onto the system via modified periodic boundary conditions, the so-called Lees-Edwards boundary conditions. Both in equilibrium and under shear, the system is coupled to a dissipative particle dynamics (DPD) thermostat.

The systems were first evolved to a steady-state at different shear rates  $\dot{\gamma}$ . As starting configurations (i.e. before switching on shear) we used both fully equilibrated samples in the supercooled state at the temperature  $T = 0.14$  (corresponding approximately to critical mode coupling temperature of the system) and samples in the glass state at the temperature  $T = 0.05$ . Note that in the liquid state at  $T = 0.14$  the typical time scale of structural relaxation at equilibrium,  $\tau$ , exceeds the time scale  $1/\dot{\gamma}$  by a factor of 100-1000 in all considered cases. Fig. 1 shows the relaxation of shear stresses after suddenly switching off shear in the steady state. Whereas in the supercooled liquid a relatively fast decay on the time scale  $1/\dot{\gamma} \ll \tau$  is observed, a two step decay is seen for the glass states where the fast  $1/\dot{\gamma}$  decay is followed by a plateau. This peculiar behavior of the shear stresses is revealed by relating it to structural changes, mean-squared displacements and local fluctuations of stresses.

We acknowledge funding in the framework of the SFB TR 6 of the Deutsche Forschungsgemeinschaft (DFG).

\* Corresponding author: juergen.horbach@dlr.de

[1] J. Zausch, J. Horbach, M. Laurati, S. Egelhaaf, J. M. Brader, Th. Voigtmann, and M. Fuchs, *J. Phys.: Condens. Matter* **20**, 404120 (2008).

[2] J. Zausch and J. Horbach, *EPL* **88**, 60001 (2009).

## Nonlinear response of dense colloidal suspensions under oscillatory shear

J.M. Brader,<sup>1,\*</sup> M. Siebenbürger,<sup>2</sup> M. Ballauff,<sup>2</sup> K. Reinheimer,<sup>3</sup>  
M. Wilhelm,<sup>3</sup> S.J. Frey,<sup>4</sup> F. Weysser,<sup>5</sup> and M. Fuchs<sup>5</sup>

<sup>1</sup>Department of Physics, University of Fribourg, CH-1700 Fribourg, Switzerland

<sup>2</sup>Helmholtz Zentrum für Materialien und Energie, D-14109 Berlin, Germany

<sup>3</sup>Karlsruhe Institute of Technology, D-76128 Karlsruhe, Germany

<sup>4</sup>Institut Charles Sadron, Université de Strasbourg,  
CNRS UPR 22, 23 rue du Loess, 67034 Strasbourg, France

<sup>5</sup>Fachbereich Physik, Universität Konstanz, D-78457 Konstanz, Germany

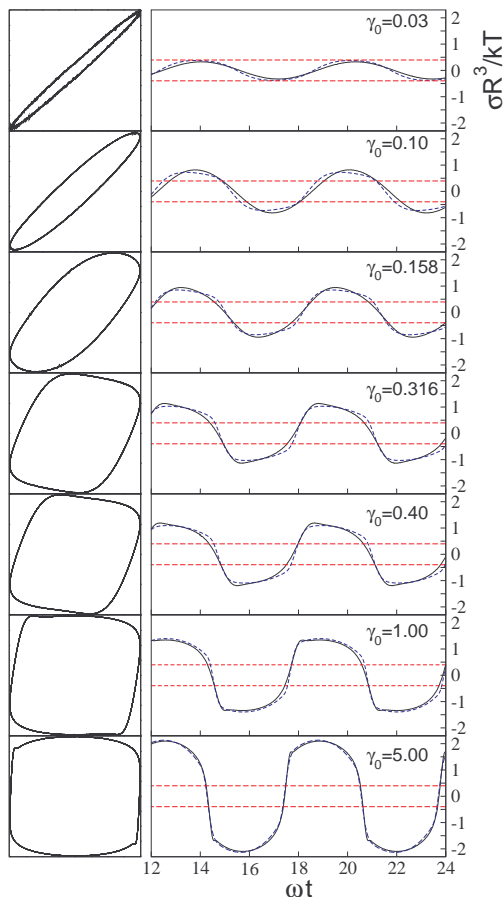


FIG. 1. The experimentally measured stress response to a shear strain  $\gamma(t) = \gamma_0 \sin(\omega t)$  (black line) and the associated Lissajous figures. The experiments are performed using PNIPAM particles at  $T = 15.1^\circ\text{C}$  (a glassy state) and at a frequency of  $1\text{Hz}$ . At  $\gamma_0 = 0.03$  the response is almost entirely elastic, emphasising the proximity of the quiescent state to the glass transition. At  $\gamma_0 = 5$  the system is almost purely viscous. The increase in dissipation with increasing  $\gamma_0$  is reflected in the increasing area enclosed by the closed Lissajous curves. The dynamic yield stress is indicated by the broken red lines.

Using a combination of theory, experiment and simulation we investigate the nonlinear response of dense colloidal suspensions to large amplitude oscillatory shear flow [1]. The time-dependent stress response is calculated using a recently developed schematic mode-coupling-type theory describing colloidal suspensions under externally applied flow [2]. For finite strain amplitudes the theory generates a nonlinear response, characterized by significant higher harmonic contributions. An important feature of the theory is the prediction of an ideal glass transition at sufficiently strong coupling, which is accompanied by the discontinuous appearance of a dynamic yield stress. For the oscillatory shear flow under consideration we find that the yield stress plays an important role in determining the non linearity of the time-dependent stress response. Our theoretical findings are strongly supported by both large amplitude oscillatory (LAOS) experiments (with FT-rheology analysis) on suspensions of thermosensitive core-shell particles dispersed in water and Brownian dynamics simulations performed on a two-dimensional binary hard-disc mixture. In particular, theory predicts nontrivial values of the exponents governing the final decay of the storage and loss moduli as a function of strain amplitude which are in good agreement with both simulation and experiment. A consistent set of parameters in the presented schematic model achieves to jointly describe linear moduli, nonlinear flow curves and large amplitude oscillatory spectroscopy.

\* Corresponding author: joseph.brader@unifr.fr

[1] J.M. Brader *et al.*, ArXiv:1010.2587 (2010).

[2] J.M. Brader, Th. Voigtmann, M. Fuchs, R.G. Larson and M.E. Cates, Proc. Natl. Acad. Sci. U.S.A. **106** 15186 (2009).

## Startup experiments of concentrated suspensions

Miriam Siebenbürger,<sup>1,\*</sup> M. Ballauff,<sup>1</sup> and Thomas Voigtmann<sup>2,3,4</sup>

<sup>1</sup>*Helmholtz-Zentrum für Materialien und Energie, 14109 Berlin, Germany*

<sup>2</sup>*Fachbereich Physik, Universität Konstanz, 78457 Konstanz, Germany*

<sup>3</sup>*Zukunftskolleg, Universität Konstanz, 78457 Konstanz, Germany*

<sup>4</sup>*Institut für Materialphysik im Weltraum, Deutsches Zentrum für Luft- und Raumfahrt (DLR), 51170 Köln, Germany*

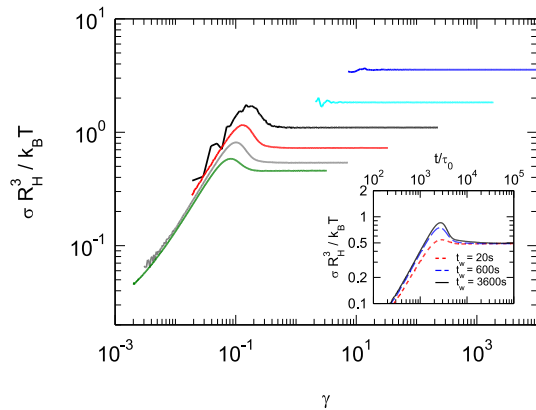


FIG. 1. Startup of shear. Reduced stress for a polydisperse suspension at  $\phi_{eff} = 0.65$  vs. the deformation  $\gamma = \dot{\gamma} \cdot t$ . The startup was performed at these Peclet numbers:  $Pe_0 = 4.03 \cdot 10^{-1}$  (dark blue),  $Pe_0 = 4.03 \cdot 10^{-2}$  (light blue),  $Pe_0 = 4.03 \cdot 10^{-3}$  (black),  $Pe_0 = 4.03 \cdot 10^{-4}$  (red),  $Pe_0 = 4.03 \cdot 10^{-5}$  (grey) and  $Pe_0 = 4.03 \cdot 10^{-6}$  (green). This measurements were performed after a pre-shear and a waiting time  $t_w = 600s$ . The inset shows the waiting time dependency at  $Pe_0 = 4.03 \cdot 10^{-5}$ .

A suspension of colloids, consisting of poly(styrene)-cores and thermosensitive poly(N-isopropylacrylamide)-shells in an aqueous  $0.05 \text{ mol L}^{-1}$  KCl solution, was investigated in the glassy state. The colloids show a sufficiently high polydispersity to suppress crystallization. The volume fraction of the glass transition was determined in a previous study [1] at  $\phi \approx 0.64$ .

The work focuses on the transient dynamics of startup of shear and stress. Startup experiments of shear at  $\phi = 0.65$  found a linear regime for small deformations, an stress overshoot for the yielding regime at  $\gamma \approx 0.1$  and the steady state shear rate at high deformations. This overshoot is connected with the super-diffusive dynamics during the yielding process [2]. It can be calculated by the microscopic model of the mode coupling theory (MCT), and was also found in simulations [2]. As can be seen by the inset of figure 1, the stress overshoot is aging dependent. It is found to increase in height with increasing waiting time after a pre-shear.

The second experiment, the startup of stress also called creep experiment, characterizes the material behavior and time dependent failure during load. Here a linear regime (with some residual oscillations) is found for small times (see figure 2). The yielding regime at  $\gamma \approx 0.1$  shows a strong ageing dependency as well. This was also found for multi-arm star polymers [3]. The creep experiment shows an ageing dependency during yielding as well, whereas in the complete shear molten state, the steady sheared state is independent in context of ageing.

\* Corresponding author: miriam.siebenbuerger@helmholtz-berlin.de

- [1] M. Siebenbürger, M. Fuchs, H. Winter, and M. Ballauff, *J. Rheol.* **53**, 707 (2009).
- [2] J. Zausch, J. Horbach, M. Laurati, S.U. Engelhaaf, J.M. Brader, Th. Voigtmann, and M. Fuchs, *J. Phys.: Condens. Matter* **20**, 404210 (2008).
- [3] C. Christopoulou, G. Petekidis, B. Erwin, M. Cloitre, and D. Vlassopoulos, *Phil. Trans. R. Soc. A* **A71**, 367 (2009).

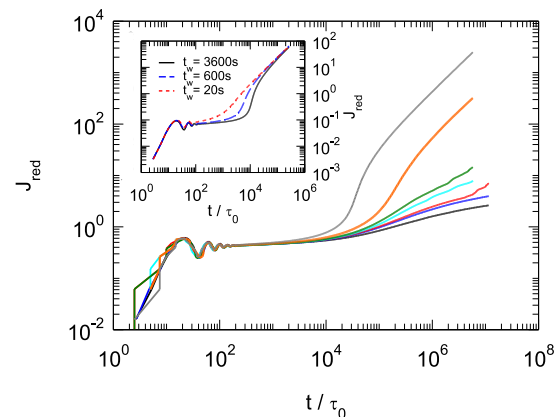


FIG. 2. Reduced creep compliance  $J_{red}$  for a polydisperse suspension at  $\phi_{eff} = 0.65$  vs. the reduced time  $t/\tau_0$ . The creep was performed at reduced shear stresses: 0.563 (grey), 0.469 (orange), 0.413 (green), 0.375 (light blue), 0.375 (red), 0.357 (dark blue) and 0.282 (black). This measurements were performed after a pre-shear and a waiting time  $t_w = 600s$ . The inset shows the waiting time dependency at a reduced shear stress of 0.912.

## A mixture of binary hard discs at the glass transition under shear

Joseph M. Brader,<sup>1</sup> Matthias Fuchs,<sup>1</sup> David Hajnal,<sup>2</sup> Matthias Krüger,<sup>1</sup>  
Rolf Schilling,<sup>2</sup> Thomas Voigtmann,<sup>1</sup> and Fabian Weysser<sup>1,\*</sup>

<sup>1</sup>Fachbereich Physik, Universität Konstanz, D-78457 Konstanz, Germany

<sup>2</sup>Institut für Physik, Johannes Gutenberg-Universität Mainz, D-550799 Mainz, Germany

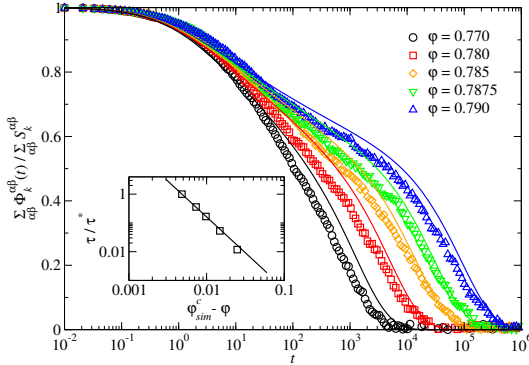


FIG. 1. MCT fits to a system of binary hard discs with radius ratio 1 : 1.4 and equal number concentrations. The inset shows the relaxation times obeying the power law  $\tau \sim |\phi - \phi^c|^{-\gamma}$  with predetermined  $\gamma = 2.4969$

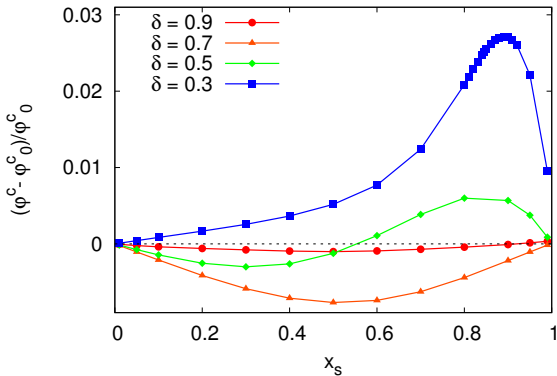


FIG. 2. Glass transition lines for different radius ratios  $\delta$  as a function of the concentration of small particles  $x_s$ . The glass is stabilized for small radius ratios while the liquid is stabilized for large radius ratios.

The glass transition in two dimensions is studied in detail by Brownian dynamics simulations of bidisperse hard discs. We investigate quiescent and steadily sheared states. An analysis for the quiescent system with the focus on the glass transition point and mixing effects is performed in the framework of mode coupling theory MCT for binary mixtures testing the predictions of Hajnal et. al. [1].

Fig. 1 shows a fit of MCT calculations to the coherent density correlation functions extracted from the simulation. Among other things we are able to verify two nontrivial mixing effects with our simulations: For small size disparities we confirm that increasing the concentration of small particles while keeping constant the total packing fraction results in a stabiliza-

tion of the glass. However for large size disparities we can confirm that increasing the concentration of small particles leads to a stabilization of the liquid (see Fig. 2).

Determining the MCT glass transition point to  $\phi^c \approx 0.795$  for a special system with radius ratio 1 : 1.4 and equal number concentrations we are able to deepen our analysis of the system when driven far from equilibrium by a steady shear flow. In the integration through transients approach (ITT) within MCT [2] microscopic calculations for two dimensional glass formers are feasible and lead to a quantitative comparison of static quantities like the distortion of the static structure factor and stress tensors [3].

Furthermore incoherent dynamic correlation functions are now accessible within MCT [4] and allow us to investigate super diffusive motion, for transient and stationary correlators.

Fig. 3 shows an MCT-ITT fit to the system from Fig. 1 under shear. Applying shear flow to a glassy state results in breaking the local structure and causing super diffusive particle motion at long times which can be understood within the framework of MCT-ITT.

\* Corresponding author: fabian.weysser@uni-konstanz.de

- [1] D. Hajnal, J. M. Brader, and R. Schilling, Phys. Rev. E **80**, 021503 (2009).
- [2] M. Fuchs and M. E Cates, J. Rheol. **53**, 957 (2009).
- [3] O. Henrich, F. Weysser, M. E. Cates, and M. Fuchs, Phil. Trans. R. Soc. A **367**, 5033 (2009).
- [4] M. Krüger, F. Weysser, and Th. Voigtmann, Phys. Rev. E **81**, 061506 (2010).

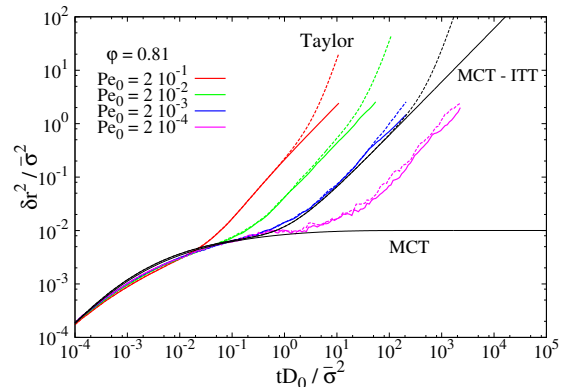


FIG. 3. MCT-ITT fits to mean squared displacements (solid in flow direction, dashed perpendicular to flow) of the system in Fig. 1 under shear and for a glassy state. The dimensionless Peclet number  $Pe_0 = \dot{\gamma}\sigma^2/D_0$  compares the shear rate to the dilute Brownian diffusion time.

## Active and Nonlinear Microrheology

Ch. J. Harrer,<sup>1,\*</sup> M. V. Gnann,<sup>1</sup> M. Fuchs,<sup>1</sup> and Th. Voigtmann<sup>1,2,3</sup>

<sup>1</sup>*Fachbereich Physik, Universität Konstanz, 78457 Konstanz, Germany*

<sup>2</sup>*Zukunftskolleg Universität Konstanz, 78457 Konstanz, Germany*

<sup>3</sup>*Institut für Materialphysik im Weltraum, Deutsches Zentrum für Luft- und Raumfahrt (DLR), 51170 Köln, Germany*

Active microrheology is a new method to probe viscous and elastic properties of complex fluids. By using a tracer particle that is driven by external means such as laser tweezers or magnetic forces it is possible to obtain information on the local rheological properties of the host liquid. This technique allows to probe the response in the nonequilibrium and usually nonlinear regime on multiple length scales. Due to its local character it can shed additional light on the microscopic mechanisms governing the dynamics in dense liquids - provided it is properly analysed.

In our work we focus on a theoretical description of constant-forcing active microrheology of colloidal glass formers. One quantity of interest is the microscopic friction coefficient  $\zeta(F^{ex})$ , which relates the steady-state velocity of the tracer particle to the applied force.

$$\zeta \langle \vec{v} \rangle_{t \rightarrow \infty} = \vec{F}^{ex} \quad (1)$$

The force dependence of this quantity is found to be highly nonlinear in experiments as well as in simulations. The well understood linear response regime at small forces is followed by a decrease of  $\zeta(F^{ex})$  by many orders of magnitude within a narrow window of the force. At high forces a second plateau is found. Within the mode coupling picture of the glass transition the decline in the friction coefficient can be considered as a force induced breaking of transient cages hindering the motion of the tracer particle before they can open up due to structural relaxation. In a glassy state the cages are permanent, so that in this case the deformation and finally the breaking of them introduces a delocalization transition by local melting. Both cases are strongly connected as the strength of the cages sets a scale for the relevant force.

By means of the integration through transients (ITT) formalism we derive a formally exact, generalized nonequilibrium Green-Kubo relation for  $\Delta\zeta(F^{ex})$ . Applying approximations in the spirit of mode coupling theory it can be expressed through fluctuations  $\phi_{\mathbf{q}}^s(t)$  and  $\phi_{\mathbf{q}}$  of the tracer and the bath particle densities [1].

$$\Delta\zeta = \frac{1}{144\pi^2\varphi} \int_0^\infty dt \int d\mathbf{k} \frac{k^2 S_k^s}{S_k} \phi_{-\mathbf{k}}(t) \phi_{\mathbf{k}}^s(t) \quad (2)$$

For the correlation functions we derive and solve numerically schematic [2] as well as microscopic [1] mode coupling equations. They have a fully microscopic foundation as they are based on the Smoluchowski

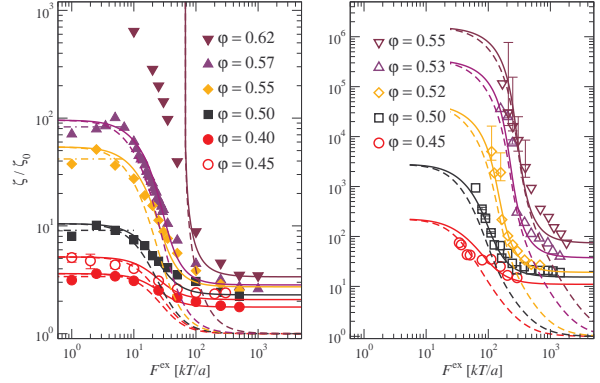


FIG. 1. Dependence of the microscopic friction on the external force in simulation (left) and experiment (right). Dashed lines are fits with a simple schematic model, solid lines with an improved schematic model taking the anisotropic nature of the fluctuations into account. Plots taken from [2].

equation and only require the equilibrium static structure factor as an input. This allows us to examine various properties of the system under consideration, e.g. one can pose the question how the local structure of the liquid does deform in response to the single-particle forcing. As the force breaks the rotational symmetry fluctuations are strongly anisotropic. The influence of fluctuations in different directions on the microscopic friction can be inspected. For host materials that are in a glassy state the nature of the delocalization transition is analysed. The details of the local melting and values for the critical force needed to delocalize the particle can be obtained. By varying the size of the tracer particle one can get even more detailed information on the microscopic processes. Finally the question of the connection between the micro-rheological and the macro-rheological properties which is important for the interpretation of micro-rheological experiments can be addressed.

This work has been supported by the Deutsche Forschungsgemeinschaft Transregio-SFB TR6.

\* Corresponding author: christian.harrer@uni-konstanz.de

- [1] I. Gazuz, A. M. Puertas, Th. Voigtmann, and M. Fuchs, Phys. Rev. Lett. **102**, 248302 (2009).
- [2] M. V. Gnann, I. Gazuz, A. M. Puertas, M. Fuchs, and Th. Voigtmann, Soft Matter **7**, 1390 (2011).

## Flow of soft jammed materials – linking global flow to local properties

Pinaki Chaudhuri,<sup>1,\*</sup> Pierre Jop,<sup>2</sup> Annie Colin,<sup>2</sup> Ludovic Berthier,<sup>3</sup> and Lyderic Bocquet<sup>1</sup>

<sup>1</sup>*Laboratoire de Physique de la Matière Condensée et Nanostructures,  
Université Claude Bernard Lyon 1, Villeurbanne, France*

<sup>2</sup>*Rhodia Laboratoire du Futur, Unité mixte Rhodia-CNRS, Université Bordeaux I, Bordeaux, France*

<sup>3</sup>*Laboratoire Colloides, Verres et Nanomatériaux,  
Université de Montpellier II, Montpellier, France*

Amorphous materials are ubiquitous in nature as well as in industrial applications. A characteristic property of these systems is that they flow only when the externally applied stress exceeds a threshold, which becomes useful in designing materials. Therefore, it is necessary to develop a complete description of how flow is initiated and sustained in these systems. A wide range of experiments and numerical simulations have revealed that, in these glassy materials, flow builds up via the occurrence of local structural rearrangements. However, the physical link between these local events and the observed macroscopic rheology, is still missing.

Recent theoretical studies have predicted that these structural rearrangements are spatially correlated - one event triggers another in its neighbourhood and this cascades on for flow to develop, with the local viscosity being the key parameter characterizing the dynamical state. Further, it has been predicted that the lengthscale for this co-operative dynamics is related to the strength of the externally applied stress, diverging as the yielding point is approached from higher stress values. Using numerical simulations and experiments, we investigate this flow scenario [1].

Our experimental system consists of a polydisperse emulsion, whose flow is observed using confocal microscopy. In numerical simulations, we study the flow of polydisperse harmonic disks, a model jammed system. In both experiments and simulations, we use the Poiseuille geometry, within which a wide range of local strain rates can be accessed. In our setups, we are able to follow the trajectory of the particles, and therefore we can identify and count the events of structural rearrangements. Our measurements show that the local viscosity is directly related to the rate of

these local events. We also observe a scaling behaviour between local velocity fluctuations and the local viscosity. Thus, we are able to demonstrate the link between the microscopic dynamical fluctuations and macroscopic rheology. Further, we quantify the cooperative dynamics among the particles and demonstrate that the flow gets increasingly correlated and heterogeneous with decreasing strain rate, in agreement with theoretical predictions.

In pursuance of studying the appearance of heterogeneities in flow, we address another puzzling question in this domain - the formation of shear bands, i.e the existence of coexisting regions of varying viscosities, during the flow of glassy systems. Such macroscopic features have been observed in a range of amorphous materials, from metallic glasses to gels. However, there is no consistent understanding of how these heterogeneities develop and sustain and how they are related to microscopic properties. In a two-dimensional planar Couette geometry, using numerical simulations, we study the change in the macroscopic features of the flow of soft particles, by tuning the interparticle interactions. We demonstrate that shear bands are more likely to occur as the applied strain rate is decreased, and this effect is further enhanced by the inclusion of attractive forces among the particles. Our observations are in agreement with a range of recent experiments.

We acknowledge funding from ANR SYSCOM.

\* Corresponding author: pinaki@thph.uni-duesseldorf.de

[1] P. Jop, P. Chaudhuri, A. Colin, L. Bocquet, submitted (2010).

## Shear banding and flow-concentration coupling in colloidal glasses

R. Besseling,<sup>1,\*</sup> L. Isa,<sup>1</sup> P. Ballesta,<sup>2</sup> G. Petekidis,<sup>2</sup> M. E. Cates,<sup>1</sup> and W. C. K. Poon<sup>1</sup>

<sup>1</sup>*SUPA, School of Physics & Astronomy, The University of Edinburgh, Kings Buildings, Mayfield Road, Edinburgh EH9 3JZ, United Kingdom.*

<sup>2</sup>*IESL-FORTH and Department of Materials Science and Technology, University of Crete, Heraklion 71110, Crete, Greece*

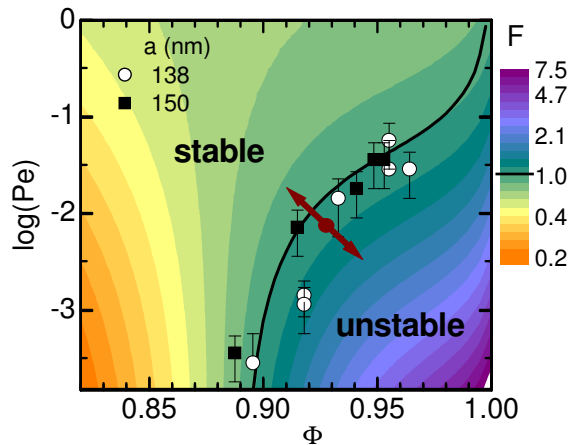


FIG. 1. Flow-stability of concentrated hard-sphere colloids versus reduced concentration  $\Phi$ . Symbols: experimental data of the reduced critical flow rate  $Pe_c$  below which shear banding occurs. Line: theoretical prediction for  $Pe_c(\Phi)$  based on Eq. (1). Colors show the value of  $F$ . The arrow shows a possible evolution of an unstable state.

Shear banding is widespread in the flow of glassy materials, including metallic glasses, pastes, gels and emulsions. It is known that banding is closely linked to the nonlinear flow and yielding properties of these systems, but experiments and theory have given conflicting pictures on its origin and possible universality, in particular for soft glasses. Two main mechanisms that have been proposed are (i) mechanical instability due to positive feedback between flow and structural breakup [1] and (ii) cooperative effects where local plastic events enhance the fluidity of the system over a characteristic length [2]. Yet various simulations and experiments can not be explained in these terms.

Here we show by experiment and theory that concentrated hard-sphere (HS) colloids, a well know soft-glassy model system, can exhibit a new type of shear banding caused by an instability due to shear-concentration coupling (SCC) [3]. In this scenario, the combined effect of a shear induced increase in pres-

sure  $\Pi$ -spatial gradients in which cause concentration variations- and the strong concentration dependence of the nonlinear viscosity, can amplify concentration fluctuations during flow. This can lead to spatially non-uniform shear and, close to the yield stress, strong shear localization.

We performed rheology and simultaneous flow-imaging experiments on glassy HS suspensions which show precisely this behavior. Below a characteristic shear rate  $\dot{\gamma}_c$  and for concentrations  $\Phi = \phi/\phi_{rcp} \gtrsim 0.9$  (with  $\phi_{rcp}$  the random close packing value) we observe increasingly nonlinear velocity profiles developing into strongly localized flow near yielding. Furthermore, the characteristic rate  $\dot{\gamma}_c$  grows rapidly with  $\Phi$ . This is illustrated in Fig. 1, which shows experimental results for the characteristic Pelet number  $Pe_c = \dot{\gamma}_c \tau_B$  (with  $\tau_B$  the Brownian time) below which shear banding sets in.

We have developed a theory, starting from the work in [3] on SCC-induced flow instability for non-linear fluids, which successfully describes this behavior. The flow stability is determined by the concentration ( $\sim \Phi$ ) and shear rate ( $\sim Pe$ ) dependence of the shear stress  $\sigma$  and the pressure  $\Pi$ . The system is linearly unstable to growth of concentration fluctuations when:

$$F \equiv \frac{\partial_{Pe} \Pi}{\partial_{\Phi} \Pi} \frac{\partial_{\Phi} \sigma}{\partial_{Pe} \sigma} > 1. \quad (1)$$

The line and color scale in Fig. 1 show our theoretical prediction based on Eq. (1), using the strongly nonlinear Herschel-Bulkley type constitutive relations for  $\Pi$  and  $\sigma$  appropriate for HS glasses [4]. The theory shows convincing agreement with the experimental data.

\* Corresponding author: rbesseli@ph.ed.ac.uk

- [1] P. Moller *et al.*, Phys. Rev. E **77**, 041507 (2008); G. Picard *et al.*, Phys. Rev. E **66**, 051501 (2002); S. M. Fielding *et al.*, Soft Matter **5**, 2378 (2009).  
 [2] L. Bocquet *et al.*, Phys. Rev. Lett. **103**, 036001 (2009).  
 [3] V. Schmitt *et al.*, Phys. Rev. E **52**, 4009 (1995).  
 [4] R. Besseling *et al.*, arXiv:1009.1579 (2010).

# Facilitation effects in supercooled liquids as a key ingredient for the dynamics

Andreas Heuer,\* Christian Rehwald, Oliver Rubner, and Carsten Schroeer

*Institute of Physical Chemistry, Westfälische Wilhelms-Universität Münster, 48149 Münster, Germany*

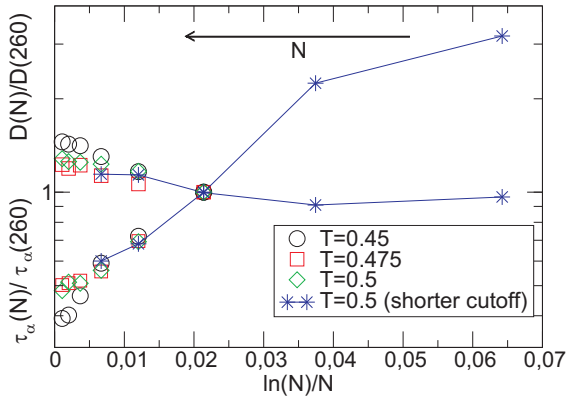


FIG. 1. The size-dependence ( $N = 65, 130, 260, \dots, 8320$ ) of the diffusion constant  $D$  (open symbols) and the structural relaxation time  $\tau_\alpha$  (filled symbols) in relation to its value for  $N = 260$ . Whereas the diffusion constant only displays very minor finite size effects, dramatic effects are observed for the structural relaxation time.

When cooling a glass-forming system many fascinating features such as the emergence of dynamic length scales occur. Many different models have been suggested to characterize the dynamics. These models (e.g. the kinetically constrained models (KCMs) [1] or the mosaic approach [2]) strongly vary with respect to the choice of the elementary subsystems as well as their mutual coupling. Whereas in the KCMs the whole physics is embedded in the facilitation rules and the elementary subsystems are just single spins, in the mosaic approach the elementary subsystems are defined via thermodynamic arguments and the coupling between mosaics is mainly taken into account in a simple mean-field sense [2].

Previously, we have identified the elementary subsystems and characterized them via the potential energy landscape [3]. In this contribution we analyze the facilitation or dynamic coupling effects between different subsystems. In a first step we analyze finite-size effects [4]. By increasing the system size beyond the elementary size the dynamic coupling effects become relevant. Whereas the diffusivity does not display any relevant finite-size effects, an effect of nearly one order of magnitude is observed for the structural relaxation time (Fig.1). Together with other characteristics of the finite-size effects a minimum model for facilitation effects is formulated which can reproduce all these observations. In contrast to the KCMs the elementary subsystem already contain important information about the thermodynamics and the dynamics of the system and one does not need different coupling

rules for strong and fragile systems. Furthermore, we show the corresponding results for the non-linear response and discuss the results in the context of the underlying physical mechanisms.

In a second step we analyze the dynamic coupling on a more microscopic level. Starting from a non-equilibrium configuration with extremely low mobility we study the effect of one local relaxation process and observe how it triggers other relaxation processes. Without a causal relation between different relaxation processes they would display a spatially homogeneous distribution. However, as shown in Fig.2, one observes a very strong distance-dependence from the location of the initial relaxation processes. The closer regions are significantly more mobile. Thus, beyond the finite-size effects we have a second route to characterize the nature of the facilitation effects.

Finally, we investigate our model predictions for the temperature dependence of (i) the degree of non-exponentiality, (ii) the dynamic length scales, and (iii) the violation of the Stokes-Einstein relation.

We acknowledge support by the DFG within FOR 1394 and SFB 458.

\* Corresponding author: andheuer@uni-muenster.de

- [1] Y.J. Jung, J. P. Garrahan, and D. Chandler, Phys. Rev. E **69**, 061205 (2004).
- [2] X. Xia and P.G. Wolynes, Phys. Rev. Lett. **86**, 5526 (2001).
- [3] A. Heuer, J. Phys. Condens. Matter **20**, 373101 (2008).
- [4] C. Rehwald, O. Rubner, and A. Heuer, Phys. Rev. Lett. **105**, 117801 (2010).

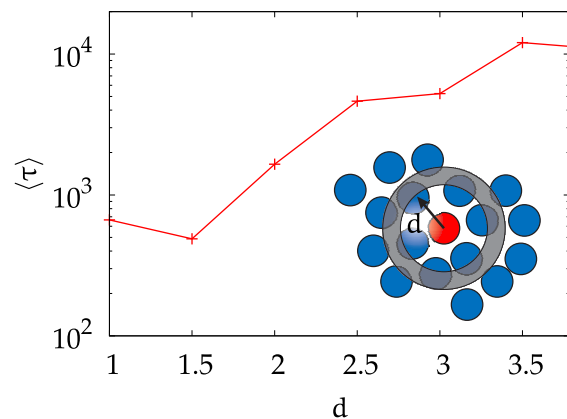


FIG. 2. The average first relaxation processes in a distance  $d$  of the initial relaxation process (location of the red particle) in a slow non-equilibrium system. The  $d$ -dependence of  $\langle \tau \rangle$  is a direct indication of causal facilitation processes.

## Cooperatively rearranging regions and their interfaces close to the glass transition

Paolo Verrocchio,<sup>1,2,\*</sup> Andrea Cavagna,<sup>3,4</sup> and Tomás S. Grigera<sup>5,6</sup>

<sup>1</sup>*Dipartimento di Fisica, Università di Trento, via Sommarive 14, 38050 Povo, Trento, Italy*

<sup>2</sup>*Istituto Sistemi Complessi (ISC-CNR), Via dei Taurini 19, 00185 Roma, Italy*

<sup>3</sup>*Istituto Sistemi Complessi (ISC-CNR), UOS Sapienza, Via dei Taurini 19, 00185 Roma, Italy*

<sup>4</sup>*Dipartimento di Fisica, Università "Sapienza", P.le Aldo Moro 2, 00185 Roma, Italy*

<sup>5</sup>*Instituto de Investigaciones Fisicoquímicas Teóricas y Aplicadas (INIFTA) and Departamento de Física, Facultad de Ciencias Exactas, Universidad Nacional de La Plata, c.c. 16, suc. 4, 1900 La Plata, Argentina*

<sup>6</sup>*CCT La Plata, Consejo Nacional de Investigaciones Científicas y Técnicas, Argentina*

It is common wisdom that the spectacular slowing down of supercooled liquids at low temperature is caused by the growth of a correlation length of some sort. The underlying idea is that of cooperativity: at lower temperatures, larger numbers of particles must move together in order to fully relax. Those cooperatively rearranging regions (CRRs), though, are hard to detect, as no obvious domain or structure can be observed. Recently, some progress has been achieved by using amorphous boundary conditions (ABC) [1–3], which exploits a fundamental idea of statistical mechanics, namely that thermodynamic states may be selected using appropriate boundary conditions. Within the framework of glass-forming liquids the method goes as follows [1]. Consider a low temperature equilibrium configuration of a liquid and freeze all particles outside a certain region. This region (or cavity) is then let free to evolve and thermalize, subject to the pinning field produced by all the frozen particles surrounding it. Clearly, the smaller the region the stronger the effect of the pinning field, hence keeping the region in a very restricted portion of its own phase space. The idea, then, is to check how large the region must be to emancipate from the boundary conditions, *i.e.* to restore ergodicity and thermalize into a state which has nothing to do with the surrounding one. The advantage of this method is that the system chooses its own definition of ‘order’ by means of the amorphous boundary conditions, and we do not need to have any *a priori* knowledge of the nature of such order. It turns out that the correlation between the original region’s configuration (that of the frozen surrounding) and that achieved after the region has equilibrated subject to the amorphous boundary conditions decays over a length-scale,  $\xi$ , which increases on lowering the temperature  $T$ .

Here we shall present recent numeric results as obtained using ABC with two different geometries of the cavity.

**Spherical geometry.** By studying the relaxation time  $\tau$  within a sphere of radius  $R$  we find that:

$$T \log \tau(R) \sim \begin{cases} R^\psi & \text{for } R < \xi, \\ \xi^\psi & \text{for } R > \xi, \end{cases} \quad (1)$$

This seems to indicate that the correlation length  $\xi$  is the typical size of the cooperatively rearranging regions, which dominate activated dynamics at low temperatures. Note that Eq. (1) for  $R < \xi$  can be used to

estimate the value of the barrier exponent  $\psi$ . Former investigations [4] suggest  $\psi = 1$ . This is confirmed by the present study, although the value  $\psi = 1.5$  is equally compatible with the data.

**Sandwich geometry.** A different implementation of ABC, which emphasizes the existence of interfaces between CRR, is the following. Consider two equilibrium configurations,  $\alpha$  and  $\beta$ , and build a system with a sandwich-geometry, made by three different regions. The size of the central region is  $L \times L \times d$  (with  $d \ll L$ ), and it is let to equilibrate under the influence of the configurations  $\alpha$  and  $\beta$ , which are placed in the left and right regions and frozen. Using this geometry, it has been measured in numeric simulation the excess energy

$$\Delta E \equiv E_{\alpha\beta} - (E_{\alpha\alpha} - E_{\beta\beta})/2 \quad (2)$$

for different values of  $d$ , finding a positive value which decreases upon increasing  $d$ . This suggests that the excess energy in this equilibrium configurations is due to the surface tension between CRRs. By varying  $T$ , one finds that  $\Delta E$  decreases at high temperatures, confirming the possible existence of the spinodal point found in Ref. [5] using inherent structures (ISs). Finally, the stiffness exponent  $\theta$  has been determined by fitting our data with the scaling form

$$\Delta E \sim d^{\theta-2} \exp(-d/\lambda) \quad (3)$$

yielding  $\theta \sim 2$ , which also confirms IS results [5].

The work of TSG was supported in part by grants from ANPCyT, CONICET, and UNLP (Argentina). PV has been partly supported through Research Contract Nos. FIS2009-12648-C03-01, FIS2008-01323 (MICINN, Spain).

\* Corresponding author: paolo.verrocchio@unitn.it

- [1] Jean-Philippe Bouchaud and Giulio Biroli, *J. Chem. Phys.* **121**, 7347 (2004).
- [2] Andrea Cavagna, Tomás S. Grigera, and Paolo Verrocchio, *Phys. Rev. Lett.* **98**, 187801 (2007).
- [3] G. Biroli, J.-P. Bouchaud, A. Cavagna, T. S. Grigera, and P. Verrocchio, *Nature Phys.* **4**, 771 (2008).
- [4] Chiara Cammarota, Andrea Cavagna, Giacomo Gradenigo, Tomás S. Grigera, and Paolo Verrocchio, *J. Chem. Phys.* **131**, 194901 (2009).
- [5] C. Cammarota, A. Cavagna, G. Gradenigo, T. S. Grigera, and P. Verrocchio, *J. Stat. Mech.* L12002 (2009).

## First steps towards a renormalization group approach for glasses

Marco Tarzia,<sup>1,\*</sup> Chiara Cammarota,<sup>2</sup> Giulio Biroli,<sup>2</sup> and Gilles Tarjus<sup>1</sup>

<sup>1</sup>*LPTMC, Université Pierre et Marie Curie, Paris, France*

<sup>2</sup>*IPhT, CEA Saclay, France*

Although there is a broad consensus on the importance of understanding the nature of the glass and the glass transition, there remains a wide divergence of views concerning the appropriate theoretical framework. In the ongoing search for a general theory of glass formation, the random first-order transition (RFOT) approach has proven to be a strong candidate, establishing what appears to be an intricate mean-field (MF) description of supercooled liquids and glasses [1, 2]. This MF treatment predicts a scenario with two critical temperatures  $T_d$  and  $T_K$ , the upper one  $T_d$  being a dynamical singularity akin to the mode-coupling transition and the lower one  $T_K$  a thermodynamic ideal glass transition characterized by a vanishing of the configurational entropy (defined as the logarithm of the number of metastable states).

The RFOT theory assumes that this MF picture retains some validity in finite-dimensional systems. Yet, in finite dimension, finite barriers between metastable states allows ergodicity restoration. It is postulated that this happens between  $T_d$  and  $T_K$  via entropy driven “nucleation” processes: the escape process from a metastable state is impeded by the free-energy mismatch with the surrounding, but, on large enough length scales, the entropic gain due to the large number of metastable states that the system can sample eventually wins. In this picture the typical equilibrium configuration is a mosaic of patches of different coexisting amorphous states [1–3]. Testing the validity of this appealing but still fragile scenario is of major interest. In addition to computer simulations of model liquids [4], some analytical work has so far been done, taking the MF result as a starting point. Going beyond these approaches however requires a renormalization group (RG) treatment.

In this talk I would like to discuss the first steps towards a RG treatment of glass formation beyond the RFOT MF theory [5]. To this end, we consider the Migdal-Kadanoff (MK) real-space RG of a Ginzburg-Landau model which is commonly taken to be in the “universality class” of structural glass-formers as it displays the two-temperature scenario at the MF level. Our starting point is the replica MF theory of structural glasses, in which one studies the distribution of putative metastable glassy states by introducing  $m$  copies (or replicas) of the same liquid system coupled with a small attractive interaction whose amplitude is

set to zero after taking the thermodynamic limit [6].

Between  $T_d$  and  $T_K$ , we find that asymptotically the system flows to a trivial disordered fixed point corresponding to a “normal” liquid with uncoupled replicas, where the boundary conditions in the metastable glassy state do not affect the deep interior of the liquid. This behavior takes place along the RG flow beyond the so called “point-to-set” length scale,  $\ell_{PS}$ , which we find to depend on the temperature as  $\ell_{PS}(T) \sim (T - T_K)^{-1}$ . Interestingly, there appears to be another characteristic length scale  $\ell_b$ , which we call the “penetration length” as it describes how far the amorphous order fixed by the metastable boundary condition penetrates into the liquid. This length grows as  $\ell_b(T) \sim (T - T_K)^{-1/d}$ . This behavior is strongly reminiscent of that observed in a conventional first-order transition, with the point-to-set length playing the role of the scale above which the metastable phase disappears and the penetration length corresponding to standard “persistence length” [7].

Our analysis shows that the physics in the vicinity of a RFOT to an ideal glass is controlled by a first-order discontinuity fixed point with standard exponents. Although the resulting physical picture is similar to the phenomenological one put forward in [1, 3], the values of the exponents differs from [1]. Recent computer simulations of an atomic glass-forming liquid model [4], find that some exponents are indeed standard, but others are not. It is therefore worth discussing the limitations of the present RG analysis.

\* Corresponding author: marco.tarzia@gmail.com

- [1] T. R. Kirkpatrick, D. Thirumalai, and P. G. Wolynes, *Phys. Rev. A* **40**, 1045 (1989).
- [2] G. Biroli and J.-P. Bouchaud, preprint arXiv:0912.2542 (2009).
- [3] J.-P. Bouchaud and G. Biroli, *J. Chem. Phys.* **121**, 7347 (2004).
- [4] A. Cavagna, T. S. Grigera, and P. Verrocchio, *Phys. Rev. Lett.* **98**, 187801 (2007); G. Biroli *et al*, *Nature Phys.* **4**, 771 (2008); C. Cammarota *et al*, *J. Chem. Phys.* **131**, 194901 (2009); *J. Stat. Mech.* (2009) L12002.
- [5] C. Cammarota, G. Biroli, M. Tarzia, and G. Tarjus, preprint arXiv:1007.2509 (2010), submitted to *Phys. Rev. Lett.*
- [6] R. Monasson, *Phys. Rev. Lett.* **75**, 2847 (1995).
- [7] M. E. Fisher and A. N. Berker, *Phys. Rev. B* **26**, 2507 (1982).

## Field Theory of Fluctuations in Glasses

Silvio Franz,<sup>1,\*</sup> Giorgio Parisi,<sup>2</sup> Federico Ricci-Tersenghi,<sup>2</sup> and Tommaso Rizzo<sup>2</sup>

<sup>1</sup>*LPTMS, CNRS and Université Paris-Sud, UMR8626, Bat. 100, 91405 Orsay, France*

<sup>2</sup>*Dipartimento di Fisica, Università di Roma 'La Sapienza', 00185 Rome, Italy*

We develop a field-theoretical description of fluctuations in supercooled liquids close to the (avoided) MCT singularity. This is based on inclusion of fluctuations in the theory of effective potential, so far developed within mean field theory. We separate the different sources of fluctuations and show that the most relevant ones are relative to variations of self-induced disorder. Our main result is that fluctuations can be studied through a cubic field theory with an effective random temperature term. We argue that our theory provides a reparametrization invariant description of dynamical fluctuations, for times between the late beta and the early alpha regimes. It ensues perturbative dimensional reduction and an upper critical dimension equal to 8. The heterogeneous character of glassy dynamics has been subject of extensive study in the last decade. Experiments, simulations and theory converge to a description of supercooled liquids where, on approaching the glass transition, relaxation requires cooperative motions on high mobility regions of increasing size and life time. An important theoretical step in the understanding of dynamical heterogeneities was to realize that the current theory of glassy dynamics, the Mode Coupling Theory (MCT), predicts a growing dynamical length as the MC critical point is approached. This was first observed in the context of disordered mean field systems where MCT is exact, and later confirmed with diagrammatic approaches to the dynamics of liquids. In the resulting picture, dynamical heterogeneities are captured by a time dependent four point correlation function, whose associated dynamical length diverges at the MC critical point. As is well known, this divergence, genuine in mean-field, is in real systems an artefactual consequence of MCT that neglects activated processes. Accordingly the divergence is cut off as the MCT dominated regime at high temperature crosses over to the barrier dominated regime at low temperature. With this caveat, the MCT prediction of a pseudo-critical growth of dynamical correlations has been largely confirmed in simulations and experiments. Our scope is to study corrections to MCT that should be at work as soon as the mean-field approximation is not exact. Two kinds of interrelated corrections can be expected: first one due to critical fluctuations which are not well described by mean-field theory, second one due to barrier jumping. Clarification of both kind of fluctuations, necessary to accomplish a theory of glassy dynamics, has been the subject of research in the last few years. Unfortunately both kind of phenomena are poorly understood. We present an in depth analysis of critical fluctuations around MCT which clarify the nature of the former, and suggest a possible path to study the latter. The MC transition is often presented as a pure dynamical ergod-

icity breaking phenomenon without structural consequences. It is sometimes stated that MC freezing can not be detected with equilibrium techniques. This is an unfortunate misconception. The MC transition describes ergodicity breaking where a system prepared in an equilibrium initial condition remains confined in its vicinity. The space of equilibrium configuration is then partitioned in metastable states that (within the MC approximation) are arguably present in an exponentially large number. As any metastability problem, the MC dynamical freezing can be studied introducing appropriate constraints in the equilibrium measure. The corresponding free-energy as a function of the constrained variables can be used to set up a purely static field theoretical description of the MC ergodicity breaking transition. This correspondence between statics and dynamics has been indeed crucial to the first recognition that the growth of a dynamical susceptibility is accompanying the growth of the relaxation time at the transition. We exploit this to make a theory of critical fluctuations on time scales where dynamical correlation functions are close to the plateau value using constrained equilibrium measures and expressing time dependent quantities in *reparametrization invariant* form i.e. eliminating the time dependence in favor of a dependence on the correlation function itself. The main thesis is that reparametrization invariant fluctuations for temperatures close to the mode coupling temperature  $T_d$  and values of the correlations close to the plateau value can be described in terms of a field theory of the kind

$$H[\phi|\delta\epsilon(x)] = \int dx \frac{1}{2}(\nabla\phi(x))^2 + (\epsilon + \delta\epsilon(x))\phi(x) + g\phi^3(x)$$

where  $\phi(x)$  is a local fluctuation of the overlap away from the plateau value,  $\epsilon = T - T_d$  is the deviation from the critical temperature,  $g$  is a coupling constant and  $\delta\epsilon(x)$  is an effective random temperature term, distributed with gaussian statistics and delta correlated in space. The random temperature term is the ultimate consequence of dynamic heterogeneity and is a formal expression of “self-induced disorder” sometimes advocated to describe structural glasses. The role of this term in perturbation theory is crucial, leading to perturbative dimensional reduction and changing the scaling properties of the cubic theory. The upper critical dimension above which fluctuations can be expected to have a Gaussian nature is found to be eight rather than six as naively expected.

\* Corresponding author: silvio.franz@gmail.com

## Characterizing order in amorphous systems

François Sausset<sup>1,\*</sup> and Dov Levine<sup>2</sup>

<sup>1</sup>*Université Paris Sud, CNRS, LPTMS, UMR 8626, Orsay F-91405, France*

<sup>2</sup>*Department of Physics, Technion, Haifa 32000, Israel*

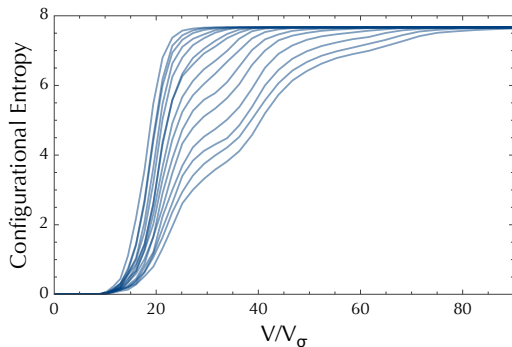


FIG. 1. Evolution of the configurational entropy of patches with their volume when cooling the system (see [3]).  $V_\sigma$  is the volume of a single particle. Note the three regimes of the entropy: constant and near zero for small sizes, then a linear behaviour, and finally a saturation (finite size effects).

Is the dramatic viscous slowing down encountered in glassy systems associated with the growth of some static amorphous order? This fundamental question remains unanswered for two main reasons: First, the nature of the hypothetical order has not been firmly established, and second, the experimental implementation of the various proposals is unclear.

Recently, a generic method to define and quantify order has been proposed [1, 2]. Roughly, it consists of measuring the configurational entropy of patches (local clusters of varying size) in the system, and studying its scaling with patch volume  $V$ . For small patches, this patch entropy is expected to grow sub-linearly in  $V$ , while for large clusters, it grows linearly. This crossover enables us to define and measure a correlation length with no a-priori knowledge of the order involved.

We will discuss the implementation of this new proposal on atomic models of glass forming liquids and colloidal systems. As a benchmark, we will study a well-characterized numerical model of a glass forming

liquid [3], and will compare various proposed measures, including bond-orientation and point-to-set correlation lengths.

This new method can also be used to access the symmetries of the local order, without any a priori knowledge of it. For this model, it is illustrated in Fig. 2 where the hexagonal order is, as expected, recovered.

We will also show first applications to experimental data (3D colloidal systems) allowing to access both order extension and symmetries.

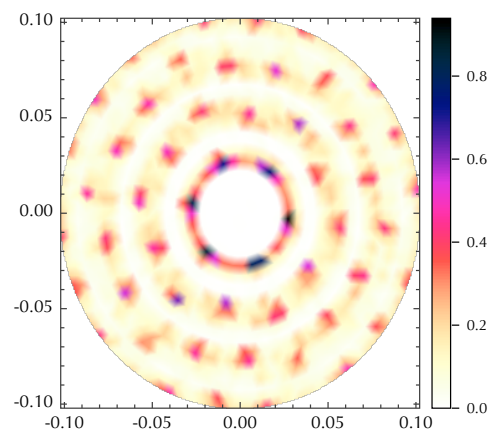


FIG. 2. Density profile of the mean patch of the most repeating class of patches. Dark spots indicate the most probable positions of particles inside of patch of this diameter. The density profile clearly displays an hexagonal symmetry characteristic of the local order in this system [3].

\* Corresponding author: francois.sausset@lptms.u-psud.fr

- [1] J. Kurchan and D. Levine, arXiv:0904.4850 (2009).
- [2] J. Kurchan and D. Levine, arXiv:1008.4068 (2010).
- [3] F. Sausset et G. Tarjus, Phys. Rev. Lett. **104**, 065701 (2010).

## Heterogeneous dynamics in dense monodisperse emulsions

Frédéric Cardinaux,<sup>1,2,\*</sup> Thomas G. Mason,<sup>2,3</sup> and Frank Scheffold<sup>1</sup>

<sup>1</sup>*Department of Physics and Fribourg Center for Nanomaterials,  
University of Fribourg, CH-1700 Fribourg, Switzerland.*

<sup>2</sup>*Department of Chemistry and Biochemistry, University of California Los Angeles, Los Angeles, CA 90095, USA.*

<sup>3</sup>*Department of Physics and Astronomy, University of California Los Angeles, Los Angeles, CA 90095, USA.*

An emulsion is a dispersion of a liquid within another, immiscible liquid. Modern emulsification techniques allow to produce monodisperse emulsions with sizes ranging from several microns down to few tenth of nanometers [1]. Additionally, coalescence can be prevented by coating the droplet surfaces with additives, thus rendering the system long-lived. Interesting properties emerge from the liquid nature of both the continuous and the dispersed phase. In particular, emulsion droplets are spherical colloids that can be deform at constant volume, with the compression been essentially controlled by the Laplace pressure. This situation typically occurs at volume fraction beyond  $\phi_{RCP}$ , the random close packing of hard spheres, where deformation results from the contact forces exerted by individual droplets on each other.

As a consequence, the physical properties of dense emulsions depends on whether droplets deform or not. Most notably, it strongly impacts on the rheology of the non-equilibrium states found at high volume fractions [2, 3]. Similarly to hard spheres, emulsions undergoes a glass transition where entropic contributions to their rheology are important. Above  $\phi_{RCP}$ , the Laplace pressure of individual droplets becomes the key parameter to understand their rheology [2].

In this study, we present our work on the dynamical properties of dense emulsions at volume fraction ranging from  $0.4 < \phi < 0.72$ . We use an experimental approach that allows spatially resolved dynamic light scattering in highly turbid media [4, 5]. An example of the results for a compressed emulsion at  $\phi = 0.699$  is shown in Fig.1. Here we constructed a dynamical activity map using the intensity structure function  $d_2(\tau, \mathbf{r})$ , where each pixel contains the dynamical contribution of a small volume of linear dimension of approximately 30 droplets diameter. Domains of high and low dynamical activity are color-coded by warm and cold colors, respectively. At these length scales, we observe a dynamics that is extremely het-

erogeneous. Our experiments allow to characterize the size and spatial distribution of dynamical heterogeneities. We aim at connecting our observations to a dynamical transition from thermally driven regime below compression, to a stress-relaxation regime as droplets starts to be in a compressed state.

We acknowledge financial support by the Swiss National Science Foundation (Grant PBF2-123104) and the Adolphe Merkle Foundation.

\* Corresponding author: frederic.cardinaux@unifr.ch

- [1] T. G. Mason *et al.*, *J. Phys.:Condens. Matter* **18**,R635-R666 (2006).
- [2] T. G. Mason, J. Bibette, and D. A. Weitz, *Phys. Rev. Lett.* **75**, 2051 (1995).
- [3] H. Gang *et al.*, *Phys. Rev. E* **59**, 715 (1999).
- [4] P. Zakharov and F. Scheffold, *SOFT MATERIALS* **8**, 102 (2010).
- [5] S. E Skipetrov *et al.*, *Opt. Express* **18**, 14519 (2010).

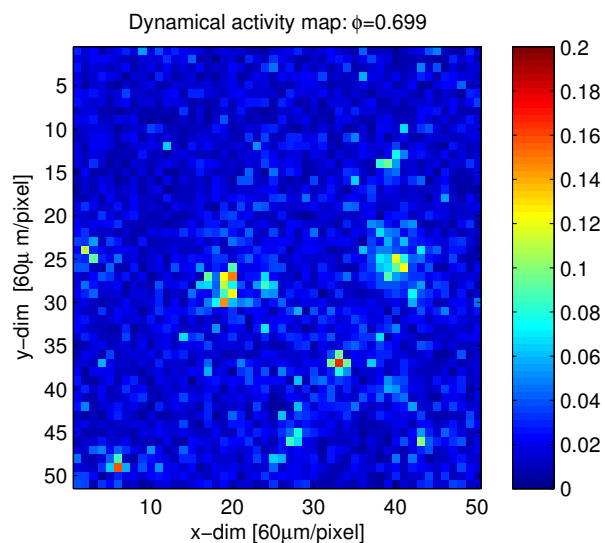


FIG. 1. Dynamical activity map constructed with the intensity structure function  $d_2(\tau = 1s, \mathbf{r})$  for a sample at  $\phi = 0.699$ .

## Dynamics and local order in a 2D colloidal glass former

Sylvain Mazoyer,<sup>1,2</sup> Florian Ebert,<sup>2</sup> Georg Maret,<sup>2</sup> and Peter Keim<sup>2,\*</sup>

<sup>1</sup>University of Crete, Heraklion, Crete, Greece

<sup>2</sup>University of Konstanz, Konstanz, Germany

Using positional data from video-microscopy we study a bi-disperse colloidal mixture (of big and small particles) in two dimensions. Since the colloids are super-paramagnetic a magnetic field induces a dipolar repulsion between the particles (ten times larger for the big ones compared to the small ones) acting as an inverse temperature. At low magnetic fields (high temperature) the system is in a disordered fluid state. Increasing the magnetic field strength (decreasing the temperature) the system traverses from a fluid to a dynamically arrested state while staying amorphous on a global scale. The mean square displacement (MSD) is in good agreement with Mode Coupling Theory for a hard disc glass former and the system does not show long range order. Nevertheless small crystallites with distinct stoichiometries appear on a local scale in the supercooled state. The basic vectors of the local unit cells are used to interpret the position of the peaks in the pair correlation function of the 2D system. The statistics of the crystalline unit cells show a continuous increase of local order with decreasing system temperature [1].

In the supercooled state dynamic heterogeneities appear on the timescale of the  $\alpha$ -relaxation and the self part of the Van Hove function shows an exponential tail [2]. Using a local cage-relative mean square displacement with respect to the nearest neighbours we are able to show that particles in a local high symmetry configuration have slower dynamics. In Figure 1 this cage relative mean square displacement (CR-MSD) is plotted for particles sitting in different local environments. The black curve is the CR-MSD averaged over all big particles, the red curve is for big

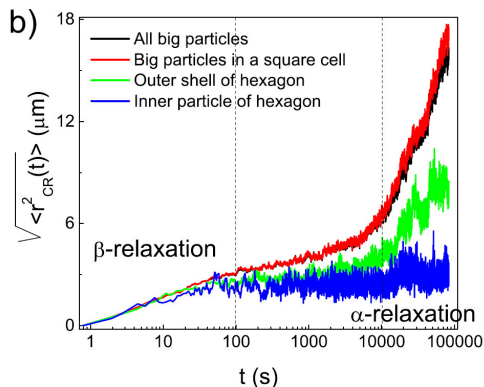


FIG. 1. Cage relative mean square displacement for particles sitting in different local configurations. Vertical dashed lines indicate the limits between the different regimes of the CR-MSD.

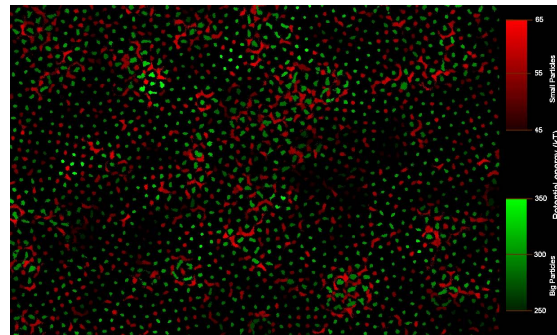


FIG. 2. Cage relative trajectories for big particles in green and small particles in red. The intensity of the color is proportional to the potential energy of the particle averaged over the duration of the experiment ( $t=80000$ s).

particles sitting in a square cell and the green and blue curve are big particles belonging to the shell and the center of a hexagon. Especially the latter show a plateau in the local mean square displacement over the duration of the experiment indicating that the particle found its local energetic minimum.

Since we know the interaction between the particles precisely we can calculate the potential energy from the positions of the colloids ab initio for all particles. Figure 2 shows this energy landscape with the magnitude of the local potential energy encoded in the brightness. Note, that the patterns are stable even far beyond the onset of the alpha relaxation. On the other hand Figure 2 shows the trajectories of the two species of particles. Dynamical heterogeneities are clearly visible and we can map them to the energy landscape. Particles sitting in an minimum with a level higher than the average level have a large radius of gyration of the local trajectory. On the other hand particles sitting in a deep minimum (where local symmetry is close to a ground state configuration) have a small radius of gyration of the trajectory. This way structural and dynamical heterogeneities are correlated.

Financial support of the DFG (Deutsche Forschungsgemeinschaft) is gratefully acknowledged.

\* Corresponding author: Peter.Keim@uni-konstanz.de

[1] F. Ebert, P.Keim, G. Maret, *Euro. Phys. Jour. E* **26**, 161 (2008)

[2] S. Mazoyer, F. Ebert, G. Maret, P. Keim, *Euro. Phys. Lett.* **88**, 66004 (2009)

## Glass-like dynamics of colloids in modulated potentials

Cécile Dalle-Ferrier,<sup>1,2,\*</sup> Matthias Krüger,<sup>3</sup> Richard D.L. Hanes,<sup>1</sup>  
Stefan Walta,<sup>1</sup> Matthew C. Jenkins,<sup>1</sup> and Stefan U. Egelhaaf<sup>1</sup>

<sup>1</sup>Condensed Matter Physics Laboratory, Heinrich Heine University, 40225 Düsseldorf, Germany

<sup>2</sup>Soft Matter and Chemistry, ESPCI-CNRS, 75005 Paris, France

<sup>3</sup>Department of Physics, Massachusetts Institute of Technology, Cambridge, Massachusetts 02139, USA

Heterogeneities and (growing) dynamic length scales are widely discussed in the context of the glass transition. It has been recently suggested [1] that the size and characteristics of such length scales (or clusters) can be probed by an external potential. For this situation, an extension of the Mode Coupling Theory to inhomogeneous situations provides predictions for the dependence of the three-point correlation functions with the length scale independently imposed by the external potential. While these predictions apply to all types of glass-forming liquids, we tested them using colloids.

Colloids are widely used as model systems for the study of the glass transition. Thanks to the micrometer size of the particles, individual trajectories can be experimentally followed by optical microscopy. This allows us to obtain the dynamics of the system including microscopic details. Colloidal particles can furthermore be manipulated using light by exploiting the force exerted on particles with a refractive index different from the solvent, as it is done in optical tweezers. Exploiting these possibilities, we measured the self dynamics of a colloidal suspension in a modulated light field [3]. We investigated the effect of the wavelength and amplitude of this potential as well as the particle size on the mean square displacement, the distribution of displacements, the non-Gaussian parameter and the dynamical heterogeneities via the three-point correlation function. Moreover, our results are compared to theoretical predictions available in the literature [1, 2].

Interestingly, not only the concentrated but also the very dilute, non-interacting samples exhibit a relation to supercooled liquids. In particular, we found that the time-dependent mean square displacements determined in a very dilute system in the modulated potential are surprisingly close to the ones in a quasi-two dimensional colloidal supercooled liquid (Fig. 1) with the role of the colloid volume fraction played by the amplitude of the potential [3]. The similarity of the mean square displacements is particularly striking since an individual colloidal particle in a periodic potential represents a considerably simpler situation

than a highly concentrated multi-particle system.

\* Corresponding author: cecile.dalle-ferrier@uni-duesseldorf.de

- [1] G. Biroli, J.-P. Bouchaud, K. Miyazaki, D. R. Reichman Phys. Rev. Lett. **97**, 195701 (2006).
- [2] B. Vorselaars, A. V. Lyulin, K. Karatasos, and M. A. J. Michels, Phys. Rev. E **75**, 011504 (2007).
- [3] C. Dalle-Ferrier, M. Krüger, R. D. L. Hanes, S. Walta, M. C. Jenkins, and S. U. Egelhaaf, Soft Matter, accepted.
- [4] R. Zangi and S. A. Rice, Phys. Rev. Lett. **92**, 035502 (2004).
- [5] B. Cui, B. Lin, and S. A. Rice, J. Chem. Phys. **114**, 9142 (2001).

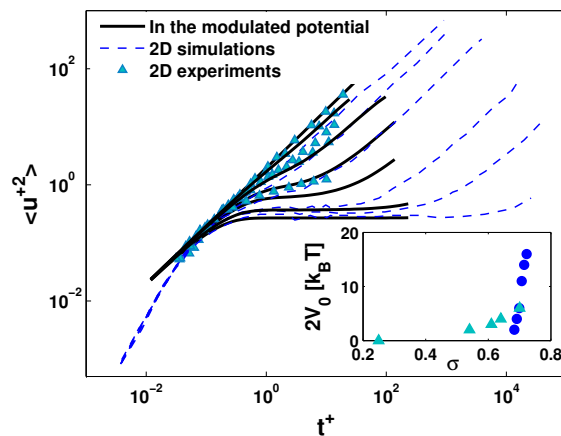


FIG. 1. Dimensionless mean square displacement  $\langle \Delta u^{+2}(t^+) \rangle = L^{-2} \langle \Delta y^2(t^+) \rangle$  as a function of dimensionless time  $t^+ = L^{-2}Dt$ , where  $L$  is a typical length scale and  $D$  the short-time diffusion constant. Our results for dilute colloidal particles in a sinusoidal potential with dimensionless amplitude  $V_0^* = 0.0, 1.0, 2.0, 3.0, 4.0, 6.0$  and  $8.0$  (solid lines, top to bottom) are shown. They are compared to another system without an external potential: Quasi two-dimensional concentrated hard-spheres, where the dashed lines represent simulations at surface fractions  $\sigma=0.68$  to  $0.723$  [4] and the triangles represents experimental data at surface fractions  $\sigma=0.25$  to  $0.70$  [5].

## Glass transition in confined geometry: A mode-coupling theory

Simon Lang,<sup>1,\*</sup> Vitalie Boțan,<sup>2</sup> Martin Oettel,<sup>2</sup> David Hajnal,<sup>2</sup> Thomas Franosch,<sup>1</sup> and Rolf Schilling<sup>2</sup>

<sup>1</sup>*Institut für Theoretische Physik, Universität Erlangen-Nürnberg, Staudtstraße 7, 91058, Erlangen, Germany*

<sup>2</sup>*Institut für Physik, Johannes Gutenberg-Universität Mainz, Staudinger Weg 7, 55099 Mainz, Germany*

The mode-coupling theory of the glass transition has made a series of nontrivial predictions for bulk systems which have been confirmed in the last two decades by experiments and computer simulations [1]. Meanwhile, also the expansion on the two dimensional case has been accomplished successfully [2], whereas a theoretical interpolation in between is rather missing. Recently, significant experimental and simulational research effort has been made to confine the liquid to small pores, films, or tubes, since they may hold the key to provide further insight into the nature of the glass transition. In particular, computer simulations reveal that the wall-fluid interaction significantly alters the transition temperatures [3, 4] and that the diffusivities depend sensitively on the distance of the walls [5]. Experiments on colloidal suspension confined between parallel plates have demonstrated that the mean-square displacements are strongly correlated with the layering of the fluid induced by the wall [6].

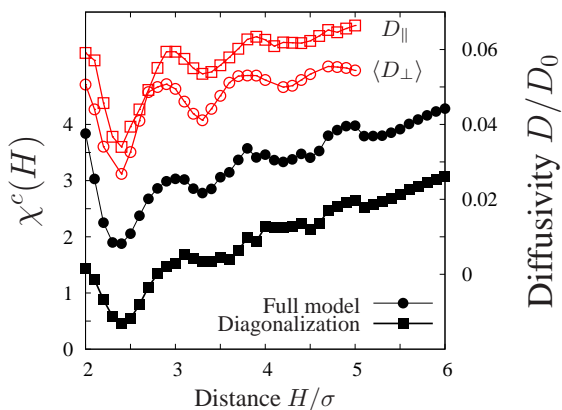


FIG. 1. The parameter  $\chi_c(H)$  reflecting the critical packing fraction for confined liquids oscillates in phase with the diffusivities  $D_{||}$  and  $D_{\perp}$  at fixed density [5].

Motivated by these intriguing observations, we have extended MCT to inhomogeneous liquids confined between two parallel flat hard walls without surface roughness [7]. The theory employs spatial Fourier modes for the density fluctuations

$$\rho_{\mu}(\vec{q}, t) = \sum_{n=1}^N \exp[iQ_{\mu}z_n(t)] e^{i\vec{q}\cdot\vec{r}_n(t)}, \quad (1)$$

where  $\vec{r}_n(t) = (x_n(t), y_n(t))$  and  $z_n(t)$  denote the position of the  $n$ -th particle parallel and perpendicular to the wall, respectively. The discrete values  $Q_{\mu}$  ac-

count for the confined geometry and the continuous set  $\vec{q} = (q_x, q_y)$  refers to the wave vector parallel to the walls. Then the basic quantities are matrix-valued density correlation function

$$S_{\mu\nu}(q, t) = \frac{1}{N} \langle \rho_{\mu}(\vec{q}, t) \rho_{\nu}(\vec{q}, 0) \rangle, \quad (2)$$

for which we derive exact equations of motion relying on the Zwanzig-Mori formalism. As a peculiarity, one has to decompose the currents into components parallel and perpendicular to the walls to reproduce the limits of a two-dimensional and a three-dimensional system. The memory kernels are approximated by a mode-coupling procedure and a closed set of integro-differential equations is obtained. In particular the nonergodicity parameters at the transition line can be evaluated numerically and the non-equilibrium phase diagram can be predicted.

As an example, we have considered a hard sphere fluid and determined the glass transition line within different approximation schemes, see Fig. 1. We observe an oscillatory behavior as a result of the structural changes connected to layering. The glass transition is facilitated at half-integer values of the distance with respect to the hard-sphere diameter in qualitative agreement with the suppression of diffusion by confinement [5]. In contrast, at commensurate packing particles can more easily slide along the walls and therefore fluid behavior is favoured.

T.F. and M.O. gratefully acknowledge support via the DFG research unit FOR-1394 (T.F.) and SFB-TR6 (N01, M. O. and V. B.)

\* Corresponding author: simon.lang@physik.uni-erlangen.de

- [1] W. Götze, *Complex Dynamics of Glass-Forming Liquids – A Mode-Coupling Theory* (Oxford University Press, Oxford, UK, 2009).
- [2] M. Bayer et al., Phys. Rev. E **76**, 011508 (2007).
- [3] P. Scheidler, W. Kob, and K. Binder, Europhys. Lett. **52**, 277 (2000); **59**, 701 (2002)
- [4] F. Varnik, J. Baschnagel, and K. Binder, Phys. Rev. E **65**, 021507 (2002).
- [5] J. Mittal, T.M. Truskett, J.R. Errington, and G. Hummer, Phys. Rev. Lett. **100**, 145901 (2008).
- [6] C. R. Nugent, K.V. Edmond, H. N. Patel, and E. R. Weeks, Phys. Rev. Lett. **99**, 025702 (2007).
- [7] S. Lang, V. Boțan, M. Oettel, D. Hajnal, T. Franosch, and R. Schilling, Phys. Rev. Lett. **105**, 125701 (2010).

## Slow dynamics in cluster crystals and cluster glasses

Daniele Coslovich,<sup>1,\*</sup> Lukas Strauss,<sup>2</sup> Gerhard Kahl,<sup>3</sup> and Angel Moreno<sup>4</sup>

<sup>1</sup>*Laboratoire de Colloïdes, Verres et Nanomatériaux,  
Université Montpellier II, Montpellier (France)*

<sup>2</sup>*Institut für Meteorologie und Geophysik, Universität Wien, Vienna (Austria)*

<sup>3</sup>*Institut für Theoretische Physik, Technische Universität Wien, Vienna (Austria)*

<sup>4</sup>*Centro de Física de Materiales CSIC-UPV/EHU, San Sebastián (Spain)*

We perform a comparative simulation study of the dynamical properties of ultrasoft particles in cluster phases. We focus on the generalized exponential model (GEM) [1], a prototypical model for ultrasoft colloids, such as dendrimers and microgels. In the GEM of order  $n$ , particles interact through the potential  $u(r) = \epsilon \exp[-(r/\sigma)^n]$ , where  $\sigma$  and  $\epsilon$  are length and energy scales, respectively. For  $n > 2$  the GEM displays crystalline phases with multiply-occupied sites, i.e., it forms *cluster crystals* [1, 2]. We present extensive simulation results on the hopping dynamics of the GEM with  $n = 4$  in the fcc cluster phase [3] and report the first simulation evidence of *cluster glasses* in a bidisperse version of the model.

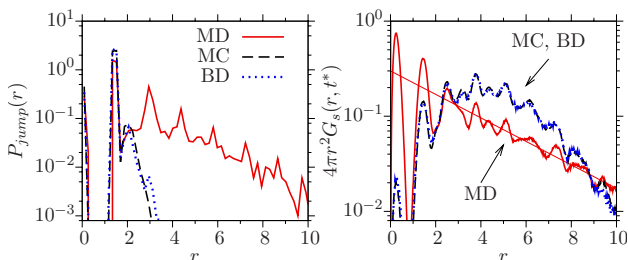


FIG. 1. Comparison of jump length distributions  $P_{\text{jump}}(r)$  and van Hove correlation functions  $4\pi r^2 G_s(r, t^*)$  obtained from MD, MC, and BD simulations in the fcc cluster crystal ( $\rho = 6.4$ ,  $T = 0.8$ ).  $t^*$  is given by  $\langle \delta r^2(t^*) \rangle = 25$ .

The dynamics of the model in the fcc cluster phase is investigated through a combination of molecular dynamics (MD), Brownian dynamics (BD) and Monte Carlo (MC) simulations. We study the activated dynamics of particles as they hop from site to site in the cluster structure, and analyze the statistics of jump events. We find that the diffusion mechanism depends sensitively on the microscopic dynamics. In MD simulations particles can jump over several cluster site in a correlated fashion, leading to a broad distribution of jump lengths  $P_{\text{jump}}(r)$ . In MC and BD simulations, by contrast, particles hop only to nearest neighbor sites. The underlying distributions of jump lengths affect the long time dynamics of the particles, giving rise, for instance, to qualitatively different shapes of the van Hove correlation functions (see Fig. 1). We attribute these differences to the suppression of momentum correlation in the two stochastic methods. The agreement between MC and BD simulations support the view that MC dynamics effectively incorporate solvent effects in a simulation of model colloids [4].

We then extend our investigations to a binary mixture

of particles with  $n = 4$  and size ratio  $\sigma_{11}/\sigma_{22} = 1.4$ , simulated over a wide range of densities. As the fluid is slowly quenched from high  $T$ , we observe the formation of stable clusters, whose centers of mass eventually arrest into a disordered configuration. The location of the cluster glass transition does not depend sensitively on the quench rate and is associated to a fragile-to-strong crossover in the  $T$ -dependence of the partial diffusion coefficients. In the cluster glass, particles hop from cluster to cluster. Unlike in cluster crystals, however, long range jumps are suppressed in MD simulations due to the disorder of the underlying cluster structure. We attribute the ability to form amorphous cluster phases to the size bidispersity of the particles. Clusters formed at low  $T$  are mostly homo-coordinated, leading to an effective binary mixture of *clusters*. This, in turn, frustrates crystallization of the clusters' centers of mass. This interpretation is supported by the comparison with a variant of the model with continuous size polydispersity, which inevitably crystallized in an fcc cluster crystal. Our observations thus suggest a viable route to cluster glass formation in a more ample class of colloidal fluids, such as systems with competing interactions.

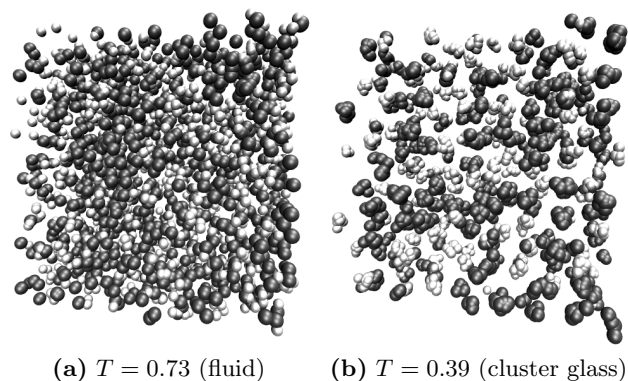


FIG. 2. Representative snapshots of the binary mixture for two different temperatures at density  $\rho = 6.0$ . For clarity, only a vertical slice of the system is displayed.

\* Corresponding author: coslovich@lcvn.univ-montp2.fr

- [1] B. M. Mladek, D. Gottwald, G. Kahl, M. Neumann, and C. N. Likos, Phys. Rev. Lett. **96**, 045701 (2006).
- [2] A. J. Moreno and C. N. Likos, Phys. Rev. Lett. **99**, 107801 (2007).
- [3] D. Coslovich, L. Strauss, and G. Kahl, Soft Matter (2010, in press); arXiv:1006.4982.
- [4] G. Brambilla *et al.*, Phys. Rev. Lett. **102**, 085703 (2009).

## Highly nonlinear dynamics in a slowly sedimenting colloidal gel

S. Buzzaccaro,<sup>1,\*</sup> G. Brambilla,<sup>2</sup> R. Piazza,<sup>1</sup> L. Berthier,<sup>2</sup> and L. Cipelletti<sup>2</sup>

<sup>1</sup>*Dipartimento di Chimica, Politecnico di Milano, 20131 Milano, Italy*

<sup>2</sup>*Laboratoire des Colloïdes, Verres et Nanomatériaux, UMR 5587, Université Montpellier II and CNRS, 34095 Montpellier, France*

Gels and attractive glasses resulting from the aggregation of colloidal particles form an important class of materials. Although they exhibit solid-like mechanical properties, colloidal gels are easily disrupted by small perturbations, such as gravitational forces. While a large body of macroscopic observations of gels under gravitational stress exists [1], very little is known on the microscopic processes at play during sedimentation, thus limiting our ability to understand and predict the behavior of sedimenting gels. We study gels formed by attractive colloidal hard spheres with radius  $R = 82 \pm 3$  nm, suspended in an aqueous solvent at an initial volume fraction  $\phi_0 = 0.123$ . Gelation is induced by attractive depletion forces [2] obtained by adding micelles of a nonionic surfactant. To probe the sedimentation process with unprecedented resolution, we use a custom-designed light scattering apparatus, which allows us to measure with both temporal and spatial resolution the local volume fraction, sedimentation velocity and microscopic relaxational dynamics within a single experiment. Briefly, a low magnification image of the sample is formed onto a CCD sensor, using light scattered at  $\theta = 90^\circ$ . Two crossed polarizers are used to detect only the depolarized light, which intensity is an accurate probe of the local particle concentration  $\phi(z, t)$  [2]. We obtain simultaneously the evolution of the local sedimentation velocity profiles,  $v(z, t)$ , using an Image Correlation Velocimetry (ICV) algorithm [3]. Our detailed set of measurements allows us to perform a rigorous quantitative test of the modelling of gels as “poroelastic” medium [1, 4]. Our velocimetry analysis indicates that there is no horizontal component of the displacement resulting from the compression of the gel, i.e. that the (effective) Poisson ratio of the gel is negligible, a remarkable property that was discussed before [5] but could not be measured experimentally. We find that the poroelastic model captures very well both  $\phi(z, t)$  and  $v(z, t)$  demonstrating its efficient modelling of the gel sedimentation kinetics at both macroscopic and mesoscopic scales. To investigate the link between microscopic rearrangements and the macroscopic gel compaction, we examine intensity correlation functions (ICFs),  $g_2(z, t, \tau) - 1$ , measured at various heights and times. We correct the ICFs for the drift due to sedimentation, so that they measure the particle motion between times  $t$  and  $t + \tau$  in the cosedimenting frame where  $v = 0$ . We find that the very slow macroscopic deformation occurs via irreversible plastic events at the microscopic scale. Remarkably, the gel behavior

at all scales is controlled by a single parameter, the time-dependent compression rate  $\dot{\epsilon} = \partial v(z, t)/\partial z$ , in striking analogy with recent observations on deformed polymer glasses [6] and sheared colloidal glasses [7]. Our results provide firm microscopic basis for future modeling of the mechanical and dynamical properties of colloidal gels in various situations of fundamental and industrial interests.

\* Corresponding author: stefano.buzzaccaro@mail.polimi.it

- [1] R. Buscall and L. R. White, J. Chem. Soc. Faraday Trans. I **83**, 873 (1987).
- [2] S. Buzzaccaro, R. Rusconi, and R. Piazza, Phys. Rev. Lett. **99**, 098301 (2007).
- [3] P. T. Tokumaru and P. E. Dimotakis, Exp. Fluids **19**, 1 (1995).
- [4] Kim *et al.*, Phys. Rev. Lett. **99**, 028303 (2007).
- [5] Manley *et al.*, Phys. Rev. Lett. **94**, 218302 (2005).
- [6] Lee *et al.*, Science **323**, 231 (2009).
- [7] R. Besseling *et al.*, Phys. Rev. Lett. **99**, 028301 (2007).

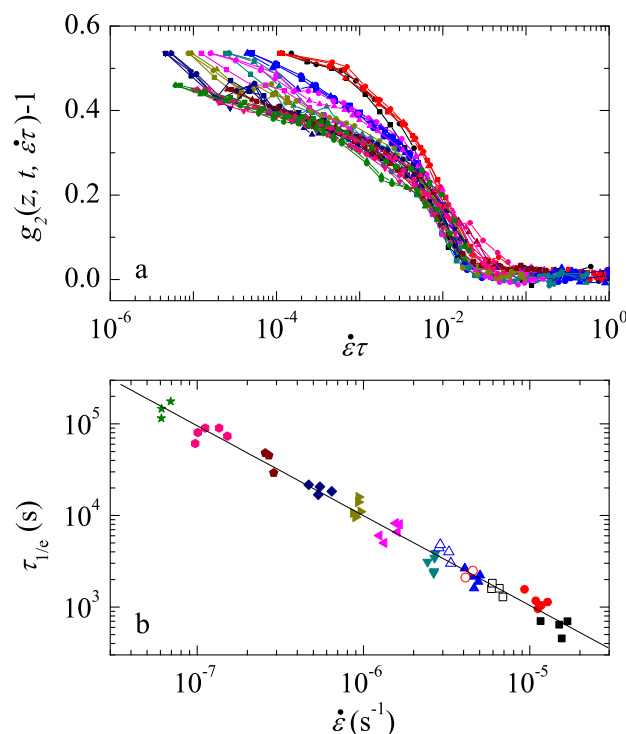


FIG. 1. a-The final relaxation ICFs collapses when plotted as a function of a rescaled time,  $\dot{\epsilon}\tau$  showing that the microscopic gel dynamics is directly related to its macroscopic deformation. b-Double logarithmic plot of the relaxation time  $\tau_{1/e}$  of the ICFs shown in a) as a function of  $\dot{\epsilon}$ .

## Phase Separation and Equilibrium gels in a colloidal clay

B. Ruzicka,<sup>1,\*</sup> E. Zaccarelli,<sup>2</sup> L. Zulian,<sup>3</sup> R. Angelini,<sup>1</sup>  
M. Sztucki,<sup>4</sup> A. Moussaïd,<sup>4</sup> T. Narayanan,<sup>4</sup> and F. Sciortino<sup>2</sup>

<sup>1</sup>CNR-IPCF and Dipartimento di Fisica, Università di Roma “La Sapienza”, Piazzale A. Moro 2, I-00185, Rome, Italy

<sup>2</sup>CNR-ISC and Dipartimento di Fisica, Università di Roma “La Sapienza”, Piazzale A. Moro 2, I-00185, Rome, Italy

<sup>3</sup>CNR-ISMAL via Bassini 15, 20133 Milan, Italy

<sup>4</sup>European Synchrotron Radiation Facility, B.P. 220 F-38043 Grenoble, Cedex France

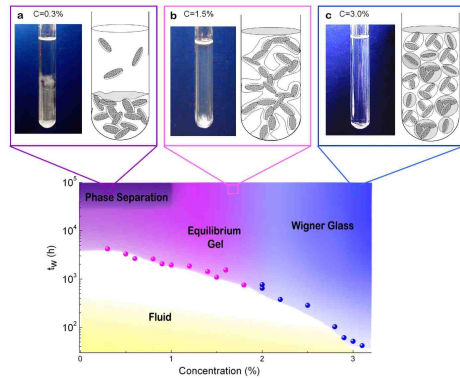


FIG. 1. Phase diagram of diluted Laponite suspensions, in the waiting time vs. concentration plane, resulting from the combined experimental and numerical results. Symbols correspond to experimental waiting time values requested to observe non ergodic behavior according to Dynamic Light Scattering [2]; boundaries inside colored regions are guides to the eye. For long waiting times, three different regions are identified, whose representative macroscopic behavior and a pictorial microscopic view are reported in **a-c**. **a**, Phase-separated sample with colloid-poor (upper part) and colloid-rich (lower part) regions for  $C_w \leq 1.0\%$ . **b**, Equilibrium gel for  $1.0 < C_w < 2.0\%$ , characterized by a spanning network of  $T$ -bonded discs. **c**, Wigner glass, expected for  $2.0 \leq C_w \leq 3.0\%$  [4], where disconnected platelets are stabilized in a glass structure by the electrostatic repulsion, progressively hampering the formation of  $T$ -bonds.

The relevance of anisotropic interactions in colloidal systems has recently emerged in the context of the rational design of novel soft materials. Patchy colloids of different shapes, patterns and functionalities are considered the novel building blocks of a bottom-up approach toward the realization of self-assembled bulk materials with pre-defined properties. New concepts such as empty liquids and equilibrium gels have been formulated[1]. Yet no experimental evidence of these predictions has been provided. Here we report the first observation of empty liquids and equilibrium gels in a complex colloidal clay, and support the experimental findings with numerical simulations.

We investigate dilute suspensions of Laponite, an industrial synthetic clay made of nanometer-sized discotic platelets with inhomogeneous charge distribution and directional interactions. The anisotropy of the face-rim charge interactions combined with the discotic shape of Laponite produce a very rich phase

diagram including aging dynamics towards disordered gels and glasses states reached respectively at low and high clay concentrations [2–4]. In this work we extend the observation time for low concentration samples to time-scales significantly longer than those previously studied and discover that, despite samples appear to be arrested on the second timescale, a significant evolution takes place on the year timescale[5]. Samples undergo an extremely slow, but clear phase separation process into clay-rich and clay-poor phases that are the colloidal analog of gas-liquid phase separation. Spectacularly the phase separation terminates at a finite *but very low* clay concentration, above which the samples remain in a homogeneous arrested state. Moreover, the slow aging dynamics peculiar of Laponite suspensions drive an arrest transition through a very slow rearrangement, so that equilibrium gels are formed. The observed features are instead strikingly similar to those predicted in simple models of patchy particles, suggesting that Laponite forms an (arrested) empty liquid at very low concentrations. Furthermore, differently from gels generated by depletion interactions or from molecular glassformers, where arrest occurs after the phase separation process has generated high-density fluctuation regions, here phase separation takes place in a sample which is already a gel. These new phenomenologies have been observed by direct visual inspection and by Small Angle X-ray measurements performed for very long time (up to more than one year). Furthermore the experimental results for the phase separation and for the structural properties in the various region of the phase diagram have been confirmed by extensive numerical simulations with a primitive model of patchy Laponite discs.

\* Corresponding author: barbara.ruzicka@roma1.infn.it

- [1] E. Bianchi, J. Largo, P. Tartaglia, E. Zaccarelli, and F. Sciortino, Phys. Rev. Lett. **97**, 168301 (2006).
- [2] B. Ruzicka, L. Zulian, and G. Ruocco, Phys. Rev. Lett. **93**, 258301 (2004).
- [3] S. Jabbari-Farouji, G. H. Wegdam, and D. Bonn, Phys. Rev. Lett. **99**, 065701 (2007).
- [4] B. Ruzicka, L. Zulian, E. Zaccarelli, R. Angelini, M. Sztucki, A. Moussaïd and G. Ruocco, Phys. Rev. Lett. **104**, 085701 (2010).
- [5] B. Ruzicka, E. Zaccarelli, L. Zulian, R. Angelini, M. Sztucki, A. Moussaïd, T. Narayanan, and F. Sciortino, Nature Materials (in press).

# Nonequilibrium fluctuations of a Brownian particle in a quenched gelatin droplet

Juan Ruben Gomez-Solano,\* Artyom Petrosyan, and Sergio Ciliberto

Laboratoire de Physique, Ecole Normale Supérieure de Lyon,  
CNRS UMR 5672, 46, Allée d'Italie, 69364 Lyon CEDEX 07, France.

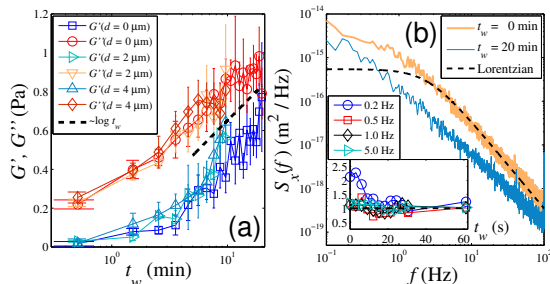


FIG. 1. (a) Time evolution of the storage and loss moduli ( $f = 5$  Hz) after the quench in different places inside the droplet (b) Power spectral density of fluctuations of  $x$  at two different  $t_w$ . Inset: Time evolution of the ratio  $\pi f S_x(f)/(2k_B T \text{Im}\{\chi(f)\})$  at different frequencies.

Gelatin is a thermoreversible gel that displays striking nonequilibrium phenomena when subjected to temperature variations due to their intricate microscopic structure. Aqueous gelatin solutions have a random coil structure above the gelation temperature  $T_{gel}$  resulting in a macroscopic viscous phase (sol) whereas below  $T_{gel}$  the formation of a helical cross-linked network leads to elastic behavior (gel) [1]. After a quench to a final temperature  $T < T_{gel}$  they exhibit physical ageing. Bulk rheological properties have been exhaustively studied along ageing in macroscopic samples showing that they share some common qualitative features with glassy systems [2].

In the present work we investigate whether complex nonequilibrium effects arise when the quench is locally performed in a micron-sized region within the gelatin bulk. In particular, we experimentally study the fluctuations of the position of a Brownian silica bead (radius =  $1\mu\text{m}$ ) surrounded by a gelatin droplet quenched through  $T_{gel} = 28^\circ\text{C}$ . A macroscopic sample (type-B pig skin gelatin, 10%wt in water) is kept at constant temperature  $26^\circ\text{C}$ . Then a laser beam ( $\lambda = 980$  nm, 200 mW) is tightly focused in the bulk using a microscope objective to locally rise the temperature  $12^\circ\text{C}$ . Therefore a sol droplet (radius =  $5\mu\text{m}$ ) is melted at  $T_0 = 38^\circ\text{C}$  in the gel bulk. The focused beam simultaneously confines the Brownian motion of the particle inside the droplet. Next, the laser power is suddenly decreased to 35 mW so that the temperature is homogenized by heat diffusion into the bulk in a few milliseconds resulting in an effective quench of the droplet to a final temperature  $T = 27.0^\circ\text{C}$ .

Immediately after the quench we measure the time evolution of a single coordinate  $x$  of the trapped particle. We use the particle as a mechanical probe to apply a small oscillatory shear and locally measure the

storage  $G'(f)$  and loss  $G''(f)$  moduli of the droplet at different frequencies  $f$  (active microrheology), see Fig. 1(a). We find that at a short waiting time  $t_w \lesssim 1$  min after the quench the droplet is purely viscous:  $G'(f) \approx 0$ . As  $t_w$  increases the droplet exhibits ageing similar to macroscopic quenches:  $G'(f)$  and  $G''(f)$  increase reaching a logarithmic growth  $\sim \log t_w$  in a few minutes. Active microrheology is also performed in other locations inside the droplet by displacing the position of the trap a distance  $d$  from the center. We find that the time evolution of  $G'$  and  $G''$  does not significantly change across the droplet and no abrupt variation of their values is detected. Thus the gelation of the droplet is not driven by a slow progressive front propagation of the gel phase into the sol phase but it is a collective evolution of the whole droplet.

Next, we study the influence of the droplet gelation on the fluctuations of the particle motion. We measure the time evolution of the power spectrum  $S_x(f)$  of  $x$  when the particle is subjected to the harmonic force of the optical trap and the fluctuating force of the gelatin chains. We observe that anomalous nonequilibrium fluctuations appear at  $t_w < 1$  min. If the droplet were in thermal equilibrium one should expect the Lorentzian power spectrum shown in Fig. 1(b). However, low frequency deviations ( $f < 1$  Hz) are observed whereas the high frequency side is well fitted by the equilibrium Lorentzian spectrum. We compare  $S_x(f)$  with the imaginary part of the Fourier transform  $\text{Im}\{\chi(f)\}$  of the linear response function of  $x$  when performing active microrheology at frequency  $f$  (inset of Fig. 1(b)). At very low frequencies the fluctuation-dissipation relation  $S_x(f) = 2k_B T \text{Im}\{\chi(f)\}/(\pi f)$  is violated, then the violation vanishes after a timescale of  $\sim 30$  s. As one approaches the high frequency side  $f > 1$  Hz the equilibriumlike fluctuations-response relation is satisfied for all  $t_w$ . Thus for early ageing times one can split the fluctuations of the droplet into a fast equilibriumlike component due to the thermal motion of the gelatin chains plus a slow nonequilibrium one due to the formation of the viscoelastic gel network. Once that the viscoelastic phase ( $G'(f) > 0$ ) is formed, the anomalous fluctuations vanish and the particle motion behaves as in equilibrium with the collective behavior of the droplet at the temperature of the gelatin bulk.

\* Corresponding author: juan.gomez\_solano@ens-lyon.fr

[1] M. Djabourov, J. Leblond and P. Papon, *J. Phys. France* **49**, 319 (1988).  
[2] A. Parker and V. Normand, *Soft Matter* **6**, 4916 (2010).

## Faceted polyhedral colloidal ‘rocks’: low-dimensional slow networks

Rebecca Rice,<sup>1</sup> Roland Roth,<sup>2</sup> and C. Patrick Royall<sup>1,\*</sup>

<sup>1</sup>*University of Bristol*

<sup>2</sup>*Friedrich-Alexander-University of Erlangen-Nurnberg*

Among the most basic models of condensed matter are hard particles with an attractive interaction. Attractive hard spheres, epitomized experimentally by colloidal suspensions with added polymer whose entropy mediates an effective attraction between the particles. These colloid-polymer mixtures exhibit the phases of gas, liquid and crystal and form a benchmark in statistical mechanics as their behaviour is well understood [1]. Much attention focuses on states with slow dynamics such as metastable gels. Here spinodal phase separation into a gas and liquid phase is suppressed due to the high density of the liquid phase such that it exhibits slow dynamics. These slow dense regions form a network which becomes the ‘arms’ of the gel [2, 3]. However, ultimately such gels undergo phase separation [4]. Stabilisation of gels may be achieved by reducing valency [5, 6] or with competing interactions which lead to a complex energy landscape and stable gels [4, 7].

Here we consider another approach to producing a long-lived network: particle geometry. We exploit the opportunity presented by the current explosion in anisotropic colloidal particles [8] to produce nanostructures with novel architectures. Although colloids with a huge variety of shapes have been synthesized, systematic studies of bulk systems are limited. Gels of colloidal rods have been produced [9] and polyhedra can frustrate long-ranged ordering at high density [10].

We introduce a new colloidal model system, of faceted polyhedra, or ‘rocks’ and study its gelation behaviour. Despite striking similarities with equilibrium gels formed from reduced valency systems, here we argue that phase separation is suppressed, not by slow dynamics due to the high local colloid density of the ‘arms’ as is the case of spherical particles, but instead that the polyhedral nature of these particles leads to rigid structures and networks of low dimensionality. We use confocal microscopy and real space analysis at the single particle level to study the gelation behaviour of both ‘rocks’ and spheres.

This change in particle geometry has two main consequences. Firstly, the overlap volume around two approaching rocks from which the centre of mass of polymer coils is excluded, which leads to the depletion attraction, is much reduced [Fig. 1(e)]. Thus we expect that more polymer is required in the case of the ‘rocks’, for a given degree of attraction. Secondly, two bonding between two ‘rocks’ is rigid.

We also introduce a model which we argue captures the geometric essence of the colloidal rocks: wireframe dodecahedra populated with 109 spheres as shown in Fig. 1(b). Each sphere interacts via a short-ranged

square-well interaction. Here we use kinetic Monte Carlo with a very short step length and rotations through a small angle, which approximates Brownian dynamics.

Confocal images of gels of rocks and spheres are shown in Fig. 1(c) and (d). The difference is striking, in that rocks form one-particle wide chains and spheres form more densely packed structures. The polymer mass fraction for gelation  $c_p^{gel}$  in the case of rocks is around five times that in required for the spheres, reflecting the difference in overlap volume. One might expect, from Figs. 1(c) and (d) that gels of rocks have a lower fractal dimension than spheres. This we indeed find, both in experiment and simulation. We access the dynamics of gel coarsening with simulation and find that the ‘rock’ geometry vastly increases the lifetime of the gel.

RR and CPR gratefully acknowledge the Royal Society for funding.

\* Corresponding author: paddy.royall@bristol.ac.uk

- [1] W. C. K. Poon, *J. Phys.: Condens. Matter* **14**, R859 (2002).
- [2] N. A. M. Verhaegh, D. Asnaghi, H. N. W. Lekkerkerker, M. Giglio, and L. Cipelletti, *Physica A* **242**, 104 (1997).
- [3] P. J. Lu *et al.*, *Nature* **435**, 499 (2008).
- [4] E. Zaccarelli, *J. Phys.: Condens. Matter* **19**, 323101 (2007).
- [5] E. Bianchi, J. Largo, P. Tartaglia, E. Zaccarelli, and F. Sciortino, *Phys. Rev. Lett.* **97**, 168301 (2006).
- [6] E. Del Gado and W. Kob *Soft Matter* **6**, 1547 (2010).
- [7] C. L. Klix, C. P. Royall, and H. Tanaka, *Phys. Rev. Lett.* **104**, 165702 (2010s).
- [8] S. C. Glotzer and M. J. Solomon, *Nature Materials* **6**, 557 (2007).
- [9] G. M. H. Wilkins, P. T. Spicer, and M. J. Solomon, *Langmuir* **25**, 8951 (2009).
- [10] R. P. A. Dullens *et al.*, *Phys. Rev. Lett.* **96**, 028304 (2006).

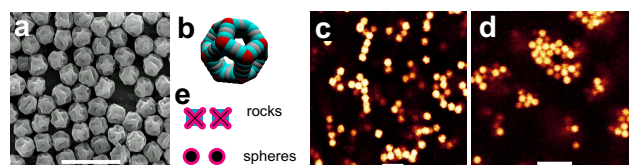


FIG. 1. **a** SEM image of colloidal ‘rocks’. **b** dodecahedral wireframe model rock populated with 109 spheres. Colors denote vertex, vertex neighbour mid-side spheres. **c** confocal microscopy image of a gel of rocks  $c_p/c_p^{gel} = 1.13$ . **d** confocal microscopy image of a gel of spheres  $c_p/c_p^{gel} = 1.44$ .  $c_p$  is polymer concentration. Scale bars in a,c,d are  $10\ \mu\text{m}$ . Both **c** and **d** correspond to a colloid packing fraction  $\phi_c = 0.05$ .

## Six ‘critical’ packing fractions for disordered hard sphere systems

Ludovic Berthier\*

*Laboratoire des Colloïdes, Verres et Nanomatériaux, Université Montpellier 2,  
34095 Montpellier, France & CNRS UMR 5587*

Hard spheres have emerged as one of the simplest model systems to study various phenomena in condensed matter physics. In recent years, they have in particular attracted interest in the context of the glass transition observed in liquids, with experimental realizations in colloidal systems, and in the context of the athermal jamming transition, where they can be seen as idealized granular materials. In the literature, the most often quoted relevant packing fractions associated to these two transitions are  $\phi_{\text{glass}} \simeq 0.58$  for the glass transition, and  $\phi_{\text{jamming}} \simeq 0.64$  for the jamming transition, which both stem from pioneering experimental work on colloids and grains. However, the glass transition is sometimes located very close to  $\phi = 0.64$ , while theoretical concepts used for one transition are often applied to the other (in both directions). Progress to disentangle (or merge) these two problems have been slow, in particular because it is hard both in practice and at the conceptual level to rigorously locate, define, and thus compare the location of these transitions.

Here, we review the outcome of a recent numerical and theoretical effort aiming at clarifying the location of the various transitions in a particular hard sphere model in three dimensions, see Table I. The studied model is a 50:50 binary mixture of spheres with diameter ratio 1.4, which is empirically found to be particularly robust against crystallization, so that crystalline ordering does not interfere with the obtained results.

In a first effort, the relaxation dynamics of the system at thermal equilibrium was investigated in detail, allowing the relaxation time to be followed over a very broad window, using both direct fitting [1], and an original scaling approach involving a soft version of the hard sphere potential [2]. This allowed the determination, for this particular system, of three ‘critical’ packing fraction, depending on the precise way the dynamic divergence is determined. We used a mode-coupling theory algebraic fit, and two distinct exponential divergences, with results indicated in Table I. Note that the mode-coupling description breaks down dramatically near and above  $\phi_{\text{mct}}$ , suggesting no genuine dynamic singularity occurs at this density. The glass transition then occurs at much higher volume fraction, closer to  $\phi_{\text{jamming}}$  than previously thought.

These findings suggested the need for a second effort, to locate more precisely the jamming transition for the same particular system at hand. We thus investigated the purely geometric, far from equilibrium problem of sphere packing in the absence of thermal fluctu-

ations. In this context also, it was found that defining rigorously, and measuring precisely the location of

Definition	Volume fraction
Onset of glassy dynamics	$\phi_{\text{onset}} \approx 0.56$
Mode-coupling theory	$\phi_{\text{mct}} = 0.592$
Vogel-Fulcher-Tamman	$\phi_{\text{vft}} = 0.615$
Dynamic scaling	$\phi_0 = 0.635$
Diverging pressure (upper bound)	$\phi_{\text{up}} = 0.648$
Diverging pressure (lower bound MC)	$\phi_{\text{low}} = 0.662$
Diverging pressure (lower bound REMC)	$\phi_{\text{low}} = 0.669$

TABLE I. Values of the relevant volume fractions characterizing the physical behaviour of the fluid dynamics for a particular hard sphere binary mixture. We report three critical packing for the equilibrium dynamics, and three values for the location of the geometric jamming transition where the pressure of the packing diverges.

the jamming density is a difficult problem, even when crystalline ordering does not play any role. We found that the jamming transition actually occurs along a continuous range of volume fractions, and we report in Table I numerical estimates for the boundaries of the numerically accessible range of jamming packing fractions.

In particular, we find that compressing hard spheres more slowly (while avoiding crystallization) produces larger jamming densities. This suggests that if one takes the view that glass and jamming transitions occur together, then they should occur at least above  $\phi = 0.669$ , a lower bound which we recently found using an efficient replica exchange Monte Carlo algorithm [4]. In the opposite view that both transitions are distinct phenomena, one should understand better the possible existence of sharp boundaries for the occurrence of the jamming transition, and obtain more data to understand more precisely not only the location but also the nature of the glass transition.

\* Corresponding author: berthier@lcvn.univ-montp2.fr

- [1] G. Brambilla, D. El Masri, M. Pierno, G. Petekidis, A. B. Schofield, L. Berthier, and L. Cipelletti, *Phys. Rev. Lett.* **102**, 085703 (2009).
- [2] L. Berthier and T. A. Witten, *Europhys. Lett.* **86**, 10001 (2009).
- [3] P. Chaudhuri, L. Berthier, and S. Sastry, *Phys. Rev. Lett.* **104**, 165701 (2010).
- [4] G. Odriozola and L. Berthier, arXiv:1010.5607.

## Glass Transition in Driven Granular Matter

Matthias Sperl\*

*Institut für Materialphysik im Weltraum, Deutsches Zentrum für Luft- und Raumfahrt (DLR), 51170 Köln, Germany*

\* Corresponding author: [matthias.sperl@dlr.de](mailto:matthias.sperl@dlr.de)

This abstract is not available in this version.

## Microscopic many-body theory of the jamming transition

Hugo Jacquin,<sup>1,\*</sup> Ludovic Berthier,<sup>2</sup> and Francesco Zamponi<sup>3</sup>

<sup>1</sup>*Laboratoire Matière et Systèmes Complexes, UMR CNRS 7057, Université Paris Diderot – Paris 7, 10 rue Alice Domon et Léonie Duquet, 75205 Paris cedex 13, France*

<sup>2</sup>*Laboratoire des Colloïdes, Verres et Nanomatériaux, UMR CNRS 5587, Université Montpellier 2, 34095 Montpellier, France*

<sup>3</sup>*Laboratoire de Physique Théorique, École Normale Supérieure, 24 Rue Lhomond, 75231 Paris Cedex 05, France*

In 1998, Liu and Nagel proposed their provocative “jamming phase diagram” [1], where they suggested that the glass state of liquids and the jammed state of granular materials can be unified into a single phase diagram, with density, temperature and shear as control parameters. The glass transition would be seen, in this picture, as a dynamical arrest controlled by the jamming transition.

In this work, we show that reverting Liu’s idea, and considering the jamming transition with theoretical tools usually used to describe the glass transition can lead to quantitatively satisfying predictions on the jamming transition.

Pioneer works of Monasson [2] and Mézard and Parisi [3, 4], and following work by Parisi and Zamponi [5] showed the way to apply the mean-field concepts originated from spin-glasses, such as complexity and the replica method, in order to predict glass transitions for hard spheres and high temperature liquids, and the jamming point of hard spheres. However, the Mézard-Parisi (MP) approach breaks down at low temperature, while the Parisi-Zamponi (PZ) approach is valid only for hard spheres. In order to assert the critical nature of the jamming point in the jamming phase diagram, we need to have at least two control parameters, thus reconcile these two approaches.

We applied, and extended when necessary, the replica calculations of MP and PZ to a model system that can interpolate between finite temperature glasses and hard spheres: the model of harmonic spheres, an assembly of  $N$  spherical particles of diameter  $\sigma$  enclosed in a volume  $V$  in three spatial dimensions, interacting with a soft repulsion of finite range. We choose the pair potential

$$V(r \leq \sigma) = \epsilon(1 - r/\sigma)^2, \quad V(r > \sigma) = 0, \quad (1)$$

where  $r$  is the interparticle distance, and  $\epsilon$  controls the strength of the repulsion. The model (1), originally proposed to describe wet foams [6], has become a paradigm in numerical studies of the  $T = 0$  jamming transition [7, 8]. The model has the two needed control parameters: the temperature,  $T$ , (expressed in units of  $\epsilon$ ), and the fraction of the volume occupied by the particles in the absence of overlap:  $\phi = \pi N \sigma^3 / (6V)$ .

To address the purely geometrical packing problem of soft spheres, we studied first the statistical mechanics

of the model (1) at finite temperatures, before taking the  $T \rightarrow 0$  limit where jamming occurs. Our central theoretical achievement is an approximation scheme that interpolates between those of MP and PZ, allowing us to explore the jamming phase diagram, verify theoretically a large number of observed behaviours of harmonic spheres, and predict new results for the correlation functions of this system around the jamming transition.

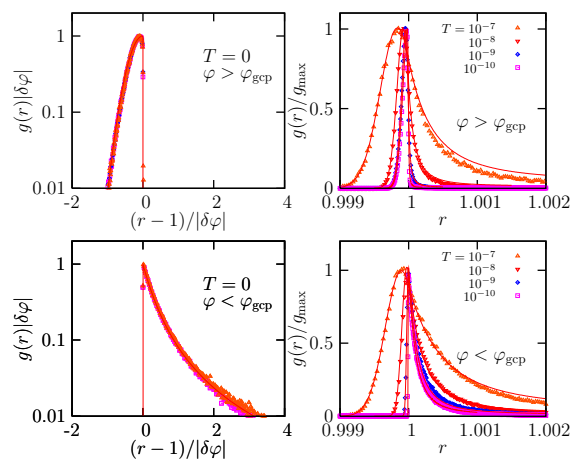


FIG. 1. The pair correlation near jamming predicted by theory (full lines) and measured in numerical simulations (symbols). Left panels: scaling behaviour at  $T = 0$  above (top) and below (bottom) the jamming transition showing the convergence of the first peak near  $r = 1$  to a delta function with asymmetric scaling functions on both sides of the transition. Right panels: the first peak of the pair correlation broadens when  $T$  increases at constant  $\phi$  above (top:  $\delta\phi = 2.8 \cdot 10^{-4}$ ) and below the transition (bottom  $\delta\phi = -3.5 \cdot 10^{-4}$ ). To ease visualisation, we show the evolution of  $g(r)/g_{max}$ , where  $g_{max}$  is the maximum of the pair correlation function.

\* Corresponding author: hugo.jacquin@univ-paris-diderot.fr

- [1] A. J. Liu and S. R. Nagel, *Nature* **396**, 21 (1998).
- [2] R. Monasson, *Phys. Rev. Lett.* **75**, 2847 (1995).
- [3] M. Mézard and G. Parisi, *J. Chem. Phys.* **111**, 1076 (1999).
- [4] M. Mézard and G. Parisi, *Phys. Rev. Lett.* **82**, 747 (1999).
- [5] G. Parisi and F. Zamponi, *Rev. Mod. Phys.* **82**, 789 (2010).
- [6] D. J. Durian, *Phys. Rev. Lett.* **75**, 4780 (1995).
- [7] C. S. O’Hern, S. A. Langer, A. J. Liu, and S. R. Nagel, *Phys. Rev. Lett.* **88**, 075507 (2002).
- [8] M. van Hecke, arXiv:0911.1384v1 (2009).

## Structural Correlations in Jammed and Glass-Forming Hard Sphere Fluids

Patrick Charbonneau,<sup>1,\*</sup> Benoit Charbonneau,<sup>2</sup> Yuliang Jin,<sup>3</sup> and Francesco Zamponi<sup>4</sup>

<sup>1</sup>*Departments of Chemistry and Physics, Duke University, Durham, North Carolina 27708, USA*

<sup>2</sup>*St. Jerome's University and Department of Pure Mathematics, University of Waterloo, Waterloo, Ontario N2L 3G1, Canada*

<sup>3</sup>*Levich Institute and Physics Department, City College of New York, New York, New York 10031, USA*

<sup>4</sup>*LPTENS, CNRS UMR 8549, associée à l'UPMC Paris 06, 24 Rue Lhomond, 75005 Paris, France*

Glass formation and jamming are intimately related, and theoretical approaches to describe the two are gradually converging [1, 2]. For instance, recent studies have detected the presence of a growing static lengthscale associated with the glassy dynamical slowdown [3], and attempted to characterize the static correlations found in jammed structures [4]. Yet no satisfying microscopic description of a growing static lengthscale has yet been formulated. In this presentation, we discuss recent progress made on this question from two different theoretical approaches. To simplify the geometrical characterization, we consider frictionless monodisperse hard spheres, which are good structural models for dense fluids. Though in two and three dimensions rapid crystallization interferes with the study of deeply supersaturated fluids, going to higher dimensions dramatically reduces this interference [5]. Higher-dimensional systems are also less affected by fluctuations – and dynamical heterogeneity [6], which simplifies the geometrical analysis. Explicitly considering the dimensional dependence further constrains the microscopic description to be generalizable to systems in which the number of nearest neighbors is large.

We first study the role of correlations in sphere packings by generalizing to arbitrary dimensions the jamming limit obtained from Edwards' statistical mechanics [7], using a liquid-state theory description [4]. The approach provides a general method for relating the isostatic surface constraint to the global packing properties. Eliminating most other structural correlations and contact fluctuations give an asymptotic scaling  $\phi \sim d2^{-d}$  that is similar to that of more elaborate approaches, such as replica theory and density functional theory, but with a different prefactor. This consistency suggests that in amorphous packings of spheres spatial correlations are suppressed or at least renormalizable in high dimensions. The various structural approximations in low dimensions are assessed by comparing with three- to six-dimensional isostatic packings from simulations, which provides an error estimate for the earlier study of 3D jamming [7]. The simplicity of the approach offers a starting point to systematically obtain a geometrical understanding of the higher-order correlations present in jammed packings. Possible inclusions of relevant correlations to two- and three-dimensional packings will be discussed.

Second, we critically evaluate the hypothesis that correlated structural defects could lead to a growing

length scale and relaxation time in deeply supersaturated fluids [8]. Though a clear structural signature of a developing order in increasingly supersaturated systems is found (see Fig. 1), the resulting defect geometry does not lead to a growing length scale based on the Frank-Kasper defect scenario [9]. A dimensional perspective further supports a vanishing contribution of such structures to the dynamical slowdown. The dimensionally generalizable nature of the defects themselves, however, provide other avenues for describing microscopic length scales. Different proposals will be discussed.

\* Corresponding author: patrick.charbonneau@duke.edu

- [1] G. Parisi and F. Zamponi, *Rev. Mod. Phys.* **82**, 789 (2010).
- [2] S. Torquato and F. H. Stillinger, *Rev. Mod. Phys.* **82**, 2633 (2010).
- [3] G. Biroli, J. P. Bouchaud, A. Cavagna, T. S. Grigera, and P. Verrocchio, *Nature Physics* **4**, 771 (2008).
- [4] Y. Jin, P. Charbonneau, S. Meyer, C. Song, and F. Zamponi, *Phys. Rev. E*, in press (2010).
- [5] J. A. van Meel, B. Charbonneau, A. Fortini, and P. Charbonneau, *Phys. Rev. E* **80**, 061110 (2009).
- [6] P. Charbonneau, A. Ikeda, J. A. Van Meel, and K. Miyazaki, *Phys. Rev. E* **81**, 040501(R) (2010).
- [7] C. Song, P. Wang, and H. A. Makse, *Nature* **453**, 629 (2008).
- [8] D. R. Nelson, *Defects and geometry in condensed matter physics* (Cambridge University Press, Cambridge, 2002).
- [9] B. Charbonneau and P. Charbonneau, in preparation (2010).

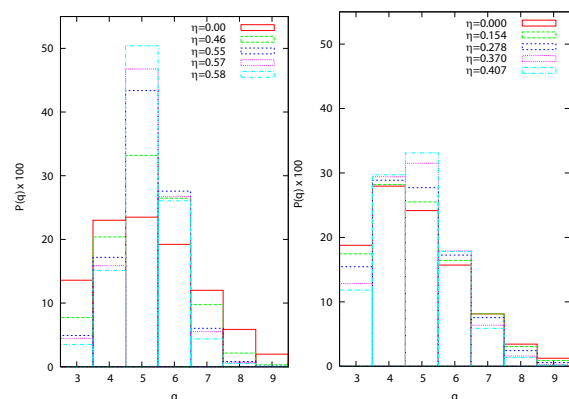


FIG. 1. The spindle order  $q$  (defect) distribution in bidisperse 3D (left) and monodisperse 4D (right) hard spheres shows a growing structural order as the volume fraction  $\eta$  of the fluid increases [9].

# Macroscopic, mesoscopic and microscopic regimes for the dynamical properties of disordered systems

Giulio Monaco\*

European Synchrotron Radiation Facility, 6 rue Jules Horowitz, BP 220, 38043 Grenoble Cedex, France

It is largely accepted that disordered systems are characterized by a short range order usually very similar to that of the corresponding crystalline phase at the same density. It is less clear to what extent dynamic properties of disordered systems and crystals can be compared. In particular, high-frequency collective excitations reminiscent of phonons in solids exist as well in disordered systems. They are traditionally discussed in terms of relaxation processes characteristic of the disordered state [1].

We present here a quantitative comparison of the collective excitations in liquid and polycrystalline sodium [2]. We show that liquid sodium exhibits acoustic excitations of both longitudinal and transverse polarization at frequencies strictly related to those of the corresponding crystal. The only relevant difference between the liquid and the polycrystal appears in the broadening of the excitations: an additional disorder-induced contribution comes into play in the case of the liquid, which we show to be related to the distribution of local structures around the average one. This is then the microscopic regime for the dynamics of a disordered system, and it corresponds to the short range order lengthscale.

On the opposite side of the lengthscale, in the macroscopic regime the dynamical properties of a disordered system can be described treating it as an isotropic continuum. This regime is well known in many details [1]. It is clear that the macroscopic and microscopic regimes must be separated by an intermediate regime, the mesoscopic one. We present here an experimental [3] and numerical [4] study of this mesoscopic regime looking at the acoustic dynamics of glasses.

We study in particular how, on decreasing the acoustic wavelength, the continuum, Debye approximation for the acoustic dynamics breaks down. In crystals, this takes place when the wavelength approaches the interatomic distance. We show here that in glasses this instead takes place on the lengthscale characteristic of the medium range order. Specifically, we find that the acoustic excitations with nanometric wavelengths show the clear signature of being strongly scattered. This crossover region is accompanied by a characteristic softening of the acoustic excitations that marks the breakdown of the Debye approximation, see Fig. 1.

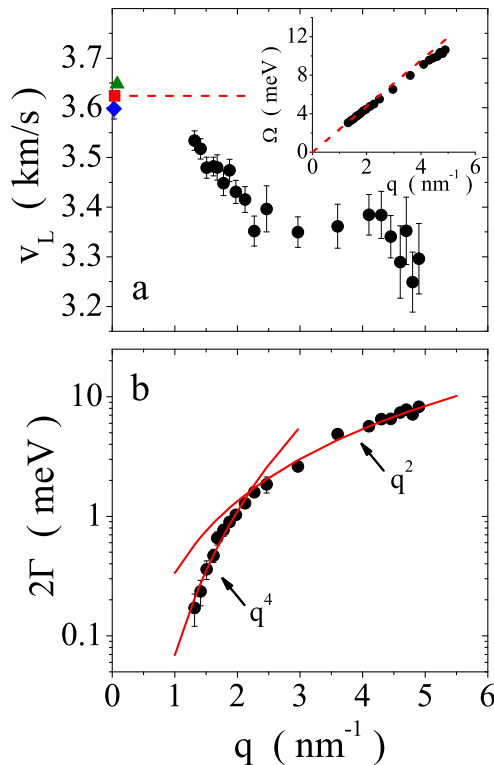


FIG. 1. Breakdown of the Debye approximation in glasses for the acoustic modes with nanometric wavelengths. Up:  $q$ -dependence of the apparent longitudinal phase velocity of a glycerol glass at 150.1 K derived from an inelastic x-ray scattering (IXS) experiment (black circles) and from lower frequency techniques: stimulated Brillouin gain spectroscopy (blue rhomb), Brillouin light scattering (red square), and inelastic ultraviolet scattering (green triangle), see Ref. [3] for the references to the original publications. The dashed line indicates the macroscopic sound limit. Insert: the low  $q$  portion of the acoustic-like dispersion curve (black circles). The dashed line corresponds to that in the main panel. Down:  $q$  dependence of the broadening (FWHM) of the acoustic excitations derived from IXS (black circles). The red lines correspond to the best  $q^4$  and  $q^2$  functions fitting the low and the high- $q$  portion of the IXS data, respectively.

\* Corresponding author: gmonaco@esrf.fr

- [1] J. P. Boon and S. Yip, *Molecular Hydrodynamics* (Dover, New York, 1991).
- [2] V. Giordano and G. Monaco, Proc. Natl. Acad. Sci. USA (accepted).
- [3] G. Monaco and V. Giordano, Proc. Natl. Acad. Sci. USA **106**, 3659 (2009).
- [4] G. Monaco and S. Mossa, Proc. Natl. Acad. Sci. USA **106**, 3659 (2009).

## Nanophase Separation and Anomalous Dynamics in Comb-like Polymers

A. Arbe,<sup>1,\*</sup> A. Moreno,<sup>1</sup> and J. Colmenero<sup>1,2</sup>

<sup>1</sup>*Centro de Física de Materiales (CSIC, UPV/EHU) and Materials Physics Center MPC, Paseo Manuel de Lardizabal 5, E-20018 San Sebastián, Spain*

<sup>2</sup>*Donostia International Physics Center, Paseo Manuel de Lardizabal 4, 20018 San Sebastián, Spain.*

The structure and dynamics of comb-like polymers have been extensively studied by different experimental techniques. In most of the systems investigated the side-group (SG) contains an alkyl chain of varying length, and the backbone is much more rigid, like in poly(*n*-alkyl methacrylates) (PnMAs). From X-ray diffraction, a kind of nano-phase separation has been suggested: SGs of different monomeric units would tend to aggregate, forming self-assembled nanodomains. The existence of two different glass-transitions was also proposed: one associated to the freezing of the motions within the alkyl nanodomains and the other with that of the main-chain (MC) dynamics (see, e. g. [1]). Such a scenario mainly rests on calorimetric, dielectric, mechanical and X-ray studies, that are not selective for MC and SG contributions.

We have exploited neutron scattering capabilities combined with isotopic labeling to *selectively* study the MC and SG components in some PnMAs [2, 3]. Our diffraction experiments provide strong support to the nanosegregated structure. Moreover, while the structural relaxation of the MCs shows standard features (Fig. 1), anomalous behavior for the dynamics of the SGs emerge: extremely stretched functional forms, decoupling of self- and collective motions (Fig. 1) and Arrhenius-like behavior. Two main possible ingredients might be invoked to account for these peculiarities: distributions of relaxation times along the SGs and confinement by the much slower relaxation of the rigid MC-matrix. In this framework, the dynamic asymmetry found between MC and SGs (see the large difference in characteristic times in Fig. 1) would play an essential role. Several questions remain unsolved, e. g.: Is nanosegregation induced by incompatibility of MCs and SGs, or does it arise just from the architecture of the polymer? Do MCs show 'standard' behavior also at length scales smaller than the average inter-molecular distances? Are the distributions of mobilities within the SGs as broad as those deduced from the experiments (several orders of magnitude!)?

To get a deeper insight, we have performed extensive simulations of a bead-spring model for comb copolymers with dynamic asymmetry, namely with the slow and fast components located respectively at the MC and at the SGs [4]. The static and dynamic correlators obtained from simulations reproduce the trends observed in the experiments on PnMAs. We confirm the proposed scenario of nanodomain formation. Moreover we show that the latter can have a purely entropic origin, and takes place even for homopolymer

combs provided that the density of branch points is high enough. In analogy with the experiments, the analysis of scattering functions reveals a decoupling of self- and collective dynamics for the fast component in the arms, and strongly stretched relaxation. Characterization of dynamic heterogeneity shows that stretching is an intrinsic feature and is not necessarily related to gradients of mobility. Due to the generic character of the bead-spring model, we suggest that the observed scenario will be a general feature of comb copolymers with dynamic asymmetry.

We thank A.-C. Genix, S. Arrese-Igor, P. Fouquet and D. Richter for their participation in the experimental works. We acknowledge support from the European Commission NoE SoftComp, Contract NMP3-CT-2004-502235 and the projects MAT2007-63681, IT-436-07 (GV) and the Spanish Ministerio de Educación y Ciencia (Grant No. CSD2006-53).

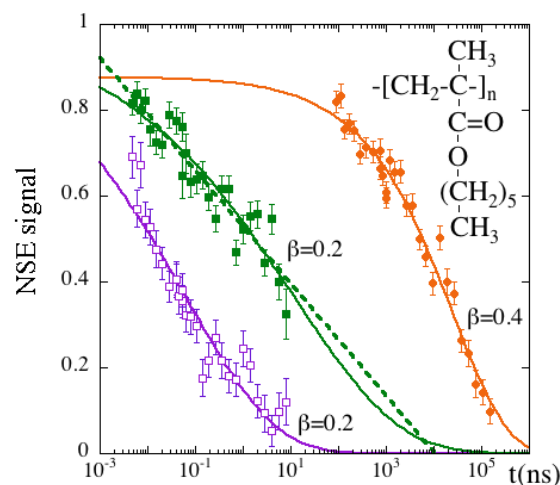


FIG. 1. Neutron Spin Echo signal measured on poly(hexyl methacrylate) probing the structural relaxation of MCs (full squares) and within the nanodomains (full circles), and the self-motions of SG-hydrogens (empty squares) at  $T \approx 320$  K (full circles have been measured at 480 K and shifted). Solid lines: fits to stretched exponentials  $A \exp[-(t/\tau)^\beta]$ ; dotted line: logarithmic description.

\* Corresponding author: a.arbe@ehu.es

- [1] M. Beiner, *Macromol. Rapid Commun.* **22**, 869 (2001).
- [2] A. Arbe, A.-C. Genix, J. Colmenero, D. Richter, and P. Fouquet, *Soft Matter* **4**, 1792 (2008).
- [3] A. Arbe, A.-C. Genix, S. Arrese-Igor, J. Colmenero, and D. Richter, *Macromolecules* **43**, 3107 (2010).
- [4] A. Moreno, A. Arbe, and J. Colmenero, submitted to *Macromolecules*.

## Computer simulation study of structure and dynamics of elementary excitations in model glass forming liquids

David Chandler,<sup>1</sup> Aaron S. Keys,<sup>1,\*</sup> Lester O. Hedges,<sup>2</sup> Sharon C. Glotzer,<sup>3</sup> and Juan P. Garrahan<sup>4</sup>

<sup>1</sup>University of California Berkeley, California 94720 USA

<sup>2</sup>Lawrence Berkeley National Laboratory, Berkeley, California 94720 USA

<sup>3</sup>University of Michigan, Ann Arbor, Michigan 48109 USA

<sup>4</sup>University of Nottingham, Nottingham NG7 2RD

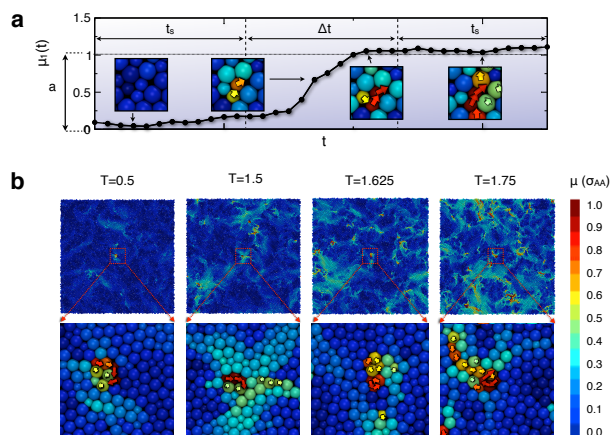


FIG. 1. Elementary excitations of length scale  $a$  for a  $d = 2$  glass forming liquid mixture at several supercooled temperatures. The onset temperature for this system is  $T_0 = 2.6$ . Panel (a) illustrates the meaning of excitation times  $\Delta t$  and  $t_s$  for a tagged particle a distance  $\mu_1(t)$  from its initial position. Panel (b) illustrates typical excitations within the context of surrounding dynamic heterogeneity. Color code indicates the distance particles move from initial conditions in a time  $\Delta t + 2t_s$ .

For several atomistic models of glass formers, at conditions below their glassy dynamics onset temperatures,  $T_0$ , we use importance sampling of trajectory space [1] to study the structure, statistics and dynamics of elementary excitations, all of which we relate to dynamic heterogeneity. We define elementary excitations in terms of irreversible particle displacements. At supercooled conditions, we find that these excitations are sparse and localized, with an average radius that is temperature independent. This radius is larger than a single particle displacement,  $a$ , but it is no larger than a few molecular diameters. As a function of temperature,  $T < T_0$ , the equilibrium concentration of these excitations is proportional to  $\exp[-J_a(1/T - 1/T_0)]$ , where the energy  $J_a$  is dependent upon the displacement length. For  $a$  between 0.2 and 2 molecular diameters, we find  $J_a \propto \ln a$ . We further find that the onset temperatures found from this fitting are the same as those found from the structural relaxation time [3],  $\tau \propto \exp[J^2(1/T - 1/T_0)^2]$ , and the variation of  $J$  with respect to changing density is identical to that for  $J_{\bar{a}}$ , where  $2\pi/\bar{a}$  is the value of the wave-vector at the principal peak in the liquid structure factor.

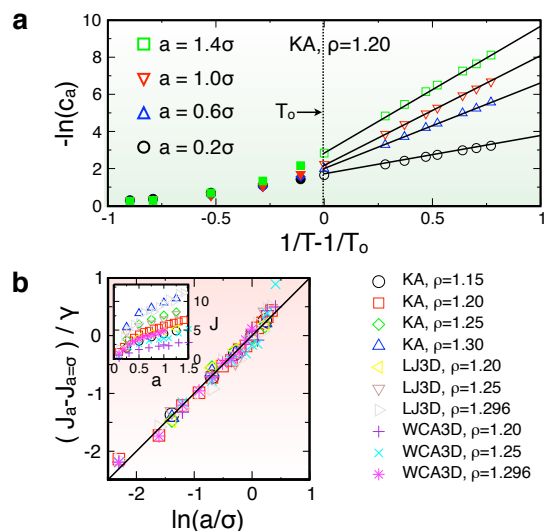


FIG. 2. Temperature dependence of elementary excitation concentrations (a) and energy scales of elementary excitations (b) for several displacement lengths,  $a$ , for various glass forming liquid mixtures.

Figures 1 and 2 illustrate some of our findings. The scalings we establish are consistent with the hierarchical dynamics of the arrow model [2], which in  $d = 1$  is the East model [4]. In particular, the structure of the elementary excitations are microcosms of larger scale dynamic heterogeneity that emerges from the facilitated dynamics of the elementary excitations. A growing length scale that directly relates to the slowing of dynamics upon cooling or compressing the liquids is the growing distance between localized excitations. In resolving the facilitated nature of the dynamics, all length scales must be accounted for. Too crude a spatial resolution can obscure the role of facilitation, especially as temperature decreases.

This research has been supported by the NSF, the DOE, and the EPSRC.

\* Corresponding author: askeys@berkeley.edu

- [1] P. G. Bolhuis et al., *Annu. Rev. Phys. Chem.* **59**, 291 (2002).
- [2] J. P. Garrahan and D. Chandler, *Proc. Natl. Acad. Sci. USA* **100** 9710 (2003).
- [3] Y. S. Elmatad, D. Chandler and J.P. Garrahan, *J. Phys. Chem. B* **113**, 5563 (2009).
- [4] F. Ritort and P. Sollich, *Adv. Phys.* **52**, 219 (2003).

## The role of attractive forces in visquous liquids and its consequence for theories of the glass transition

Gilles Tarjus<sup>1,\*</sup> and Ludovic Berthier<sup>2</sup>

<sup>1</sup>*LPTMC, CNRS-UMR 7600, Université Pierre et Marie Curie, boîte 121, 4 Pl. Jussieu, 75252 Paris cédex 05, France*

<sup>2</sup>*LCVN, Université Montpellier II and CNRS, 34095 Montpellier, France*

The so-called ‘van der Waals picture of liquids’, *i.e.* the predominance of the short-ranged repulsive part of the intermolecular potentials in determining the structure of dense nonassociated liquids, has proved very fruitful for predicting the pair correlation functions, the thermodynamics, and the dynamics of liquids. More recently, this picture has been transposed to the viscous (supercooled) liquid regime and a number of approaches have either suggested or taken for granted that the structure and the dynamics of viscous glass-forming liquids are also controlled by the short-ranged repulsive forces. Prior to our work, this hypothesis however had never been directly studied. We have filled this gap by comparing via Molecular Dynamics simulation the structure and the dynamics of a standard model of glass-forming liquid, a binary Lennard-Jones mixture (LJ), and its reduction to the purely repulsive part of the pair potentials, truncated at the minimum of the full pair potential, proposed by Weeks, Chandler and Andersen (WCA).

We have found that the viscous slowing down of the two systems is quantitatively and qualitatively different over a broad range of density, whereas the static pair correlations remain very close: see Fig. 1. The qualitative difference in the dynamics shows up as an impossibility to rescale even approximately the dynamics of the two systems through a single effective energy/temperature parameter. In particular, the isochoric fragility of the LJ liquid is essentially independent of density, as also found experimentally in glass-forming liquids and polymers, while that of the WCA liquid is strongly dependent on density [1].

We discuss the consequences of these results for several approaches of the glass transition that describe the dynamics in the supercooled regime on the basis of the static pair correlations, such as the mode-coupling theory in its common implementation. How far can one go with the idea that a small change in the static pair correlations can be extremely amplified in the dynamics? We show that the answer is not favorable for the mode-coupling theory[1] and a few other approaches. Our results also raise a question about the actual role of the attractive forces in glass formation. The WCA reduction of the LJ poten-

tial actually involves two distinct aspects: neglecting the attractive forces (which are only included in the thermodynamics as a cohesive background) and truncating the range of the potential to a finite distance. Which one of these two procedures is the more severe for the dynamics? We address this issue on the basis of recent studies by us [2] and others. Our findings cast some serious doubts on the relevance of the jamming scenario, in which the slowing down of relaxation is controlled by a critical point J that is only defined for a truncated repulsive potentials, for glassforming liquids and polymers.

\* Corresponding author: tarjus@lptl.jussieu.fr

- [1] L. Berthier and G. Tarjus, *Phys. Rev. Lett* **103**, 170601 (2009); *Phys. Rev. E* **82**, 031502 (2010).  
 [2] L. Berthier and G. Tarjus, in preparation.

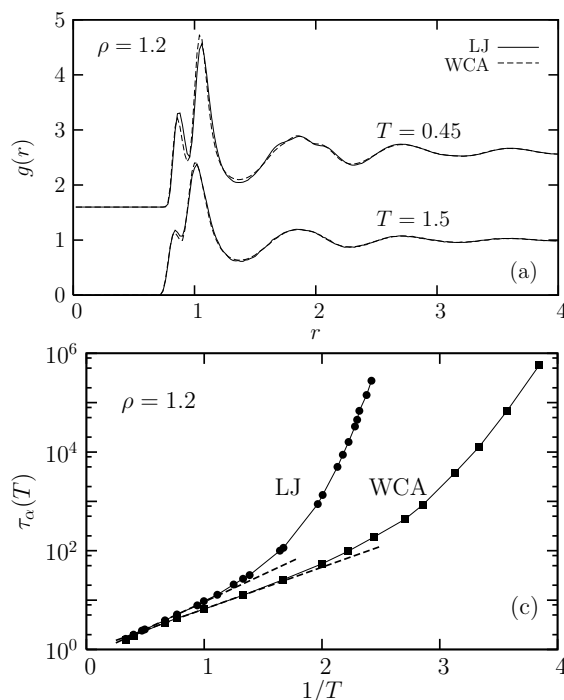


FIG. 1. Comparison between the LJ and its WCA description at the liquid density  $\rho = 1.2$ . Top: Static pair correlation functions. Bottom: Arrhenius plot of the relaxation time.

## Structural signature of slow dynamics in supercooled liquids: Critical-like glassy structural ordering

Hajime Tanaka,<sup>1,\*</sup> Takeshi Kawasaki,<sup>1,2</sup> and Mathieu Leocmach<sup>1</sup>

<sup>1</sup>*Institute of Industrial Science, University of Tokyo, Meguro-ku, Tokyo 153-8505, Japan*

<sup>2</sup>*Present Address: Department of Physics, Kyoto University, Sakyo-ku, Kyoto 606-8502, Japan*

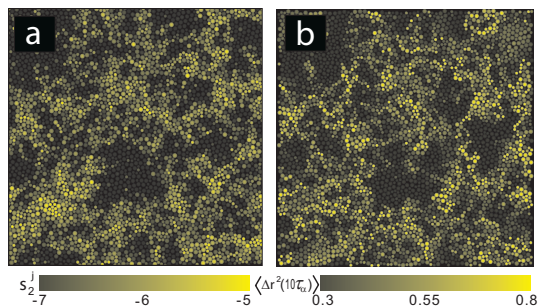


FIG. 1. Structural ordering and its link to dynamics in 2DBC. (a) Spatial distribution of the local structural entropy  $\bar{s}_2^j$ , which is averaged over  $10\tau_\alpha$ . (b) Spatial distribution of the mean square displacement over  $10\tau_\alpha$ ,  $\langle \Delta r^2(10\tau_\alpha) \rangle$ .

Glassy states are formed if crystallization is avoided upon cooling or increasing density. However, the physical factors controlling the ease of vitrification and the nature of glass transition remain elusive. Among various glass forming systems, colloidal liquids are one of the most ideal glass forming systems because of the simplicity and controllability of the interactions. We tackled both of these longstanding questions by using numerical simulations and experiments of polydisperse and binary colloidal systems.

For polydisperse systems, we systematically control the polydispersity, which can be regarded as the strength of frustration effects on crystallization [1–3]. We reveal that crystal-like bond orientational order grows in size and lifetime with an increase in the colloid volume fraction or with a decrease in polydispersity (or, frustration). We stress that bond orientational ordering in hard-sphere-like systems is a direct consequence of dense packing and a manifestation of low configurational entropy. Our study suggests an intriguing scenario that the strength of frustration controls both the ease of vitrification and the nature of glass transition. Vitrification may be a process of hidden crystal-like ordering under frustration [4].

For 2D binary colloidal mixtures (2DBC), on the other hand, slow dynamics is not associated with any obvious structural order in the usual sense. Glassy order responsible for slow dynamics is associated with a structure of low configurational entropy [4]. Such a structural signature can be picked up by using local structural entropy  $s_2$  (see Fig. 1), suggesting a structural origin for slow dynamics also for 2DBC.

We also confirmed that the degree of frustration effects on crystallization controls not only the glass-forming

ability but also the fragility of liquid [5] for both colloidal liquids [1, 6, 7] and spin liquids [8]. Despite the difference in the origin of frustration effects on crystallization (geometrical vs energetic), the behaviour is remarkably similar between them: Hidden glassy structural ordering may be the common origin of dynamic heterogeneity and slow dynamics in these systems and the degree of frustration on ordering controls the fragility.

Our study leads to the following tentative conclusions on the link between structure and dynamics [9, 10]. (1) There is a static structural signature responsible for slow dynamics and it is this signature that controls dynamic heterogeneity. We call this structural order ‘glassy order’. (2) This glassy order exhibits critical-like fluctuations, whose correlation length and amplitude tend to diverge towards the ideal glass transition point. (3) When the strength of frustration on crystallization is rather weak, glassy order is a bond orientational order which has a link to the symmetry of the equilibrium crystal. On the other hand, when the strength of frustration on crystallization is so strong that crystallization must involve fractionation or phase separation, glassy order no longer has a link to the symmetry of the crystal, but is associated with an apparently disordered structure of low configurational entropy. We note that bond orientational order is also regarded as a structure of low configurational entropy. Thus, we may say that there is an intrinsic link between structure and dynamics in glass-forming materials: slow dynamics is linked to structuring (‘glassy ordering’) towards low configurational entropy. The universality of this physical picture is to be checked carefully for various glass-forming systems.

\* Corresponding author: tanaka@iis.u-tokyo.ac.jp

- [1] T. Kawasaki, T. Araki, and H. Tanaka, Phys. Rev. Lett. **99**, 215701 (2007).
- [2] T. Kawasaki and H. Tanaka, Phys. Rev. Lett. **102**, 185701 (2009).
- [3] K. Watanabe and H. Tanaka, Phys. Rev. Lett. **100**, 158002 (2008).
- [4] H. Tanaka, T. Kawasaki, H. Shintani, and K. Watanabe, Nature Mater. **9**, 324 (2010).
- [5] H. Tanaka, J. Phys.: Condens. Matter **10**, L207 (1998).
- [6] T. Kawasaki and H. Tanaka, J. Phys.: Condens. Matter **22**, 232102 (2010).
- [7] T. Kawasaki and H. Tanaka, Proc. Nat. Acad. Sci. U.S.A. **107**, 14036 (2010).
- [8] H. Shintani and H. Tanaka, Nature Phys. **2**, 200 (2006).
- [9] H. Tanaka, J. Phys.: Condens. Matter (in press).
- [10] H. Tanaka, J. Stat. Phys. (in press).

## Crystallization Mechanism of Hard Sphere Glasses

Eduardo Sanz,<sup>1,\*</sup> Chantal Valeriani,<sup>1</sup> Emanuela Zaccarelli,<sup>2</sup> W. C. K. Poon,<sup>1</sup> P. N. Pusey,<sup>1</sup> and M. E. Cates<sup>1</sup>

<sup>1</sup>*SUPA, School of Physics and Astronomy, University of Edinburgh,  
Mayfield Road, Edinburgh, EH9 3JZ, Scotland*

<sup>2</sup>*CNR-ISC and Dipartimento di Fisica, Università di Roma “La Sapienza”, P.le A. Moro 2, I-00185 Roma, Italy*

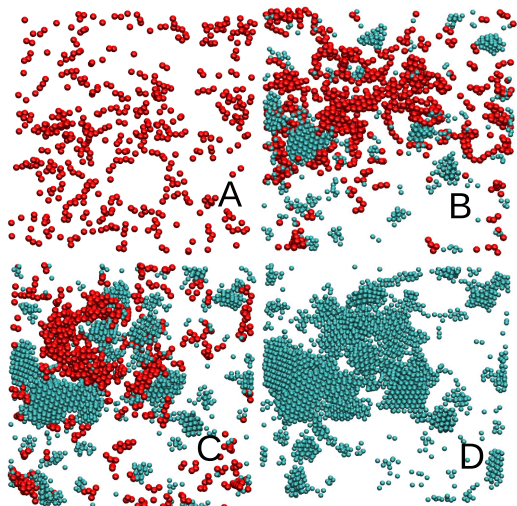


FIG. 1. Slab in the  $xy$  plane showing the 5% most mobile particles (in red) and the crystalline particles (in light blue) at time  $t = 0$  (A),  $t = 320$  (B),  $t = 640$  (C) and  $t = 1280$  (D). Mobile particles are ranked by the distance they move between the time of the frame at which they are shown and the subsequent frame. They are spatially correlated with crystalline ones and have a higher tendency to become crystalline than “average” amorphous particles.

In supercooled liquids, vitrification generally suppresses crystallization [1]. Yet some glasses can still crystallize despite the arrest of diffusive motion [2]. This ill-understood process may limit the stability of glasses, but its microscopic mechanism has not been probed yet. Here we present extensive computer simulations addressing the crystallization of monodisperse hard-sphere glasses at constant volume (as in a colloid experiment). Multiple crystalline patches appear without particles having to diffuse more than one diameter. As these patches grow, the mobility in neighbouring areas is enhanced, creating dynamic heterogeneity with positive feedback. The future crystallization pattern cannot be predicted from the particle coordinates alone: crystallization proceeds by a sequence of stochastic micro-nucleation events, correlated in space by emergent dynamic heterogeneity.

Figure 2 shows the evolution of an initial state with periodic density pattern, following two different tra-

jectories (white arrows) from identical initial particle coordinates, but with different initial velocity choices (drawn at random from the thermal distribution). The black arrow shows a run where velocities are randomized after  $X$  reaches 0.05. The subsequent evolution is again altered, even though significant crystallinity was already present. At no stage do we find the future evolution to depend reproducibly on coordinates alone, although crystallites are more likely to form in regions of high  $Q_6$  than elsewhere. The crystallization mechanism thus comprises a sequence of stochastic ‘micro-nucleation’ events.

\* Corresponding author: esanz@ph.ed.ac.uk

- [1] P. G. Debenedetti and F. H. Stillinger, *Nature* **410**, 259 (2001).  
 [2] E. Zaccarelli and C. Valeriani and E. Sanz and W. C. K. Poon and M. E. Cates and P. N. Pusey, *Phys. Rev. Lett.* **103**, 135704 (2009).

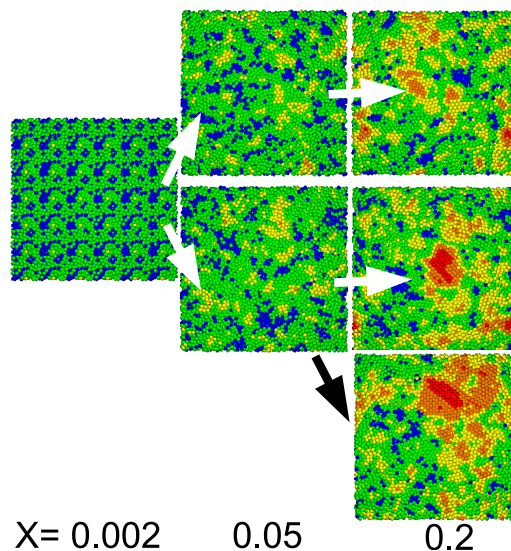


FIG. 2. Slab of the system for various values of the evolving crystallinity  $X$ . Particles are coloured according to the degree of crystalline order in their neighbourhood (blue,  $0 < Q_6 < 0.15$ ; green  $0.15 < Q_6 < 0.25$ ; yellow  $0.25 < Q_6 < 0.35$ ; orange  $0.35 < Q_6 < 0.45$ ; red  $0.45 < Q_6 < 0.55$ ). The initial state (left) has a periodic density pattern that is quickly forgotten.

## An evaluation of the “ideal glassformer” concept, using van der Waals ellipsoids in the Gay-Berne model

Vitaly Kapko, Dmitry V. Matyushov, and C. Austen Angell\*

*Department of Chemistry and Biochemistry, Arizona State University, Tempe, AZ85287-1604*

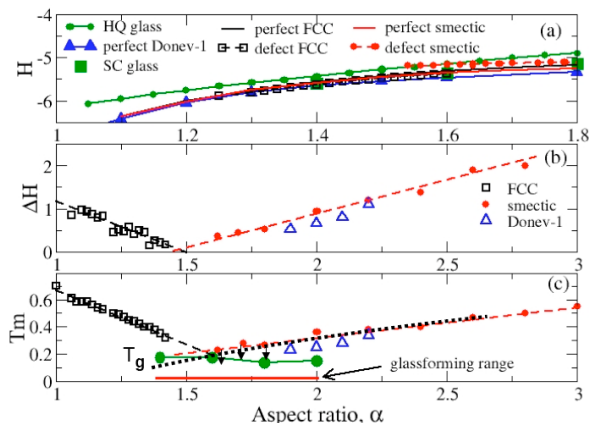


FIG. 1. (a) Crystal enthalpies  $H$  for perfect crystals FCC, Smectic B and Donev-1 at  $T = 0.1$ , compared with  $H$  of glasses (SlowCooled and HyperQuenched) and defect crystals obtained from freezing liquids at aspect ratios  $\alpha = 1.1, 3.0$ , and  $2.2$ , respectively, and then tuning  $\alpha$  within the crystal state (b) enthalpies of fusion (c)  $T_m$  and  $T_g$

We report on an adaption of the empirics of industrial age coal briquetting (for maximum trucking efficiency) [1], to the design of model molecular glassformers. Already in the study of packing of hard particles it has been found that ellipsoids of certain aspect ratios can pack with efficiencies approaching those of ordered packing [2]. We have examined the van-der Waals equivalent in which the system has independent temperature and pressure variables, and melting points and glass transition temperatures  $T_g$  can be determined.

It is generally assumed that liquids are always supercooled when they vitrify, but it is not proven that this needs to be the case. Elsewhere we have raised the possibility that the so-called “2/3” rule of glassforma-

tion ( $T_g = 2/3T_m$ ) is a tautology. Here we examine the possibility that an “ideal glassformer” for which  $T_m < T_g$  might exist.

For the van der Waals ellipsoid study, we carry out potential tuning studies of melting by the method of Molinero et al [3], using the Gay-Berne model of liquid crystals [4] in the low aspect range which has not been previously studied. We find that the FCC crystal stable at aspect ratio  $\alpha = 1.0$  undergoes rapid decrease of  $T_m$  with increasing  $\alpha$  and that at  $\alpha = 1.5$ , the enthalpy of fusion vanishes and the crystal spontaneously disorders at any  $T > 0K$ . Likewise the enthalpy of fusion of the Gay-Berne smectic crystal B (stable at higher aspect ratios) decreases with decreasing  $\alpha$  and vanishes near  $\alpha = 1.5$ . The packing mode found most efficient in hard ellipsoid studies is encountered in crystallization at  $\alpha = 2.2$ , but proves less stable than smectic B to which it transforms during reheating. This packing mode also has no stability at  $\alpha = 1.4–1.5$ . Certainly liquid states in this range of  $\alpha$  never crystallize.

At  $\alpha = 1.4–2.0$ , crystallization of the liquid could be avoided during steady cooling. Density and enthalpy showed hysteresis across the ergodicity-breaking (glass transition) range for  $a = 2.0$  and  $1.8$  but, at  $1.4–1.6$ , glass transition without hysteresis was observed, indicating exceptional fragility according to Wang’s hysteresis analysis [5]. Static and dynamic correlations, and their lengthscales, are being analyzed.

\* Corresponding author: austenangell@gmail.com

- [1] D. Frenkel, *Physics* **3**, 37 (2010).
- [2] A. Donev, *Science* **303**, 990 (2004).
- [3] V. Molinero, S. Sastry, and C. A. Angell, *Phys. Rev. Lett.* **97**, 075701 (2006).
- [4] J. G. Gay and B. J. Berne, *J. Chem. Phys.* **74**, 3316 (1981).
- [5] L.-M. Wang, *J. Phys. Chem.* **113**, 5168 (2009).

## The dynamic crossover temperature is as important as the glass transition temperature: Evidence from liquid transport coefficients

Francesco Mallamace,<sup>1,2,3,\*</sup> Carmelo Corsaro,<sup>4</sup> Sow-Hsin Chen,<sup>2</sup> and H. Eugene Stanley<sup>3</sup>

<sup>1</sup>*Dipartimento di Fisica and CNISM, Università di Messina, I-98166, Messina, Italy*

<sup>2</sup>*Department of Nuclear Science and Engineering, Massachusetts Institute of Technology, Cambridge, MA 02139 USA*

<sup>3</sup>*Center for Polymer Studies and Department of Physics, Boston University, Boston, MA 02215 USA*

<sup>4</sup>*Dipartimento di Fisica and CNISM, Università di Messina I-98166, Messina, Italy*

It is becoming common practice to partition glass-forming liquids into two classes based on the dependence of the shear viscosity  $\eta$  on temperature  $T$ . In an Arrhenius plot,  $\ln \eta$  vs  $1/T$ , a *strong* liquid shows linear behavior while a *fragile* liquid exhibits an upward-curvature [super-Arrhenius (SA) behavior], a situation customarily described by using the Vogel-Fulcher-Tammann (VFT) law.

Here we analyze existing data of the transport coefficients of 84 glass-forming liquids. We show the data are consistent, on decreasing temperature, with the onset of a well-defined dynamical crossover  $\eta_\times$ , where  $\eta_\times$  has the same value,  $\eta_\times \approx 10^3$  Poise, for all 84 liquids. The crossover temperature,  $T_\times$ , located well above the calorimetric glass transition temperature  $T_g$ , marks significant variations in the system thermodynamics, evidenced by the change of the SA-like  $T$ -dependence above  $T_\times$  to Arrhenius behavior below  $T_\times$ . We also show that below  $T_\times$  the familiar Stokes-Einstein (SE) relation  $D/T \sim \eta^{-1}$  breaks down and is replaced by a *fractional* form  $D/T \sim \eta^{-\zeta}$ , with  $\zeta \approx 0.85$ .

By taking into account for these transport parameters a scaling law approach (similar to that of the Mode Coupling Theory), we obtain that the arrested process may be characterized by a crossover in the dynamical properties. In addition, we have already the demonstration that the singularity implied by a genuine structural arrest appears not to be supported by the existing experimental data, and the VFT equation seems to lose any physical basis. We thus conclusively demonstrated that this phenomenon is a general property of all glass-forming liquids. From these considerations it emerges that:

- (i) The FS crossover phenomenon has a larger generality than the traditional Angell classification of liquids into two separate classes of glass-formers: fragile and strong;
- (ii) Transport coefficients [and the isothermal compressibility  $K(T)$ ] show significant change of be-

havior but only near  $T_\times$ ;

- (iii) The FS crossover, the appearance of the fractional Stokes-Einstein violation, the Debye-Stokes-Einstein violation, and the dynamical heterogeneities are directly linked with  $T_\times$ .

Thus we conclude that: (a)  $T_\times$  appears to be more relevant than  $T_g$  or  $T_0$  for understanding the physics of dynamical arrest phenomena; and (b) the universality attained in the master curves from the scaled description of the Stokes-Einstein (SE) and of the Debye-Stokes-Einstein (DSE) violations appears as a “ground-breaking” reality indicating a new route to explore arrested processes. A situation illustrated in the Figure 1 where are represented in a log-log plot the behaviors of the self diffusion constant and the relaxation time as a function of the shear viscosity.

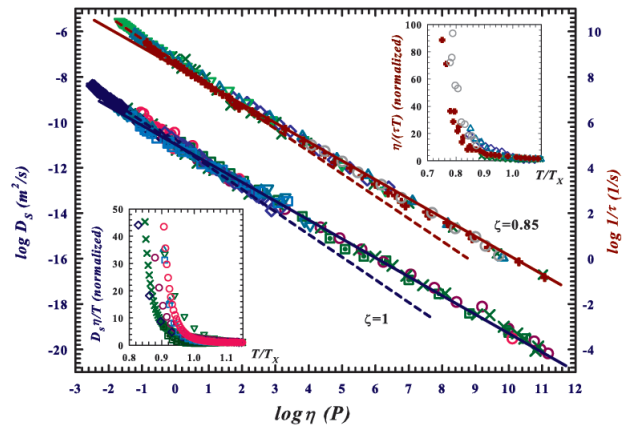


FIG. 1. Lower inset: the onset of the breakdown of the SE law for 9 liquids analyzed. Upper inset: the breakdown of the DSE law for 6 liquids. In both cases the breakdowns occur just below the corresponding crossover temperature, identified using the power law approach. The main plot shows a scaled representation of the *fractional* SE and of the *fractional* DSE, lower and upper data respectively. In both cases, for all the liquids studied, the scaling exponent  $\zeta$  takes almost the same value,  $\zeta = 0.85 \pm 0.02$ . We note that the onset of the breakdown of the *fractional* SE and DSE takes place at the same value of viscosity,  $\eta_\times \approx 10^3$  Poise. These data demonstrate a remarkable degree of universality in the temperature behavior of the transport properties of supercooled liquids.



### **3.2 Posters A**

## Decoupling of viscosity from diffusive mobility in a molecular liquid, caused by isothermal introduction of 2nm structural inhomogeneities

Kazu Ueno and C. Austen Angell\*

*Department of Chemistry and Biochemistry, Arizona State University, Tempe, AZ85287-1604*

One of the most intensively researched aspects of glassforming liquids is the heterogeneity that develops in their dynamic properties as temperature is decreased from above the melting point to deep in the supercooled liquid state [1, 2]. Near  $T_g$  the “slow” domains have dimensions of  $\sim 2$ nm. It has been a common belief that static structure and its fluctuations are not of great importance, but this has been questioned recently by demonstration of a structural “propensity” for mobility [3]. To support structural/enthalpic interpretation of the decoupling of diffusivity from viscosity that accompanies the development of heterogeneity [4, 5] and which leads to breakdown of the Stokes-Einstein equation, we demonstrate, in Figure 1, that the introduction of 2nm structural inhomogeneities into a homogeneous glassformer leads to the same two orders of magnitude decoupling of diffusion from viscosity as is observed during the cooling of orthoterphenyl OTP between  $T_A$ , where Arrhenius behavior is lost, and its  $T_g$  (but mostly in the last 30K [6] (below  $1.1T_g$ )).

Our liquid is cresol which has low viscosity and intermediate fragility, hence has no heterogeneities of its own. The 2nm inhomogeneities are cresol-soluble asymmetric derivatized tetrasiloxo- based (POSS) molecules. We measure diffusive mobility precisely via the equivalent conductivity (Nernst-Einstein relation) and compare with viscosity. The decoupling we report in Figure 1 is the phenomenon predicted by Onsager in 1945 in discussing the approach to a liquid-liquid phase separation with decreasing temperature. In the present case the decoupling observed implies that the 2nm lengthscale for non-mobile domains in liquids near  $T_g$  can arise from structural fluctuations anticipating an isocompositional liquid-liquid transition that, in fragile liquids, is hidden below  $T_g$  [5].

The same phenomenon occurs in water but at much lower viscosities because, in that case the transition giving rise to the fluctuations occurs far above  $T_g$ , near 220K, and it is above this temperature that the breakdown in Stokes-Einstein behavior has been reported over the years (for summary of experimental data see [7] and of simulations see [8]). In strong

liquids the decoupling should not be observed, since fluctuation lengthscales decrease in magnitude as  $T_g$  is approached [9].

It is worth noting that a similar decoupling can be expected as small globular proteins (diameters 2–3 nm) are dissolved in dilute aqueous solutions or in protic ionic liquids.

\* Corresponding author: austenangell@gmail.com

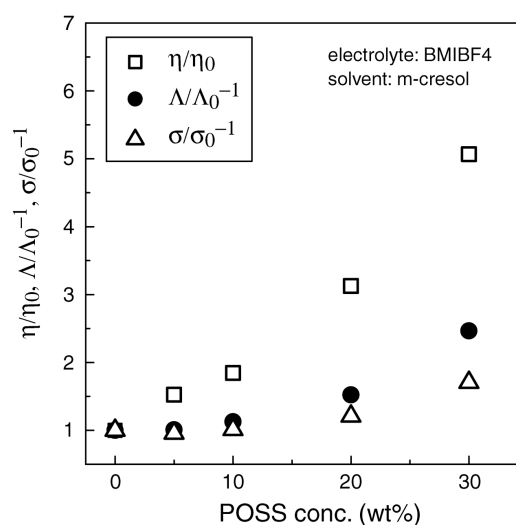


FIG. 1. Relative changes in conductivity (ion mobility) and viscosity, in relation to amount of 2 nm POSS molecules added to solvent cresol.

- [1] M. D. Ediger, *Ann. Rev. Phys. Chem.* **51**, 99 (2000).
- [2] R. Richert, *J. Phys.: Condens. Matter* **14**, R703 (2002).
- [3] A. Widmer-Cooper and P. Harrowell, *J. Phys.: Condens. Matter* **17**, S4025 (2005).
- [4] C. Cammarota *et al.*, *Phys. Rev. Lett.* **105**, 055703 (2010).
- [5] D. V. Matyushov and C. A. Angell, *J. Chem. Phys.* **126**, 094501 (2007).
- [6] M. K. Mapes, S. F. Swallen, and M. D. Ediger, *J. Phys. Chem. B* **110**, 507 (2006).
- [7] K. R. Harris, *J. Chem. Phys.* **132**, 231103 (2010).
- [8] L. Xu *et al.*, *Nature Physics* **5**, 565 (2009).
- [9] S. Wei, I. Gallino, R. Busch, and C. A. Angell, *Nature Physics* (online Nov. 28, 2010).

# Mesoscopic natures of the anomalous viscous transport and viscoelasticity in supercooled liquids

Akira Furukawa\* and Hajime Tanaka

*Institute of Industrial Science, University of Tokyo, Meguro-ku, Tokyo 153-8505, Japan*

The steep increase in the *macroscopic* viscosity near the glass transition is a highlight of the transport anomaly of supercooled liquids. So far, this viscosity anomaly has been regarded as a particle-scale phenomenon (*simple-liquid picture*): jamming of density fluctuations with wavelengths comparable to the cage size ( $\sim$  particle size) is the essential origin of the excessive slowing down of macroscopic structural relaxation. However, contrary to the conventional understanding, here we show by three-dimensional molecular dynamics simulations, that the viscous transport and the viscoelasticity of glass-forming liquids have far more complicated spatio-temporal hierarchical structures in mesoscopic scales [1], similar to usual *complex* liquids and soft materials [2].

(i) The wavenumber ( $k$ )-dependent shear viscosity  $\eta(k)$  and the viscoelastic relaxation time  $\tau_{ve}(k)$  show distinct crossovers from their microscopic to macroscopic values at a characteristic wavelength, which is comparable to the correlation length of dynamic heterogeneity (DH) and grows with an increase in the degree of supercooling [Fig. 1]: At high-temperature normal-liquid states,  $\eta(k)$  smoothly approaches its macroscopic ( $k = 0$ ) value with an increase in  $k$ , already at a wavelength comparable to the particle size. This suggests that there is no important lengthscale beyond the cage size in a normal-liquid state. On the contrary, in supercooled states the  $k$ -dependence of  $\eta(k)$  becomes more pronounced for lower  $T$ . In a highly supercooled state,  $\eta(k)$  increases almost  $10^4$  times when  $k$  decreases from the microscopic to macroscopic value. This nonlocality strongly suggests that a growing dynamic correlation dominates the viscosity anomaly. To verify this, we study a standard measure of dynamic correlation length,

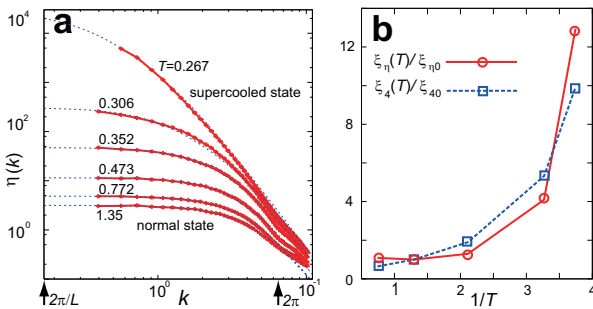


FIG. 1. (a) The  $k$ -dependence of  $\eta$  for several temperatures.  $\eta(k)$  can be well fitted by the empirical function,  $\eta(k = 0, T)/(1 + (\xi_\eta(T)k)^2 + (\lambda_\eta(T)k)^4)$  (dashed curves), where  $\eta(k = 0, T)$  is the macroscopic shear viscosity obtained by the Green-Kubo formula. (b)  $\xi_\eta$  and  $\xi_4$  scaled by their values at  $T = 1.15$  are plotted against  $1/T$ .

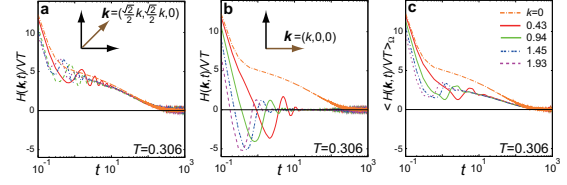


FIG. 2. The decay of the shear stress autocorrelation function  $H(\mathbf{k}, t) = \langle \sigma_{xy}(\mathbf{k}, t) \sigma_{xy}(-\mathbf{k}, 0) \rangle$  for a supercooled state. (a) is for  $\mathbf{k} = (k/\sqrt{2}, k/\sqrt{2}, 0)$ , and (b) is for  $\mathbf{k} = (k, 0, 0)$ . The angular average is plotted in (c).

$\xi_4$ , which is the characteristic length of DH, and we find that  $\xi_\eta$  and  $\xi_4$  grow in quite a similar manner [Fig. 1(b)].

(ii) Strongly anisotropic decay of the shear-stress autocorrelation at a finite wavenumber, which indicates intrinsic decoupling between the longitudinal and transverse dynamics: In Fig. 2 the shear stress autocorrelation function,  $H(\mathbf{k}, t) = \langle \sigma_{xy}(\mathbf{k}, t) \sigma_{xy}(-\mathbf{k}, 0) \rangle$  is plotted for several  $\mathbf{k}$ 's for a supercooled state. Here  $\sigma_{xy}(\mathbf{k}, t)$  is the microscopic expression of the  $xy$ -component of the shear stress. For  $\mathbf{k} = (k/\sqrt{2}, k/\sqrt{2}, 0)$ ,  $\sigma_{xy}(\mathbf{k}, t)$  is directly coupled to the *longitudinal* modes.  $H(\mathbf{k}, t)$  very slowly decays in a time scale of the  $\alpha$ -relaxation and nearly collapses on a single curve for a long time ( $t \gtrsim \tau_\alpha$ ) [see Fig. 2(a)]. For  $\mathbf{k} = (k, 0, 0)$ , on the other hand,  $\sigma_{xy}(\mathbf{k}, t)$  is the almost purely *transverse* shear stress. Along this direction,  $H(\mathbf{k}, t)$  decays very quickly within the  $\beta$ -relaxation time scale except  $k = 0$ , while exhibiting a pronounced anti-correlation [see Fig. 2(b)]. It is worth noting that this decoupling becomes more pronounced for a lower temperature.

These novel dynamic features, (i) and (ii), strongly suggest a fundamental importance of a growing dynamic correlation which may specify the anomalous transport properties and mechanical behaviors. Furthermore, we show that the conventional mode coupling theory (MCT) cannot capture our simulation results. The discrepancies may be attributed to the lack of the essential longer-range correlation than the cage size in the framework of MCT. Our findings should call for a new physical picture beyond a simple mean-field theory with the scalar density field, such as conventional MCT.

\* Corresponding author: furu@iis.u-tokyo.ac.jp

- [1] A. Furukawa and H. Tanaka, Phys. Rev. Lett. **103**, 135703 (2009).  
 [2] A. Furukawa, J. Phys. Soc. Jap **72**, 209 (2003); A. Furukawa, J. Chem. Phys. **121**, 9716 (2004).

## Dynamical heterogeneity in structural glasses and correlated fluctuations of the time variables

Horacio E. Castillo,<sup>1,\*</sup> Karina E. Avila,<sup>1</sup> and Azita Parsaeian<sup>2</sup>

<sup>1</sup>*Department of Physics and Astronomy, Ohio University, Athens, OH, 45701, USA*

<sup>2</sup>*Materials Research Center, Northwestern University, Evanston, IL 60208-3108, USA*

In this work we use numerical simulation data from four atomistic glass-forming models to test the hypothesis that dynamical heterogeneities near the glass transition [1] are associated to soft (Goldstone) modes originating in a broken continuous symmetry under time reparametrizations  $t \rightarrow h(t)$  [2–4]. We construct coarse grained observables that probe the dynamical heterogeneity [5], decompose the fluctuations of these observables into two *transverse* components and a *longitudinal* component, and study the probability distributions and spatial correlations of all the components [6]. The transverse components  $\pi_1$  and  $\pi_2$  are associated with fluctuating reparametrizations of the time variable,  $t \rightarrow h_{\mathbf{r}}(t)$ , i.e. the correlation  $C_{\mathbf{r}}(t, t_w)$  between the state of a coarse-grained region at two times  $t_w$  and  $t$  takes the form  $C_{\mathbf{r}}(t, t_w) = C(h_{\mathbf{r}}(t), h_{\mathbf{r}}(t_w))$ . The *longitudinal* component  $\sigma$  contains all other fluctuations [6]. We find that the transverse fluctuations become dominant and correlate over longer lengthscales than the longitudinal ones as the system becomes more glassy, i.e. as the temperature is lowered and the timescales are increased.

We simulated [6] an 80:20 mixture of particles interacting via Lennard-Jones (LJ) potentials (dataset C), an 80:20 mixture of particles interacting via purely repulsive Weeks-Chandler-Andersen (WCA) potentials (datasets D-H), and short (10-monomer) polymer systems interacting via either LJ potentials (dataset A) or via WCA potentials (dataset B). Nearest neighbors along the polymer chains were held together by FENE anharmonic spring potentials. The ratio of the final temperature  $T$  to the Mode Coupling critical temperature  $T_c$  was  $T/T_c \sim 0.9$  for datasets A-D,  $T/T_c = 1.10$  for datasets E-F and  $T/T_c = 1.52$  for datasets G-H. For datasets F and H, the samples were in equilibrium, but for all the others they were aging. To probe the dynamical heterogeneities, we used the local two-time correlation  $C_{\mathbf{r}}(t, t_w) \equiv \frac{1}{N(B_{\mathbf{r}})} \sum_{\mathbf{r}_j(t_w) \in B_{\mathbf{r}}} \cos(\mathbf{q} \cdot (\mathbf{r}_j(t) - \mathbf{r}_j(t_w)))$ . Here  $\mathbf{r}_j(t)$  is the position of particle  $j$  at time  $t$ ,  $B_{\mathbf{r}}$  is a small coarse graining box around the point  $\mathbf{r}$ , the wavevector  $\mathbf{q}$  is chosen at the main peak of the static structure factor  $S(\mathbf{q})$ , and the sum runs over the  $N(B_{\mathbf{r}})$  particles present in  $B_{\mathbf{r}}$  at the waiting time  $t_w$ . The *global* correlation function  $C(t, t_w) = C_{\text{global}}(t, t_w)$ , defined by extending the average to all of the  $N$  particles in the system, is the self part of the intermediate scattering function. We found that the form

$$C(t, t_w) = g(\varphi(t) - \varphi(t_w)), \quad (1)$$

provides a good fit for the global correlation. Here  $g$

is a stretched exponential  $g(\theta) = q_{EA} \exp[-(\theta/\theta_0)^\beta]$ , and the fitting parameters  $q_{EA}$ ,  $\beta$  and  $\theta_0$  vary little from one dataset to another. The function  $\varphi(t)$  is of the form  $\varphi(t) = \ln^\alpha(t/t_0)$  for aging polymers,  $\varphi(t) = (t/t_0)^\alpha$  for aging particles, and  $\varphi(t) = t/t_0$  for any system in equilibrium. We use this result to define  $\kappa_{ab} \equiv g^{-1}[C(t_a, t_b)]$ , with  $a, b \in \{1, 2, 3\}$ . If Eq. (1) is satisfied, we have  $\kappa_{ab} = \varphi(t_a) - \varphi(t_b)$ . We can analogously define the local quantities  $\kappa_{ab, \mathbf{r}} \equiv g^{-1}[C_{\mathbf{r}}(t_a, t_b)]$ , and extract the longitudinal component of the fluctuations  $\sigma_{\mathbf{r}} \equiv \frac{1}{\sqrt{3}}(\kappa_{12, \mathbf{r}} + \kappa_{23, \mathbf{r}} - \kappa_{13, \mathbf{r}})$ , and the transverse components  $\pi_{1, \mathbf{r}} \equiv \frac{1}{\sqrt{2}}(\kappa_{12, \mathbf{r}} - \kappa_{23, \mathbf{r}})$  and  $\pi_{2, \mathbf{r}} \equiv \frac{1}{\sqrt{6}}(\kappa_{12, \mathbf{r}} + \kappa_{23, \mathbf{r}} + 2\kappa_{13, \mathbf{r}})$ . Time reparametrization fluctuations are characterized by  $\sigma_{\mathbf{r}} = 0$ , i.e. they are purely transverse. We have studied the joint probability distributions  $\rho(\sigma_{\mathbf{r}}, \pi_{1, \mathbf{r}}, \pi_{2, \mathbf{r}})$  and found that for large enough coarse graining regions, as the dynamics of the system becomes slower by reducing the temperature and increasing the observation timescales (for aging systems), the longitudinal fluctuations becoming weaker than the transverse fluctuations. We have also studied the spatial correlations of the fluctuations, and we have found that at low temperatures the correlation volume for the transverse fluctuations is comparable to the correlation volume for the dynamical heterogeneities, but the correlation volume for the longitudinal fluctuations is much smaller than either of them.

H. E. C. thanks L. Cugliandolo and C. Chamon for suggestions and discussions. This work was supported in part by DOE under grant DE-FG02-06ER46300, by NSF under grant PHY05-51164, and by Ohio University. Numerical simulations were carried out at the Ohio Supercomputing Center. H. E. C. acknowledges the hospitality of the Aspen Center for Physics and the Kavli Institute for Theoretical Physics.

\* Corresponding author: castillh@ohio.edu

- [1] M. D. Ediger, Annu. Rev. Phys. Chem. **51**, 99 (2000).
- [2] C. Chamon, M. P. Kennett, H. E. Castillo, and L. F. Cugliandolo, Phys. Rev. Lett. **89**, 217201 (2002).
- [3] H. E. Castillo, C. Chamon, L. F. Cugliandolo, and M. P. Kennett, Phys. Rev. Lett. **88**, 237201 (2002); H. E. Castillo, C. Chamon, L. F. Cugliandolo, J. L. Iguain, and M. P. Kennett, Phys. Rev. B **68**, 134442 (2003).
- [4] H. E. Castillo, Phys. Rev. B **78**, 214430 (2008).
- [5] L. D. C. Jaubert, C. Chamon, L. F. Cugliandolo, and M. Picco, J. Stat. Mech. **2007**, P05001, (2007).
- [6] K. E. Avila, A. Parsaeian, and H. E. Castillo, arXiv:1007.0520; H. E. Castillo and A. Parsaeian, Nat. Phys. **3**, 26 (2007); A. Parsaeian and H. E. Castillo, Phys. Rev. Lett. **102**, 055704 (2009); A. Parsaeian and H. E. Castillo, arXiv:0811.3190 (2008).

# Atomistic molecular dynamics simulations of polybutadiene at graphite: Slowing down in confined melt vs. bulk

Leonid Yelash,<sup>1,\*</sup> Peter Virnau,<sup>1</sup> Kurt Binder,<sup>1</sup> and Wolfgang Paul<sup>2</sup>

<sup>1</sup>*Institute of Physics, Johannes-Gutenberg-University Mainz, 55099 Mainz, Germany*

<sup>2</sup>*Institute of Physics, Martin-Luther-University Halle-Wittenberg, 06099 Halle, Germany*

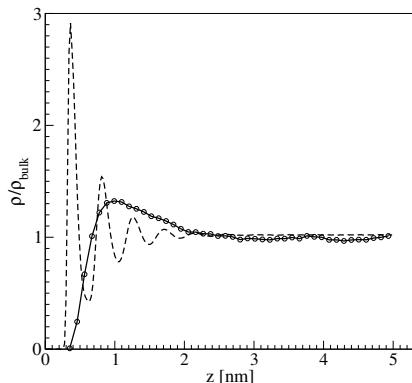


FIG. 1. Layering effect in the monomer density (dashed line) and chain center-of-mass density (circles) of a confined 1,4-polybutadiene melt. Both curves are normalized by the corresponding density in the bulk [4].

A nanoscopic thin film of 1,4-polybutadiene confined between two graphite surfaces is studied using molecular dynamics simulations. The polymer is described using an united atom model [1, 2]; the crystalline surface is modeled by several layers of graphite atoms placed at their crystallographic positions [3].

Our study has shown that the confinement affects the statics as well as the dynamics of the polymer melt in a wide range of scales. E.g., monomer density and chain center-of-mass density as function of distance  $z$  from the solid surface show layering caused by the presence of the crystalline surfaces (Fig. 1).

Dynamical properties, which we analyzed resolving by layers, located at distance  $z$  parallel to solid wall, and in directions parallel ( $xy$ ) and perpendicular ( $z$ ) to the wall, show heterogeneity too, which are not present in bulk. Fig. 2 shows, for example, the chain mean square displacement, which exhibits a bulklike lateral diffusion, whereas the interlayer exchange dynamics (i.e., diffusion perpendicular to the surface) is significantly slowed down due to very slow chain desorption kinetics at solid support [4]. We discuss results of our analysis of simulation data for the bond orientation relaxation  $C(t) = \langle P_2\{\cos[\theta(t)]\} P_2\{\cos[\theta(0)]\} \rangle$  (Fig. 3), dielectric relaxation, and incoherent scattering in bulk and confined systems. Some of the functions which we discuss here can be accessed experimentally, e.g., using NMR measurements [5], dielectric spectroscopy [6], or neutron scattering techniques [7].

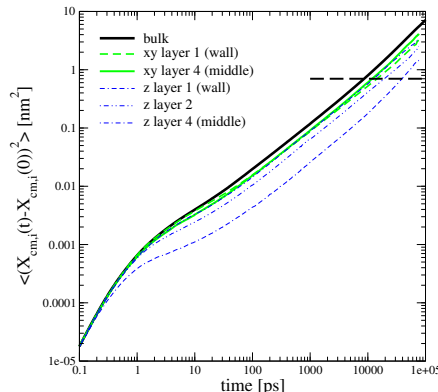


FIG. 2. Mean-square-displacement of the center-of-mass of chains in bulk and in different film layers, in directions parallel ( $xy$ ) and perpendicular ( $z$ ) to the solid wall [4].

- [2] Krushev, S., Diss. Mainz 2002.
- [3] Steele, W.A., Surf. Sci. **36**, 317 (1973).
- [4] Yelash, L., Virnau, P., Binder, K., and Paul, W., Phys. Rev. E **82**, 50801R (2010).
- [5] Saalwächter, K., Prog. NMR Spec. **51**, 1 (2007).
- [6] Serghei, A., Tress, M., and Kremer, F., J. Chem. Phys. **131**, 154909 (2009).
- [7] Krutyeva, M., Martin, J., Arbe, A., Colmenero, J., Mijangos, C., Schneider, G., Unruh, T., Su, Y., Richter, D., J. Chem. Phys. **131**, 174901 (2009).

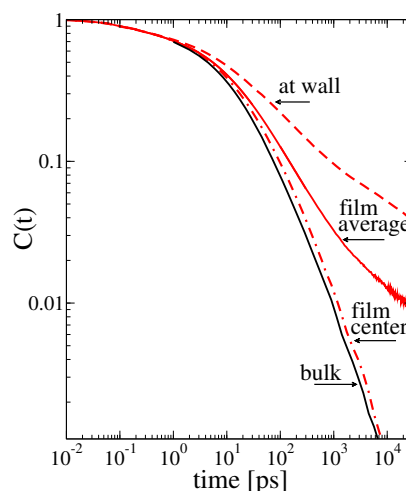


FIG. 3. Inhomogeneous relaxation functions for double-bond rotation dynamics in two different layers of confined polymer: In film center we obtain similar dynamics as in bulk, whereas at solid wall the relaxation is slowed down significantly, which also affects the average signal from the whole film (as it can be measured in NMR experiments).

\* Corresponding author: yelash@uni-mainz.de

[1] Smith, G.D., and Paul, W., J. Phys. Chem. A **102**, 1200 (1998).

## Viscous properties of water

J. S. Hansen,<sup>1,\*</sup> Henrik Bruus,<sup>2</sup> B.D. Todd,<sup>3</sup> and Peter J. Daivis<sup>4</sup>

<sup>1</sup>*DNRF Centre "Glass and Time", Department of Sciences, Roskilde University, P.O. Box 260, Roskilde DK-4000, Denmark*

<sup>2</sup>*Department of Micro- and Nanotechnology, Technical University of Denmark, DTU Nanotech Building 345 East, Kongens Lyngby DK-2800, Denmark*

<sup>3</sup>*Centre for Molecular Simulation, Swinburne University of Technology, P.O. Box 218, Hawthorn, Victoria 3122, Australia*

<sup>4</sup>*Applied Physics, School of Applied Sciences, RMIT University, G.P.O. Box 2476, Melbourne, Victoria 3001, Australia*

In the fluid dynamical description of macroscopic systems the coupling of the fluid's molecular degrees of freedom to the hydrodynamical degrees of freedom are usually disregarded because the former can often safely be ignored. However, this coupling does exist [1] and recently it has been showed via molecular dynamics (MD) that the coupling between the molecular intrinsic angular momentum and the fluid translational motion can become important on small length scales [2]. The effect of the coupling is governed by a total of four phenomenological coefficients for an incompressible isotropic fluid, namely, the shear viscosity, the rotational viscosity, and the two spin viscosities.

The coefficients are defined via the corresponding linear constitutive relations. Thus, for a fluid composed of uniaxial molecules the rotational viscosity  $\eta_r$  is given via [3]

$$\overset{d}{\mathbf{P}} = -\eta_r (\nabla \times \mathbf{u} - 2\boldsymbol{\Omega}) \quad (1)$$

where  $\overset{d}{\mathbf{P}}$  is the vector dual of the antisymmetric part of the pressure tensor,  $\mathbf{u}$  is the velocity field, and  $\boldsymbol{\Omega}$  is the angular velocity field. The rotational viscosity thus describes the decay of the antisymmetric stress: this process is a fast local process and originates from molecular intrinsic angular momentum relaxation. The spin viscosities  $\zeta_0$  and  $\zeta_r$  are in general given by the relations [4]

$$\overset{os}{\mathbf{Q}} = -2\zeta_0 (\nabla \boldsymbol{\Omega}) \quad \text{and} \quad \overset{d}{\mathbf{Q}} = -\zeta_r (\nabla \times \boldsymbol{\Omega}) \quad (2)$$

Here  $\overset{os}{\mathbf{Q}}$  is the traceless symmetric part of the couple tensor and  $\overset{d}{\mathbf{Q}}$  is the vector dual of the antisymmetric part of the couple tensor. The spin viscosities are both related to angular momentum diffusion. In this talk I show MD results of the viscosity coefficients for water.

The calculated values of the viscosities are used in the extended Navier-Stokes equations that include the molecular details and I analyze two simple nanofluidic flows, namely, a planar Poiseuille flow and a flow generated by a rotating electrical field, illustrated in Fig 1. It is shown that a flow driven by an external field the coupling will reduce the flow rate significantly for nanoscale geometries. The coupling also enables conversion of rotational electrical energy into fluid linear momentum and we find that in order to obtain measurable flow rates the electrical field strength must be in the order of  $0.1 \text{ MV m}^{-1}$  and rotate with a frequency of more than 100 MHz.

\* Corresponding author: jschmidt@ruc.dk

- [1] H. Grad, *Commun. Pure Appl. Math.* **5**, 455 (1952).  
 [2] J. S. Hansen, P. J. Daivis, and B. D. Todd, *Phys. Rev. E* **80**, 046322 (2009).  
 [3] S. R. de Groot and P. Mazur, *Non-Equilibrium Thermodynamics* Dover, (Mineola, 1984).  
 [4] D. J. Evans and W. B. Streett, *Mol. Phys.* **36**, 161 (1978).

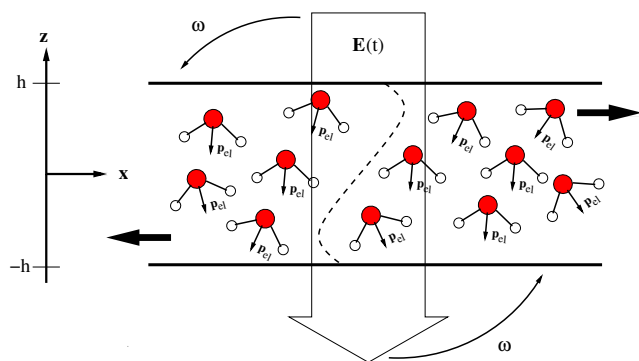


FIG. 1. Illustration of flow generation using a rotating electrical field,  $\mathbf{E}(t)$ . The water molecules have a permanent electrical dipole, here denoted  $\mathbf{p}_{el}$  which is not perfectly aligned with the field due to thermal fluctuations. The velocity profile is indicated by the dotted line and illustrates the opposite flow directions as shown by the thick black arrows.

## Short time dynamics of a medium length polyethylene melt

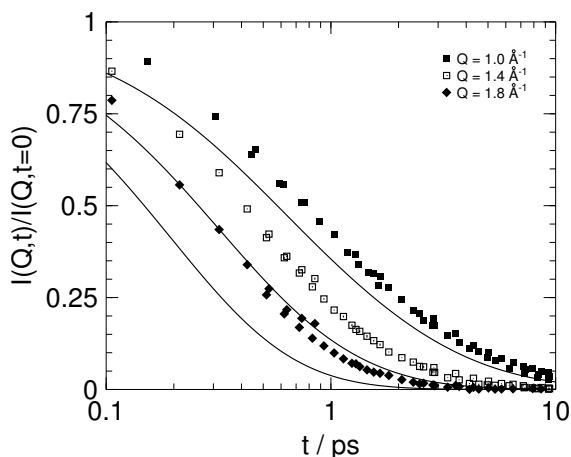
Humphrey Morhenn,<sup>1,\*</sup> Sebastian Busch,<sup>1</sup> and Tobias Unruh<sup>1,2</sup><sup>1</sup>Technische Universität München, Forschungs-Neutronenquelle Heinz Maier-Leibnitz und Physik Department E13, 85747 Garching, Germany<sup>2</sup>Friedrich-Alexander-Universität Erlangen-Nürnberg, Lehrstuhl für Kristallographie und Strukturphysik, 91058 Erlangen, Germany

FIG. 1. Normalized incoherent intermediate scattering function for  $n\text{-C}_{100}\text{H}_{202}$  (symbols) and the Rouse prediction (solid lines) for three values of momentum transfer  $Q$ .

The description of transport mechanisms in molecular liquids is a challenging task. Especially the mechanism of molecular self-diffusion in liquids of organic medium-chain molecules is not yet completely understood. With time-of-flight quasielastic neutron scattering (TOF-QENS), it is possible to get experimental access to the motions on a molecular length scale in the pico- to nanosecond time regime. In this regime one has to assume a superposition of several (intra)molecular motions ranging from methyl group rotation to long-range diffusion.

It could be shown previously that the diffusion coefficients of short- and medium-chain  $n$ -alkanes measured by TOF-QENS deviate increasingly from the long-time long-range values determined by pulsed-field gradient nuclear magnetic resonance (PFG-NMR) with increasing chain length of the molecules and decreasing temperature [1].

It has also been demonstrated by molecular dynamics (MD) simulations for the  $n$ -alkane  $\text{C}_{32}\text{H}_{66}$  that in the 1 ps time range tumbling motions of the hydrogen atoms dominate while small chain deformations dominate after 20 ps [2]. By extending this work to samples with different molecular weight and several temperatures, we might be able to construct a complete picture of short time dynamics.

The Rouse model may be considered as the standard model for polymer chain dynamics. It is a bead-spring

model developed to describe large scale chain motions, consisting of long range diffusion and slightly faster dynamics. It considers a chain consisting of  $N$  freely joint Gaussian segments in a heat bath where springs stand for the entropic forces between the hypothetical beads. Excluded volume effects are disregarded. The solution of the Langevin equation results in a spectrum of normal modes which account for the internal motion of the chain [3]. Since the tumbling motions of hydrogen atoms in polyethylene melts at short times are not taken into account by the Rouse model, it should predict a too slow decay of the correlation function in this time regime.

Our data show the contrary, where the observed dynamics are slower than the decay predicted by the Rouse model. In order to test the model, TOF-QENS experiments were performed on a polyethylene melt ( $n\text{-C}_{100}\text{H}_{202}$ ). The chains are long enough to show gaussian chain statistics in their confirmations but are still in the unentangled regime so that it was possible to check the validity of the Rouse model on this time and length scale.

Fig. 1 shows the measured intermediate scattering function and the Rouse prediction for several values of the momentum transfer  $hQ$ . It can clearly be seen that the Rouse predictions lie throughout below the measured data. Thus the Rouse model predicts a faster decay than actually measured. Any additional models, accounting for further motions, cannot enhance the description of the data.

A modified Rouse model, contributing only to the motion of lower modes (slower, large scale motion), might allow the integration of additional terms. By combining resolution resolved TOF-QENS experiments with MD simulations, it might be possible to identify the motions, which occur on timescales faster than long range diffusion.

The authors gratefully acknowledge D. Richter (JCNS) for fruitful discussions and for providing the sample.

\* Corresponding author: hmorhenn@frm2.tum.de

- [1] C. Smuda, S. Busch, G. Gemmeker and T. Unruh, *J. Chem. Phys.* **129**, 014513 (2008).
- [2] T. Unruh, C. Smuda, S. Busch, J. Neuhaus, W. Petry, *J. Chem. Phys.* **129**, 121106 (2008)
- [3] D. Richter, M. Monkenbusch, A. Arbe, J. Colmenero, *Neutron Spin Echo in Polymer Systems*, *Advances in Polymer Science*, 174 (2005)

## From caging to Rouse dynamics in polymer melts with intramolecular barriers: a critical test of the Mode Coupling Theory.

Marco Bernabei,<sup>1,\*</sup> Angel J. Moreno,<sup>2</sup> Emanuela Zaccarelli,<sup>3</sup> Francesco Sciortino,<sup>3</sup> and Juan Colmenero<sup>1,4,5</sup>

<sup>1</sup>*Donostia International Physics Center, Paseo Manuel de Lardizabal 4, E-20018 San Sebastián, Spain.*

<sup>2</sup>*Centro de Física de Materiales (CSIC, UPV/EHU) and Materials Physics Center MPC, Paseo Manuel de Lardizabal 5, E-20018 San Sebastián, Spain*

<sup>3</sup>*Dipartimento di Fisica and CNR-ISC, Università di Roma La Sapienza, Piazzale Aldo Moro 2, I-00185, Roma, Italy*

<sup>4</sup>*Centro de Física de Materiales (CSIC, UPV/EHU) and Materials Physics Center MPC, Paseo Manuel de Lardizabal 5, E-20018 San Sebastián, Spain.*

<sup>5</sup>*Departamento de Física de Materiales, Universidad del País Vasco (UPV/EHU), Apartado 1072, E-20080 San Sebastián, Spain.*

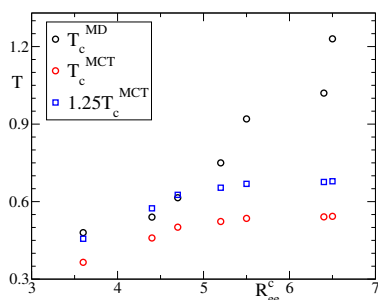


FIG. 1. Critical temperature  $T_c$  as a function of the end-to-end radius  $R_{ee}^c$  (measured at  $T_c^{MD}$ ). The theoretical values  $T_c^{MCT}$  are compared with the simulation values  $T_c^{MD}$ .

By means of computer simulations and solution of the equations of the Mode Coupling Theory (MCT), we investigate the role of the intramolecular barriers on several dynamic aspects of non-entangled polymers [1]. The investigated dynamic range extends from the caging regime characteristic of glass-formers to the relaxation of the chain Rouse modes. We review our recent work [2, 3] on this question, provide new results and critically discuss the limitations of the theory. Solutions of the MCT for the structural relaxation reproduce qualitative trends of simulations for weak and moderate barriers, see Fig. 1. However a progressive discrepancy is revealed as the limit of stiff chains is approached. This disagreement does not

seem related with dynamic heterogeneities, which indeed are not enhanced by increasing barrier strength. It is not connected either with the breakdown of the convolution approximation for three-point static correlations, which retains its validity for stiff chains. These findings suggest the need of an improvement of the MCT equations for polymer melts. Concerning the relaxation of the chain degrees of freedom, MCT provides a microscopic basis for time scales from chain reorientation down to the caging regime. It rationalizes, from first principles, the observed deviations from the Rouse model on increasing the barrier strength. These include anomalous scaling of relaxation times, long-time plateaux, and non-monotonous wavelength dependence of the mode correlators.

We thank S.-H. Chong, T. Franosch, M. Fuchs, M. Sperl, and J. Baschnagel for useful discussions. We acknowledge financial support from the projects FP7-PEOPLE-2007-1-1-ITN (DYNACOP, EU), MAT2007-63681 (Spain), IT-436-07 (GV, Spain), ERC-226207-PATCHYCOLLOIDS (EU), and ITN-234810-COMPLOIDS (EU).

\* Corresponding author: sckbernm@ehu.es

- [1] M. Bernabei, A. J. Moreno, E. Zaccarelli, F. Sciortino, J. Colmenero, arXiv:1003.6015
- [2] M. Bernabei, A. J. Moreno, J. Colmenero, J. Chem. Phys. **131**, 204502 (2009).
- [3] M. Bernabei, A. J. Moreno, J. Colmenero, Phys. Rev. Lett. **101**, 255701 (2008).

# Glassy and polymer dynamics in confining geometry as revealed by NMR

M. Hofmann,\* S. Gradmann, and E. A. Rössler

University Bayreuth, Experimentalphysik II, D-95440 Bayreuth, Germany

We investigate molecular glass formers and polymers in confining geometry by solid state NMR and  $^1\text{H}$  field-cycling NMR (FCNMR), respectively.

We studied the dynamics of the glass former tricesyl phosphate (TCP) embedded in different porous systems like MCM and SBA matrices by 2D  $^{31}\text{P}$  NMR. Fig. 1 (left) shows a comparison of the reorientational correlation functions  $F_2(t)$  of bulk TCP and of TCP in confinement of pores with different sizes. In the smallest confinement ( $r = 3.61$  nm), an interpolation with a Kohlrausch function, as it is possible in the case of bulk TCP (50 nm pores), is not appropriate. In order to describe the decay curves we assume that a spatially varying correlation time is present in the pores: the closer the molecules are to the walls of the cylindrical pores the slower are the dynamics. The decay curves are then calculated by a superposition of Kohlrausch functions with the weight of the corresponding cylinder shell. The needed “distance law” for the correlation time has been taken as the fit function. Fig. 1 (right) demonstrates the result for the spatial dependence of the correlation time for different temperatures ( $r = 7.25$  nm pores) and for different pore sizes ( $T = 224$  K). While at high temperature the slowing-down of the correlation time does not penetrate much into the liquid, this effect is much stronger at low temperatures. 2D  $^{31}\text{P}$  NMR spectra, however, indicate that the scenario of completely heterogeneous dynamics does not strictly hold.

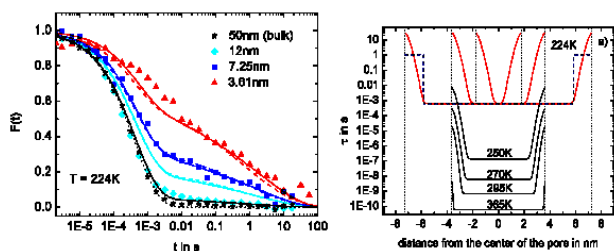


FIG. 1. Orientational correlation function for bulk TCP and in confinement of different pore sizes; solid-line: model interpolation for different pore sizes with a single “distance law” (cf. right). (right): correlation times as a function of the distance (“distance law”) from the pore centre for different temperatures and pore sizes [1].

Regarding polymers in confinement of anodic aluminum oxide (AAO) we applied FCNMR relaxometry which allows probing both local and collective polymer dynamics by measuring the dispersion of the spin-lattice relaxation time  $T_1(\omega)$ . Previous work by Fatkullin et al. [2] state that for pore sizes

even much larger than the polymer radius of gyration a strong confinement effect exists which they call “corset effect”. Chain dynamics as predicted by the tube/reptation model are observed for polyethylene oxide (PEO) confined in a porous solid methacrylate matrix (SMM) (Fig. 2). The effect emerges for molecular weights below and above the critical molecular weight  $M_c$  and is independent from the pore diameter.

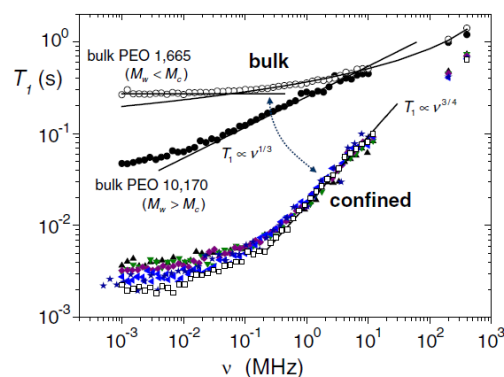


FIG. 2.  $T_1(\omega)$  as measured by FCNMR [2] of bulk PEO (upper curves) and confined in SMM (lower curves) for pore diameters of 8nm, 13nm, 21nm, 33nm and 58nm at 358K.

Studying polybutadiene (Pb) in AAO channels (Fig. 3 (left)) with diameters of 60nm and 20nm, we find no significant difference between bulk and confined Pb except a shift in the glass transition temperature  $T_g$  (Fig. 3 (right)). There is no indication for a corset effect.

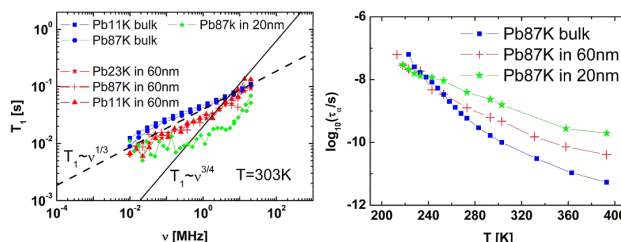


FIG. 3.  $T_1(\omega)$  of bulk Pb ( $M_w=87\text{KDa}$ ,  $23\text{KDa}$  and  $11\text{KDa}$ ) and infiltrated in 20nm and 60nm pores. The lines represent the power laws predicted by tube/reptation ( $T_1 \propto \nu^{3/4}$ ) and renormalized Rouse theory ( $T_1 \propto \nu^{1/3}$ ).

\* Corresponding author: marius.hofmann@uni-bayreuth.de

- [1] S. Gradmann, P. Medick, E.A. Rössler, J. Phys. Chem. **113**, 8443 (2009)
- [2] N. Fatkullin, R. Kimmich, E. Fischer, C. Mattea, U. Beginn, M. Kroutieva, New J. Phys. **6**, 46 (2004)

## Heterogeneities of segmental dynamics in lamellar phases of diblock copolymers

Mohammed Zakaria Slimani,<sup>1,\*</sup> Angel J. Moreno,<sup>2</sup> and Juan Colmenero<sup>1,2,3</sup>

<sup>1</sup>*Donostia International Physics Center, Paseo Manuel de Lardizabal 4, 20018 San Sebastián, Spain.*

<sup>2</sup>*Centro de Física de Materiales (CSIC, UPV/EHU)  
and Materials Physics Center MPC, Apartado 1072, 20080 San Sebastián, Spain.*

<sup>3</sup>*Departamento de Física de Materiales, Universidad del País  
Vasco (UPV/EHU), Apdo. 1072, 20080 San Sebastián, Spain.*

By means of computer simulations, we investigate the segmental dynamics in the lamellar phase of a simple bead-spring model of diblock copolymers. We characterize dynamic heterogeneity in mean squared displacements and bond reorientations. This is done as a function of the position of the monomers along the chain and of the distance to the nearest interface between consecutive domains. Both characterizations of dynamic heterogeneity reveal moderate gradients of mobility in the investigated temperature range, which qualitatively probes time scales up to 100 ns. Thus, the obtained distribution of relaxation times spreads

over less than a decade. However extrapolation of the former analysis to lower temperatures suggest an increasing spread over several time decades. Apparently, the observed dynamic heterogeneity cannot be explained by invoking gradients of density over the domains. Indeed such gradients are absent and the local density in the domains is, within statistics, identical to that of the corresponding homopolymers.

\* Corresponding author: sckslimz@ehu.es

## Unusual dynamics of polymer grafted nanoparticles

Sunita Srivastava, Sivasurender Chandran, C. K. Sarika, Ajoy K Kandar, and Jaydeep K Basu\*

*Department of Physics, Indian Institute of Science, Bangalore, India*

Soft colloids have been widely studied over the past few years due to their interesting structural and dynamical phase behavior [1–7]. Block copolymer micelles [3], star polymers [4–6], microgel particles [1, 2] constitute few examples of such materials which have been extensively studied. However, hybrid nanoparticles [7–10] having an inorganic core and organic or polymeric shell, which also belong to the same class of materials, have not received as much attention. Recent effort [7, 8] has focused on understanding the conformation of the grafted polymer chains as a function of various parameters like grafting density or chain length etc. However, no effort has been made in understanding their dynamics, especially for concentrated solutions or melts where these hybrid nanostructures are expected to form gel, glass or crystalline phases. Here we present results of temperature and wave vector dependent dynamics in such hybrid nanoparticles. The results presented here are based on hybrid particles with core of gold nanoparticles and corona of thiol terminated polystyrene (PST) synthesised by a method described earlier [9, 10]. Both the core size as well as the grafting density of PST chains on the gold surface were varied to obtain hybrid particles with various sizes. Binary mixtures of two such hybrid particles, having different sizes, were prepared by mixing them in tetrahydrofuran solutions. X-ray photon Correlation Spectroscopy (XPCS) measurements, on these samples, were performed at the Advanced Photon Source in Argonne National Laboratory at the 8 - ID beam line with monochromatic x - rays of energy 7.35 KeV.

In Fig. 1 (a) we summarise the behaviour of relaxation time  $\tau$  with functionality,  $f$  as extracted from the intermediate scattering function measured using XPCS. Since no theoretical or experimental data is available for the variation of structural relaxation time of nanoparticle grafted polymer chain with functionality, we have compared the data with that available for star polymers. Contrary to expectation based on data from star polymer melts [11] we find non-monotonic dependence of  $\tau$  on  $f$ . Clearly, there seems to be a cross-over in the behavior of relaxation time  $\tau$  above a certain value of  $f$ . Thus the dynamics of our hybrid nanoparticles in the high  $f$  regime seems to resemble that of polymer core colloidal melt [11] but the low  $f$  ( $f \leq 100$ ) regime shows anomalous behavior.

In Fig. 1(b) we also display the dependence of relaxation time  $\tau$  as a function of  $\phi$ , for the binary mixture samples. This behavior is very reminiscent of glass melting and re-vitrification for binary mixtures

of colloids and polymers in solution [12]. However, in such cases the volume fraction of added polymer for glass melting is much higher than what we observe here. Further, the size ratio (size of polymer compared to colloid),  $\delta$ , at which such behavior has been observed is also much smaller than the case of our hybrid nanoparticles. The observed behaviour is explained in terms of the subtle interplay between the soft repulsion between grafted chains and the van der Waals attraction between the inorganic gold cores.

We acknowledge DST, India for financial support and the beamline staff at 8-ID, APS for technical support.

\* Corresponding author: basu@physics.iisc.ernet.in

- [1] Z. Zhang et al, *Nature*, **459**, 203 (2009).
- [2] J. Mattsson et al, *Nature*, **462**, 83 (2009).
- [3] I. W. Hamley, *The Physics of Block Copolymers*. (Oxford University Press - New York, 1998).
- [4] C. N. Likos, *Soft Matter*, **2**, 2, 478 (2006).
- [5] C. Mayer et al, *Nat. Mater.* **7**, 780 (2008).
- [6] E. Zaccarelli et al, *Phys. Rev. Lett.* **95**, 268301 (2005).
- [7] D. Dukes et al, *Macromolecules* **43**, 1564(2010).
- [8] A. Jayaraman and K. S. Schweizer, *Macromolecules* **42**, 8423(2009).
- [9] A. K. Kandar et al *J.Chem.Phys.* **130**, 121102 (2009).
- [10] S. Srivastava et al *J.Chem.Phys.* **133**, 151105 (2010).
- [11] T. Pakula, et. al., *Macromolecules*, **31**, 8931 (1998).
- [12] T. Eckert and E. Bartsch, *Phys. Rev. Lett.*, **89**, 125701 (2002)

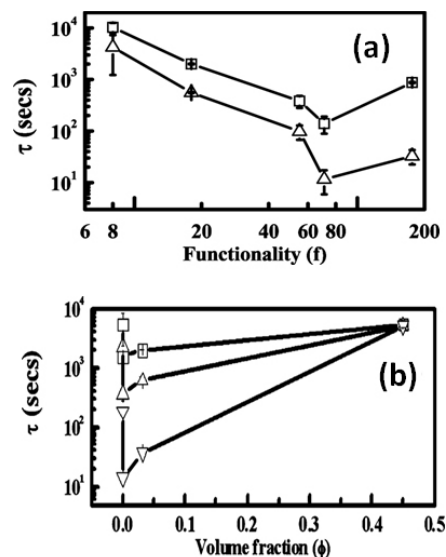


FIG. 1. (a)  $\tau$  vs  $f$  for polymer grafted nanoparticles and (b)  $\tau$  vs volume fraction,  $\phi$  for their binary mixtures. In (a) squares represent data collected at 100<sup>o</sup>C and uptriangle for data collected at 115<sup>o</sup>C for  $q = 0.03 \text{ \AA}^{-1}$ . In panel (b) data is shown for 105<sup>o</sup>C and same  $q$  as in (a).

## Specific volume and activation volume scalings in viscous systems

A. Grzybowski,\* M. Paluch, K. Grzybowska, A. Swiety, and K. Koperwas

*Institute of Physics, Silesian University, Uniwersytecka 4, 40-007 Katowice, Poland*

Thermodynamic scaling in viscous systems has been intensively studied for last years in search of a proper relation between thermodynamics, dynamics, and effective intermolecular interactions, which would be able to explain prior observations that some dynamic quantities  $x$  such as primary relaxation time  $\tau$  and viscosity  $\eta$ , mainly collected for van der Waals liquids and polymers near the glass transition, can be plotted onto one master curve in terms of a general equation

$$\log_{10}(x) = J(\Gamma) \text{ with } \Gamma = T^{-1}v^{-\gamma} \quad (1)$$

where  $T$  and  $v$  are temperature and specific volume, and the scaling exponent  $\gamma$  is a material constant independent of thermodynamic conditions. This subject is hotly debated and its theoretical grounds is still under discussion. Usually, an approximation of the generalized Lennard-Jones potential, whose dominant part is a repulsive inverse power law (IPL) term  $\propto r^{-3\gamma_{IPL}}$ , is suggested to be responsible for the thermodynamic scaling. According to this interpretation, we have found [1] an isothermal equation of state (EOS),

$$\left(\frac{v_0}{v}\right)^{\gamma_{EOS}} = 1 + \frac{\gamma_{EOS}}{B_T^{conf}(p_0^{conf})} (p^{conf} - p_0^{conf}) \quad (2)$$

which is derived from such a potential, i.e.,  $\gamma_{EOS} \approx \gamma_{IPL}$ . This EOS valid for the low compressibility region describes the scaled specific volume as a linear function of the configurational pressure  $p^{conf}$ , using the isothermal configurational bulk modulus  $B_T^{conf}(p_0^{conf})$  at a chosen reference state  $p_0^{conf} = p^{conf}(v_0) = p_0 - RT/(Mv_0)$  where  $v_0 = v(p_0)$ ,  $R$  is the gas constant and  $M$  is molar mass of the system. Similar EOS can be also derived for non-configurational quantities from the definition of the isothermal bulk modulus  $B_T(p_0)$ . Both the EOSs result [1] in very well fits of PVT experimental data and lead them to scale with  $\gamma_{EOS} \gg \gamma$  (that enables to scale dynamic quantities in terms of Eq. (1)). Another discrepancy has been also known. Although the thermodynamically defined Grüneisen constant  $\gamma_G$  is identified with  $\gamma$  according to a very promising temperature-volume version of the entropic Avramov model suggested by Casalini et al. [2], it follows from experimental data that  $\gamma_G \ll \gamma$ . We found [3, 4] that a progress in this field can be achieved by a reasonable modification of one assumption of the model, replacing a constant maximal energy barrier  $E_{max}$  with its volume scaled counterpart  $E_{max} \propto (v_0/v)^{\gamma_{EOS}}$ . Then, for instance, primary relaxation times can be described as follows

$$\log_{10} \tau = \log_{10} \tau_0 + \left(\frac{A}{Tv^\gamma}\right)^D \quad (3)$$

$$\text{with } \gamma = \gamma_G + \gamma_{EOS}/D \quad (4)$$

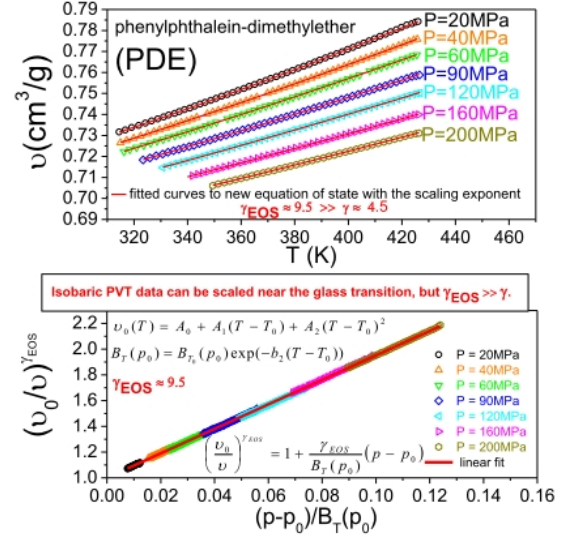


FIG. 1. The upper panel shows a successful fit of PVT data for PDE to a non-configurational isobaric counterpart of Eq. (2). The scaling of the specific volume in terms of this equation is presented in the lower panel.

where  $\tau_0$ ,  $A$ ,  $D$ , and  $\gamma$  are fitting parameters. The latter relation can be verified by fitting PVT data to Eq. (2) and calculating  $\gamma_G$  from heat capacity and PVT data. In this way we have very successfully tested it for supercooled van der Waals liquids [3], and even for one ionic liquid [4]. Eq. (4) seems to be meaningful to the thermodynamic scaling theory under construction, because it provides a linkage between the scalings of specific volume and dynamic quantities.

Next, some latest findings will be shown at the Workshop, i.e., equations of state, based on Eq. (2) and its non-configurational counterpart, which can scale both isobaric and isothermal PVT data (see in Fig. 1). Finally, a very intriguing observation will be reported: an unknown until recently scaling of the activation volume  $v^{act}(P) = RT(\partial \ln \tau / \partial P)_T$  in terms of an equation analogous to Eq. (2). The quantity is a very useful parameter to characterize relaxation processes in glass-forming liquids. Thus, its scaling can give a new insight into the thermodynamic scaling idea.

\* Corresponding author: andrzej.grzybowski@us.edu.pl

- [1] A. Grzybowski, S. Haracz, M. Paluch, and K. Grzybowska, *J. Phys. Chem. B* **114**, 11544 (2010).
- [2] R. Casalini, U. Mohanty, and C. M. Roland, *J. Chem. Phys.* **125**, 014505 (2006)
- [3] A. Grzybowski, M. Paluch, K. Grzybowska, S. Haracz, *J. Chem. Phys.* **133**, 161101 (2010)
- [4] M. Paluch, S. Haracz, A. Grzybowski, M. Mierzwa, J. Pionteck, A. Rivera-Calzada, and C. Leon, *J. Phys. Chem. Lett.* **1**, 987 (2010)

## Identification of the molecular origin of secondary relaxation process which is commonly observed in the whole family of the saccharides.

K. Kaminski,\* P. Włodarczyk, K. Adrjanowicz, Z. Wojnarowska, and M. Paluch

*Institute of Physics, University of Silesia, ul. Uniwersytecka 4, 40-007 Katowice, Poland*

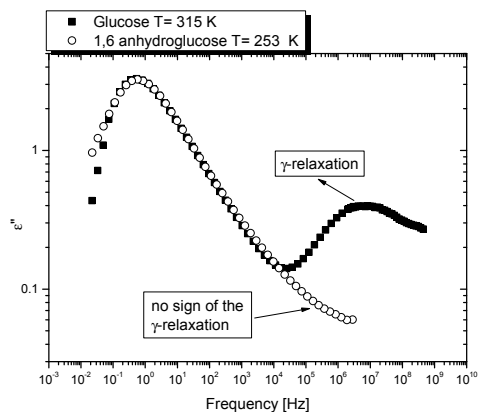


FIG. 1. No sign of  $\gamma$ -relaxation in the 1,6-anhydro-glucose.

Broadband dielectric relaxation studies were performed on a D-glucose and an 1,6-anhydro-D-glucose. In the liquid phase of both systems, one can observe structural relaxation processes. In the glassy phase of the former system, two secondary relaxations can be seen. The slower one, hardly detectable in the loss spectra, was identified as the Johari-Goldstein type (JG) relaxation. On the other hand, the  $\gamma$ -relaxation is visible as pronounced peak. Origin of this process was a subject of hot debate. Different authors speculated about origin of this relaxation, but no consensus was reached. Moreover, application of so sophisticated method such as NMR and MD simulations

[1, 2] have not resolved this problem. Comparison of the dielectric loss spectra measured for the D-glucose and the 1,6-anhydro-D-glucose, together with other experimental findings coming from NMR or acoustical studies enabled us to certify unquestionably, that the rotation of hydroxymethyl group is the origin of  $\gamma$ -relaxation in D-glucose. Since this relaxation is observed in the whole family of saccharides [3] we can be sure that our research will be very helpful in understanding molecular dynamics of oligo or polysaccharides, which are materials of high practical importance.

The authors (K. K., P.W, K.A., Z. W. and M. P.) are deeply thankful for the financial support of their research within the framework of the project entitled From Study of Molecular Dynamics in Amorphous Medicines at Ambient and Elevated Pressure to Novel Applications in Pharmacy, which is operated within the Foundation for Polish Science Team Programme cofinanced by the EU European Regional Development Fund. Moreover P. W. would like to thank Foundation for Polish Science for awarding grants within the framework of the START Programme (2010).

\* Corresponding author: kaminski@us.edu.pl

- [1] V. Molinero and W. A. Goddard, *Phys. Rev. Lett.* **95**, 045701 (2005).
- [2] G. R. Moran, K. R. Jeffrey, J. M. Thomas, and J. R. Stevens, *Carbohydr. Res.* **328**, 573 (2000).
- [3] K. Kaminski, E. Kaminska, K. L. Ngai, M. Paluch, P. Włodarczyk, A. Kasprzycka, and W. Szeja, *J. Phys. Chem. B* **113**, 10088 (2009).

## Removal of hydrogen-bond-induced clusters in m-fluoroaniline by mixing with aromatic compounds: emergence of genuine Johari-Goldstein relaxation

M. Romanini,<sup>1,\*</sup> S. Capaccioli,<sup>1,2</sup> A. N. Murugan,<sup>1</sup> L.C. Pardo,<sup>1</sup> M. Barrio,<sup>1</sup> and J. Ll.Tamarit<sup>1</sup>

<sup>1</sup>*Grup de Caracterització de Materials, Departament de Física i Enginyeria Nuclear. ETSEIB, Universitat Politècnica de Catalunya, Diagonal 647 Barcelona 08028. Catalonia*

<sup>2</sup>*Dipartimento di Fisica, University of Pisa, Largo Pontecorvo 3, 56127 Pisa (Italy)*

The dielectric loss spectra of the glass former, m-fluoroaniline (m-FA) show up, at higher frequencies than the structural relaxation, a faster resolved secondary relaxation. In the past this secondary relaxation was identified in the literature as the universal Johari-Goldstein (JG)  $\beta$ -relaxation [1]. The JG relaxation involves essentially all parts of the molecule and has certain specific characteristics [2] including a strong correlation with the structural relaxation timescale on a wide range of pressure and temperature variations. Actually, dielectric studies carried out on m-FA at moderate [3] and high [4] pressure show, respectively, a peculiar aging behavior and significant changes in the dielectric spectra. In particular, in glasses obtained at very high pressure and high temperature, the secondary relaxation observed at ambient pressure in m-FA is suppressed, and a new secondary relaxation emerges with properties of a genuine JG relaxation like in toluene [4]. The guess that comes from these results is that the secondary relaxation observed in m-FA at ambient pressure could originate from some internal processes in the hydrogen-bond-induced clusters. In fact, published elastic neutron scattering and simulation data [5] showed clearly the presence of hydrogen-bond-induced clusters of limited size in m-FA at low pressure and temperature as a pre-peak in the static structure factor  $S(Q)$ . The intensity of the pre-peak almost vanishes at high temperature and it is weakly affected by pressure. In the range of very high pressure and temperature these clusters are suppressed. The aim of our study was to validate that hypothesis using a different way to suppress the hydrogen-bond-induced clusters in m-FA: mixing it with aromatic compounds, in particular with m-xylene (m-X). In fact, variable shape variable size Monte Carlo simulations in isothermal-isobaric ensemble were carried out for pure and mixed solutions of m-FA and m-X in ambient condition. Except for pure m-X system, in all other systems we observed a pre-peak in the center of mass distribution function and structure factor, which we attribute to intermolecular hydrogen bonding. The intensity of this peak decreases with decrease in concentration of m-FA which suggests a similar decreasing of the population of intermolecular hydrogen bonded pairs. Vibrational spectra from infrared spectroscopy also confirmed that the N-H stretching was considerably changed at low m-FA molar fraction.

We performed broadband dielectric spectroscopy on  $(m\text{-FA})_{1-x}(m\text{-X})_x$  mixtures at different molar fraction  $x$  spanning all the supercooled and glassy temperature

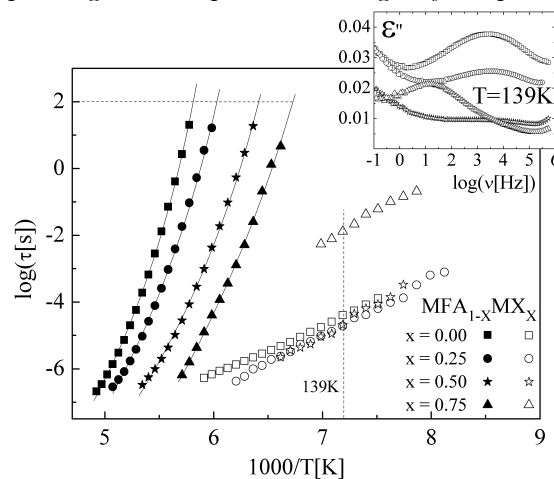


FIG. 1. Relaxation map for  $\alpha$ - and  $\beta$ - relaxation times (filled and open symbols respectively) in binary mixtures of m-FA and m-X. Inset shows a comparison of dielectric losses for different mixtures at  $T=139$  K in the glassy state.

range. As in the case of high pressure experiment, the main result was a complete suppression of the secondary relaxation observed in m-FA, substituted already at  $x=0.75$  m-X molar fraction by a slower process with higher activation energy, with characteristics of the universal JG  $\beta$ -relaxation (see Fig.1).

S.C. thanks Ministerio de Education de España for financial support of the program *Estancias de Jovenes Extranjeros en Centros Españoles* SB2009-0130.

\* Corresponding author: michela.romanini@upc.edu

- [1] A. Kudlik, S. Benkhof, T. Blochowicz, C. Tschirwitz, and E. Rössler, *J. Mol. Struct.* **479**, 201 (1999)
- [2] K. L. Ngai and M. Paluch, *J. Chem. Phys.* **120**, 857 (2004).
- [3] A. Reiser, G. Kasper, and S. Hunklinger, *Phys. Rev. Lett.* **92**, 125701 (2004).
- [4] S. Hensel-Bielówka, M. Paluch, K. L. Ngai, *J. Chem. Phys.* **123**, 014502 (2005).
- [5] D. Morineau, C. Alba-Simionesco, M. C. Bellissent-Funel, and M. F. Lauthie, *Europhys. Lett.* **43**, 195 (1998); D. Morineau and C. Alba-Simionesco, *J. Chem. Phys.* **109**, 8494 (1998).

## Identification the origins of non-JG secondary modes. Conformational interconversion as JG secondary mode.

P. Włodarczyk,\* M. Paluch, K. Kaminski, K. Adrjanowicz, and Z. Wojnarowska

*Institute of Physics, University of Silesia, ul. Uniwersytecka 4, 40-007 Katowice, Poland*

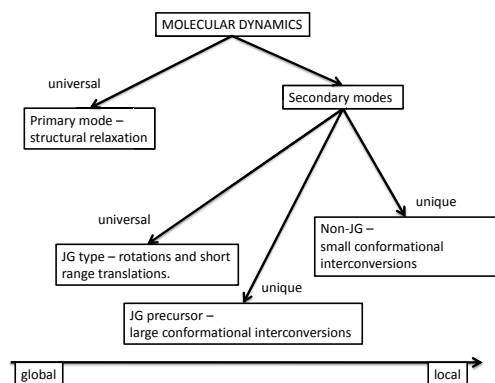


FIG. 1. Classification of secondary modes proposed by our group. It includes unique large JG-like interconversions.

Secondary modes can be divided into two groups. To the first one belong processes related to rotations and short-range translation of molecule which is entrapped in the cage created by its neighbors. This type of movements is called Johari-Goldstein. To the second group belong all processes which cannot be classified as Johari-Goldstein. These processes are called non-Johari-Goldstein. Non-JG processes were intensively studied in our group. We found, that every relaxation process which is classified as non-JG is in fact change of conformation. All conformational interconversions in studied molecules were connected with the certain relaxation modes by comparison of experimental activation energy with the one obtained from density functional theory (DFT) calculations. It is simple method to identify origin of the non-JG secondary mode. During our studies we found in few compounds

interconversions, in which large parts of molecules are involved. These interconversions are such space demanding that they have positive activation volume. Therefore, molecules interact with surroundings while they are changing their conformation. In such scenario they should be classified rather as JG, however they are not universal. Such type of movement doesn't exist in small and rigid molecules. This is explained in the scheme presented in the abstract (fig.1). We have already studied such molecules as D-glucose [1], maltose [2], perhydroisoquinoline [3], tetralone, glibenclamide, glimepiride, butyl phthalate, isobutyl phthalate and few more. Some of the data are not yet published.

The authors (P. W., K. K., Z. W., K. A. and M. P.) are deeply thankful for the financial support of their research within the framework of the project entitled From Study of Molecular Dynamics in Amorphous Medicines at Ambient and Elevated Pressure to Novel Applications in Pharmacy, which is operated within the Foundation for Polish Science Team Programme cofinanced by the EU European Regional Development Fund. Moreover P. W. would like to thank Foundation for Polish Science for awarding grants within the framework of the START Programme (2010).

\* Corresponding author: pwlodarc@us.edu.pl

- [1] K. Kaminski, P. Włodarczyk, K. Adrjanowicz, E. Kaminska, Z. Wojnarowska, and M. Paluch, *J. Phys. Chem. B* **114**, 11272 (2010).
- [2] P. Włodarczyk, K. Kaminski, K. Adrjanowicz, Z. Wojnarowska, B. Czarnota, M. Paluch, J. Ziolo, and J. Pilch, *J. Chem. Phys.* **131**, 125103 (2009).
- [3] P. Włodarczyk, B. Czarnota, M. Paluch, S. Pawlus, and J. Ziolo, *J. Mol. Struct.* **975**, 200 (2010).

## Visualizing Coherent Acoustic Phonons in Disordered Materials

Tullio Scopigno\*

*Dipartimento di Fisica and IPCF-CNR, Università di Roma "La Sapienza", Italy*

\* Corresponding author: [tullio.scopigno@phys.uniroma1.it](mailto:tullio.scopigno@phys.uniroma1.it)

This abstract is not available in this version.

## Temperature-independent decoupling between the characteristic time scales of five independent linear response functions

Bo Jakobsen,\* Tina Hecksher, Kristine Niss, Tage Christensen, Niels Boye Olsen, and Jeppe C. Dyre

*DNRF centre “Glass and Time”, IMFUFA, Department of Sciences,  
Roskilde University, Postbox 260, DK-4000 Roskilde, Denmark*

The temperature dependence of the characteristic time scale of the structural relaxation is a major parameter characterizing viscous liquids. However, it is not possible to assign one unique time scale, as this depends on the type of response that is analyzed.

We have in the Roskilde group developed a number of techniques allowing for measuring a number of complex frequency- or time-dependent linear response functions on very viscous liquids close to the glass transition temperature: The shear modulus ( $G(\nu)$ ) [1], the adiabatic bulk modulus ( $K_S(\nu)$ ) [2] [which can be inverted to give the complex frequency-dependent adiabatic compressibility ( $\kappa_S(\nu)$ )], the longitudinal thermal expansion coefficient ( $\alpha_l(t)$ ) [3], the longitudinal specific heat [4] ( $c_l(\nu)$ ), and the dielectric constant ( $\epsilon(\nu)$ ). All techniques utilize the same custom-built cryostat [5] and electronics setup [6].

In this work [7] we compare the characteristic time scales from these methods for two molecular glass-formers the silicone oil Tetramethyltetraphenyltrisiloxane (the Dow Corning diffusion pump oil DC704) and Polyphenylether (Santovac®5 Diffusion Pump Fluid). Fig. 1 shows the characteristic time scales as function of temperature, covering in total 9 decades in time scales.

Three major observations are discussed:

**First,:** the data establish a “time scale order” for the response functions:

$$\tau_G < \tau_{K_S} < \tau_{\kappa_S} < \tau_\epsilon < \tau_{\alpha_l} < \tau_{c_l}. \quad (1)$$

**Secondly,:** it is surprisingly observed that the time scales follow each other closely as function as temperature, that is:

$$\frac{\tau_x(T)}{\tau_y(T)} = \text{Constant}_{x,y} \quad (2)$$

for any pair of the observed response functions.

**Third,:** we evaluated the temperature dependency of the spectral shape for  $\epsilon(\nu)$ ,  $G(\nu)$ ,  $K_S(\nu)$ ,  $\alpha_l(t)$ , and found that the shape of these response functions to a very good approximation is temperature independent (we speculate that all the measured response functions have similar behavior).

The consequences of the specific choice of thermo-mechanical boundary conditions on the time scale are

discussed. Based on information on the absolute levels of the response functions [8] we discuss the time scales for the more well-known response functions,  $c_P(\nu)$ ,  $\alpha_P(\nu)$ , and  $K_T(\nu)$ .

To summarize, we show that these two liquids have a surprisingly simple behavior, with time scales following each other closely and temperature independent shapes of their linear response functions.

The center for viscous liquid dynamics “Glass and Time” is sponsored by the Danish National Research Foundation.

\* Corresponding author: boj@ruc.dk

- [1] T. Christensen and N. B. Olsen, Rev. Sci. Instrum. **66**, 5019 (1995).
- [2] T. Christensen and N. B. Olsen, Phys. Rev. B **49**, 15396 (1994).
- [3] K. Niss, N. B. Olsen, and J. C. Dyre, In preparation.
- [4] T. Christensen and J. C. Dyre, Phys. Rev. E **78**, 021501 (2008); B. Jakobsen, N. B. Olsen, and T. Christensen, Phys. Rev. E **81**, 061505 (2010).
- [5] B. Igarashi, T. Christensen, E. H. Larsen, N. B. Olsen, I. H. Pedersen, T. Rasmussen, and J. C. Dyre, Rev. Sci. Instrum. **79**, 045105 (2008).
- [6] B. Igarashi, T. Christensen, E. H. Larsen, N. B. Olsen, I. H. Pedersen, T. Rasmussen, and J. C. Dyre, Rev. Sci. Instrum. **79**, 045106 (2008).
- [7] B. Jakobsen, T. Hecksher, K. Niss, T. Christensen, N. B. Olsen, and J. C. Dyre, In preparation.
- [8] D. Gundermann, U. R. Pedersen, T. Hecksher, et al., In preparation.

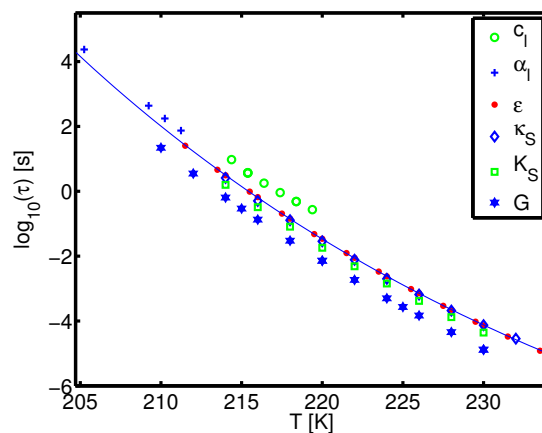


FIG. 1. Characteristic time scales (defined from loss-peak positions) as function of temperature for the six response functions of Tetramethyltetraphenyltrisiloxane (DC704). The line is a fit of the dielectric data to an Avramov function ( $\tau(T) = \tau_0 \exp(B/T^m)$ ), used for extrapolation of the dielectric data to low temperatures.

## Experimental connection between density scaling and the Prigogine-Defay ratio of a glass-forming liquid

Ditte Gundermann,<sup>1,\*</sup> Ulf R. Pedersen,<sup>1,2</sup> Tina Hecksher,<sup>1</sup> Nicholas Bailey,<sup>1</sup>  
Bo Jakobsen,<sup>1</sup> Tage Christensen,<sup>1</sup> Thomas B. Schröder,<sup>1</sup> Daniel Fragiadakis,<sup>3</sup>  
Ricardo Casalini,<sup>3</sup> Mike Roland,<sup>3</sup> Jeppe C. Dyre,<sup>1</sup> and Kristine Niss<sup>1</sup>

<sup>1</sup>*DNRF Centre Glass and Time, IMFUFA, Department of Sciences,  
Roskilde University, Postbox 260, DK-4000 Roskilde, Denmark*

<sup>2</sup>*Department of Chemistry, University of California, Berkeley, California 94720-1460, USA*

<sup>3</sup>*Chemistry Division, Naval Research Laboratory, Washington, DC 20375-5342, USA*

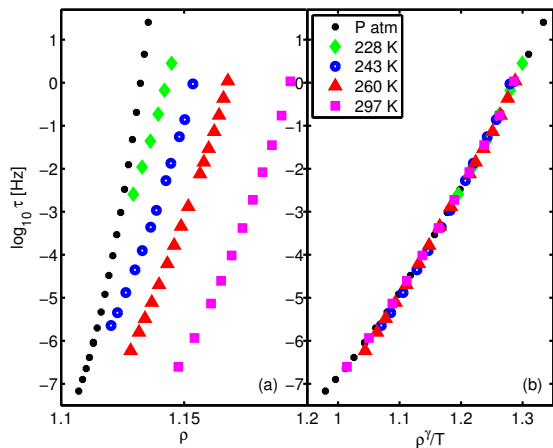


FIG. 1. Relaxation time ( $\tau = 1/\omega_{max}$ ) as a function of (a) density and (b)  $\rho^\gamma/T$  for DC704.  $\gamma = 6.1$

We present the first experimental test of an important prediction for strongly correlating liquids [1], namely that the density scaling exponent may be calculated from equilibrium fluctuations at a single state point as showed in computer simulations [2, 3]. The equilibrium fluctuations are probed via the fluctuation-dissipation theorem, which relates linear-response functions to fluctuations. The experiments were performed on a van der Waals bonded and stable glass-forming liquid DC704 (tetramethyltetraphenyltrisiloxane). Fig. 1 shows scaled and unscaled dielectric data for DC704 ( $\gamma_{scale} = 6.1$ ) and Fig. 2 shows examples of the measured frequency dependent viscoelastic response functions. The table shows the calculated  $\gamma$  together with  $\gamma_{scale}$  obtained from density scaling (Fig. 1):

$\Pi_{pT}^{lin}$	1.1
$\Pi_{VT}^{lin}$	1.2
$R$	0.92
$\gamma$	$6.2 \pm 2$
$\gamma_{scale}$	$6.1 \pm 0.2$

We find that for DC704 the prediction for the density scaling exponent obtained from linear-response data taken at a single state point,  $\gamma = 6.2 \pm 2$ , is in good agreement with the exponent found from density scaling of the dielectric data,  $\gamma_{scale} = 6.1$  (Fig. 1(b)). The large uncertainty on  $\gamma$  reflects the fact that measuring the absolute values of the fre-

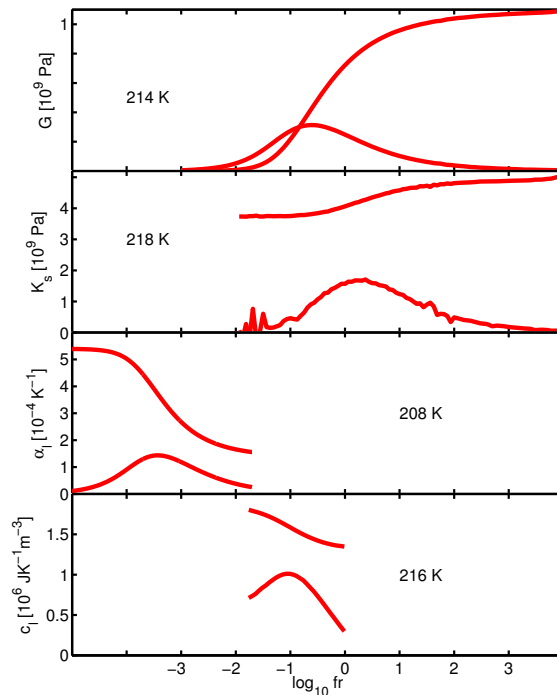


FIG. 2. Examples of the frequency-dependent data, from top: shear modulus  $G(\omega)$ , adiabatic bulk modulus  $K_s(\omega)$ , longitudinal expansion coefficient,  $\alpha_l(\omega)$  and the longitudinal heat capacity  $c_l(\omega)$ . Imaginary parts of  $K_s(\omega)$  and  $c_l(\omega)$  have been multiplied by a factor of 5.

quency dependent thermo-mechanical response functions is still very challenging.

Finally we show that the correlation coefficient is given by the linear P-D ratio [4] and show that a compilation of literature data on classical P-D ratios supports the general conjecture that van der Waals bonded liquids are strongly correlating, and hence constitute a class of simple liquids.

\* Corresponding author: ditteg@ruc.dk

- [1] U. R. Pedersen, N. P. Bailey, T. B. Schröder and J. C. Dyre, *Phys. Rev. Lett.* **100**, 015701 (2008).
- [2] D. Coslovich and C. M. Roland, *J. Chem. Phys.* **131**, 151103 (2009).
- [3] T. B. Schröder, U. R. Pedersen, N. P. Bailey, S. Toxværd, and J. C. Dyre, *Phys. Rev. E* **80**, 04150 (2009).
- [4] N. L. Ellegaard, T. Christensen, P. V. Christiansen, N. B. Olsen, U. R. Pedersen, T. B. Schröder, and J. C. Dyre, *J. Chem. Phys.* **126**, 074502 (2007).

## Dynamic thermal expansivity of a molecular liquid near the glass transition

Kristine Niss,\* Niels B. Olsen, and Jeppe C. Dyre

*DNRF Centre Glass and Time, IMFUFA, Department of Sciences,  
Roskilde University, Postbox 260, DK-4000 Roskilde, Denmark*

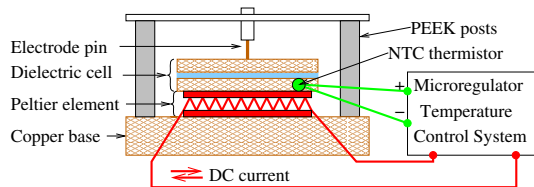


FIG. 1. Sketch of the experimental setup. An NTC-bead in the lower capacitor-plate measured the temperature. It is connected to a temperature-control system which controls the heating and cooling done by the Peltier element. The whole setup is placed in our main cryostat. (Figure taken from [2].)

Glass-forming liquids are viscoelastic close to the glass-transition and all the thermodynamic response functions are therefore dynamic. That is the response is time (or equivalently frequency) dependent: at short times the response is solid-like but it is liquid-like at long time. While this is well known, and while it is clear that both the temperature dependence of the relaxation time and the absolute level of these quantities play a central role for understanding the viscous liquids, data is very scarce in literature.

Here we present data on the dynamical expansion coefficient  $\alpha(t)$  for a glass-forming liquid in the ultra viscous range. The experiment is performed on a novel home-built setup which follows the principle suggested by Bauer [1]. The dynamical range has been extended by making time domain experiments, and by making very small and fast temperature steps. The modelling of the experiment has moreover been developed.

The principle of the experiment is to make an “instantaneous” temperature step and then to measure the capacitance at a fixed frequency as a function of time. From the capacitance we calculate the time-dependent expansion coefficient. The actual time of a temperature step is 10 s. In order for this to be “instantaneous” compared to the timescale of the liquid dynamics, the relaxation time needs to be 100 s or preferably longer. To obtain a linear response the temperature steps need to be very small, because the relaxation time is extremely temperature dependent. This also means that the change in volume and thereby measure capacitance is very small, the relative changes are in capacitance  $dC/C$  are in the order of magnitude  $10^{-4}$ . The fast temperature step and the required long time temperature stability is achieved by using our microregulator which changes temperature on a time scale of a few seconds and keeps fluctuations below  $100\mu\text{K}$

[2, 3]. The setup is illustrated in Fig. 1.

We measure  $\frac{1}{C_m} \frac{dC_m(t)}{dT}$ , and show that this is proportional to  $\alpha(t)$  with a proportionality constant that depends on  $\epsilon_\infty$  and the degree of filling of the capacitor,  $f$ , but not on the geometrical capacitance or the distance between the plates. The principle and the idea follows the derivations shown in Ref. 1, but we moreover consider the situation where the capacitor is not full because the liquid contracts when cooling from room temperature down to around  $T_g$  (which is typically around 200 K for molecular liquids).

Data is presented on the molecular glass-former Tetramethyltetraphenyltrisiloxane (DC704). The data are shown in Fig. 2. We find that the relaxation obeys TTS and that the temperature dependence of the relaxation time follows the same behavior as the dielectric relaxation. The absolute value of the expansion coefficient is used in combination with other data to determine the linear Prigogine-Defay ratio.

This work was supported by the Danish National Research Foundation’s DNRF center for viscous liquid dynamics “Glass and Time”.

\* Corresponding author: kniss@ruc.dk

- [1] C. Bauer *et al.*, Phys. Rev. E **61** 1755 (2000), C. Bauer *et al.* J. Non-cryst Solids **262** 276 (2000)
- [2] T. Hecksher *et al.*, J. Chem. Phys. **133**, 174514 (2010)
- [3] B. Igarashi *et al.* Rev. Sci. Instrum. **79**, 045105 (2008).

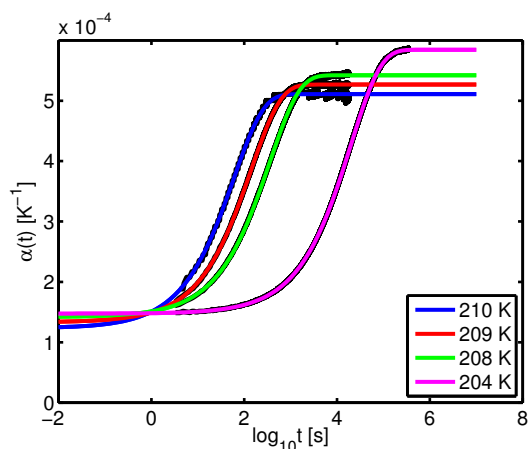


FIG. 2. Time dependent linear thermal expansion coefficient of Tetramethyltetraphenyltrisiloxane (DC704). The black lines are data and the colored lines are fits.

## Investigation of infinite frequency shear and bulk moduli on strongly correlating liquids

Lasse Bøhling\* and Thomas B. Schrøder

*DNRF Center “Glass and Time”, IMFUFA, Department of Sciences,  
Roskilde University, P.O. box 260, DK-4000 Roskilde Denmark*

It has recently been suggested that the high frequency shear moduli expressed in reduced units is an isomorph invariant for strongly correlating liquids[1] and no prediction has been proposed for the bulk moduli[2]. Here we investigate the invariance of the moduli on an isomorph. From computer simulations it is possible to calculate the high frequency limit of the shear and bulk moduli from the radial distribution function[3]. The moduli has been examined for the strongly correlating generalized Lennard-Jones potential. The shear moduli is to a certain approximation invariant on an isomorph. The bulk moduli is equally invariant, but the origin of this is different from the shear moduli.

Furthermore a prediction for the shear and bulk mod-

uli, using Rosenfeld Tarazona scaling[4], on a isochore is presented.

The center for viscous liquid dynamics “Glass and Time” is sponsored by the Danish National Research Foundation (DNRF).

\* Corresponding author: lasseb@ruc.dk

- [1] U. R. Pedersen, N. P. Bailey, T. B. Schrøder, and J. C. Dyre, *Phys. Rev. Lett.* **100**, 015701 (2008).
- [2] N. Gnan, T. B. Schrøder, U. R. Pedersen, N. P. Bailey, and J. C. Dyre, *J. Chem. Phys.* **131**, 234504 (2009).
- [3] R. Zwanzig and R. D. Mountain, *J. Chem. Phys.* **43**, 12 (1965).
- [4] Y. Rosenfeld and P. Tarazona, *Mol. Phys.* **95**, 141 (1998).

## Perturbation theory approach to determining the effective inverse power-law exponent for strongly correlating liquids.

Nicholas P. Bailey,\* Thomas B. Schröder, and Jeppe C. Dyre

*DNRF Center “Glass and Time”, IMFUFA, Dept. of Sciences,  
Roskilde University, P.O. Box 260, DK-4000 Roskilde, Denmark*

Recent work has demonstrated that a class of model liquids exhibit certain scaling properties normally associated with systems which interact via inverse power-law (IPL) potentials[1–6]. These include (1) strong correlation between instantaneous potential energy  $U$  and virial  $W$  under conditions of fixed volume; (2) “density-scaling” of structure and dynamics, that is to say that all structural and dynamical properties, when expressed in appropriate “reduced units”, depend only on the combination  $\Gamma = \rho^\gamma/T$ , where  $\gamma$  is the slope in the  $W, U$  plot[3]; (3) jumps made along curves of constant  $\Gamma$  bring the system immediately to equilibrium without any relaxation, even though the relaxation time may be large[4, 5]. The above statements are exactly true for systems interacting with an IPL potential  $v(r) = A/r^n$ , where the exponent  $n$  determines  $\gamma = n/3$ . What has newly been appreciated is that Lennard-Jones (LJ)-like systems exhibit the same properties. The explanation can be traced to the fact that the LJ potential is well approximated by an extended IPL (eIPL)—an IPL with exponent  $n \sim 18$  plus a linear term which fluctuates little at fixed volume and therefore has little effect on structure or dynamics[2].

The observed slope  $\gamma$  in the  $W, U$  plot is state-point dependent, so one cannot expect to be able to look at the LJ potential and figure out exactly what the effective IPL exponent should be. It has generally been assumed to be  $3\gamma$ , that is, given by looking at the fluctuations in  $U$  and  $W$ [7]. It is of interest to see if this matches the “thermodynamically optimal” exponent. In the present work we use methods of liquid-state perturbation theory to provide a variational estimate of the effective IPL exponent. That is we use the IPL potential to define reference system. It is well-known that the following inequality is strictly valid:

$$F_{LJ} \leq F_{IPL} + \langle \Delta U \rangle_{IPL} \quad (1)$$

where  $F$  represents the Helmholtz free energy, and the last term is the expectation value of the difference in potential energy between the LJ system and the IPL system. Since the right hand side depends on the IPL parameters  $A$  and  $n$ , minimizing the right hand side with respect to them provides the thermodynamically optimal choice.

Our initial attempts involved using standard analytical techniques for approximating the structure of the reference system by use of mapping to an equivalent hard-sphere system. This approach turned out not to be sufficiently accurate, despite using recent formulations of the hard-sphere radial distribution function and equation of state, due to the accuracy of the mapping from hard to soft systems being systematically worse as  $n$  decreases. Instead all reference free-energies were calculated by simulation with a precision better than 0.002 (LJ units). This allowed us to find the optimal  $A$  and  $n$  as a function of state point ( $\rho, T$ ) and compare with the exponent determined from the fluctuations i.e.,  $3\gamma$ . Results will be presented for the single-component LJ fluid as well as for the Kob-Andersen binary LJ system which is a good model of a glass-forming liquid.

The centre for viscous liquid dynamics “Glass and Time” is sponsored by the Danish National Research Foundation (DNRF).

\* Corresponding author: nbailey@ruc.dk

- [1] N. P. Bailey et al., *J. Chem. Phys.* **129**, 184507 (2008).
- [2] N. P. Bailey et al., *J. Chem. Phys.* **129**, 184508 (2008).
- [3] T. B. Schröder et al., *J. Chem. Phys.* **131**, 234503 (2009)
- [4] N. Gnan et al., *J. Chem. Phys.* **131**, 234504 (2009).
- [5] N. Gnan et al., *Phys. Rev. Lett.*, **104**, 125902 (2010).
- [6] T. B. Schröder et al., *Phys. Rev. E* **80**, 041502 (2009).
- [7] U. R. Pedersen et al, *Phys. Rev. Lett.*, **105**, 157801 (2010).

## NVU dynamics: Replacing Newton's 2nd law with Newton's 1st law

Trond S. Ingebrigtsen,\* Søren Toxvaerd, Thomas B. Schrøder, and Jeppe C. Dyre

DNRF Centre "Glass and Time", IMFUFA, Department of Sciences, Roskilde University, Denmark

This abstract considers geodesic motion on the constant potential energy hypersurface,  $\Omega$ , defined by

$$\Omega = \{(\mathbf{r}_1, \dots, \mathbf{r}_N) \in R^{3N} \mid U(\mathbf{r}_1, \dots, \mathbf{r}_N) = U_0\}. \quad (1)$$

$U(\mathbf{r}_1, \dots, \mathbf{r}_N)$  is the potential energy function of the system. The geodesic motion defines a molecular dynamics entitled *NVU* dynamics [1, 2]. Geodesic curves are well known in mathematics: on a sphere they are the great circles. The geodesic curves on  $\Omega$  are defined via

$$\delta \int dl = 0, \quad (2)$$

where  $dl$  is the infinitesimal distance measure on  $\Omega$ .

*NVU* dynamics considers only the configuration space with equal probability (and potential energy) for all points on  $\Omega$ . *NVU* dynamics thus invites to a different view on the dynamics of a classical mechanical system, than provided by for instance the potential energy landscape.

From Eq. (2) we derived a discrete algorithm for tracing out geodesic curves on  $\Omega$  [1]. The corresponding algorithm is very similar to the well-known Verlet algorithm and has the same excellent stability. The discrete *NVU* algorithm is

$$\mathbf{R}_{i+1} = 2\mathbf{R}_i - \mathbf{R}_{i-1} + \frac{2\mathbf{F}_i \cdot (\mathbf{R}_i - \mathbf{R}_{i-1})}{\mathbf{F}_i^2} \cdot \mathbf{F}_i. \quad (3)$$

In this paper [2] *NVU* dynamics is compared to different dynamics, stochastic as well as deterministic, in the viscous regime for the Kob-Andersen (*KA*) binary Lennard Jones mixture [3]. Amongst these dynamics is the standard energy conserving *NVE* dynamics given by Newton's 2nd law (Verlet algorithm). Selected results from this comparison are given in Fig. (1) and (2).

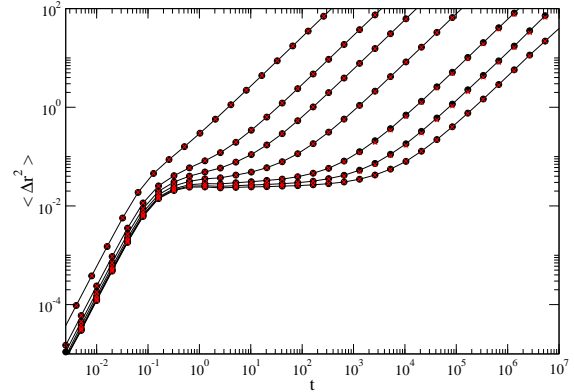


FIG. 1. The mean-square displacement at  $\rho = 1.2$  and  $T = 2.0, 0.80, 0.60, 0.50, 0.44, 0.42$  and  $0.405$  (left to right) for the *KA* binary mixture. The *NVE* dynamics is given by filled black circles and the *NVU* dynamics as red crosses.

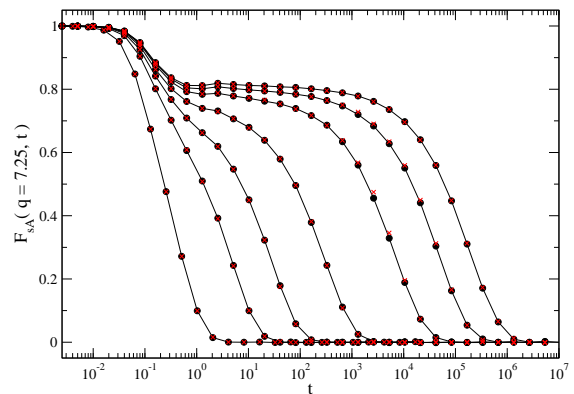


FIG. 2. The incoherent intermediate scattering function at  $\rho = 1.2$  and  $T = 2.0, 0.80, 0.60, 0.50, 0.44, 0.42$  and  $0.405$  (left to right) for the *KA* binary mixture. The *NVE* dynamics is given by filled black circles and the *NVU* dynamics as red crosses.

*NVU* and *NVE* dynamics are not identical, but the two dynamics are seen to agree very well – one may say that they are equivalent. This equivalence can furthermore be justified from the discrete algorithm given in Eq. (3) or from Hamilton's principle in the thermodynamic limit.

The centre for viscous liquid dynamics "Glass and Time" is sponsored by the Danish National Research Foundation (DNRF).

\* Corresponding author: trond@ruc.dk

- [1] *NVU* dynamics. I. Geodesic motion on the constant-potential-energy hypersurface (in preparation).
- [2] *NVU* dynamics. II. Comparing to four other dynamics (in preparation).
- [3] W. Kob and H. C. Andersen, Phys. Rev. E **51**, 4626 (1995); *ibid.* **52**, 4134 (1995).

## Theory of isomorphs: applications to generalized Lennard-Jones liquids

Thomas B. Schröder,\* Nicoletta Gnan, Ulf R. Pedersen, Nicholas P. Bailey, and Jeppe C. Dyre

*DNRF center “Glass and Time,” Roskilde University, Denmark*

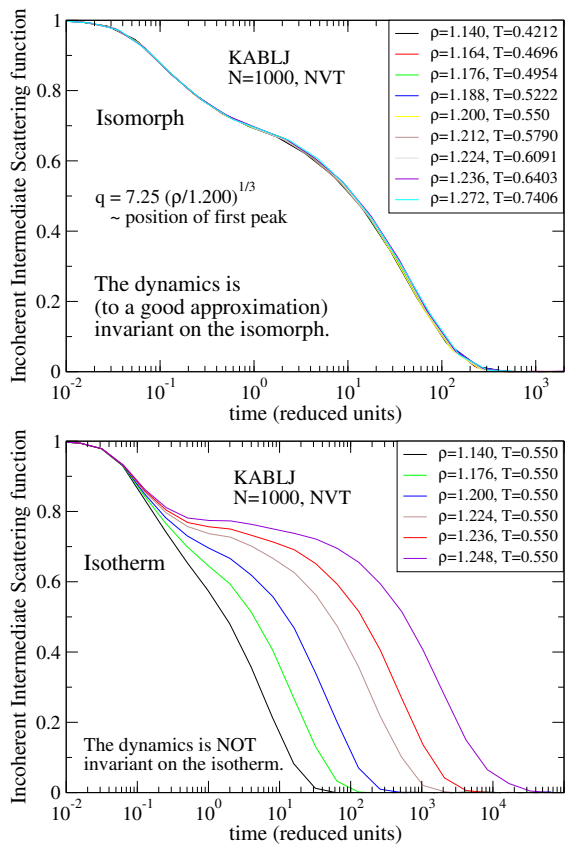


FIG. 1. Upper panel: Invariance of the incoherent intermediate scattering function on an isomorph. State points on isomorph chosen to keep  $S^{ex}$  constant. Lower panel: Corresponding isotherm with slightly less density change.

The theory of isomorphs in liquids is derived [1] from a single assumption: Two state points  $(\rho_1, T_1)$  and  $(\rho_2, T_2)$  are defined to be *isomorphic* if they obey the following: Any two physically relevant configurations  $(\mathbf{r}_1^{(1)}, \dots, \mathbf{r}_N^{(1)})$  and  $(\mathbf{r}_1^{(2)}, \dots, \mathbf{r}_N^{(2)})$  that trivially scale into one another,

$$\rho_1^{1/3} \mathbf{r}_i^{(1)} = \rho_2^{1/3} \mathbf{r}_i^{(2)} \quad (i = 1, \dots, N), \quad (1)$$

have proportional configurational Boltzmann weights:

$$e^{-U(\mathbf{r}_1^{(1)}, \dots, \mathbf{r}_N^{(1)})/k_B T_1} = C_{12} e^{-U(\mathbf{r}_1^{(2)}, \dots, \mathbf{r}_N^{(2)})/k_B T_2}. \quad (2)$$

Here  $U(\mathbf{r}_1, \dots, \mathbf{r}_N)$  is the potential energy function and  $C_{12}$  depends only on the two state points.

Only IPL liquids have exact isomorphs, but it can be shown [1] that “strongly correlating liquids” (with strong correlations between potential energy  $U(t)$  and virial  $W(t)$  in NVT simulations [2]) to a good approximation have isomorphs.

From Eq. (2) a number of properties can be derived [1], e.g., the excess entropy  $S^{ex}$  and heat capacity  $C_V^{ex}$  are invariant on an isomorph (curve in the state diagram along which all state points are isomorphic). Furthermore, both structure and dynamics (Fig. 1) are isomorphic invariant (in the proper reduced units). For multi-component generalized Lennard-Jones (LJ) systems further properties can be derived [3]. The predicted shape of isomorphs in the  $WU$  phase diagram is in excellent agreement with simulations, see Fig 2. Shapes only depend on the LJ exponents, thus all isomorphs of all standard LJ systems (with exponents 12 and 6) are identical - and can be scaled onto to a single curve (Fig. 2). Building on the isomorph theory, an equation of state is derived [3] for generalized LJ systems.

The center for viscous liquid dynamics “Glass and Time” is sponsored by the Danish National Research Foundation (DNRF).

\* Corresponding author: tbs@ruc.dk

- [1] N. Gnan, T. B. Schröder, U. R. Pedersen, N. P. Bailey, and J. C. Dyre, *J. Chem. Phys.* **131**, 234504 (2009).
- [2] U. R. Pedersen, N. P. Bailey, T. B. Schröder, and J. C. Dyre, *Phys. Rev. Lett.* **131**, 015701 (2008).
- [3] T. B. Schröder, N. Gnan, U. R. Pedersen, N. P. Bailey, and J. C. Dyre, *Phys. arXiv:1004.5142* (2010).

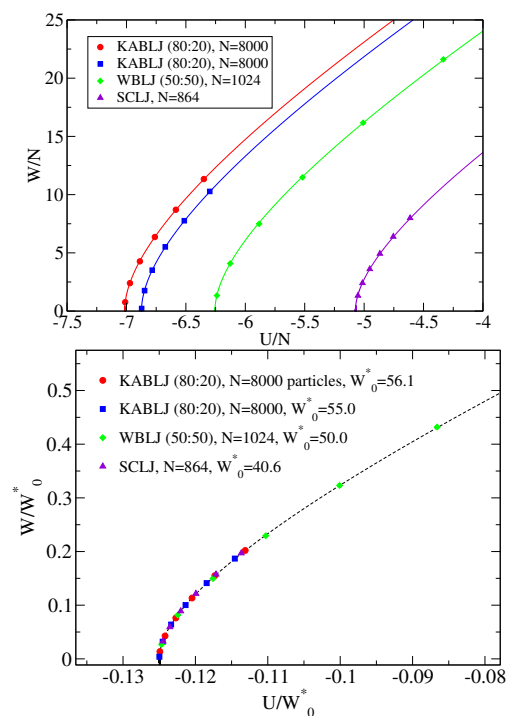


FIG. 2. Upper panel: Isomorphs in the  $WU$  phase diagram for three different 12-6 LJ systems, Points: simulations, Lines: isomorph prediction. Lower panel: Same isomorphs scaled onto the “master isomorph”.

## Relation between the shear fluctuation spectrum and the dielectric fluctuation spectrum in highly viscous liquids

U. Buchenau\*

*Institut für Festkörperforschung, Forschungszentrum Jülich,  
Postfach 1913, D-52425 Jülich, Federal Republic of Germany*

A promising approach for the study of the flow process in highly viscous liquids is its comparison in different techniques. One usually finds the dielectric absorption peak close to the heat capacity one, but the shear modulus peak about half a decade higher in frequency [1]. In a broad distribution of relaxation times, a modulus peak always appears at a higher frequency than a susceptibility (compliance) peak. The question is whether this explains the faster shear peak.

In order to answer this question, one has to extract a susceptibility out of the shear modulus  $G(\omega)$ . There are two equivalent textbook descriptions of the shear spectrum of a liquid [2], a relaxation spectrum  $H(\tau)$  for the description of the complex shear modulus  $G(\omega)$  ( $\tau$  relaxation time)

$$G(\omega) = \int_{-\infty}^{\infty} \frac{H(\tau)i\omega\tau}{1+i\omega\tau} d \ln \tau \quad (1)$$

and a retardation spectrum  $L(\tau)$  for the description of the complex shear compliance

$$J(\omega) = \frac{1}{G} + \int_{-\infty}^{\infty} \frac{L(\tau)}{1+i\omega\tau} d \ln \tau - \frac{i}{\omega\eta}. \quad (2)$$

Here  $G$  is the infinite frequency shear modulus and  $\eta$  is the viscosity. A third material constant hidden in this equation is the recoverable compliance  $J_e^0$ , the elastic compliance plus the integral over the retardation processes

$$J_e^0 = \frac{1}{G} + \int_{-\infty}^{\infty} L(\tau) d \ln \tau. \quad (3)$$

Eq. (2) makes a separation of two independent contributions to the compliance, the retardation spectrum and the viscosity. From our gradually growing understanding of the highly viscous liquid, we know that both parts must come from thermally activated transitions between inherent states, stable structures corresponding to minima of the potential energy landscape. The retardation spectrum is due to back-jumps into the initial inherent state, the viscosity is due to the no-return jumps. The retardation description separates these two influences, the relaxation description does not.

It is interesting to consider a liquid with no back-jump preference. For a stationary flow in such a liquid, the removal of the constant shear stress would only result in the immediate recoverable compliance  $1/G$ . Afterward, there would be no reason for a further back-flow.

There would be no retardation spectrum, the Maxwell time  $\tau_M = \eta/G$  would be the only relaxation time and  $GJ_e^0 = 1$ . The consideration shows that the stretching observed universally in experiment is due to the back-jump preference, a fact that has never been clearly stated before.

In a real liquid, one finds an extremely broad spectrum of relaxation times and measured values of  $GJ_e^0$  of the order of three. Numerical simulations also find a large back-jump probability for the thermally activated transitions between the inherent states. Thus it is always possible to define a normalized shear retardation susceptibility  $\chi_{sr}$

$$\chi_{sr}(\omega) = \frac{G}{GJ_e^0 - 1} \int_{-\infty}^{\infty} \frac{L(\tau)}{1+i\omega\tau} d \ln \tau. \quad (4)$$

$\chi_{sr}$  is normalized with respect to the compliance step; the function begins with the value 1 at low frequency and ends with 0 at high frequency.

With  $J(\omega) = 1/G(\omega)$  and eq. (2), one can translate eq. (4) to

$$\chi_{sr}(\omega) = \frac{1}{GJ_e^0 - 1} \left( \frac{G}{G(\omega)} - 1 + \frac{i}{\omega\tau_M} \right). \quad (5)$$

One can argue that this susceptibility should equal the normalized  $\chi_e$  describing the decay of the electric dipole moment of the sample. The no-return transitions of the viscosity should assist the decay in a similar way in both cases. However, this is just a plausibility argument and no proof. The proof must come from a comparison of experimental spectra.

The comparison was done for literature data, taken under carefully controlled conditions to ensure the same samples and the same temperature control in both measurements [3]. The normalized shear compliance agrees with the normalized dielectric susceptibility in two substances at all measured temperatures. In two other substances, one can argue that there are good reasons for the deviations that one finds.

\* Corresponding author: buchenau-juelich@t-online.de

- [1] K. Schröter and E. Donth, *J. Non-Cryst. Solids* **307-310**, 270 (2002)
- [2] D. J. Ferry, *Viscoelastic properties of polymers*, chap. 3, 3rd ed., John Wiley, New York 1980
- [3] K. Niss, B. Jakobsen and N. B. Olsen, *J. Chem. Phys.* **123**, 234510 (2005); B. Jakobsen, K. Niss and N. B. Olsen, *J. Chem. Phys.* **123**, 234511 (2005); data available at the website <http://glass.ruc.dk/data/>

## Cooling by Heating - new phenomenon establishes subtle thermomechanical coupling

Jon Papini\* and Tage Christensen

Department of Sciences, DNRF Centre "Glass and Time", IMFUFA,  
Roskilde University, P.O. Box 260, DK-4000 Roskilde, Denmark

Given the thermoviscoelastic nature of liquids and the fascinating phenomena of flow that follow, it comes as no surprise that measurements of liquid properties are met with numerous problems. Interpretation of results become increasingly difficult as the glass transition is approached, and subtleties enter your considerations. Specifically the stresses that arise from thermal waves relaxing on the timescale of experiment (due to a high shear modulus) inevitably lead to broken hydrostatic conditions [1].

The equations for displacement and temperature fields (in a spherically symmetric case under quasi-static elastic conditions) couple through the pressure coefficient  $\beta_V = \frac{\partial p}{\partial T}|_V$ , which is related to the isobaric thermal expansion coefficient  $\alpha_p$  and isothermal bulk modulus  $K_T$  through  $\beta_V = \alpha_p K_T$ . This means that the ordinary heat diffusion equation fails, unless there is no thermal expansion,  $\alpha_p = 0$  or a vanishing shear modulus,  $G = 0$  [2].

Interacting thermally with a viscous system through its boundaries will lead to broken hydrostatic conditions, even in cases where the boundaries are mechanically non-clamped; the principal stresses will be equal only when the shear modulus has relaxed.

This non-trivial thermomechanical coupling is given by the ratio  $\gamma_l = \frac{c_l}{c_p}$  (as opposed to the often seen (trivial) ratio  $\gamma = \frac{c_p}{c_v}$ ), where the *longitudinal* specific heat,  $c_l$ , is given by  $c_l = \frac{M_S}{M_T} c_v$  where  $M = K + \frac{4}{3}G$ .

It can be shown that the relative deviation between  $c_l$  and  $c_p$  is  $\frac{c_p - c_l}{c_p} = \frac{4}{3} \cdot \frac{G}{M_T} \cdot \frac{c_p - c_v}{c_p}$ . This implies that the deviation from isobaric conditions is only significant at the glasstransition where upon increasing frequency the first factor  $[G/M_T]$  increases while the second  $[(c_p - c_v)/c_p]$  decreases. The situation is illustrated in the *sketch* in Fig. 1.

To establish the relative difference between the two specific heats, we propose an experiment where a temperature step is applied at the surface of a sphere (solid or liquid) while measuring temperature at the center. We present analytical results in the thermoelastic case (solid) as well as a numerical analysis (based on a single-order parameter model with parameters determined by Glycerol data) pertaining to the thermoviscoelastic case (liquid and solid). An example from the numerical results is given in Fig. 2 and shows a remarkable effect: The temperature initially decrease at the center of the sphere as the temperature at the boundary is increased!

The phenomenon reflects the non-isotropic character of the thermal expansion and the qualitative behavior

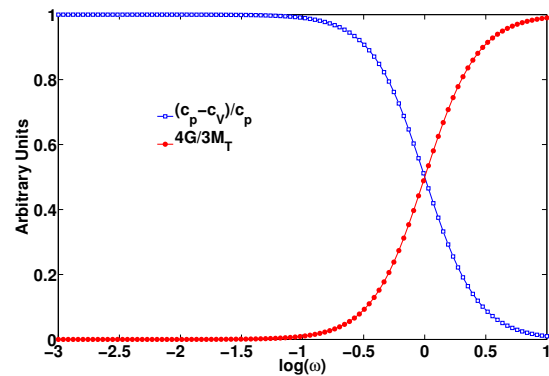


FIG. 1. Sketch of overlapping relaxations of  $G/M_T$  and  $(c_p - c_v)/c_p$ . The relative difference  $(c_p - c_l)/c_p$  depends on the product of the two relaxing functions. The higher a value at the inflection point, the bigger a difference between  $c_l$  and  $c_p$ .

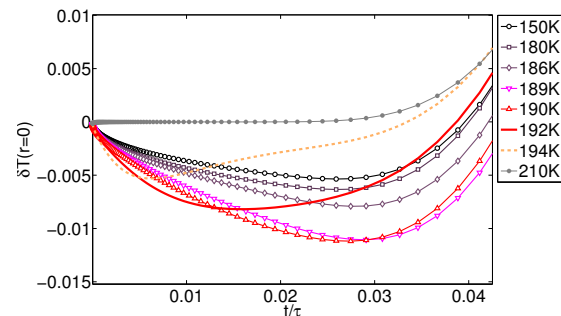


FIG. 2. Change in temperature,  $\delta T$  at the center of a sphere after a temperature step of  $\Delta T = 1$  has been applied at the surface (radius  $r = 10\text{mm}$  and parameters determined by Glycerol data). Time is scaled with the characteristic heat diffusion time  $\tau = \frac{r^2}{D}$  -  $D$  being the heat diffusion constant. The maximum occurs just above  $T_g$  (around 186K in Glycerol) where both shear modulus and isobaric expansion coefficient are expected to be large.

of the phenomenon makes it possible to experimentally establish the difference between  $c_l$  and  $c_p$ .

The numerical results (based on Glycerol data) indicate that a change in temperature at the center is on the order of 10mK with a duration of approximately 30 seconds when the temperature is increased by 1K on the surface of a sphere of radius  $r = 10\text{mm}$ .

\* Corresponding author: papini@ruc.dk

- [1] T. Christensen, N. B. Olsen and J. C. Dyre, Phys. Rev. E **75**, 041502 (2007)
- [2] T. Christensen and J. C. Dyre, Phys. Rev. E **78**, 021501 (2008)

## Thermodynamic and kinetic properties of glass-forming monoalcohols

Miguel A. Ramos,\* Merzak Hassaine, and Bisher Kabtoul

*Laboratorio de Bajas Temperaturas, Departamento de Física de la Materia Condensada,  
Universidad Autónoma de Madrid, Cantoblanco, E-28049 Madrid, Spain*

The fundamental understanding of the glass transition and related phenomena, as well as its connection to the unexpected low-temperature dynamics of non-crystalline solids, still represents an open challenge in condensed-matter physics and chemical physics.

In particular, much interest has been recently paid to molecular glass-forming liquids, among other reasons because they usually solidify either into crystal or glassy states at temperatures between liquid-nitrogen and room temperatures, therefore providing easy access to the different states of the substance for many experimental techniques. They often also include manifestations of polymorphism and even polyamorphism, that makes them interesting model systems to be studied.

In this work we present and discuss earlier and recent calorimetric experiments and specific-heat measurements performed on simple aliphatic glass-forming monohydroxy alcohols  $H(CH_2)_nOH$  at moderately low temperatures.

Firstly, we discuss how the gradual elongation of the molecule with increasing number of ethyl groups affects the vitrification vs crystallization kinetics for primary monoalcohols (that is, when the hydrogen bond is fixed at the end of the molecule). The competition between crystallization rate and glass-forming ability seems to depend mainly on the aspect ratio of the molecules, ranging from the easiest crystal former methanol to the best glass former propanol. The intermediate glass former ethanol (its phase diagram is schematically depicted in Fig. 1) presents the added value of a rich polymorphism [1]. On the other hand, our recent experiments on 1-butanol [2] supported the previous view [3] that the so-called “glacial state” of 1-butanol, presented as an evidence of *polyamorphism*, is rather a mixture of many nanocrystallites embedded in a disordered matrix, essentially due to an aborted crystallization originated by a high nucleation rate in a temperature range where the crystal growth is low.

It was found that the boson peaks of the *structural* (i.e. amorphous) glass and the *orientational* glass (i.e. orientationally-disordered crystal, ODC) of ethanol were very similar. In contrast, noticeable changes occur in the lattice dynamics and hence in the low-temperature properties of both glass and crystal states when different chemical isomers are compared, e.g. 1-propanol vs 2-propanol and 1-butanol vs 2-butanol [4].

Finally, we have compiled available thermodynamic data of all these monoalcohols, at the glass and crystal melting transitions, and have studied [4] whether proposed correlations in the literature [5, 6] of those

with liquid fragility could shed light on the observed

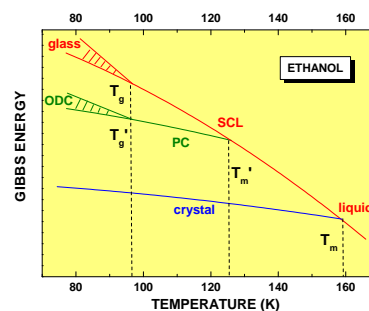


FIG. 1. Schematic Gibbs-energy phase diagram for ethanol. When the supercooled liquid (SCL) below the melting point  $T_m$  is quenched fast enough, the glass state is obtained. By heating the glass above  $T_g = 97K$  or by cooling the SCL more slowly, a plastic crystal (PC) is obtained, which becomes an orientationally-disordered crystal (ODC) below a glass-like transition at  $T'_g = 97K$ . The PC melts at  $T'_m = 125K$  and immediately transforms into a fully-ordered monoclinic crystal.

behaviour. By comparing kinetic and thermodynamic data, we have found that those proposed phenomenological correlations for the fragility of undercooled liquids is not fulfilled at all for these (and probably other) hydrogen-bonded liquids, which seem to behave kinetically as strong liquids but thermodynamically as fragile ones. For them, the entropy of crystal melting and the specific-heat jump at the glass transition do not directly correlate with the kinetic fragility index of the supercooled liquid. Furthermore, the glassy transition for the plastic crystal (i.e. the dynamical freezing of rotational disorder into static orientational disorder), that behaves so similarly to the canonical glass transition in many other respects, exhibits in this case a completely disparate behaviour.

\* Corresponding author: miguel.ramos@uam.es

- [1] M. A. Ramos *et al.*, *J. Non-Cryst. Solids* **352**, 4769 (2006).
- [2] M. Hassaine *et al.*, *J. Chem. Phys.* **131**, 174508 (2009); I. M. Shmyt'ko *et al.*, *J. Phys.: Condens. Matter* **22**, 195102 (2010).
- [3] A. Wypych, Y. Guinet and A. Hedoux, *Phys. Rev. B* **76**, 144202 (2007).
- [4] M. A. Ramos, B. Kabtoul and M. Hassaine, *Philos. Mag.*, first published on: 15 November 2010 (eFirst).
- [5] L.-M. Wang, C. A. Angell and R. Richert, *J. Chem. Phys.* **125**, 074505 (2006) and references therein.
- [6] V. Lubchenko and P. G. Wolynes, *J. Chem. Phys.* **119**, 9088 (2003); J. D. Stevenson and P. G. Wolynes, *J. Phys. Chem. B* **109**, 15093 (2005).

## The Kovacs effect: New insights from the Gaussian trap model

Gregor Diezemann<sup>1,\*</sup> and Andreas Heuer<sup>2</sup>

<sup>1</sup>*Institut für Physikalische Chemie, Universität Mainz, Welderweg 11, 55099 Mainz, FRG*

<sup>2</sup>*Institut für Physikalische Chemie, Universität Münster, Corrensstr. 30, 48149 Münster, FRG*

We investigate the memory effect or Kovacs effect in a simple model for glassy relaxation, the Gaussian trap model. In contrast to other models used to study non-equilibrium dynamics, in this model equilibrium is reached for long times independent of the initial conditions[1].

The protocol of the Kovacs experiment is the following: jump from a high temperature  $T_0$  to a low  $T_1 < T_0$  and stay there until the energy has reached its equilibrium value at some higher  $T_2$  ( $T_1 < T_2 < T_0$ ) at a time  $t_1$ ,  $E_{T_1}(t_1) = E_{T_2}^{\text{eq}}$  and then jump to  $T_2$ . Monitoring the energy  $E_{T_2}(t)$  afterwards, one observes a 'hump' in contrast to the naive expectation, according to which nothing changes.

First, one determines the time  $t_1$  for given  $(T_2 - T_1)$ , cf. Fig. 1. The non-monotonic behavior of  $t_1$  to the best

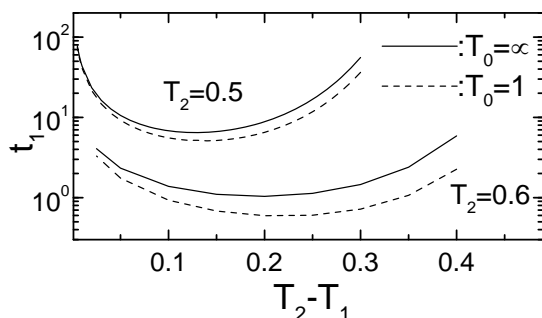


FIG. 1.  $t_1$  versus  $T_2 - T_1$  for different  $T_0$  and  $T_2$ . (Temperatures are measured in units of the width of the Gaussian density of states.)

of our knowledge has never been observed before but can be understood in terms of the relaxation behavior of the energy. The Kovacs hump  $\Delta E(t) = E_{T_2}(t) - E_{T_2}^{\text{eq}}$  is shown in Fig. 2. For this, all qualitative features

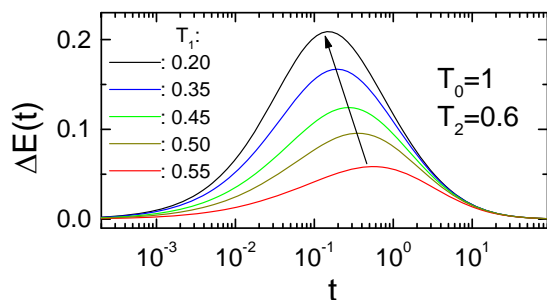


FIG. 2. Kovacs hump  $\Delta E(t)$  for the standard protocol.  $T_1$  decreases in the way indicated by the arrows.

are very similar to what has been found in many other investigations of the Kovacs effect. In particular, the maximum value increases and the time of its occurrence

decreases as a function of  $(T_2 - T_1)$ .

We also perform up-jumps and monitor the aging properties of the model for the 'inverse' Kovacs protocol. One starts from a low  $T_0$  and performs a jump to a high  $T_1$ . Here, one waits for  $t_1$  defined in the same manner as in the standard protocol and then jumps to  $T_2 < T_1$ . In this case  $t_1$  continuously decreases as a function of  $(T_2 - T_1)$ . Apart from the different sign, the temporal evolution of the Kovacs hump qualitatively behaves very similar for the two different protocols. This fact is somewhat surprising on first sight because the temporal evolution of the distribution of energies during aging is quite different[1]. However, it shows that the Kovacs hump does not allow to gather detailed information about the actual distributions.

For the trap model, one can successfully use the concept of a demarcation energy  $\epsilon_D$  defined via  $\epsilon_D(t) = -T \ln(\kappa_\infty t)$  with the attempt rate  $\kappa_\infty$  to understand the relaxation behavior. States with energies smaller than  $\epsilon_D$  are essentially frozen while those with  $\epsilon > \epsilon_D$  are relaxed[1]. This different relaxation behavior can be used to rationalize the origin of the Kovacs hump. Low energy states are still frozen at  $t_1$ , the time of the temperature jump to  $T_2$ , while high energy states respond quickly. Using this property, one can show that the Kovacs hump can approximately be described as a difference of two relaxation functions,  $\Delta E(t) \simeq \phi(t_1, t) - \psi(t)$ . Here,  $\phi$  and  $\psi$  are two different relaxation functions. This form is very reminiscent of the corresponding expression one obtains in linear response theory,  $\Delta E(t) = h_{01}C_{\text{eq}}(t_1 + t) - h_{21}C_{\text{eq}}(t)$ . Here,  $h_{nm}$  are temperature-dependent amplitudes and  $C_{\text{eq}}(t)$  is the normalized energy-autocorrelation function. Thus, a Kovacs hump is observed only for non-exponentially decaying  $C_{\text{eq}}(t)$ [2]. For the occurrence of a Kovacs hump, the most important point seems to be that there has to be slow and fast relaxation at the same time. However, the averaging inherent in the evaluation of bulk properties apparently does not allow to distinguish among different types of distributions.

We conclude with noting that the Kovacs hump for a given quantity can be qualitatively understood in terms of the linear response behavior. In the nonlinear regime mainly quantitative differences are found but we do not observe any qualitatively new features.

\* Corresponding author: diezeman@uni-mainz.de

[1] C. Rehwald, N. Ngan, A. Heuer, T. Schröder, J. Dyre and G. Diezemann; Phys. Rev. E **82** 021503 (2010)

[2] R. Böhmer, B. Schiener, J. Hemberger and R.V. Chamberlin; Z. Phys. B Cond. Mat. **99** 91 (1995)

## Identification of coupling processes in supercooled liquids

Christian Rehwald\* and Andreas Heuer

*Institut für Physikalische Chemie, Westfälische Wilhelms-Universität Münster, 48149 Münster*

Many presently discussed models (like KCMs) for the glass transition are dealing with the concept of coupled subsystems. Qualitatively speaking the macroscopic system can be decomposed into some elementary subsystems (ESs). In a recent paper [1] we have used finite-size effects in a binary mixture Lennard-Jones liquid to gain information about the nature of the ESs, as well as their mutual coupling. It turns out that on the one hand, a system containing 65 particles is large enough to contain the complete information about thermodynamics and diffusivity. On the other hand the coupling determines the structural relaxation and the emergence of dynamic length scales. However, a strict definition of an ES in a large system as well as a detailed understanding of the coupling is still missing.

While the determination of dynamic length scales in equilibrium above  $T_c$  has been studied in detail, it requires more effort to understand the transport of mobility between distinct regions in space. We are particularly interested in the response of the system to a single relaxation event, calculated from the single particle displacements. Without further knowledge about the nature of coupling, it is difficult to identify responses in equilibrium directly. Therefore we choose a different route: We use an iso-configurational ensemble of a very stable non-equilibrium configuration, generated from copies of a suitably structure of an  $N = 65$  system, where almost no dynamic noise is present. This environment enables well defined relaxation events, as well as detecting their responses.

The average propagation of mobility after the first event can clearly be identified and the corresponding velocity can be calculated. However, looking closer at this process, not every event leads to a sequence of relaxation processes which is in contrast to the concept of excitation lines in KCMs. In particular, several relaxations with following pauses are taking place until the structure is destabilized. The connection between local rearrangements and remote relaxation is highly non-trivial. This behavior gives rise to define a statistical dynamic coupling between ESs, which can be modeled within the framework of so-called coupled ideal Gaussian glass formers (IGGF). In a further step, we compare model predictions with different types of coupling (discrete, continuous and elastic) to the MD data. The predictions can in turn be used to improve the understanding of the underlying physics.

Another important question is, how much causality one can expect of a model which includes facilitation, even in equilibrium. We use our model to provide suitable quantities, which can characterize the transport of mobility. In turn, we apply this approach to the MD simulation and show, that it is possible to verify facilitation processes, even in equilibrium. The characteristics are of course much weaker than in the non-equilibrium case.

\* Corresponding author: rehwaldc@uni-muenster.de  
[1] C. Rehwald *et al.*, PRL **105**, 117801 (2010).

## Dynamic and thermodynamic properties underlying secondary processes in a mean-field exactly solvable model glass

Luca Leuzzi,<sup>1,2,\*</sup> Matteo Paoluzzi,<sup>3,2</sup> and Andrea Crisanti<sup>1,4</sup>

<sup>1</sup>*Department of Physics, Università di Roma “La Sapienza”, P.le A. Moro 2, I-00185 Rome, Italy*

<sup>2</sup>*IPCF-CNR, UOS Rome, P.le A. Moro 2, I-00185 Rome, Italy*

<sup>3</sup>*Department of Physics, University Rome 3, Via Vasca Navale 84, I-00146 Rome, Italy*

<sup>4</sup>*ISC-CNR, UOS Sapienza, P.le A. Moro 2, I-00185 Rome, Italy*

The interrelation of dynamic processes active on separated time-scales in glasses and viscous liquids is investigated. Both a thermodynamic (static) and a dynamic approach are implemented on an exactly solvable spin model with quenched disordered interactions, developed to study the nature of polyamorphism and amorphous-to-amorphous transitions [1]. On the static front, the analysis is carried out within the framework of Replica Symmetry Breaking (RSB) theory, leading to the identification of low temperature glass phases of different kinds. A typical feature of the mean-field kind of models we investigate is that the configurational entropy can be computed at the static level [2], since glassy metastable states have infinite life-time in the thermodynamic limit. Moving to the study of dynamics this allows for predictions on the system relaxation above the mode coupling (MC) temperature, that are compared with the outcomes of the equations of motion directly derived within the Mode Coupling Theory (MCT) for under-cooled viscous liquids.

The model under probe is a spherical  $s + p$  multi-spin interaction model:

$$\mathcal{H} = \sum_{i_1 < \dots < i_s} J_{i_1 \dots i_s}^{(s)} \sigma_{i_1} \dots \sigma_{i_s} + \sum_{i_1 < \dots < i_p} J_{i_1 \dots i_p}^{(p)} \sigma_{i_1} \dots \sigma_{i_p} \quad (1)$$

where  $J_{i_1 \dots i_t}^{(t)}$  ( $t = s, p$ ) are uncorrelated, zero mean, Gaussian variables of variance  $J_t^2 t! / (2N^{t-1})$  and  $\sigma_i$  are  $N$  “spherical spins” obeying the constraint  $\sum_i \sigma_i^2 = N$ . The model displays the feature of having both usual “one-step” RSB solutions, known to reproduce all basic properties of structural glasses, and a physically consistent “two-step” solution. Since the dynamic counterpart of a RSB is known to be a time-scale bifurcation [4], Eq. (1) provides a leading model to probe the behavior of characteristic time-scales in presence of secondary processes and the different mechanisms in which they can arise.

In Fig. 1 we show the phase diagram in temperature (in  $J_s$  units) and the ratio  $J_p/J_s$ , i.e., an indicative parameter for the relative weight of “few-body” to many-body interactions ( $s = 3$  for few,  $p = 16$  for many). Moving from the fluid phase, the dynamic transition between glass phases of different nature always precedes the thermodynamic one. This is the MC temperature where the plateau of the spin-spin time correlation function (analogue of the correlation between density fluctuations) extends to infinite time and ergodicity is broken. It is the highest  $T$  at which

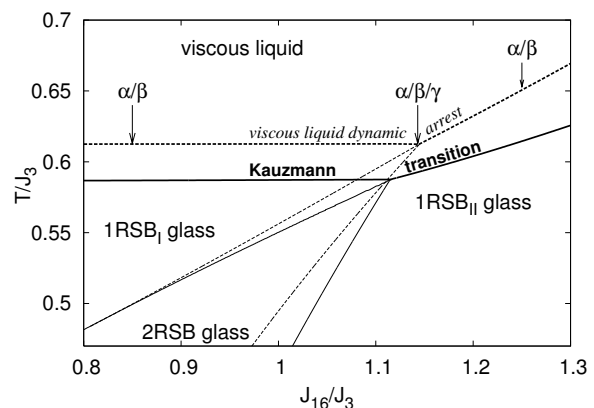


FIG. 1. Phase diagram of the 3 + 16 spherical spin model with dynamic (dashed) and thermodynamic (full) transition lines.

the lifetime of high-lying local states becomes infinite and their number grows like  $\exp(Ns_c(T))$ , with  $s_c(T)$  the configurational entropy density and  $N$  the size of the system.

Along certain cooling paths in the phase diagram, determined by analysis of the static thermodynamic properties, approaching the tricritical point MCT applied to the  $s + p$  model yields a time-correlation function with *two* plateaus at different correlation values. A first plateau occurs for  $t \gtrsim t_\gamma$  and a second one on the characteristic time-scale at which the  $\beta$  secondary relaxation occurs. We, thus, study the behavior in  $T$  of the characteristic relaxation times for processes on different time-scales and their functional interrelation. The hierarchical nesting implicit in the present approach hints that fast processes have a relevant influence on slow processes, even though taking place on well separated time-scales. This observation naturally stimulates a comparison with Ngai’s Coupling Model [6].

\* Corresponding author: luca.leuzzi@cnr.it

- [1] A. Crisanti and L. Leuzzi, Phys. Rev. B **76**, 184417 (2007).
- [2] L. Leuzzi and T.M. Nieuwenhuizen, *Thermodynamics of the glassy state* (Taylor & Francis, UK, 2007).
- [3] J.-P. Bouchaud et al., Physica A **226**, 243 (1996).
- [4] H. Sompolinsky, Phys. Rev. Lett. **47**, 935 (1981).
- [5] G.P. Johari and M.J. Goldstein, J. Chem. Phys. **53**, 2372 (1970).
- [6] K. L. Ngai, S. Capaccioli, J. Phys: Cond. Matt. **19**, 205114 (2007).

## On the Decay Exponents of Mode Coupling Theory

F. Caltagirone,<sup>1</sup> U. Ferrari,<sup>1</sup> S. Franz,<sup>2</sup> L. Leuzzi,<sup>1,3</sup> G. Parisi,<sup>1,3,4</sup> F. Ricci-Tersenghi,<sup>1</sup> and T. Rizzo<sup>1,\*</sup>

<sup>1</sup>*Dip. Fisica, Università di Roma "La Sapienza", Piazzale A. Moro 2, I-00185, Rome, Italy*

<sup>2</sup>*LPTMS, CNRS and Université Paris-Sud, UMR8626, Bat. 100, 91405 Orsay, France*

<sup>3</sup>*IPCF-CNR, UOS Rome, Università di Roma "La Sapienza", Piazzale A. Moro 2, I-00185, Rome, Italy*

<sup>4</sup>*INFN, Piazzale A. Moro 2, 00185, Rome, Italy*

An important prediction of Mode-Coupling-Theory is the relationship between the decay exponents in the  $\alpha$  and  $\beta$  regimes:

$$\frac{\Gamma^2(1-a)}{\Gamma(1-2a)} = \frac{\Gamma^2(1+b)}{\Gamma(1+2b)} = \lambda \quad (1)$$

In the original structural glass context this relationships follow from the MCT equations that are obtained making rather uncontrolled approximation. As a consequence it is usually assumed that the relationship between the exponents is correct while the parameter  $\lambda$  has to be treated like a tunable parameter. On the other hand it is known that in some mean-field spin-glass models the dynamics is precisely described by MCT. In that context the parameter  $\lambda$  can be computed exactly, but again its computation becomes difficult when we consider more complex models including finite-dimensional ones.

What was unknown up to now was the physical meaning of the parameter  $\lambda$ , *i.e.* its connection to physical observables. We have been able to unveil this connection in full generality working within an effective theory of dynamics.

In the following we sketch the outline of the derivation. The starting point is a supersymmetric effective theory for the dynamics of the model. The supersymmetric formalism allows to connect the equilibrium dynamics with the statics. The statics of the model is described by an effective replicated theory in which the order parameter is a  $n \times n$  replica symmetric matrix  $Q_{ab}$  with  $n = 1$ . One can argue that the knowledge of the Gibbs free energy as a function of the order parameter  $Q_{ab}$  allows to determine the dynamical Gibbs free energy in terms of the dynamical order parameter *i.e.* the correlations at different times.

In particular the coefficients  $w_1$  and  $w_2$  of the terms  $\text{Tr}Q^3$  and  $\sum_{ab} Q_{ab}^3$  in the static Gibbs free energy appear also in the dynamical Gibbs free energy leading to the following equation:

$$(w_1 - w_2) \delta C^2(t) + w_1 \int_0^t (\delta C(t-y) - \delta C(t)) \delta \dot{C}(y) dy = 0 \quad (2)$$

This is the standard quadratic equation describing the decay to and the departure from the plateau and it yields the desired relationship (1) with:

$$\lambda = \frac{w_2}{w_1} \quad (3)$$

The coefficients  $w_1$  and  $w_2$  of the Gibbs free energy can in turn be related to the corresponding cubic coefficients  $\omega_1$  and  $\omega_2$  of its Legendre transform *i.e.* the free energy in presence of a set of sources  $\lambda_{ab} q_{ab}$ . After a careful computation it turns out that

$$\omega_1 = \frac{1}{V} \int dx_1 dx_2 dx_3 \times \overline{\langle \rho(x_1) \rho(x_2) \rangle_c \langle \rho(x_2) \rho(x_3) \rangle_c \langle \rho(x_1) \rho(x_3) \rangle_c} ; \quad (4)$$

$$\omega_2 = \frac{1}{V} \int dx_1 dx_2 dx_3 \overline{\langle \rho(x_1) \rho(x_2) \rho(x_3) \rangle_c^2} ; \quad (5)$$

where  $\rho(x)$  is the microscopic variable, *e.g.* the density in a structural glass or the spin in a spin-glass model. In the above expressions the square brackets represent (connected) thermal averages within the set of configurations explored by the dynamics starting from a given initial (equilibrium) configuration, and the overline represents the average over different initial condition and over the quenched disorder if it is present. Inverting the Legendre transform we have  $w_1 = r^3 \omega_1$  and  $w_2 = r^3 \omega_2$  where  $r$  is the so called replicon that vanishes as  $(T - T_d)^{1/2}$  in MCT, as a consequence  $\omega_1$  and  $\omega_2$  must diverge as  $r^{-3}$ . Similar relationships can be obtained also in different theories, in particular in continuous theories like the one of the de Almeida-Thouless line in spin-glass. We are testing numerically the connection between the MCT exponents  $a$  and  $b$  and the cubic cumulants  $\omega_1$  and  $\omega_2$  in many different models.

\* Corresponding author: tommaso.rizzo@inwind.it

## Geometrical approach to the glass transition

R. Pastore, M. Pica Ciamarra,\* A. de Candia, and A. Coniglio

CNR-SPIN, Dipartimento di Scienze Fisiche, Università di Napoli Federico II

We introduce a reverse-percolation approach to the glass transition leading to a geometrical interpretation of the relaxation process, and particularly of dynamical heterogeneities [1], validated via numerical simulations of the Kob-Andersen model [2]. This approach is conveniently described focusing on the particles that never moved from time 0 to time  $t$ , also known as persistent particles. In a lattice formalism where  $n_i = 0, 1$  is the usual occupation number, the density of persistent particles is  $\rho_p(t) = 1/V \sum n_i^p(t)$ , where  $n_i^p(t) = \prod_0^t n_i(t) = 0, 1$  is a lattice variable signaling the presence/absence of a persistent particle at site  $i$ .  $\rho_p$  is related to the high wave-vector limit of the self-intermediate scattering function, and it is therefore a common relaxation function which vanishes when the system relaxes. Its fluctuations give the dynamical susceptibility  $\chi_p(t)$ , and are the volume integral of

$$g_p(r, t) = \langle n_i^p(t) n_j^p(t) \rangle - \langle n_i^p(t) \rangle \langle n_j^p(t) \rangle. \quad (1)$$

This allows to interpret the dynamical heterogeneities as the spatial correlations of persistent particles. The spatial decay of these correlation fixes the dynamical correlation length  $\xi(t)$ .

However,  $\rho_p$  can also be interpreted as a continuously decreasing occupation probability of persistent particles. This suggests the existence of a reverse-percolation transition, whereby the strength (density)  $P$  of the spanning cluster of persistent particles decreases until it vanishes at a critical density  $\rho_p^c(\rho)$ , reached at a time  $t_{\text{per}}(\rho)$ . This reverse-percolation transition is illustrated in Fig. 1, where we plot the density of persistent particles  $\rho_p$  and the strength of the spanning clusters  $P$  as a function of time, as obtained from Monte Carlo simulations of the Kob-Anderson model.

Several quantities have a critical behavior at the percolation threshold. In particular, a percolating length  $\xi_{\text{per}}$  diverges at the transition; below the transition,  $\xi_{\text{per}}$  measures the size of the largest cluster, while above the transition it measures the extension of the density correlations within the infinite cluster. This correlation length is obtained from the spatial decay of the pair-connected correlation function of persistent particles. In the absence of finite clusters of persistent particles, this function equals Eq. 1. Accordingly, the percolation length  $\xi_{\text{per}}$  equals the dynamic correlation

length  $\xi$  for a large fraction of the relaxation process, and precisely until at a time  $t_{\text{fc}}$  finite clusters of persistent particles appears. The numerical results shown in Fig. 1 confirm this interpretation.

These results and related ones clarify that the relaxation process of glass forming systems is related to an underlying correlated reverse-percolation transition of persistent particles. Dynamical quantities such the density of persistent particles, the dynamic correlation length and the dynamical susceptibility, coincide with corresponding percolating quantities over a large fraction of the relaxation process. The relevance of this geometrical approach increases on approaching structural arrest, as percolating quantities are found to coincide with the dynamical ones over a larger fraction of the relaxation process.

\* Corresponding author:

massimo.picaciamarra@spin.cnr.it

[1] R. Pastore, M. Pica Ciamarra, A. de Candia, A. Coniglio, under review.

[2] W. Kob and H.C. Andersen, Phys. Rev. E **48**, 6 (1993).

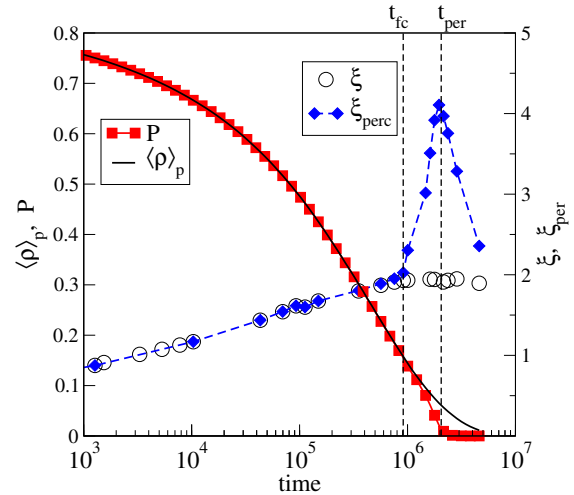


FIG. 1. Left axis: density of persistent particles  $\rho_p$  and strength of the percolating cluster  $P$ . Right axis: dynamical  $\xi$  and percolation  $\xi_{\text{per}}$  length.  $\rho_p = P$  and  $\xi = \xi_{\text{per}}$  for a large fraction of the relaxation process, until finite clusters appear at a time  $t_{\text{fc}}$ . Results refer to numerical simulation of the Kob-Anderson model at  $\rho = 0.85$ .

## Mapping the slowdown of the dynamics of soft spheres onto hard sphere behavior

Michael Schmiedeberg,<sup>1,\*</sup> Thomas K. Haxton,<sup>2</sup> Sidney R. Nagel,<sup>3</sup> and Andrea J. Liu<sup>4</sup>

<sup>1</sup>*Institut für Theoretische Physik 2: Weiche Materie,  
Heinrich-Heine-Universität Düsseldorf, 40225 Düsseldorf, Germany*

<sup>2</sup>*Theory of Nanostructured Materials, Lawrence Berkeley National Laboratory, Berkeley, CA 94720, USA*

<sup>3</sup>*The James Franck Institute, The University of Chicago, Chicago, IL 60637, USA*

<sup>4</sup>*Department of Physics and Astronomy, University of Pennsylvania, Philadelphia, PA 19104, USA*

\* Corresponding author: [schmiedeberg@thphy.uni-duesseldorf.de](mailto:schmiedeberg@thphy.uni-duesseldorf.de)

This abstract is not available in this version.

## Direct measurement of the free energy of hard sphere glasses

Rojman Zargar,<sup>1,2,\*</sup> Vijayakumar K. Chikkadi,<sup>1</sup> Peter Schall,<sup>1</sup> Bernard Nienhuis,<sup>2</sup> and Daniel Bonn<sup>1,3</sup>

<sup>1</sup>Van der Waals Zeeman Institute, University of Amsterdam, 1090 GL Amsterdam The Netherlands

<sup>2</sup>Institute for Theoretical Physics, University of Amsterdam, 1090 GL Amsterdam The Netherlands

<sup>3</sup>LPS de l'ENS, CNRS UMR 8550, 24 Rue Lhomond Paris, France 75005

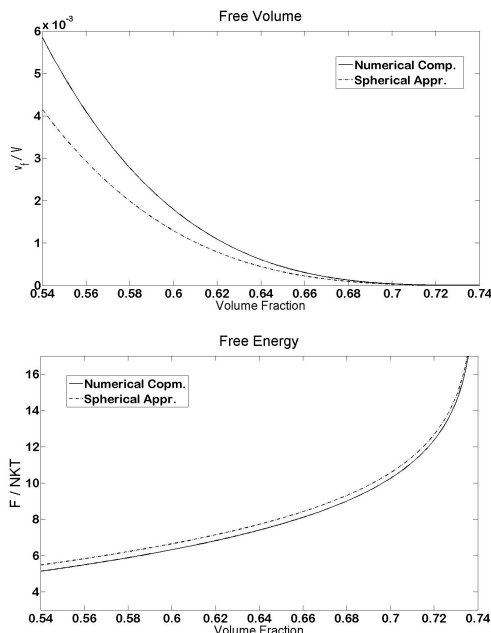


FIG. 1. Numerical free volume and free energy (solid lines) compared to those of the spherical approximation (dashed lines) versus the volume fraction.

Glasses are structurally liquidlike, but mechanically solidlike. Recently, a cell theory for liquid solids and glasses was proposed [1]. Here we apply this theory to our experimental colloidal glass; using fast confocal microscopy, we obtain direct images of hard sphere glasses and use those to measure the free energy and thermodynamic glass properties directly.

Hard sphere systems have been studied widely in order to obtain insight into intrinsic structures of solids, liquids and glasses.

As a first step we use the traditional cell theory to determine the thermodynamical properties of hard sphere crystals. We calculate the free volume numerically and using the spherical approximation, in which

the free volume of the central particle is approximated by a sphere. We then obtain thermodynamical properties of the hard sphere crystal. Results are shown in Fig. 1. Although there is a big difference between the two free volumes, but because of error cancellation the thermodynamics are very similar.

We show that the elastic constants can be determined from the free volume theory as well. The free energy difference between the deformed and undeformed fcc crystal then gives us the elastic constants. The elastic constants we obtain are in a good agreement with the results of Frenkel *et.al* [2].

In the next step, we apply a recently proposed cell theory for dense system [1] to direct measurements on colloidal hard sphere glasses. This new cell theory combines ideas of the free volume approach with the most likely structures based on the free energy landscape. We prepared a colloidal glass consisting of  $\sim 2 \times 10^5$  PMMA particles in a density and index match solvent at a volume fraction of  $\phi \sim 0.60$ . The particles have a diameter of  $\sigma = 1.3\mu\text{m}$  with a polydispersity of 7% to prevent crystallization. We used fast confocal microscopy and determined particle's positions in three dimensions. We then calculated the Voronoi volume as well as the free volume for each particle. Determining these values for each particle and exploiting the new cell theory, we will be able to calculate the free energy, the equation of state, and many other interesting thermodynamical properties of hard sphere glasses such as the chemical potential and the elastic constants. We can also use the free energy results to investigate the aging of a hard sphere glass in the picture of the free energy landscape.

\* Corresponding author: r.zargar@uva.nl

- [1] T. Aste and A. Coniglio, *Europhys. Lett.* **67**, 165 (2004).
- [2] S. Pronk and D. Frenkel, *Phys. Rev. Lett.* **90**, 255501 (2003).

## Analysis of oscillating-cup technique for measurement of density and non-Newtonian properties

Inna Elyukhina\*

*South Ural State University, Russia*

The oscillating-cup viscometer (OCV) is more suitable technique for liquid metals. One of reasons of enough contradictions in viscometric data can be linear rheological type accepted for them [1]. Mathematical modeling for OCV filled with non-Newtonian fluids has been carried out, e.g., in [2] including case of non-affine deformations. Mainly exact solutions are of interest for practice and further analysis focuses on their finding. One of such algorithms is based on equations and interpretation in terms of linear fluids [3].

For Newtonian fluids, we use  $A = 0.5MR^2/K$ ,  $\xi_0 = R/\sqrt{\nu\tau_0/(2\pi)}$ ,  $\chi = H/R$ , where  $H$ ,  $M$  and  $R$  are sample height, radius and mass;  $K$  is moment of inertia of empty system;  $\nu$  is kinematic viscosity;  $\tau_0$  is period  $\tau$  for  $M = 0$ . With growth of  $\xi_0$ ,  $\tau$  decreases mainly at  $\xi_0 \in (2, 12)$  and  $\delta(\xi_0)$  has maximum at some  $\xi_m$ . Increasing elasticity leads to growth of numbers of extrema in  $\tau(\xi_0)$ ,  $\delta(\xi_0)$  (Fig. 1, We is Weissenberg number, UCMM). If  $A$  increases, curves become steeper.

Effective values  $\xi_{\text{eff}}$ , e.g., for nonlinear viscous and linear viscoplastic fluids are  $\xi_{\text{eff}} = \xi_0/\sqrt{bD^{m-1}}$  and  $\xi_{\text{eff}} = \xi_0/\sqrt{c + \text{Bn}/D}$ , where  $\text{Bn}$  is Bingham number. In the damping, amplitude of shear rate  $D$  decreases,  $\nu_{\text{eff}}$  and  $\xi_{\text{eff}}$  change and corresponding changes of  $\tau$  and  $\delta$  are taken place depending on number of oscillation  $N$  (Fig. 2). For visco- and pseudoplastic fluids,  $\nu_{\text{eff}}$  increases, i.e.  $\tau$  increases and  $\delta$  passes through maximum, for dilatant fluids – vice versa. For viscoplastics, there are isosynchronous oscillations at the close responding to cylinder filled with solid body.

Experiment conditions (nonsteady state, high precision, small deformations, etc.) make observed weakly non-Newtonian properties, e.g., low  $\text{Bn}$ . Forced mode extends working range of viscous and particularly elastic properties. It allows to use OCV for various classes of nonlinear fluids, not only high-temperature ones,

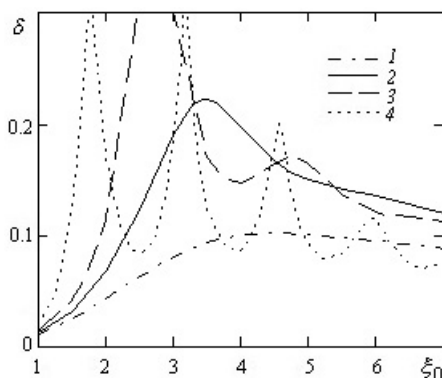


FIG. 1.  $\delta = \delta(\xi_0)$  ( $A = 0.1$ ): 1 –  $\text{We} = 0$ , 2 – 1, 3 – 2, 4 – 5

and to use algorithm for any oscillatory viscometry including external flow. Approach to analysis of alloys as non-Newtonian fluids can be also useful to relate kinetics of solidification with their properties or, e.g., to determine liquidus from change of flow behaviour. Such questions are discussed here. Note that at temperature growth above solidus, average for  $N$  values of  $\delta$  and  $\tau$  change along curves in Fig. 1 with  $\xi_0$  growth.

Viscometric equations includes density  $\rho$  that gives possibly to find  $\nu$  and  $\rho$  from the same experiment, i.e. furthermore to study fluids with weakly investigated equations of state, to eliminate errors caused by difference in temperature and pressure for independent measurements and to check consistency of data.

Behaviour in Fig. 1, 2 takes intervals of working sensitivity of fluid properties to parameters  $x$  observed in experiment ( $x$  is  $K$ ,  $R$ ,  $\tau$ , etc.): e.g., for Newtonian fluid at  $\xi_0 \sim \xi_m$ , errors of  $\nu$  is too high. Features of estimation are high sensitivity of  $\rho$  to  $\tau$  from imaginary part of viscometric function, correlation of errors of  $\nu$  and  $\rho$ , impossibility of search of  $\rho$  for  $\chi \rightarrow \infty$ , etc. Parameter sensitivity  $\psi_{\rho, x} \sim \psi_{\nu, x} \psi_{\rho, \nu}$ , where  $\psi_{\rho, \nu}$  increases with  $H$  and  $\psi_{\nu, x}$  conversely decreases (e.g., in view of  $A$ ), ceteris paribus. Taking this into account, identification methods and procedure for optimal experiment planning are developed. Data processing in numerical and full-scale experiments is carried out.

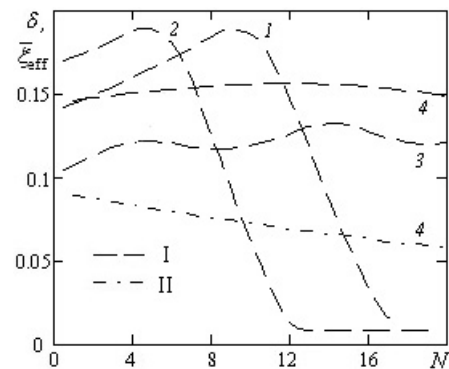


FIG. 2. Dependences of  $\delta$  (I) and  $\bar{\xi}_{\text{eff}} = 0.015\xi_{\text{eff}}$  (II) on  $N$  for linear viscoplastic (1, 2), elastic viscoplastic (3) and nonlinear viscous (4) fluids ( $\chi \rightarrow \infty$ ,  $b = 1, c = 1$ ): 1 –  $A = 0.2$ ,  $\xi_0 = 12$  ( $\text{Bn} = 0.2$ ); 2 – 0.2, 12 ( $\text{Bn} = 0.4$ ); 3 – 0.1, 10 ( $\text{We} = 1$ ,  $\text{Bn} = 0.5$ ); 4 – 0.15, 7 ( $m = 0.75$ )

Work was supported by RFBR (N 10-01-96042\_ural).

\* Corresponding author: Inna.Elyukhina@gmail.com

- [1] I. Elyukhina and G. Vyatkin, *J. Phys. CS* **98** (2008).
- [2] I. Elyukhina, *Rheol. Acta* (2011). (in press)
- [3] I.V. Elyukhina, *High Temp.* **47**, 562 (2009).

## On the viscosity and the crystallization processes of the Co-(Fe, Cr)-Si-B amorphizing melts

I.V. Sterkhova, V.I. Lad'yanov,\* and L.V. Kamaeva

*Laboratory of amorphous alloys, Physical-Technical Institute,  
Ural Branch of Russian Academy of Sciences, 132 Kirov Street, 426001 Izhevsk, Russia*

The alloys based on the Co-Si-B system are easy amorphizing alloys and they present a new type of promising soft-magnetic materials. Increasing the glass forming ability of alloys as well as improving their properties due to peculiarities of the structural state can be obtained by the choice of both the optimal chemical composition and the technology parameters of the alloys production (such as melt temperature, holding time at a given temperature and cooling rate). In connection with this the investigations of the influence of the liquid phase state on the solidification processes of the amorphizing melts based on Co-Si-B:  $\text{Co}_{69}\text{Cr}_3\text{Si}_{18}\text{B}_{10}$ ,  $\text{Co}_{65.5}\text{Cr}_{6.5}\text{Si}_{18}\text{B}_{10}$ ,  $\text{Co}_{65.5}\text{Fe}_{6.5}\text{Si}_{18}\text{B}_{10}$  have been carried out by viscosimetry, the differential thermal, X-ray structural analyses and metallography. It has been shown that the temperature dependences of the kinematic viscosity ( $\nu$ ) of the melts have non-monotone character. In the viscosity polytherms in the first heating the anomalies in the vicinity of the determined temperatures,  $T^*$ , ( $T^* = 1490\text{K}$  for  $\text{Co}_{69}\text{Cr}_3\text{Si}_{18}\text{B}_{10}$ ,  $1610\text{K}$  –  $\text{Co}_{65.5}\text{Cr}_{6.5}\text{Si}_{18}\text{B}_{10}$ ,  $1550\text{K}$  –  $\text{Co}_{65.5}\text{Fe}_{6.5}\text{Si}_{18}\text{B}_{10}$ ) and hysteresis of  $\nu$  have been first discovered. Moreover the increase of the Cr concentration from 3 to 6.5at.% result in that  $T^*$  displaces substantial to the higher temperature region. But Cr atoms replacing by Fe atoms does not significantly affects the character of the  $\nu(T)$  dependences. The observed peculiarities in the viscosity polytherms

are caused by the change of the compositional short-range ordering in the melts in the area of  $T^*$  i.e. by the transition of low-temperature structure of the melts into the high-temperature structure which being further cooled is retained up to the solidification temperature. It has been found that the changes of the structural state of melts result in the change of the processes of their solidification in the cooling conditions at 100K/min. The crystallisation ability change of the melts has been first observed in the vicinity of  $T^*$  which correlates well with the anomalies temperatures in the  $\nu$  polytherms. The increase of the supercooling of the melts after superheating above  $T^*$  is accompanied by the change of the mechanism of the nucleation and growth of  $\text{Co}_2\text{B}$  and  $\text{Co}_2\text{Si}$  for  $\text{Co}_{65.5}\text{Fe}_{6.5}\text{Si}_{18}\text{B}_{10}$ . In accordance with the obtained data we may conclude that in models of the micro-heterogeneous structure of the liquid phase the structural transformations occurring in  $\text{Co}_{69}\text{Cr}_3\text{Si}_{18}\text{B}_{10}$ ,  $\text{Co}_{65.5}\text{Cr}_{6.5}\text{Si}_{18}\text{B}_{10}$ ,  $\text{Co}_{65.5}\text{Fe}_{6.5}\text{Si}_{18}\text{B}_{10}$  melts in the vicinity of  $T^*$  have been caused by the change of the short-range ordering in the microgroups based on  $\text{Co}_2\text{B}$  and  $\text{Co}_2\text{Si}$  in depending on the alloy composition.

This work has been supported by the program of fundamental research Presidium of Russian Academy of Sciences (09P-2-1023).

\* Corresponding author: las@pti.udm.ru

## The use of the temperature and concentration dependences of viscosity for the study of structure of Me(Fe,Ni,Co)-P melts

L.V. Kamaeva,\* V.I. Lad'yanov, and A.L. Bel'tyukov

*Laboratory of amorphous alloys, Physical-Technical Institute,  
Ural Branch of Russian Academy of Sciences, 132 Kirov Street, 426001 Izhevsk, Russia*

The results of the investigation of the temperature and concentration dependences of the kinematic viscosity ( $\nu$ ) of the Ni-P, Co-P, Fe-P melts as well as the investigation of the crystallization peculiarities in the wide range of cooling rates and the initial melt temperatures have been presented in this paper. In the concentration dependences the clearly pronounced viscosity maxima of the Ni-P and Co-P melts have been observed in 16-17 and 20-22at% P (for Ni-P) and 20-22at% P (for Co-P). The availability of maxima in the isotherms points to the strong chemical interaction between the components in the melt over these concentration ranges. The presence of the  $\nu$  maxima indicates that in the Ni-P melts with 16-17 at% and 20-22 at% P and the Co-P melts with 19-21 at%P the microgroups consisted of the different sorts of atoms which stoichiometrically correspond the Ni<sub>5</sub>P, Ni<sub>4</sub>P and Co<sub>4</sub>P chemical compounds are present. It has been experimentally shown that on solidification at low rates (up to 100K/min) in the  $\nu$  maxima areas the metastable phases are initially formed. Being fur-

ther cooled they are decomposed. In the temperature dependences of viscosity of the Fe-P melts with the P concentration from 17 to 20 at% the sharp (anomalous) increase of the viscosity values is observed in the temperature interval (1410-1510 K) when the melts were initially heated. This anomaly is caused by the change of the compositional sort-range ordering. The investigation of the solidification processes of these alloys has shown that the crystallization occur according to the phase diagram when the melt is heated above the melt point. In this case the equilibrium eutectic is formed. The superheating of the melt above the anomaly temperature results in the change of the type of the crystallization and the formation of the non-equilibrium eutectic under the equal cooling conditions.

The work has been carried out thanks to the financial support of the RFFI (Grant No. 08-03-00609-a).

\* Corresponding author: lara.kam@mail.ru

## On viscosity and relaxation processes of the glass-forming AL-TM-REM melts

V. I. Lad'yanov,<sup>1</sup> S. G. Menshikova,<sup>2,1,\*</sup> A. L. Bel'tyukov,<sup>1</sup> M. G. Vasin,<sup>1</sup> and V. V. Maslov<sup>3</sup>

<sup>1</sup>*Physical-Technical Institute, Ural Branch of Russian Academy of Sciences, 426000, Izhevsk, Russia*

<sup>2</sup>*Udmurt State University, 426034, Izhevsk, Russia*

<sup>3</sup>*G. V. Kurdyumov Institute of Metal Physics,  
National Academy of Sciences of Ukraine, Kiyev, UA-03680, Ukraine*

In recent years amorphous Al-based alloys (80–90 at.%) with transition (TM) and rare-earth (REM) metals have increasingly attracted interest. Rapid solidification of aluminium alloys of the Al-TM-REM type makes it possible to produce a new generation of aluminium alloys with higher strength, plasticity, corrosion resistance as well as with increased thermal expansion and wear resistance in comparison with the properties of cast commercial alloys.

In the present paper the measuring of the temperature and time dependencies of kinematic viscosity of liquid Al-Y (up to 10 at.% Y), Al<sub>87</sub>Ni<sub>8</sub>Y<sub>5</sub>, Al<sub>86</sub>Ni<sub>8</sub>(Ce/La)<sub>6</sub>, Al<sub>86</sub>Ni<sub>6</sub>Co<sub>2</sub>Gd<sub>4</sub>(Tb/Y)<sub>2</sub> alloys was carried out by the method of damped torsional vibrations.

An irreversible non-monotonic change of the melts viscosity above the temperature of melting brought about by the destruction of their micro-heterogeneous state inherited from the multi-phase solid sample has been found out. It is shown that for the melts transition into the quasi-equilibrium state long isothermal holding is necessary. At the temperatures close to the melting temperature the relaxation times are order of 300 minutes. The relaxation time decreases with in-

crease of the melt temperature.

On the basis of the conception about of a micro-nonuniform structure of melts in view of the ultrametric dynamic theory of a molecular field the model of a non-monotonic relaxation of the non-equilibrium melts has been offered. According to the offered approach, the key parameter, which influences viscosity, is the concentration of non-equilibrium micro-groups of atoms. In the beginning of isothermal holding of melt the size of these micro-groups is great enough, but their concentration is small and does not render essential influence on viscosity. Eventually the concentration of these micro-groups is changing. That is determined by two processes: dissolution the largest and dispersion the finest of micro-groups. The first process (that is dissolution) leads to increase in concentration of non-equilibrium micro-groups in melt, the second (that is dispersion) leads to reduction of their total. Joint influence of these two processes is shown in non-monotonic change of viscosity investigated melts.

\* Corresponding author: svetlmenh@mail.ru

## Chemical disordering of crystals and its relation to liquid-liquid transitions in strong liquids

Shuai Wei,<sup>1,\*</sup> Isabella Gallino,<sup>1</sup> Ralf Busch,<sup>1</sup> and C.Austen Angell<sup>2</sup>

<sup>1</sup>Materials Science and Engineering Department,  
Universität des Saarlandes, Campus C63, 66123 Saarbrücken, Germany

<sup>2</sup>Department of Chemistry and Biochemistry, Arizona State University, Tempe, Arizona 85287, USA

The glass transition is usually considered as a structural arrest during cooling of a liquid, or a plastic crystal, trapping a metastable state of the system before it can crystallize. As the glass transition temperature  $T_g$  is approached from above, all liquids exhibit pronounced slowdown of relaxation processes. However, the origin of the dynamic slowdown has been in debate for many years. Recent studies suggest that the especially rapid slowdown in “fragile” liquids is associated with an increasing correlation length as the temperature drops towards  $T_g$ . It is suggested that the dynamic slowdown is a result of critical-like fluctuations of static structural order. Less attention has been paid on those “strong” liquids, another extreme of the fragile/strong pattern, and their correlation length.

Here we study a crystalline order-disorder system, the simple binary alloy  $\text{Fe}_{50}\text{Co}_{50}$  superlattice, in which a glass-like transition with respect to chemical disordering is observed below the order-disorder critical temperature,  $T_\lambda$ . The kinetics of this ‘glass’ transition are found to be ideally strong (fragility index  $m \approx 16$ ), when the fragility criterion is applied to this non-liquid system. We show that this ideally strong disordering system has much in common with those typical strong glass-forming liquids by comparing the kinetics and thermodynamics of  $\text{Fe}_{50}\text{Co}_{50}$  with those for  $\text{SiO}_2$ ,  $\text{BeF}_2$  and even water. The comparison of their heat capacities above  $T_g$  is shown in Figure 1.  $\text{Fe}_{50}\text{Co}_{50}$  represents the case of crossing the critical point.  $\text{SiO}_2$  and  $\text{BeF}_2$  exhibit smeared out peaks in heat capacity above their respective melting points, which are interpreted as the results of crossing the Widom line, the extension of the coexistence line beyond the liquid-liquid critical point. The Inset shows the heat capacity peak of argon that is very sharp on its liquid-gas critical point and becomes smeared out as the pressure increases beyond the critical point. The similar behavior seems to be seen also in “strong” substances.

The computer simulations of liquids based on the Jagla model by Xu et al. have found that the liquid-liquid (LL) transition slightly above the LL critical pressure is characterized by a sharp  $\lambda$  peak in heat capacity, just like the  $\lambda$  peak for  $\text{Fe}_{50}\text{Co}_{50}$ . On cooling below the critical temperature, the liquid is frozen-in (glass transition), trapping the remaining disorder. The same is also seen for  $\text{Fe}_{50}\text{Co}_{50}$ . The simulations also show that the transitions become smeared out as pressure increases beyond the critical point, like the behavior of argon near its liquid-gas critical point. The simulations together with the comparison in Fig-

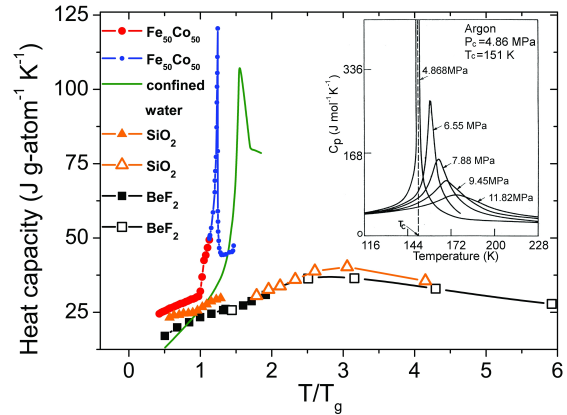


FIG. 1. Heat capacity of  $\text{Fe}_{50}\text{Co}_{50}$  through  $T_g$  compared to those for  $\text{SiO}_2$  and  $\text{BeF}_2$  as well as that for nanoconfined water. Filled symbols: experimental data. Open symbols: simulations. Inset: Heat capacity of argon in the vicinity of its liquid-gas critical point. (Taken from Ref. [1])

ure 1 imply that the behavior of strong liquids should be understood as the off-critical phenomena. Furthermore, it is clear that the static correlation length of  $\text{Fe}_{50}\text{Co}_{50}$  is diverging at the order-disorder critical point. We argue that the static correlation length of strong liquids decreases as  $T$  approaching  $T_g$  from above, which is the opposite trend to that of fragile molecular liquids whose dynamic and static correlation length are found to increase as  $T_g$  is approached from above.

There is evidence that a LL transition involved in a critical point is associated with a dynamic crossover (strong for low- $T$  phase and fragile for high- $T$  phase). Therefore, we argue that strong and fragile liquids exist on opposite flanks of the heat capacity peak of the underlying order-disorder transition, which can be a smeared out continuous transition or a (weak) first order transition under different conditions. However, on laboratory timescales, one can usually only observe either strong or fragile phase of one liquid except for the case of water and, perhaps, now also for some metallic glass-forming liquids.

The authors thank the support from Deutsche Forschungsgemeinschaft (DFG).

\* Corresponding author: shuai.wei.mailbox@gmail.com  
[1] S. Wei, I. Gallino, R. Busch & C. A. Angell, Nature Physics DOI:10.1038/NPHYS1823 (2010).

## Equilibrium viscosity, enthalpy recovery and free volume relaxation in a $\text{Zr}_{44}\text{Ti}_{11}\text{Ni}_{10}\text{Cu}_{10}\text{Be}_{25}$ bulk metallic glass

Zach Evenson\* and Ralf Busch

Universität des Saarlandes

We report on the free volume of the  $\text{Zr}_{44}\text{Ti}_{11}\text{Ni}_{10}\text{Cu}_{10}\text{Be}_{25}$  bulk metallic glass (BMG) in terms of its experimentally determined volumetric relaxation, enthalpy recovery and equilibrium viscosity below the glass transition temperature,  $T_g$ . The isothermal change in length of the amorphous samples during relaxation into the metastable equilibrium liquid was used directly to determine the change in the excess free volume of the glass. Additionally, differential scanning calorimetry was used to detect the enthalpy recovery during heating through the glass transition after isothermal annealing of the samples below  $T_g$ . The equilibrium viscosity of the samples was determined using a three-point beam-bending technique. The results obtained present a very consistent picture of structural relaxation as analyzed with calorimetric and volumetric methods.

At annealing temperatures below  $T_g$  the kinetics of volumetric and viscosity relaxation are found to be well described with a stretched exponential, or Kohlrausch-Williams-Watts function

$$\phi(t) = \phi_0 \exp(-t/\tau)^{\beta_{KWW}} \quad (1)$$

with  $\beta_{KWW}$  values approaching unity in both measured quantities as the glass transition is approached. This is in good accordance with similar investigations of the enthalpy relaxation in another Zr-based BMG system [1].

Furthermore, a linear correlation is found between the experimentally determined enthalpy of recovery and free volume reduction, giving a constant value of the formation enthalpy for free volume in the glass,  $\beta$ , determined here to be  $622.7 \pm 20 \text{ kJ g-atom}^{-1}$ , which has been interpreted as the formation enthalpy for an amount of free volume with the magnitude of one atomic volume. Since flow processes are known to occur when a critical amount of free volume is reached ( $\sim 0.1v_m$  for metallic species[3]), the formation enthalpy necessary for this critical free volume is accordingly lower. According to our results, the formation enthalpies for the critical amount of free volume needed for structural relaxation as well as for viscous flow are similar,  $\sim 180\text{-}200 \text{ kJ g-atom}^{-1}$  near the glass transition.

The free volume in the equilibrium liquid is calculated from viscosity measurements carried out below  $T_g$ . These data are described using the Cohen and Turnbull[3] and Cohen and Grest[5] models of the free volume. Additionally, an interpretation of the free volume based on the equilibrium viscosity model of Adam-Gibbs[6] is proposed as

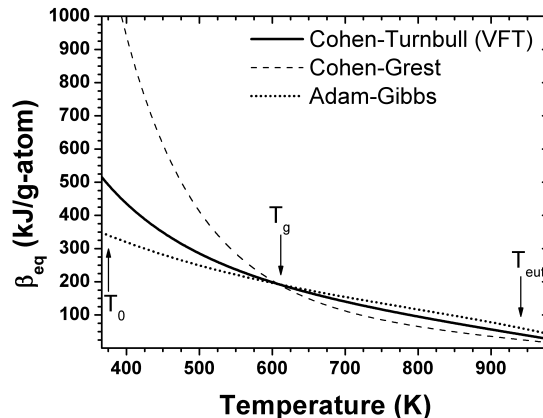


FIG. 1. Reduced free volume formation enthalpy in the equilibrium liquid,  $\beta_{eq}$ . The solid, dashed and dotted lines represent  $\beta_{eq}$  calculated according to each free volume model indicated in the legend. The temperatures shown are the VFT-temperature,  $T_0$ ; the glass transition temperature,  $T_g$ ; and the melting temperature,  $T_{eut}$ .

$$v_f/v_m = \frac{bTS_c(T)}{C}, \quad (2)$$

where  $b$  is the Doolittle parameter[4];  $T$ , the temperature;  $S_c(T)$ , the configurational entropy of the equilibrium liquid calculated according to the method in [2]; and  $C$  is the free energy barrier per particle to viscous flow in the Adam-Gibbs equation below:

$$\eta = \eta_0 \exp(C/TS_c(T)) \quad (3)$$

Analysis of the free volume and enthalpy functions of the equilibrium liquid reveals a temperature-dependent formation enthalpy for free volume that varies from  $\sim 1 \text{ eV}$  at the melting point to  $\sim 2 \text{ eV}$  near the glass transition (Fig. 1).

\* Corresponding author: z.evenson@mx.uni-saarland.de

- [1] I. Gallino, M. Shah and R. Busch, *Acta Mater* **55**, 4 (2007).
- [2] I. Gallino, J. Schroers and R. Busch, *J Appl Phys* **108**, 6 (2010).
- [3] H. Cohen and D. Turnbull, *J Chem Phys* **31**, 5 (1959).
- [4] A. Doolittle, *J Appl Phys* **23**, 2 (1952).
- [5] G. Grest and H. Cohen, *Adv Chem Phys* **48**, (1981).
- [6] G. Adam and J. H. Gibbs, *J Chem Phys* **43**, 1 (1965).

## Isotropic-nematic transition of charged disks

Sara Jabbari-Farouji,<sup>1,\*</sup> Emmanuel Trizac,<sup>1</sup> and Jean-Jacques Weis<sup>2</sup>

<sup>1</sup>LPTMS, CNRS and Université Paris-Sud, UMR8626, Bat. 100, 91405 Orsay, France

<sup>2</sup>Laboratoire de Physique Théorique d'Orsay, Bat. 210, 91405 Orsay, France

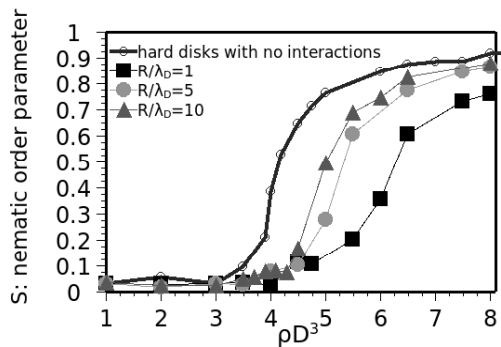


FIG. 1. The nematic order parameter defined as  $\langle P_2(\cos\theta) \rangle$  with respect to the nematic axis as a function of density for 3 ratios radius to Debye length  $R/\lambda_D$  as depicted in the legend.

Clay minerals, ubiquitous in our everyday life, are one of the fascinating instances of charged plate-like colloids with widespread applications. The anisotropic shape of clay minerals suggests that these materials could form liquid crystalline phases due to the competition between translational and orientational entropy. In practice, isotropic-nematic transition is hindered by the formation of a gel-like viscoelastic phase in most of clays including the widely studied cases of Laponite and Montmorillonite. Lately however, isotropic-nematic transition has been identified in aqueous suspensions of some natural clays [1].

Motivated by these experimental findings and to gain a better insight into the role of electrostatic interactions on isotropic-nematic transition, we have performed Monte Carlo simulations of thin charged disks. In our simulations, the electrostatic interactions be-

tween charged disks embedded in an electrolyte are implemented through an orientation-dependent two-body effective interaction potential recently developed for charged spheroids [2, 3]. We have made an extensive study of phase behavior of our model system as a function of disks density and ionic strength. In the presence of electrostatic interactions, we find that isotropic-nematic transition is shifted towards higher densities as demonstrated in Fig. 1; the larger the screening length (Debye length), the stronger the shift towards higher densities. These results suggest that charged disks surrounded by ions are effectively less anisotropic than infinitely thin disks.

To have a better understanding of the structures formed, we have also characterized the dynamics of the system by computing the intermediate scattering function. To do so, we have developed a dynamic Monte Carlo scheme in which the amplitude of translational and orientational displacements are chosen in such a way that they correspond to a physical move of particles undergoing translational and rotational Brownian motion. To conclude, we will discuss the interplay between orientational excluded volume and anisotropic electrostatic interactions and their role on the phase behavior of the system.

We would like to thank the foundation “Le Triangle de la Physique” for its financial support.

\* Corresponding author: sara.jabbari@lptms.u-psud.fr

- [1] L. J. Michot, et. al, Proc. Nat. Acad. Sci. **103**, 16101 (2006).
- [2] R. Agra, E. Trizac, L. Bocquet, Eur. Phys. J. E **15**, 345 (2004).
- [3] Carlos Alvarez and Gabriel Tellez, J.Chem. Phys. **133**, 144908 (2010).

## Nanoscale structural characterization and relaxation of the oil-in-water nanoemulsion with Hydrophobically End-Capped Poly (ethylene oxide)

Masoud Amirkhani,<sup>1</sup> Soheil Sharifi,<sup>2,\*</sup> Johan Bergenholtz,<sup>3</sup> and Othmar Marti<sup>1</sup>

<sup>1</sup>*Institut für Experimentelle Physik, Universität Ulm,  
Albert-Einstein-Allee 11 89081 Ulm, Germany*

<sup>2</sup>*Department of Physics, University of Sistan and Baluchestan, 98135-674 Zahedan, Iran*

<sup>3</sup>*Department of Chemistry, Göteborg University, SE-412 96 Göteborg, Sweden*

We study the mixture of C12E5 microemulsion with the Poly (ethylene oxide) end-cap polymer. The mass fraction of droplet and oil to the surfactant ( $mf=0.2$  and  $mC12E5/mol=1.0833$ ) kept constant while we vary the polymer concentration. The small-angle x-ray scattering has been employed to investigate the

structural behavior of the system and the dynamic light scattering is used to study dynamic behavior and possible formation of the network.

\* Corresponding author: soheil.sharifi@gmail.com

## The effect of depletion interaction on relaxation and structure of nanoemulsion

Soheil Sharifi,<sup>1,\*</sup> Masoud Amirkhani,<sup>2</sup> Johan Bergenholtz,<sup>3</sup> and Othmar Marti<sup>2</sup>

<sup>1</sup>*Department of Physics, University of Sistan and Baluchestan, 98135-674 Zahedan, Iran*

<sup>2</sup>*Institut für Experimentelle Physik, Universität Ulm,  
Albert-Einstein-Allee 11 89081 Ulm, Germany*

<sup>3</sup>*Department of Chemistry, Göteborg University, SE-412 96 Göteborg, Sweden*

The mixture of C12E5 nanoemulsion with PEG have been studied by small-angle X-ray scattering and dynamic light scattering in order to determine structure and dynamic of the system. Light scattering experiment shown an exponential relaxation for pure C12E5 nanoemulsion that with increasing of PEG concentration in the C12E5 nanoemulsion, relaxation be-

comes non-exponential, which demonstrates that increase of cooperativity. The study structure of the system with SAXS experiment, shown with increasing of PEG concentration, the size of the droplet doesn't change but interaction between droplets increases that have agreement with light scattering data's.

\* Corresponding author: soheil.sharifi@gmail.com

## Non-linear response of dipolar colloidal gels to external fields

Emanuela Del Gado<sup>1,\*</sup> and Patrick Ilg<sup>2</sup>

<sup>1</sup>*Microstructure and Rheology, Institute for Building Materials,  
Department of Civil Engineering, ETH Zurich, Switzerland*

<sup>2</sup>*Polymer Physics, Department of Materials, ETH Zurich, Switzerland*

Suspensions of dipolar colloidal particles show extremely interesting potentialities as field-responsive soft matter systems thanks to the non-trivial interplay of the external fields with the complex microstructures. They do not only form chain-like aggregates, but can also show pseudo-crystalline ordering [1] and computer simulations of colloids with extended dipoles have recently indicated that a percolating network of cross-linked chains appears at low temperatures [2]. Starting from the model system of charged soft dumbbells introduced in Ref. [2], we here analyze the properties of the network structure in different state points and investigate the response of the system to an external electric field [3].

At relatively high temperatures the system behaves like a gas of chain-like structures and its dielectric susceptibility increases smoothly with the intensity of the applied external field. The system is characterized by chain-like structures with an exponential distribution of chain lengths and an external magnetic field orients not only the particle's dipole moments but also the chain-like structures as a whole. For low temperatures instead, where the dipolar interactions are more dominant, the system undergoes a percolation transition to an interconnected network of particle chains. Below the percolation transition, almost all particles belong to the same sample-spanning network. The network regime is characterized by persistent bonds and glassy relaxational dynamics, as typically observed in colloidal gels where particles are typically bonded by short-range attractive potentials [4].

We find that this gelation dramatically, and rather irreversibly, changes the response of the material to an external electric field. In fact, since particles are strongly bound in the network, they can not easily reorient according to the field. Hence the polarizability of the gel network is initially relatively weak, as compared to the initial dipolar fluid. When the external field strength reaches a critical value, however, the particle's dipole moments orient rather abruptly along the field direction, with a strongly nonlinear increase of the polarization. This reorientation breaks the network structure and particles rearrange into oriented, bundled chains (Fig.2). Such significant structural reorganizations beyond a critical field strength allows to change the mechanics and the dielectric properties

at the same time, and could offer new applications for dipolar colloidal suspensions as field-responsive, smart materials. Because of this field-induced structural transition, the gel dielectric response displays a significant hysteresis, which is stronger for the more persistent network structures.

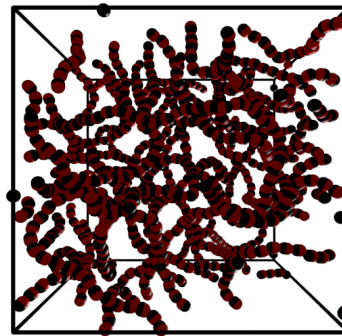


FIG. 1. 3D Snapshot of particle coordinates at  $\phi = 0.0484, T = 0.06$  without field.

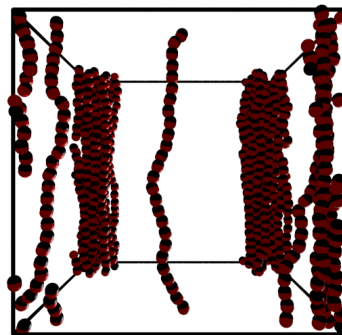


FIG. 2. 3D Snapshot of particle coordinates at  $\phi = 0.0484, T = 0.06$  in the presence of a strong field  $E = 0.75$  in the vertical direction.

\* Corresponding author: delgadoe@ethz.ch

- [1] S. Odenbach (ed.) *Colloidal Magnetic Fluids*, Lecture Notes in Physics, Springer (2008).
- [2] R. Blaak, M.A. Miller, J.-P. Hansen EPL **78** 26002 2007.
- [3] P. Ilg and E. Del Gado, *Soft Matter* (2010), DOI:10.1039/c0sm00592d.
- [4] E. Del Gado and W. Kob, *Soft Matter* **6**, 1547 (2010).

## Ultra-fast quenching of binary colloidal suspensions in external magnetic fields

René Messina,\* Lahcen Assoud, and Hartmut Löwen

*Institut für Theoretische Physik II: Weiche Materie,  
Heinrich-Heine-Universität Düsseldorf, Universitätsstraße 1, D-40225 Düsseldorf, Germany*

Temperature quenching constitutes a key processing technique to produce amorphous and crystalline solids which are considerably different from their thermodynamically stable counterparts. Possible applications can be found in metallurgy, ceramics and semiconductor doping. Such quenching techniques are most efficient when they are performed abruptly, i.e. if the system temperature changes on a time scale that is much shorter than that of a typical particle motion. While this can be realized in computer simulations, it is practically impossible to be achieved for molecular systems where the quench is performed by a contact with an external heat bath. There, it takes some time until the prescribed temperature is realized within the whole sample. However, as we shall show in this presentation, an ultra-fast quenching is possible for colloidal particles which move much slower and are highly susceptible to external fields [1].

The system under consideration consists of a (two-dimensional) suspension of two kinds of superparamagnetic colloidal particles denoted by  $A$  and  $B$ . At prescribed composition, all static properties (assuming point dipolar particles) depend uniquely on a dimensionless interaction strength  $\Gamma = \frac{\mu_0 \chi_A^2 H^2}{4\pi k_B T a^3}$  where  $k_B T$  is the thermal energy at room temperature,  $a$  the average interparticle separation between  $A$  particles,  $\mu_0$  the vacuum permeability,  $\chi_A$  the magnetic susceptibility for particles  $A$  (i.e., with large dipolar moments  $m_A = \chi_A H$ ), and  $H$  the external applied magnetic field.

Illustrative snapshots after the quench (i.e., going

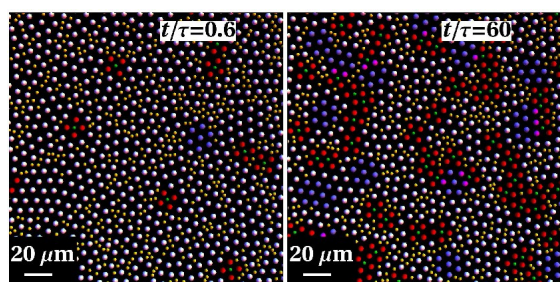


FIG. 1. Two experimental snapshots for a time  $t/\tau = 0.6$  ( $\tau$  being a typical Brownian time) just after the quench (left configuration) and a later time  $t/\tau = 60$  (right configuration) are shown. Big particles are shown in blue if they belong to a triangular surrounding and in red if they belong to a square surrounding. All other big particles are shown in white color. Few big particles belonging to both triangular and square surroundings are shown in pink color. The small particles are shown in green if they belong to a square center of big particles, otherwise they appear in yellow.

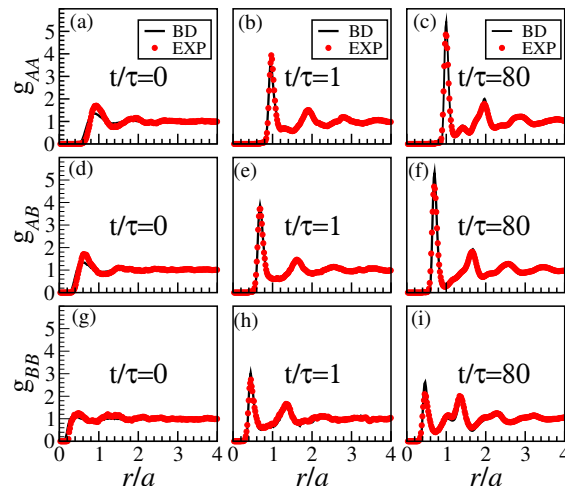


FIG. 2. Partial pair distribution functions  $g_{AA}(r)$ ,  $g_{AB}(r)$  and  $g_{BB}(r)$  of  $A$ - and  $B$ -particles versus reduced distance  $r/a$  at three different reduced times (a),(d),(g)  $t/\tau = 0$ ; (b),(e),(h)  $t/\tau = 1$ ; (c),(f),(i)  $t/\tau = 80$ . BD results (solid lines) are compared to experimental data (symbols).

from  $\Gamma = 1$  to  $\Gamma = 71$ ) are sketched on Fig. 1. From these snapshots, it is evident that the crystalline clusters form locally and grow as a function of time. Preferentially triangular structures form in an area depleted from  $B$  particles while square structures nucleate around “seeds” which possess a structure close to an underlying square.

As a more quantitative illustrative result, the time evolution of the partial pair distribution functions  $g_{AA}(r)$ ,  $g_{AB}(r)$  and  $g_{BB}(r)$  for different times is shown in Fig. 2. Thereby, the system spontaneously relaxes by exhibiting structural inhomogeneities which reflect the underlying stable crystal [2, 3] and correlate with slower regions in the dynamics.

This work was supported by the DFG (projects C2 and C3 of SFB TR6 and SPP 1296).

\* Corresponding author: messina@thphy.uni-duesseldorf.de

- [1] L. Assoud, F. Ebert, P. Keim, R. Messina, G. Maret, and H. Löwen, *Phys. Rev. Lett.*, **102** 238301 (2009).
- [2] L. Assoud, R. Messina, and H. Löwen, *Europhys. Lett.* **80**, 48001 (2007).
- [3] L. Assoud et al., *J. Phys.: Condens. Matter.*, **21** 464114 (2009).

## Theoretical study of aging and instantaneous quenches in attractive Yukawa systems

Pedro E. Ramírez-González\* and Magdalena Medina-Noyola

*Instituto de Física “Manuel Sandoval Vallarta”, Universidad Autónoma de San Luis Potosí,  
Álvaro Obregón 64, 78000 San Luis Potosí, SLP, México*

The non-stationary, slowly-evolving dynamics of deeply quenched fluids, referred to as aging, has been the subject of considerable attention over the last decade [1, 2]. Certain universal features in the irreversible evolution of these structurally-disordered and out-of-equilibrium materials, suggests the existence of an underlying common source of the observed dynamic properties. The quantitative theoretical first-principles description of these phenomena has, however, not been available until now. In this work we demonstrate that the recently-developed *non-equilibrium* self-consistent generalized Langevin equation (NE-SCGLE) theory [3, 4] provides a theoretical prediction of the dependence of the static structure factor  $S(k; t_w)$  and of the time-dependent intermediate scattering function  $F(k, \tau; t_w)$  on the evolution time  $t_w$ , that characterize the non-equilibrium evolution of these system. Thus, we apply this theory to a model mono-component fluid of particles interacting through the hard-sphere plus short-ranged attractive Yukawa potential, subjected to an instantaneous quench to a temperature below its attractive glass transition.

Let us focus our discussion on the conceptually simplest glass-forming system, namely, a mono-component fluid made of  $N$  identical spherical particles in a volume  $V$  which interact through the pair potential  $u(r)$ . Assuming that in the absence of external fields this system is initially prepared in an equilibrium state corresponding to a mean density  $\bar{n}^{(0)} = N/V$  and a temperature  $T^{(0)}$ , in which the static structure factor is  $S^{(0)}(k) = S^{eq}(k; \bar{n}^{(0)}, T^{(0)})$ . In the simplest idealized quench experiment, at the time  $t = 0$  the temperature of the system is instantaneously and discontinuously changed to a value  $T^{(f)}$ . The *non-equilibrium* self-consistent generalized Langevin equation (NE-SCGLE) theory consists of a closed self-consistent system of equations for  $S(k; t)$  and  $F(k, \tau; t)$ , which we numerically solve here for the model system above.

As illustrated in Fig. 1, after the sudden temperature change at  $t = 0$  has occurred the system evolves spontaneously, searching for its new thermodynamic equilibrium state, at which the static structure factor should be  $S^{eq}(k; \bar{n}^{(0)}, T^{(f)})$ . If the end state, however, is a dynamically-arrested state (a glass or a gel), the system may never be able to reach this equilibrium state within experimental times.

Let us stress that the theory proposed is not limited to instantaneous quench processes; in principle it is easily extendable to other quench “programs”. The

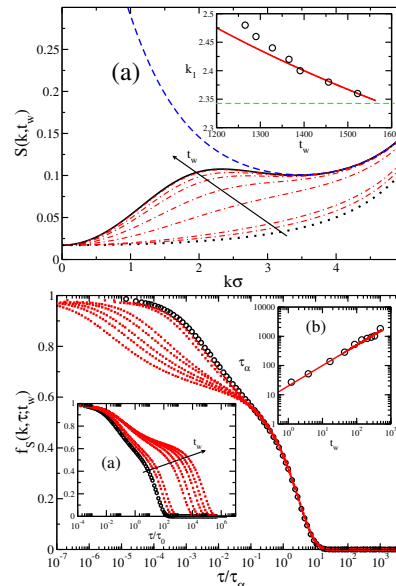


FIG. 1. Non-equilibrium evolution of the static structure factor  $S(k, t_w)$  and  $F(k, \tau; t_w)$  for a quench to a dynamically arrested state. The system, initially equilibrated at a fluid state  $(\phi_0, T_I^*)$ , with  $S(k; t = 0) = S^{eq}(k; \phi_0, T_I^*)$  (black dotted curve), is instantaneously quenched at  $t_w = 0$  to the final point  $(\phi, T_{F'})$  inside the dynamic arrest region. The static structure factor then evolves continuously along a sequence of non-equilibrium values ((red) point-dashed lines). Because we quenched to a dynamic arrest state the system cannot reach the equilibrium state  $S^{eq}(k; \phi_0, T_{F'})$  (blue dashed curve). Instead of that the static structure factor evolves asymptotically to a non-equilibrium arrested value  $S^{(a)}(k)$  (black solid line). Although this asymptotic evolution is not appreciable in the static structure factor, it is evident in  $F(k, \tau; t)$ , where the relaxation time grows indefinitely as is illustrated in the second figure (inset (a)).

present work, however, was meant to provide the first exploratory application of this general theory in the simplest possible conditions. The specific results reported here suggest that this theory provides a qualitatively and quantitatively sound basis for the first-principles theoretical discussion of the complex non-equilibrium phenomena associated with the aging of structural glass-forming colloidal systems.

\* Corresponding author: ehecatl@dec1.ifisica.uaslp.mx

- [1] L. Cipelletti and L. Ramos, J. Phys.: Condens. Matter **17**, R253, 285 (2005).
- [2] R. Bandyopadhyay, D. Liang, J.L. Harden and R.L. Leheny, Solid State Comm. **139**, 589 (2006).
- [3] P. E. Ramírez-González and M. Medina-Noyola, Phys. Rev. E (2010, submitted).
- [4] P. E. Ramírez-González PHD Thesis (2010).



### **3.3 Posters B**

## Non-linear response in glass-forming systems: Computer simulations

Carsten Schroer and Andreas Heuer\*

*Institut für Physikalische Chemie, Universität Münster, 48149 Münster, Germany*

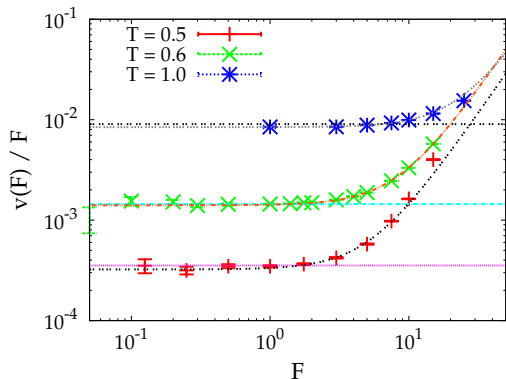


FIG. 1. The velocity of the tagged particle for different forces and temperatures. The solid lines correspond to the linear response prediction.

The non-linear behavior of glass forming system under application of external forces is of major current interest. Several experimental working groups are investigating the changes of dynamical properties, for example by examining the non-linear conductivity of glassy ionic conductors [1]. Computer simulations can give a deeper understanding and provide more microscopic information about these processes.

In this contribution we study the properties of the non-linear response of glass-forming liquids. For this purpose we perform molecular dynamics simulations of a binary mixture Lennard-Jones liquid where an additional constant force is applied to one tagged particle, see Fig. 1. Our investigations are analyzed in terms of the continuous time random walk (CTRW) and the potential energy landscape (PEL) formalism [2].

For application of the CTRW for large system it turns out to be essential to determine the waiting times in real space rather than configuration space [4]. This made it possible to define elementary jump processes for an unforced system. For systems with an external force, there is no unique way to determine the force-dependence of the mean waiting time  $\langle\tau\rangle$  and average transition distance in force direction  $\delta$ , see Fig. 2, such that the resulting velocity is just given by  $v/\langle\tau\rangle$ . We suggest a method which is most appropriate to

characterize the transition from the linear to the non-linear regime of the tagged particle velocity. In this way we can express the non-linear regime in terms of a CTRW.

Another point of interest is the investigation of finite-size effects of the non-linear behavior. Our results suggest that the onset as well as the strength of non-linearity is independent of system size beyond system sizes as small as 65 particles, see Fig. 2. This ob-

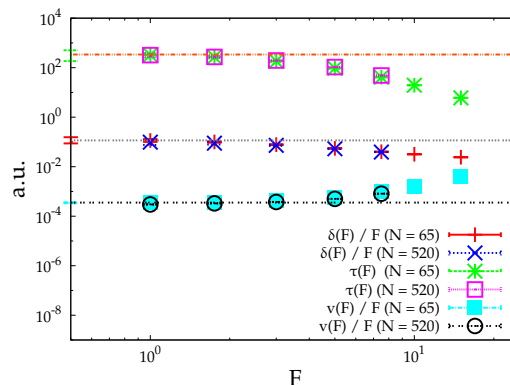


FIG. 2. Determination of the different CTRW-ingredients in dependence of force and system size.

servation makes it possible to use small systems for simulations and to express the non-linear effects in terms of the properties of the underlying PEL.

Furthermore, we use oscillating external forces to determine the frequency dependency of the non-linear behavior. These results can be compared with experimental data as obtained in the Roling-group.

We acknowledge financial support by the DFG (FOR 1394)

\* Corresponding author: andheuer@uni-muenster.de

- [1] B. Roling, S. Murugavel, A. Heuer, L. Luehning, R. Friedrich, and S. Roethel, Phys. Chem. Chem. Phys. **10**, 4211 (2008).
- [2] A. Heuer, J. Phys. Condens. Matter **20**, 373101 (2008).
- [3] O. Rubner and A. Heuer Phys. Rev. E **78**, 011504 (2008).
- [4] C. Rehwald, O. Rubner, A. Heuer Phys. Rev. Lett. **105**, 117801 (2010)

## Non-linear single-particle-response of glassforming systems to external fields

David Winter,<sup>1,\*</sup> Peter Virnau,<sup>1</sup> Kurt Binder,<sup>1</sup> and Jürgen Horbach<sup>2</sup>

<sup>1</sup>Johannes Gutenberg-Universität, Mainz, Germany

<sup>2</sup>Deutsches Zentrum für Luft- und Raumfahrt (DLR), Köln, Germany

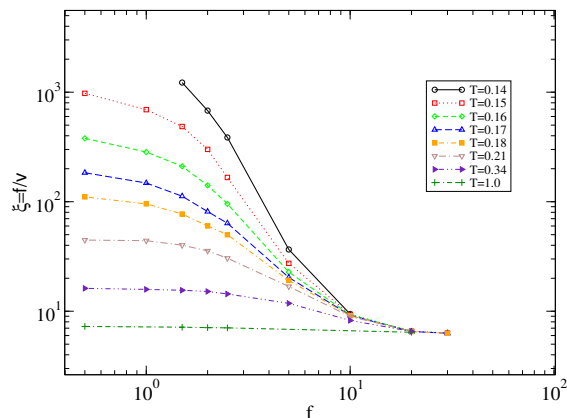


FIG. 1. Friction coefficient  $\xi$  of A particles in the binary Yukawa mixture at different temperatures as a function of the external force  $f$ .

Glassy dynamics of viscous liquids are characterized by a drastic slowing down of dynamical properties, while structural and thermodynamic quantities only show a weak gradual change. Recently, various independent studies have revealed that the interplay of the glass transition with external fields provides a wealth of new phenomena yet to be explored [1, 2]. There is hope that the understanding of the non-linear response of glassforming systems to external fields leads to new insight into the nature of the glass transition. In this work, we study the behavior of single particles in a supercooled liquid under the influence of an external force. Our model system is a 50:50 binary mixture

whose particles interact via a Yukawa potential.

$$V_{\alpha\beta}(r) = \varepsilon_{\alpha\beta} d_{\alpha\beta} \exp[-\kappa(r - d_{\alpha\beta})]/r \quad (1)$$

By choosing slightly different potentials between A and B particles we prevent the system from crystallizing. In the equilibrated system, we add a constant force field to one of these particles which as a consequence will be accelerated. After some time, this particle reaches a steady state. In this state we measure characteristic properties of the particle and the surrounding like the steady state velocity, the friction coefficient, mean square displacements and correlation functions in dependence of the external force and system temperature. Fig. 1 shows the friction coefficient measured in our simulations. We observe that for low temperatures and high enough force fields the particle leaves the linear response regime and enters the non-linear regime. Here, the friction coefficient is not constant any more. For even higher forces all curves reach a second plateau and fall on top of each other. This work also allows to check new theoretical approaches for the micro-rheology of glassforming systems in the framework of mode coupling theory [3].

Acknowledgements: Deutsche Forschungsgemeinschaft (grant TR6/A5).

\* Corresponding author: winterda@uni-mainz.de

- [1] R. G. Larson, *The Structure and Rheology of Complex Fluids* (Oxford University Press, New York, 1999).
- [2] M. Fuchs, *Nonlinear rheological properties of dense colloidal dispersions close to a glass transition under steady shear*, in 'High Solid Dispersions' ed. M. Cloitre, Vol. 236 of *Advances and Polymer Science* (Springer, Berlin, 2010), preprint arXiv:0810.2505.
- [3] I. Gazuz, A. M. Puertas, T. Voigtmann, and M. Fuchs, *Phys. Rev. Lett.* **102**, 248302 (2009).

## Yielding of colloidal glasses and gels

Nick Koumakis,<sup>1,2,\*</sup> George Petekidis,<sup>1,2</sup> and John F. Brady<sup>3</sup>

<sup>1</sup>*IESL-FORTH, Heraklion, Crete, Greece*

<sup>2</sup>*Department of Materials Science and Technology, University of Crete, Heraklion, Crete, Greece*

<sup>3</sup>*California Institute of Technology, Pasadena, California, U.S.A.*

It has been found that by adding attractions to a simple colloidal hard sphere glass, for example in the form of a short range depletion, the glass turns into an ergodic liquid, followed by a re-entrant transition to an attractive glass [1]. Simple hard sphere glasses exhibit a single step yielding under oscillatory or steady shear that is related with the entropic elasticity and breaking of the first neighbour cage at a strain corresponding to the maximum distortion of the cage, which is the structural arrest length scale at about 10%-15% strain. However, when strong attractions are added, for example in the form of a short range depletion, the system yields in a two step manner. It has been proposed that these processes reflect an initial particle bond breaking at low strains and a subsequent breaking of an attractive cage at larger strains [2].

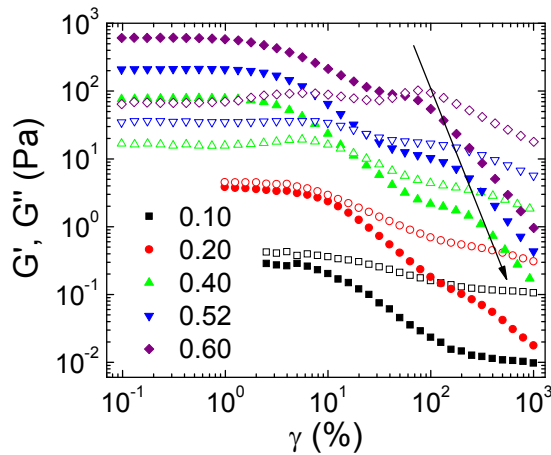


FIG. 1. Dynamic strain sweeps of different volume fractions with equal attraction strength of  $U_{dep}(2R) = -19kT$ . Note the complicated behaviour of  $G'$  (solid) with increasing strain and the dissipation of the second  $G''$  (open) yielding peak (100% strain) with decreasing volume fraction. The arrow shows the approximate shift of the second  $G''$  peak with decreasing volume fraction.

Here we attempt to elucidate the origin of the two step yielding by examining the rheological response of a series of samples with the same interparticle attraction ranging from high volume fraction attractive glasses to the low volume fraction colloidal gels ( $0.1 < \phi < 0.6$ ). We examine the linear and non-linear properties with both oscillatory and steady shear rheology. We find that the transition from a highly concentrated attractive glass to a low volume fraction colloid-polymer gel takes place gradually with the cage breaking process being substituted by a cluster dominated process as the volume fraction is decreased, leading to larger

yield strains (see fig. 1) [3].

Rheological measurements are complemented by steady shear Brownian Dynamics simulations of the gel state in order to gain insight on the microscopic rearrangements and structural changes that occur during yielding. It is found that the structural properties of the steady state under shear and after cessation are highly dependent on the shear rate. Low rates tend to increase the structural inhomogeneities compared to rest, while high rates “rejuvenate” the system by breaking up all heterogeneous structure (fig. 2).

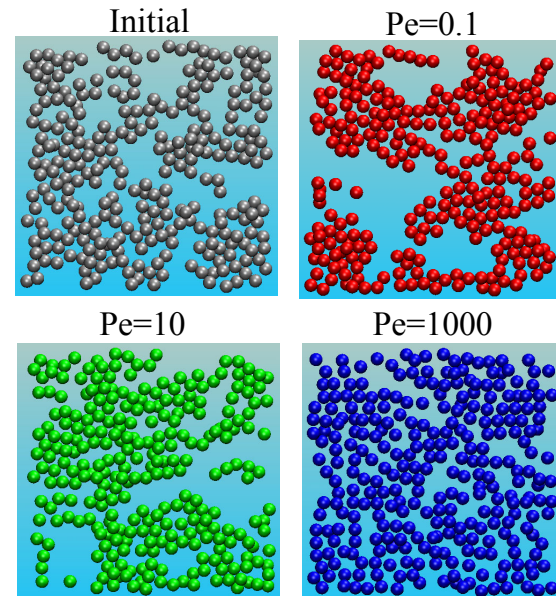


FIG. 2. BD simulation image slice of particle positions at steady states both at rest and under shear of a strong gel with  $\phi = 0.44$ , revealing different levels of heterogeneity.

This work was supported by the EU ToK project “Cosines”, the EU Network of Excellence “Softcomp” and the EU FP7 project “Nanodirect”.

\* Corresponding author: nickk@iesl.forth.gr

- [1] K. N. Pham, A. M. Puertas, J. Bergenholtz, S. U. Egelhaaf, A. Moussaid, P. N. Pusey, A. B. Schofield, M. E. Cates, H. Fuchs and W. C. K. Poon, *Science*, **296**, 104-106 (2002).
- [2] K. N. Pham, G. Petekidis, D. Vlassopoulos, S. U. Egelhaaf, W. C. K. Poon and P. N. Pusey, *Journal of Rheology* **52**, 649 (2008).
- [3] N. Koumakis and G. Petekidis, *Softmatter*, (2011, Submitted).

## Brownian dynamics simulation of extensional shear flow in dense colloidal hard-sphere systems at the glass transition

Olaf Herbst<sup>1,\*</sup> and Th. Voigtmann<sup>1,2</sup>

<sup>1</sup>*Institut für Materialphysik im Weltraum, Deutsches Zentrum für Luft- und Raumfahrt (DLR), 51170 Köln, Germany*

<sup>2</sup>*Zukunftskolleg und Fachbereich Physik, Universität Konstanz, 78457 Konstanz, Germany*

We study colloidal particles in extensional flow as a model system to understand gravity-driven convection of metallic melts in micro-gravity environment. Colloidal systems have been an active field of research for more than a century now [1–3]. As a model system for metallic melts they have the advantage of being more easily accessible in experiments, e.g. through confocal microscopy and at room temperature, than metallic melts. Our model system consists of colloidal particles at densities near the glass transition and subject to a two-dimensional extensional flow, i.e. where the solvent behaves according to a velocity field given by  $\vec{V}(\vec{r}(t), t) = \vec{V}(\vec{r}(t), 0) = \mathbf{\Gamma} \cdot \vec{r}(t)$  with a constant velocity gradient tensor  $\mathbf{\Gamma} = \begin{pmatrix} 0 & a \\ b & 0 \end{pmatrix}$  with eigenvalues  $\epsilon_i \equiv \pm\sqrt{ab}$ . An illustration is given in the left graph of Fig. 1.

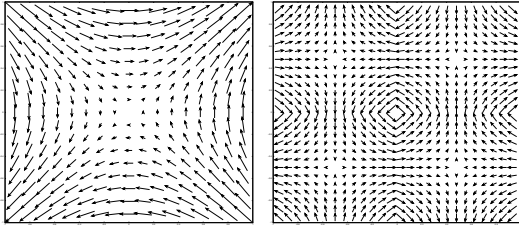


FIG. 1. Velocity field of (left) a simple extensional flow and (right) a smart periodic continuation of an extensional flow used as a simple model to study gravity-driven convection.

When a plane is plastered in a smart way with extensional flows we can construct what is shown in the right graph of Fig. 1. This flow is periodic and will be used in the computer simulations described below.

A system of colloidal particles in a solvent exhibits Brownian motion. Such a system can be described by means of a Smoluchowski equation or, equivalently, we can describe the system of an individual Brownian particle by a Langevin equation, i.e.

$$\frac{d\vec{p}}{dt} = -\gamma \left( \frac{\vec{p}}{M} - \vec{V}(\vec{r}, t) \right) + \vec{f}(t) \quad \text{and} \quad \frac{d\vec{r}}{dt} = \frac{\vec{p}}{M},$$

where  $\vec{r}$  is the position of the Brownian particle,  $\vec{p}$  its momentum,  $M$  its mass,  $\gamma$  the damping constant that depends on the interaction between the solvent and the particle, and  $\vec{V}$  is the prescribed velocity field of the solvent. The force  $\vec{f}(t)$  is chosen to be delta-correlated white noise with zero mean.

Assuming that the colloidal particles do not disturb the prescribed velocity flow field of the solvent the Langevin equation can be solved analytically by diagonalization to yield (in diagonal form)

$$\begin{aligned} \tilde{r}_i(t) &= \tilde{r}_i(0) e^{-\alpha t} \left[ \cosh(\alpha_i t) + \frac{\alpha}{\alpha_i} \sinh(\alpha_i t) \right] \\ &\quad + \frac{\tilde{p}_i(0)}{\alpha_i M} e^{-\alpha t} \sinh(\alpha_i t) \\ &\quad + \frac{1}{M \alpha_i} \int_0^t e^{-\alpha s} \sinh(\alpha_i s) \tilde{f}_i(t-s) ds \\ \tilde{p}_i(t) &= \tilde{p}_i(0) e^{-\alpha t} \left[ \cosh(\alpha_i t) - \frac{\alpha}{\alpha_i} \sinh(\alpha_i t) \right] \\ &\quad + \tilde{r}_i(0) \frac{M \alpha^2 \beta_i}{\alpha_i} e^{-\alpha t} \sinh(\alpha_i t) \\ &\quad + \int_0^t e^{-\alpha s} \left[ \cosh(\alpha_i s) - \frac{\alpha}{\alpha_i} \sinh(\alpha_i s) \right] \tilde{f}_i(t-s) ds \end{aligned}$$

where  $\alpha_i = \alpha \sqrt{1 + \beta_i}$ ,  $\alpha = \frac{\gamma}{2M}$ ,  $\beta_i = \frac{2\epsilon_i}{\alpha}$ . From this solution the covariance matrix of the stochastic variables for momentum,  $\vec{x}_1$ , and displacement,  $\vec{x}_2$ , is calculated. To calculate the effective diffusion constant for such a system we employ and adapt a novel Brownian Dynamics Event-Driven Molecular Dynamics simulation algorithm [4, 5]. The main idea is to translate the random displacements  $\vec{x}_2$  (drawn for each prescribed timestep  $\tau$  from a Gaussian with variance  $\langle \vec{x}_2 \otimes \vec{x}_2 \rangle$ ) into pseudo velocities  $\vec{v}_{\text{pseud}} := \frac{\vec{x}_2}{\tau}$  to avoid forbidden states: Instead of moving each particle according to its random displacement we let the simulation evolve for a small timestep  $\tau$ . If for a given particle no collision occurs during  $\tau$  then its total displacement will be exactly the random displacement drawn for that particle. If, however, the particle was not able to freely move the distance stochastically drawn previously then it will collide with other particles and the total displacement will be modified accordingly. This yields the new spatial configuration. In the overdamped limit considered the real velocities are drawn independently from a Gaussian (with variance  $\langle \vec{x}_1 \otimes \vec{x}_1 \rangle$  – while  $\langle \vec{x}_1 \otimes \vec{x}_2 \rangle = 0$ ).

We present effective diffusion constants for various shear rates near the glass transition and data for densities that are beyond the glass transition without shear but below the effective glass transition when sheared strongly enough. Various time and length scales are identified.

\* Corresponding author: olaf.herbst@dlr.de

- [1] A. Einstein, Ann. Phys. **17**, 549–560 (1905).
- [2] M. Smoluchowski, Ann. Phys. **21**, 756–780 (1906).
- [3] P. Langevin, C. R. Acad. Sci. **146**, 530–533 (1908).
- [4] P. Strating Phys. Rev. E **59**, 2175 (1999).
- [5] A. Scala, Th. Voigtmann, and C. de Michele J. Chem. Phys. **126**, 134109 (2007).

# Lattice-Boltzmann Simulation of Non-Newtonian Liquids

Simon Papenkort<sup>1,\*</sup> and Thomas Voigtmann<sup>1,2</sup>

<sup>1</sup>*Fachbereich Physik, Universität Konstanz and Zukunftskolleg der Universität Konstanz, 78457 Konstanz, Germany*

<sup>2</sup>*Institut für Materialphysik im Weltraum, Deutsches Zentrum für Luft- und Raumfahrt (DLR), 51170 Köln, Germany*

There are many examples of complex fluids in nature and everyday life, such as blood, paint or shampoo. Their distinct properties make them an interesting object not only for rheological studies, but also for engineering science. Unlike a Newtonian fluid the viscosity exhibits a strong dependency on the shear rate, which leads to the most interesting effects, i.e., rod-climbing, the tube-less siphon or the Kaye effect [1]. Often a simple power-law is used to approximate the influence of viscoelasticity affecting the rheological properties, but this purely phenomenological constitutive model lacks a physical motivation and interpretation.

Maxwell introduced a simple model for a viscoelastic fluid, where the time dependent shear modulus  $G_\infty$  decays exponentially with a characteristic structural relaxation time  $\tau$ . In mode coupling theory a competition of structural arrest and shear-induced motion is observed and a non-linear extension of the model is suggested [2]. In this non-linear Maxwell model the shear modulus can relax via a second shear driven process characterized by a time  $\tau^{(\dot{\gamma})} = c_*/|\dot{\gamma}|$ , with a numerical constant  $c_*$  and the shear rate  $\dot{\gamma}$ . The constitutive equation is then given by

$$\sigma = \dot{\gamma} \left( \eta_\infty + \frac{G_\infty \tau}{1 + |\dot{\gamma}| \frac{\tau}{c_*}} \right),$$

where  $\eta_\infty$  denotes the viscosity in the limit of infinite shear rates. Thanks to its upper and lower bound the model is far more robust than the power-law model. Since it does not suffer from any divergences for extreme shear rates, the model is especially useful for studying arbitrary and time-dependent flows.

The Lattice Boltzmann Method (LBM) is a powerful tool for simulating liquid flows using a discrete space and velocities [3]. The algorithm uses two alternating steps; first a collision is done locally on each lattice node and then the velocity distributions are streamed to their corresponding neighbors. Due to its local character, the LBM works very well on parallel computers and complex geometries can be implemented easily. The lattice Boltzmann calculation [4] is done in the Bhatnagar-Gross-Krook approximation of the collision operator, using only a single relaxation time  $\tau_{lb}$ . The LBM can be generalized *ad hoc* to simulate non-Newtonian liquids in two different ways. Most commonly  $\tau_{lb}$  is adjusted locally to achieve the desired ratio of stress to strain rate [5]. Here no numerical differentiation is needed and the strain rate can be obtained by the velocity distribution function. The lattice kinetic scheme [6] follows an alternative approach by adding a shear rate dependent term to the equilibrium distribution function. The collision step is much simplified, but the dynamics becomes

non-local due to numerical differentiation.

To test these approaches we consider a Poiseuille flow of a non-linear Maxwell fluid through a 2D channel  $L_x \times L_y$  and a pressure gradient  $p/L_x$  is applied with the help of generalized periodic boundary conditions [7]. The steady state velocity profile of the problem can be solved analytically and we use a honey-like liquid ( $\eta_\infty = 2$  Pa.s,  $\rho = 1360$  kg/m<sup>3</sup>) for simulation. Fig. 1 shows the velocity  $v$  for different values of  $\tau$  in dimensionless units  $v \eta_0 / (L_x L_y p / L_x)$ , where  $\eta_0 = \eta_\infty + G_\infty \tau$  is the viscosity for a vanishing shear rate  $\dot{\gamma}$  and  $\tau$  is given in values of  $\eta_\infty / G_\infty$ . The LBM is able to capture the steady state extremely well and the numerical results are in very good agreement to the analytical solution. As the parameter  $\tau$  increases shear thinning effects become more dominant and we observe a plug flow profile.

Having established this method, we are able to simulate the time dependence of non-Newtonian fluid flows in arbitrary geometries.

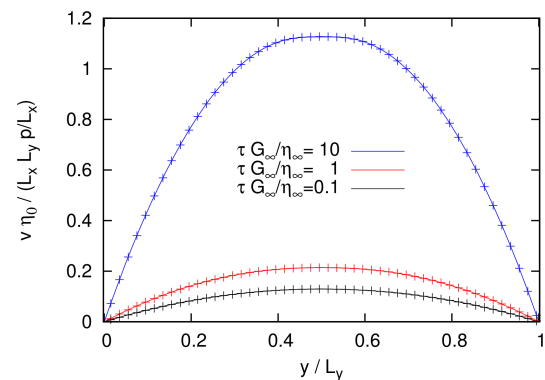


FIG. 1. Poiseuille flow of a non-linear Maxwell fluid.  $c_* = 0.1$  and  $G_\infty$  is set to 1 Pa. A pressure gradient  $\Delta p / L_x = -2$  Pa/cm with  $L_x = L_y = 1$  cm is applied.

This work was supported by the Zukunftskolleg der Universität Konstanz.

\* Corresponding author: simon.papenkort@uni-konstanz.de

- [1] R. Bird and R. Armstrong and O. Hassager, *Dynamics of Polymeric Liquids*, John Wiley & Sons (1987).
- [2] M. Fuchs and M. Cates, *Faraday Discuss.* **123**, 267 (2003).
- [3] S. Succi, *The Lattice Boltzmann Equation for Fluid Dynamics and Beyond*, Oxford University Press (2001).
- [4] <http://www.lbmmethod.org/palabos>
- [5] E. Aharonov and D. Rothman, *Geophys. Res. Lett.* **20**, 679 (1993).
- [6] T. Inamuro, *Phil. Trans. R. Soc. Lond. A* **360**, 477 (2002).
- [7] S. Kim and H. Pitsch, *Phys. Fluids* **19**, 108101 (2007).

## Transient fluidization processes leads to quantitative predictions for the Herschel–Bulkley model in Simple Yield Stress Fluids

Thibaut Divoux,<sup>1,\*</sup> Catherine Barentin,<sup>2</sup> and Sébastien Manneville<sup>1</sup>

<sup>1</sup>*Université de Lyon, Laboratoire de Physique,  
Ecole Normale Supérieure de Lyon, CNRS UMR 5672,  
46 Allée d'Italie, 69364 Lyon cedex 07, France.*

<sup>2</sup>*Laboratoire de Physique de la Matière Condensée et Nanostructures, Université de Lyon,  
CNRS UMR 5586, 43 Boulevard du 11 Novembre 1918, 69622 Villeurbanne cedex, France.*

Yield stress fluids (YSF) encompass a large amount of everyday-life and industrial complex fluids ranging from hair gels, cosmetic creams, or toothpastes to many food products or even concrete and drilling muds. They respond elastically below a certain stress threshold  $\sigma_c$ , known as the yield stress, whereas they flow as liquids if stressed above  $\sigma_c$ . The behavior of YSF still raises many fundamental and practical issues, in particular in the vicinity of this solid-to-fluid transition, often referred to as the unjamming transition [1]. Recently it was proposed to categorize YSF into two groups: (i) those with aging and memory effects that present *thixotropic* properties (clay suspensions, colloidal gels, adhesive emulsions) and (ii) those for which such effects can be neglected, which are called *simple* YSF (foams, carbopol “gels”, non-adhesive emulsions) [2].

In this work we revisit the case of a simple YSF, namely a carbopol “gel”. Indeed, in spite of a huge body of rheological work, no thorough temporally and spatially resolved study has been conducted on simple YSF. In particular, it is generally assumed that the flow remains homogeneous during its evolution towards steady state. Here we investigate the fluidization for both shear-rate and shear-stress controlled experiments using ultrasonic speckle velocimetry [3] simultaneously to standard rheological measurements.

On the one hand, shear-rate controlled experiments show that (i) the transient regime from solidlike to liquidlike behavior involves a shear-banded flow; (ii) the duration  $\tau_f$  of this transient regime decreases as a power law of the imposed shear rate:  $\tau_f = A/\dot{\gamma}^\alpha$ ; and (iii) the flow always turns out to be homogeneous after this transient shear banding. This fluidization scenario is very robust and the exponent  $\alpha$  does not depend on the gap width or on the boundary conditions. Our results not only confirm the idea that one cannot observe steady-state shear banding without thixotropy but also demonstrate that a simple YSF can present shear banding in a transient regime that can last surprisingly as long as  $10^5$  s [4].

On the other hand, shear-stress controlled experiments show that (i) the transient regime from solidlike to liquidlike behavior also involves a shear-banded flow; (ii) the duration  $\tau_f$  of this transient regime decreases as a power law of the reduced shear-stress:  $\tau_f = B/(\sigma - \sigma_c)^\beta$ , where  $\sigma_c$  stands for the yield stress of the fluid; and (iii) the flow always turns out to be homogeneous after this transient shear banding. This fluidization scenario is very robust and rules out any

analogy between the stress induced fluidization process of simple YSF and the rupture of elastic solids as recently suggested [5, 6]. Indeed, spatiotemporal diagrams of ultrasonic speckle signals show a fluidization involving the whole bulk of the gel without any fracture plane [7].

Finally, as both stress induced and shear induced fluidization processes correspond to the same scenario, namely a transient shear-banding before reaching a homogeneous steady state, one can equal the two fluidization times, which leads to:

$$\sigma = \sigma_c + (B/A)^{1/\beta} \dot{\gamma}^{\alpha/\beta} \quad (1)$$

Equation (1) is exactly the Herschel-Bulkley (HB) model that describes the rheology of carbopol very well [4, 8]. This scaling provides a quantitative prediction for the value of the exponent in the HB model as the ratio of the two fluidization exponents previously defined. For the first time, we evidence a clear link between the transient regime of the fluidization process and steady state rheology. We believe this result to be general for simple YSF, namely emulsions [9] and foams [10].

We thank the Anton Paar company for lending us a MCR301 rheometer, Y. Forterre for providing us with the carbopol, D. Tamarii for substantial help with the software and H. Feret for elegant technical solutions. We also thank L. Bocquet and S. Santucci for enlightening discussions.

\* Corresponding author: Thibaut.Divoux@ens-lyon.fr

- [1] E. Weeks, book chapter in *Statistical Physics of Complex Fluids*, eds. S Maruyama & M Tokuyama (Tokyo University Press, Sendai, Japan, 2007).
- [2] P.C.F. Møller *et al.*, *Phil. Trans. R. Soc. A* **367**, 5139 (2009).
- [3] S. Manneville, L. Bécu, and A. Colin, *Eur. Phys. J. AP* **28**, 361373 (2004).
- [4] T. Divoux *et al.*, *Phys. Rev. Lett.* **104**, 208301 (2010).
- [5] F. Caton and C. Baravian, *Rheol Acta* **47**, 601 (2008).
- [6] G. Benmoukkoef-Benbelkacem *et al.*, *Rheol Acta* **49**, 305 (2010).
- [7] T. Divoux, C. Barentin and S. Manneville, *in prep.* (nov. 2010).
- [8] J.M. Piau, *J. Non-Newtonian Fluid Mech.* **144**, 1 (2007).
- [9] L. Bécu *et al.*, *Colloids Surfaces A* **263**, 146-152 (2005); *Phys. Rev. Lett.* **96**, 138302 (2006).
- [10] G. Ovarlez, K. Krishan and S. Cohen-Addad **91**, 68005 (2010).

## Technique for Experimental Studying of Elongational Behavior of High Reactivity Viscoelastic Liquids: Application to Alkoxide-Based Sol-Gel Precursors.

Medhat Hussainov,\* Tanel Tätte, Glen Kelp, and Rait Rand

University of Tartu, Riia 142, 51014, Tartu, Estonia.

The fabrication of micro- and nanoscale metal oxide fibers has gained considerable interest because of their potential applications in nanoelectronics, nanosensors, low-loss optical wave guides, etc. For micro- and nanofibers preparation, the sol-gel method is used. The precursors are prepared from alkoxides of corresponding metals by aqueous (AQ) and non-aqueous (NAQ) (thermolysis) manner [1]. Zero shear viscosity of such precursors range between  $\sim 200$ – $2000$  Pa·s. Characteristic for the precursors of this type is that they are very highly reactive for humidity, solidifying immediately when exposed for air.

The process of fiber drawing requires detailed understanding of the key parameters of fiber fabrication at the sub-micron scale [2]. One of the most important rheological parameters of viscous-elastic liquids in the processes of fiber spinning is an apparent extensional viscosity and relaxation time. To obtain the values of these parameters, the special devices such as Capillary Breakup Extensional Rheometer (CaBER) [3–5], which is conceptually based on the designs of [6], are used.

The standard CaBER technique does not perfectly suit for studying highly reactive viscoelastic liquids due to test duration of dozens and more seconds when change in liquid properties is very probable. We propose a method for measurement the properties of such kind of liquids that are contained in a transparent reaction bulb, where a liquid under consideration has been prepared. In this case, the studied matter is in an equilibrium state with inherent vapor. For measurement, a rod of 3–5 mm in diameter was pulled down to contact with a liquid surface. When touched the surface, the rod was instantly raised up for a 10–15 mm distance which results in the formation of a liquid thread. The evolution of the thread diameter is registered by a high speed camera. From the fluid dynamics point of view, the main distinguish of the proposed method from the standard CaBER method is the presence of unlimited amount of a liquid under the rod because the rod diameter is much smaller than the diameter of the reaction bulb filled with a liquid. *In the present work, the presumable effect of this distinguish on the final test data is studied.* In the frame of this research the simulations of Newtonian and non-Newtonian fluids were conducted for the test equipments with newly elaborated and CaBER-like [3–5] configurations. The results of simulations are compared with the data obtained with the help of CaBER-like equipments as well as by the proposed method. The test data and the computational investigations show some difference in the results ob-

tained only at low values of Hencky Strain (or, in other words, at the initial period of the thread evolution) (Fig. 1). Increase in Hencky Strain leads to a good agreement between results obtained with help of CaBER-like devices and the proposed one.

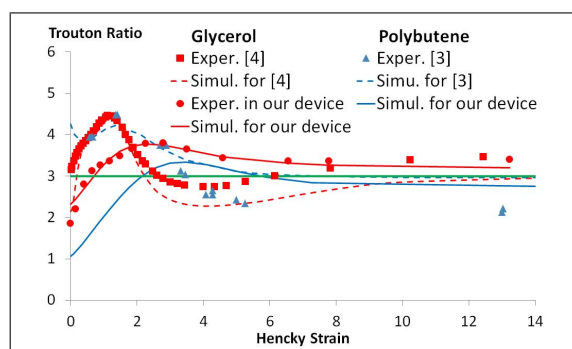


FIG. 1. Dependence of Trouton ratio on Hencky Strain for Newtonian liquids: squares - experimental data [4] for glycerol, triangles - experimental data [3] for polybutene. The dashed lines represent our simulations for corresponding liquids in CaBER-like devices [3, 4]. Circles - experimental data for glycerol in our device. The solid lines represent the simulations for our device.

Elongational behavior of precursors, obtained from alkoxides of Ti, Sn, Zr, was studied by the elaborated method. The comparative analysis of the rheological behavior of AQ and NAQ precursors, obtained from  $\text{Sn}(\text{OBU})_4$ , is also conducted. Rheological tests proved that metal alkoxide precursors are typical non-Newtonian fluids. NAQ precursor is revealing more elastic behavior as compared to AQ prepared.

The work was supported by the Estonian Science Foundation (grants No. 8377, 7612, JD120, SF0180073s07, SF0180058s07).

\* Corresponding author: medhat.hussainov@ut.ee

- [1] T. Tätte et al., Alkoxide-based precursors for direct drawing of metal oxide micro- and nanofibres, submitted to Science and Technology of Advanced Materials.
- [2] J. Crest, J. C. Nave, S. Pabba, R. W. Cohn, G. H. McKinley, submitted to J. of Non-Newtonian Fluid Dynamics.
- [3] M.I. Kolte, and P. Szabo, J. Rheology, **43** (3), pp. 609–626, (1999).
- [4] McKinley, G.H. and Tripathi, A., J. Rheol., **44** (3), pp. 653–671, (2000).
- [5] Tuladhar, T.R., Mackley, M.R., J. Non-Newtonian Fluid Mech. **148** pp. 97–108, (2008).
- [6] A.V. Bazilevsky, V.M. Entov, A.N. Rozkhov, in: *Third European Rheology Conference*, edited by D. R. Oliver, (Elsevier Applied Science, 1990), pp. 41–43.

## Avalanche size in sheared amorphous solids at low temperature

Joyjit Chattoraj,<sup>1,\*</sup> Christiane Caroli,<sup>2</sup> and Anaël Lemaître<sup>1</sup>

<sup>1</sup>Université Paris Est – Laboratoire Navier, ENPC-Paris, LCPC, CNRS UMR 8205 2 allée Kepler, 77420 Champs-sur-Marne, France

<sup>2</sup>INSP, Université Pierre et Marie Curie-Paris 6, CNRS, UMR 7588, 140 rue de Lourmel, 75015 Paris, France

After decades of research, the identification of a constitutive theory of plasticity in glassy systems is still an open question. One consensus on plasticity is that it originates from irreversible local rearrangements (or “flips”) of soft zones. Each flip emits an elastic signal which carries directional information and modifies the stress level of surroundings. This facilitates the occurrence of secondary flips and the emergence of avalanche behavior. In the article [1], Lemaître and Caroli argued that, in athermal ( $T = 0$ ) conditions the plastic deformation of amorphous solids is accompanied with avalanche dynamics for experimentally attainable strain rates. But at  $T \neq 0$  the existence of avalanches and their contribution to plasticity are yet uncertain. We thus here study avalanche behavior of a sheared amorphous solid at finite temperatures using numerical simulation.

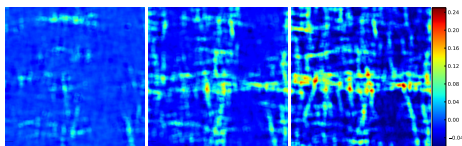


FIG. 1. The accumulated strain field with increasing macroscopic strain intervals  $\Delta\gamma = 1\%, 5\%, 10\%$  respectively at  $\dot{\gamma} = 1e-04$  and  $T = 0.025$  for  $L \times L = 160 \times 160$ .

We perform MD simulation of a 2D binary mixture which is sheared at constant strain rates ( $1e-05$  to  $1e-02$ ) and constant temperatures ( $0.025$  to  $0.3$ ): these ranging from very low to near the vicinity of the glass transition,  $T_g \approx 0.27$ . All numerical details are given in [2].

To characterize avalanche behavior we focus on the coarse-grained shear strain  $\epsilon_{xy}(\vec{r})$ , which is computed using [3]. In Fig 1, we show  $\epsilon_{xy}(\vec{r})$  with increasing macroscopic strain intervals  $\Delta\gamma = 1\%, 5\%, 10\%$  for  $\dot{\gamma} = 1e-04$  and  $T = 0.025$ . In analogy with [1], the accumulated strain field presents directional heteroge-

neous structures.

To quantify the avalanche size we next study the spatial auto-correlation of  $\epsilon_{xy}(\vec{r})$ ;  $C(\vec{r}) = \langle \epsilon_{xy}(\vec{r} + \vec{r}') \epsilon_{xy}(\vec{r}') \rangle$ . As shown in Fig 2, the strain correlation field has a quadrupolar symmetry with respect to the axes of the system. A cut of  $C(\vec{r})$  along the perpendicular direction  $y$  is shown in Fig 2 for  $T = 0.025$  and for several strain rates. We attempt to extract a correlation length  $\xi$  from the tail of  $C(y)$ . In agreement with [1], we find a critical strain rate,  $\dot{\gamma}_c$  s.t. 1) for  $\dot{\gamma} < \dot{\gamma}_c$ ,  $\xi$  has a plateau value  $\propto L$  whereas, 2) for  $\dot{\gamma} > \dot{\gamma}_c$ ,  $\xi$  decreases strongly with  $\dot{\gamma}$ . We conclude that avalanches do exist at low but finite  $T$  and have a similar behavior as found in athermal dynamics.

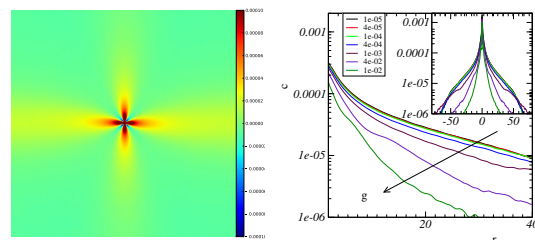


FIG. 2. Left:  $C(\vec{r})$  over  $\Delta\gamma = 1\%$  at  $\dot{\gamma} = 1e-05$ ,  $T = 0.025$  and  $L \times L = 160 \times 160$ . Right:  $C(\vec{r})$  along the perpendicular direction of applied shear, for all strain rates. We zoom in the tail of  $C(\vec{r})$ . Arrow indicates increasing of  $\dot{\gamma}$ .

\* Corresponding author: joyjitchattoraj@gmail.com

- [1] A. Lemaître and C. Caroli, *Rate-dependent avalanche size in athermally sheared amorphous solids*, Phys. Rev. Letters, 103:065501, 2009
- [2] J. Chattoraj, C. Caroli and A. Lemaître, *Universal, additive effect of temperature on the rheology of amorphous solids*, arXiv:1005.1179, 2010
- [3] I. Goldhirsch and C. Goldenberg, *On the microscopic foundations of elasticity*, Eur. Phys. J. E 9, 245–251, 2002

## Confined diffusion of probes in a colloidal suspension

Catherine Barentin,\* Laure Petit, Jean Colombani, Christophe Ybert, and Lydéric Bocquet

*Laboratoire de Physique de la Matière Condensée et Nanostructures, Université de Lyon,  
CNRS UMR 5586, 43 Boulevard du 11 Novembre 1918, 69622 Villeurbanne cedex, France.*

Soft glassy materials are complex and disordered materials. Their description is fundamentally challenging due to their intrinsic out-of-equilibrium nature, associated with the dynamical arrest in disordered state occurring at the jamming transition [1]. Among the various systems studied so far, suspension of Laponite have been used extensively due to its industrial interest, together with practical advantages associated with its transparency and the fact that it exhibits a complete phenomenological picture, from aging to shear-thinning, thixotropy and shear-banding. Laponite suspensions in their glassy state were used to study aging dynamics associated with slow structural relaxation [2] and were used also to investigate the theoretical proposal of extending the fluctuation-dissipation theorem to describe out-of-equilibrium systems, through the incorporation of an effective temperature  $T_{\text{eff}}$ . [3].

Although theoretical works suggest that the tracer characteristics dictate the way it couples to the soft glass and affect for instance the effective temperature it probes [4], it appears that very little is known on the experimental side about how changing the tracer size modifies its diffusive motion in such system. In this study, we use a Fluorescence Recovery After Photobleaching technique to investigate the diffusive motion of tracers in the Laponite suspension as a function of their size, ranging from molecular (1 nm) up to 100 nm. By varying the probe size, as well as the concentration of the colloidal glass, we evidence and quantify the deviations of the probe diffusivity from the bulk Stokes–Einstein expectations as shown on the Fig. 1. A change of diffusive behavior is indeed evidenced for probe sizes around a few tens of nanometers, which corresponds to the typical distance between the disk of clay. Far below this value, the nanospheres migrate in the solvent showing little interaction with the Laponite, and their diffusion coefficient is the same as in pure solvent. Far above this value, the motion of the nanospheres is strongly hindered by the network of Laponite platelets and their diffusion coefficient is seen to vanish. These results suggest that the probe diffusion in the dynamically arrested Laponite structure is mainly controlled by the ratio between the probe size and the typical clay platelets inter-distance. This also implies that the reduction of tracer diffusion originates mainly in the hydrodynamic interaction of the probe with the Laponite structure. We managed

to describe quantitatively the measured diffusion by a simple hindered diffusion models originating from Faxen models[5, 6].

Finally, using the FRAP technique and dense fluorescent probes, we were able to measure simultaneously

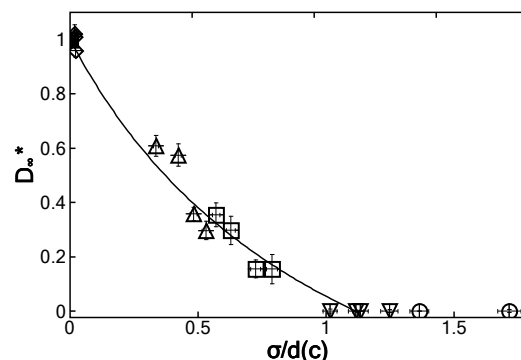


FIG. 1. Evolution of diffusion coefficient of colloidal tracers in Laponite normalized by the value measured in pure water,  $D^* = D_{\infty}(c)/D_0$ , as a function of the concentration of laponite for various tracer sizes: ( $\diamond$ ) 1 nm fluorescein molecules; ( $\triangle$ ) 25 nm diameter colloids; ( $\square$ ) 37 nm diameter colloids; ( $\circ$ ) 100 nm diameter colloids.

the sedimentation velocity and the diffusivity of the probes, allowing us to obtain the effective temperature of the laponite suspensions at various ages and concentrations. As predicted by recent theoretical works[7], it never departs from the bath temperature.

We thank Jean-Louis Barrat for many interesting discussions and suggestions. We acknowledge support from the ANR, through the program 'ANR Blanche' (Sllocdyn).

\* Corresponding author: Catherine.Barentin@univ-lyon1.fr

- [1] G. Biroli, Nature Physics **3**, 222 (2007).
- [2] B. Ruzicka, L. Zulian, and G. Ruocco, Phys. Rev. Lett. **93**, 258301, (2004).
- [3] P. Jop, J. Ruben Gomez-Solano, A. Petrosyan and S. Ciliberto, submitted to J. Stat. Mech., ArXiv:0812.1391, (2009).
- [4] L. Berthier and J.-L. Barrat, J. Chem. Phys. **116**, 6228 (2002).
- [5] A. Saugey, L. Joly, C. Ybert, J.-L. Barrat, and L. Bocquet, J. Phys. : Cond. Matt. **17**, S4075 (2005).
- [6] L. Petit *et al.*, Langmuir **25**, 12048 (2009).
- [7] J. Russo and F. Sciortino, Phys. Rev. Lett. **104**, 195701 (2010).

## Elastic Properties of Glasses

Christian L. Klix,\* Florian Ebert, Georg Maret, and Peter Keim

*Department of Physics, Universitätsstraße 10, University of Konstanz, 78457 Konstanz*

Usually, a disordered system is called a glass if its viscosity exceeds  $10^{-13}$  poise upon crossing the freezing (vitrification) temperature  $T_g$ . However, this definition is difficult to apply to soft matter systems since a measurement of the viscosity is often impracticable. Thus, other ways have been thought of to pin down  $T_g$ . Since glasses, as crystals, are categorized as solids, their mechanical behavior is similar. In particular, they exhibit a finite shear modulus  $\mu$ . A fluid, however, lacks such, at least for low frequencies. Therefore, we expect to see an abrupt change in  $\mu$  at the onset of vitrification. This should define  $T_g$  much more exactly than the rather arbitrary definition of the systems viscosity.

In this contribution, we present results on the elastic properties of a two dimensional colloidal glass former. The moduli are derived from modes in the long wavelength limit which are thermally excited. We use video microscopy on a binary system of superparamagnetic polystyrene spheres confined at a flat water-air interface. An external magnetic field lets us control the particle interactions *in situ*. This is expressed by the dimensionless system parameter  $\Gamma = E_{mag}/k_B T \propto \chi H^2/(n^{3/2}k_B T)$ , which acts as an inverse temperature. Details of the setup are described elsewhere [1].

Our approach is identical to that in [2]. Via the equipartition theorem, we connect the fourier transformed dynamical matrix  $D_{\mu\nu}(\vec{q})$  to the averaged correlation of displacements  $\langle u_\mu^*(\vec{q})u_\nu(\vec{q}) \rangle$ , where  $\mu, \nu \in x, y$ . The Eigenvalues  $\lambda_s$  of this matrix ( $s$  denotes polarization) are the spring constants of our system:  $\omega_s(\vec{q}) = \sqrt{\lambda_s(\vec{q})/m}$ . By computing

$$\frac{1}{\langle |u_s(\vec{q})|^2 \rangle} = \frac{\lambda_s}{k_B T}, \quad (1)$$

we extract the 'dispersion relation'. In doing so, we implicitly assume all modes to be plane waves. This is correct in the long wavelength limit corresponding to elastic continuum theory. There, the 2d system is considered to be a homogeneous structureless solid. For short wavelength, in contrary, the local structure matters and polarization of the waves will no longer be well defined. This results in swirling motions as described by [4, 5], where the density of states is analyzed. Interestingly, we do not find any scaling of the 'dispersion relations' with  $\Gamma$  as it is found for a crystal [2]. This hints towards a change in structure with decreasing temperature in the glassy state below  $T_g$ .

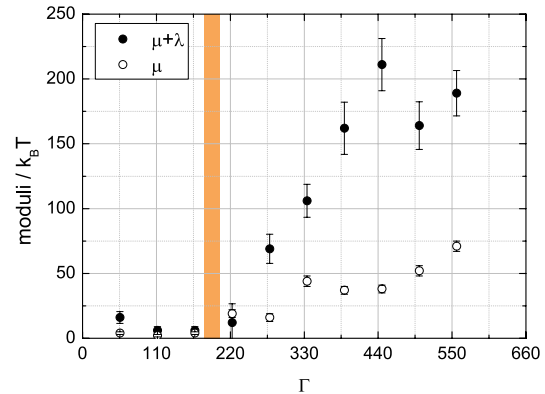


FIG. 1. Elastic moduli, extrapolated from the 'dispersion relation' for the long wavelength limit. Note the onset of a shear modulus  $\mu$  at  $\Gamma \approx 200$  (shaded region).

From the 'dispersion relation' we now extract the Lamé coefficients  $\mu$  and  $\lambda$  of continuum elasticity theory [3]. They are given by

$$\frac{2\mu + \lambda}{k_B T} = \lim_{\vec{q} \rightarrow 0} [q^2 \langle |u_{\parallel}(\vec{q})|^2 \rangle]^{-1}, \quad (2)$$

$$\frac{\mu}{k_B T} = \lim_{\vec{q} \rightarrow 0} [q^2 \langle |u_{\perp}(\vec{q})|^2 \rangle]^{-1}. \quad (3)$$

As we extrapolate  $q$  to zero, only data from the long wavelength regime is taken into account. The resulting moduli, computed from the Lamé coefficients, are shown in Fig. 1. The results are consistent with results acquired by MD simulation for an amorphous binary alloy [6]. As expected, we find an onset of a shear modulus  $\mu$  as we cool down our system. Thus, we define  $\Gamma \approx 200$  as the glass transition temperature.

Financial support of the Young Scholar Fund, University of Konstanz is gratefully acknowledged.

\* Corresponding author: Christian.Klix@uni-konstanz.de

- [1] F. Ebert, P. Dillmann, G. Maret, and P. Keim, Rev. Sci. Instr. **80**, 083902 (2009).
- [2] P. Keim, G. Maret, U. Herz, and H. H. von Grünberg, Phys. Rev. Lett. **92**, 215504 (2004).
- [3] H. H. von Grünberg, P. Keim, K. Zahn, and G. Maret, Phys. Rev. Lett. **93**, 255703 (2004).
- [4] A. Gosh, V. K. Chikkadi, P. Schall, J. Kurchan, and D. Bonn, Phys. Rev. Lett. **104**, 248305 (2010).
- [5] D. Kaya, N. L. Green, C. E. Maloney, and M. F. Islam, Science **329**, 329 (2010).
- [6] J.-L. Barrat, J.-N. Roux, J.-P. Hansen, and M. L. Klein, Europhys. Lett. **7**, 707 (1988).

## Suppression of multiple scattering effects in colloidal model systems

Achim Lederer\* and Hans Joachim Schöpe

*Institut für Physik, Johannes Gutenberg-Universität Mainz, Staudingerweg 7, 55128 Mainz*

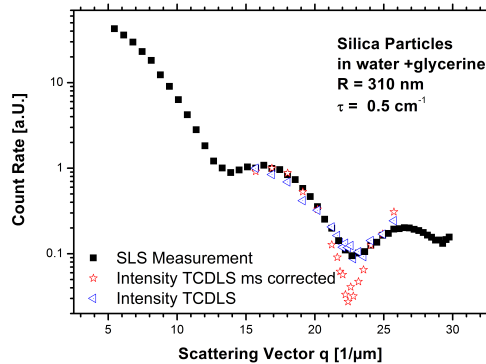


FIG. 1. Comparison of multiple scattering corrected data obtained by the new TCDLS setup with a conventional light scattering setup.

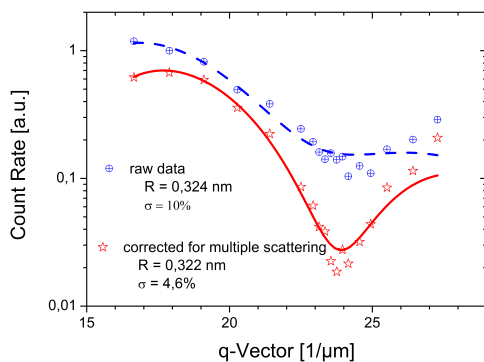


FIG. 2. Polydisperse RDG-Fit to conventional and by TCDLS corrected data. The fit is only in good agreement with the MS-free data. While both fits determine the particle size correctly, the SLS data leads to unreasonable high polydispersities.

Light scattering is one of the most powerful tools in soft matter physics to study the structure, kinetics and dynamics of the system of interest. Unfortunately effects due to multiple scattering complicate the evaluation in colloidal systems. Particularly measurements of structure factors as well as form factors (polydispersity) are affected strongly by multiple scattering. There are several techniques to suppress multiple scattering, like theoretical corrections, index matching or cross correlation techniques. In the latter, two identical but distinguishable dynamic light scattering experiments are performed simultaneously. Scattered photons are correlated and hence detected in the normalized cross correlation function, as long as their scattering vectors and their origins are identical. Multiple scattered light has different  $q$ -vectors and origins and hence does not contribute [1, 2].

In Mainz we recently developed a new TCDLS Setup. Unlike previous TCDLS experiments we realized a small and compact setup with fibre optical illumination and detection. This ensures an easy and long time stable alignment. The machine is in the test stage. Measurements by the new designed TCDLS setup are compared with conventional SLS data. The performance of the TCDLS will be discussed.

We thank Bill van Meegen and Gary Bryant for fruitful discussions. We gratefully acknowledge the financial support of the DFG (SCHO1054/3-2).

\* Corresponding author: lederer@uni-mainz.de

[1] K. Schätzel, *J. Modern Opt.* **38**, 1849 (1991).

[2] P. N. Pusey, *Current Opinion in Colloid Interface Science* **4**, 177 (1999).

## Shear Melting and Shear Flows in a 2D Complex (Dusty) Plasma

Vladimir Nosenko,\* Alexei Ivlev, and Gregor E. Morfill

*Max-Planck-Institut für extraterrestrische Physik, D-85741 Garching, Germany*

A complex plasma is an ionized gas that has small particles of solid matter in it [1]. Micron-size particles carry large negative charges. Due to their mutual interaction and external confinement, the particles can self-organize in structures that can have a crystalline or liquid order. Such ordered structures are vastly softer than molecular materials and even colloidal crystals, so that they can be easily manipulated, e.g., by applying laser beams [2]. In plasma crystals, the interparticle distance is of the order of 0.1 – 1 mm and characteristic dynamic frequencies  $\omega_d$  are of the order of 1 – 100 Hz, which makes it possible to observe the motion of individual particles – proxy “atoms” – in real time. In contrast to colloidal dispersions, the particle dynamics in plasma crystals is virtually undamped – the damping rate  $\nu$  for individual particles (caused by the friction on rarefied neutral gas) is weak,  $\nu \ll \omega_d$ .

Two-dimensional (2D) complex plasmas that can form in the presence of gravity are an especially attractive model system to study various phenomena at an atomistic level. In a 2D complex plasma, a fully resolved dynamics of particles can be observed, providing a complete kinetic description of experimental system.

In this work, we studied the response of a 2D complex plasma to a suddenly applied shear stress.

Our experimental setup was a modified GEC (Gaseous Electronics Conference) rf reference cell. Argon plasma was produced using a capacitively-coupled rf discharge.

A single layer of dust particles was suspended in the plasma sheath of the lower rf electrode. The microspheres were made of Melamine Formaldehyde, had a diameter of  $9.19 \pm 0.09 \mu\text{m}$ , and acquired an electric charge of  $Q = -17\,000 \pm 1500e$ . The suspension included  $\approx 6000$  particles and had a diameter of  $\approx 60$  mm. The gas damping rate was  $\nu = 0.77 \text{ s}^{-1}$ .

At our experimental conditions, the particle suspension self-organized in a highly ordered triangular lattice. To apply a shear stress to the particle suspension, we used a laser manipulation scheme. A powerful laser beam was focused down to a fraction of the interparticle spacing and it was rapidly ( $\approx 300$  Hz) scanned to draw a rectangular stripe on the suspension. The particles reacted to the averaged radiation pressure. The shear stress was controlled by varying the output laser power  $P_{\text{laser}}$ .

Beginning with an undisturbed lattice, we applied increasing levels of shear stress, and we observed that the particle suspension passes through four stages: elastic deformation, defect generation while in a solid state, onset of plastic flow, and fully developed shear

flow. Particles were confined so that after flowing out of the field of view they circulated around the suspension’s perimeter and re-entered the field of view, and the suspension did not buckle in the vertical direction.

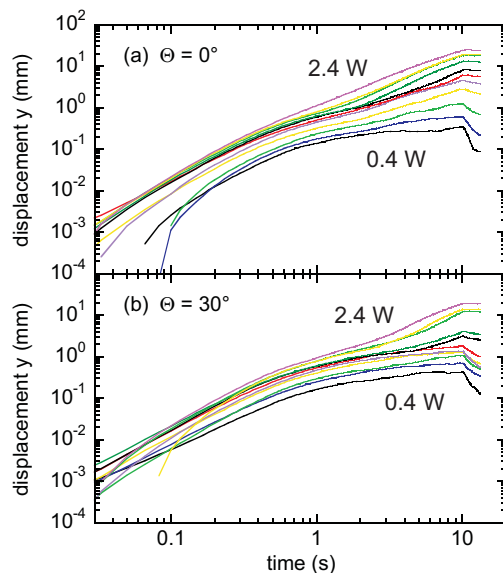


FIG. 1. Displacement of the laser-irradiated particle stripe as a function of time, for two principal orientations of the triangular lattice. Different curves are for the manipulation laser power  $P_{\text{laser}}$  ranging from 0.4 W to 2.2 W, in increments of 0.2 W. The laser is switched off at  $t = 10$  s.

We measured the displacement of the laser-irradiated particle stripe by integrating the average particle velocity in the stripe, see Fig. 1. After the laser is switched on at  $t = 0$  the displacement scales as  $\propto t^2$ , which is indicative of the ballistic motion. After  $t_0 \approx 0.4$  s, the particle motion slows down. As long as  $P_{\text{laser}}$  is below a threshold the curves tend to saturate, whereas above the threshold the lattice shear-melts. The melting occurs more easily for  $\Theta = 0^\circ$ , when nucleating dislocations glide in the direction of the laser beam. For  $\Theta = 30^\circ$ , the lattice deformation occurs via dislocations gliding at that angle with respect to the laser beam. Therefore the melting happens at higher  $P_{\text{laser}}$  and has a more pronounced threshold character, with the displacement  $\propto t^\alpha$ , where  $\alpha = 0.9 - 1.7$ . We note a final push-back, even of melted lattice after the laser was switched off at  $t = 10$  s.

We thank Jürgen Horbach for valuable discussions.

\* Corresponding author: nosenko@mpe.mpg.de

- [1] G. E. Morfill and A. V. Ivlev, *Rev. Mod. Phys.* **81**, 1353 (2009).
- [2] V. Nosenko, S. K. Zhdanov, A. V. Ivlev, C. A. Knapek, and G. E. Morfill, *Phys. Rev. Lett.* **103**, 015001 (2009).

## Particle influence on the viscosity measurements of molten slags

Arne Bronsch\* and Patrick J. Masset

Centre for Innovation Competence Virtuhcon, Freiberg University of  
Mining and Technology, Fuchsmühlenweg 9, 09596 Freiberg, Germany

Coal still remains an important source for power generation and also an important feedstock for chemical products. One way to use coal as a raw material are coal gasification techniques to generate the required amounts of syngas for further production steps, e.g. fuel production. There are several coal gasification techniques in development, like the entrained coal gasifier. One of the most important features of this process is the formation of a solid slag layer onto the water cooled inner walls of the gasifier. Due to the high temperature in the reactor the liquid slag is flowing on the top of the solid layer. The flowing conditions depend on the temperature, the environment and the slag composition [1].

The knowledge of the viscosity of molten slags is actively researched since a few decades. Several investigations were done and models for calculating the slag viscosity were developed. A weak point of the former investigations is the range of viscosity measurement. The empirical described models were developed for temperature ranges with completely molten phases [2, 3] or for supercooled silicate melts [4]. The influence of particles in a solid-liquid mixture on the viscosity of slags was investigated by few authors [5, 6]. Results were linked to the Einstein-Roscoe-Model [7].

This work deals with the introduction of the particle influence on the viscosity of molten slags and silicate liquids. Up to 13 viscosity models were modified using the Einstein-Roscoe-Model, see Eq. (1)

$$\eta = \eta_0(1 - af)^{-n} \quad (1)$$

where  $\eta$  and  $\eta_0$  are the viscosities of particle-containing and particle-free slags, respectively. Factor  $f$  is the volume fraction of solid particles,  $a$  and  $n$  are constants which are set to 1.35 and 2.5, respectively. The solid fraction for each sample was determined by calculating complex equilibria using the software FactSage<sup>TM</sup>.

For example a silica-free slag was experimentally investigated and measurements were compared to computed viscosities. Each model underestimate the measured viscosity by two orders of magnitudes and even more, but with improvements by Einstein-Roscoe-Model better results were recognized, see Fig. 1.

Results obtained with a silica-free and a silica-rich real slag from German lignites will be presented, discussed and compared with a synthetic mixture of SiO<sub>2</sub>-CaO exhibiting a melting point close to 1600 °C.

\* Corresponding author: arne.bronsch@vtc.tu-freiberg.de

- [1] C. Higman and M. van der Burgt, *Gasification Processes*, in: *Gasification* (Gulf Professional Publishing, Burlington, 2nd edition, 2008), pp. 91–191.
- [2] J. O. M. Bockris and D. C. Lowe, *Proceedings of the Royal Society of London A* **226**, 423 (1954).
- [3] G. Urbain *et al.*, *Transactions & Journal of the British Ceramic Society* **80**, 139 (1981).
- [4] D. R. Neuville and P. Richet, *Geochimica et Cosmochimica Acta* **55**, 1011 (1991).
- [5] S. Wright *et al.*, *Metallurgical and Materials Transactions B* **31**, 97 (2000).
- [6] W. Song *et al.*, *AIChE Journal*, DOI:10.1002/aic.12293
- [7] R. Roscoe, *British Journal of Applied Physics* **3**, 267 (1952).

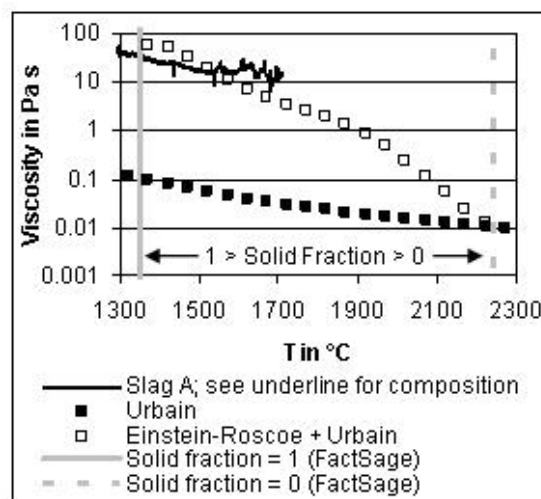


FIG. 1. Comparison of measured, normal calculated and solid-liquid calculated viscosities. Slag composition is Al<sub>2</sub>O<sub>3</sub> = 1.0; CaO = 39.2; Fe<sub>2</sub>O<sub>3</sub> = 11.8; K<sub>2</sub>O = 1.6; MgO = 23.1; Na<sub>2</sub>O = 5.0; SO<sub>3</sub> = 16.8 (values in mass-%, trace amounts were neglected).

# Determination of physical chemical properties of molten slags using molecular dynamics simulation

Aurélie Jacob,<sup>1,\*</sup> Patrick J. Masset,<sup>1</sup> and Angus Gray-Weale<sup>2</sup>

<sup>1</sup>TU Bergakademie Freiberg, Centre for Innovation Competence Virtuhcon, Group "Multiphase Systems", Fuchsmühlenweg 9, Reiche Zeche, D-09596 Freiberg, Germany

<sup>2</sup>School of Chemistry, Monash University, Melbourne, Victoria 3800, Australia

The chemistry of molten slags represents an important feature of high temperature processes (metallurgy, gasification, glass industry...). Molecular dynamics (MD) simulation was used to study molten slags by employing simple model called rigid ion model. This model was used to study binary systems such as silica-calcia (CS) and calcia-alumina (C3A) taking the potential models from Seo et al.[1] and Thomas et al. model [2] respectively. Before calculating the materials properties, the accuracy of the model was checked by calculating the radial distribution function (RDF) (see Fig. 1) that was compared with experimental data (Table 1).

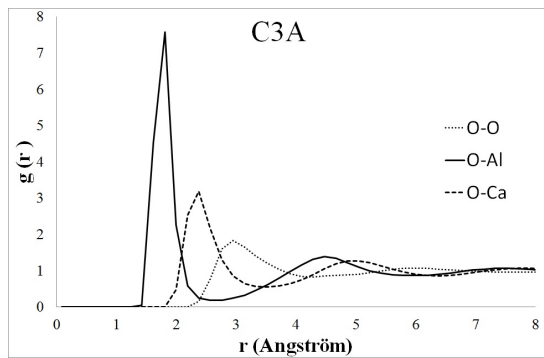


FIG. 1. RDF for cation-anion and anion-anion for binary system calcia-alumina (C3A).

C3A					
Present Work			Experimental Data [3]		
$r_{Al-O}$ (Å)	$r_{Ca-O}$ (Å)	$r_{O-O}$ (Å)	$r_{Al-O}$ (Å)	$r_{Ca-O}$ (Å)	$r_{O-O}$ (Å)
1.81	2.38	2.95	1.82	2.30	2.90

CS					
Present Work			Experimental Data [4]		
$r_{Si-O}$ (Å)	$r_{Ca-O}$ (Å)	$r_{O-O}$ (Å)	$r_{Si-O}$ (Å)	$r_{Ca-O}$ (Å)	$r_{O-O}$ (Å)
1.64	2.36	2.64	1.64	2.40	2.66

Table 1 - Comparison of the calculated and experimental interatomic distances for ion pairs in C3A and CS systems.

Using the rigid ion model it allows to calculate the radial distribution function of binary mixtures CS and C3A and a rather good agreement was obtained with experimental data from diffraction measurements using levitation method [3] (see Table 1). From these calculations, materials properties such as density and viscosity were calculated. In Fig. 2, densities as a function of the composition from MD simulation are compared with experimental data taken from [5].

The diffusion coefficients of the species were calculated for different compositions and as a function of

the temperature. The diffusion coefficient of species  $i$  is given by Eq. 1. To calculate the transport properties the velocity autocorrelation function was used.

$$D_i = \frac{1}{3} \int_0^\infty \langle v_i(t) \cdot v_i(0) \rangle dt \quad (1)$$

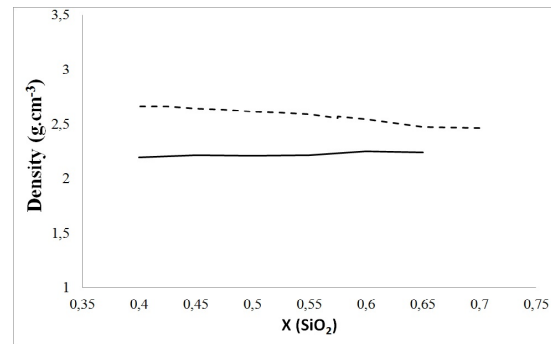


FIG. 2. Comparison of calculated (full line) and experimental (dash line) density of  $(CaO)_{1-x}-(SiO_2)_x$  mixtures at 2000 K.

Once the diffusion coefficient has been calculated, the viscosity can be calculated introducing the stress tensor  $P_{\alpha\beta}$  (Eq. 2) :

$$\eta = \frac{V}{k_B T} \int_0^\infty \langle P_{\alpha\beta}(t) \cdot P_{\alpha\beta}(0) \rangle dt \quad (2)$$

Viscosity values are more subject to statistical error compared to diffusion coefficient since the stress tensor is not a function of the number of ions used for MD simulation but a function of the total size of the simulation box. To reduce the statistical error in viscosity determinations, average component of the stress tensor has been used ( $\alpha\beta = xy, yz, zx$ )

These different calculations are compared with experimental data for some simple systems (CS or C3A). Once this approach is validated with binary systems, it would be applied to more complex mixtures to investigate multicomponent systems.

\* Corresponding author:  
Aurelie.Jacob@vtc.tu-freiberg.de

- [1] W. Seo et al., ISIJ International **11**, 1817-1825 (2004).
- [2] B. Thomas et al., J. of Phys. Condens. Matter. **18**, 4697-4708 (2006).
- [3] V. Cristiglio et al., J. of Non-Crystalline Solids **356**, 2492-2496 (2010).
- [4] X. Kuandy et al., Science in China **42**, 77-82 (1999).
- [5] Slag Atlas, 2<sup>nd</sup> Edition, p. 322 (2008).

## Star-linear polymer mixtures: a subtle balance between depletion and osmotic shrinkage

Domenico Truzzolillo,<sup>1,\*</sup> Dimitris Vlassopoulos,<sup>1,2</sup> and Mario Gauthier<sup>3</sup>

<sup>1</sup>*F.O.R.T.H, Institute of Electronic Structure and Laser, GR-71110 Heraklion, Crete, Greece*

<sup>2</sup>*University of Crete, Department of Materials Science and Technology, GR-71110 Heraklion, Crete, Greece*

<sup>3</sup>*Univ. Waterloo, Dept. Chem., Polymer Res. Inst., Waterloo, ON N2L 3G1, Canada*

Star polymers with high functionality have emerged as a new class of ultrasoft colloidal particles, characterized by soft repulsive wide ranging interactions [1]. The dynamic arrest described as glasslike gelation occurring in concentrated star polymer solutions, bears many similarities with both colloidal glass formation (crowding of single particles) and colloidal gelation (formation of clusters). A challenge with the liquid-solid transitions is how to achieve their molecular control that would have a significant scientific and technological impact paving the way for the design of soft materials with desired properties. Mixtures of star polymers with linear polymers are an obvious choice (as many soft matter systems occur as mixtures), which however have not been widely investigated.

The polymer-induced reduction of the star-star repulsions, the melting of the ultrasoft colloidal gel mediated by the presence of linear chains, and the subsequent reentrant gelation were previously studied [2] in the low linear polymer's concentration region of the phase diagram [see fig.1]. Via linear and non-linear rheological measurements we are investigating the high concentration linear chains' region of the phase diagram in order to shed light on the possible presence of reentrances (liquid-to-solid) or solid-to-solid transition for high molecular weights of chains. As a first result we found the lack of the attractive glassy phase for high concentration of chains (depletants) (size ratio  $q = 0.17$ ), whose addition in the concentrated star polymer solution produces the melting of the glass, establishing that the liquid phase extends up to the "nanocomposite-limit" where the star and linear polymer melts are merged. The effect of the isotropic osmotic pressure exerted by the chains on the star polymers that has been neglected at low volume fraction of chains, turns up as a good candidate to be the dominant effect that could even prevent the reentrance of the "liquid lake" in the case of low mobility of linear chains as well [4]. In order to gain some knowledge on the transition between a star polymer glass and a linear polymer melt, we also performed rheological measurements on star/linear polymer mixtures diluting the glassy phase of star polymers using different polymer melts. Both the linear (frequency depen-

dence of the complex modulus  $G^*(\omega)$ ) and non linear rheological properties of the mixtures (post yielding power law behaviour of  $G'(\gamma)$  and  $G''(\gamma)$ , extension of the linear regime and Fourier spectrum of stress waveforms at high strain amplitude) clearly show the existence of a critical concentration of chains above which

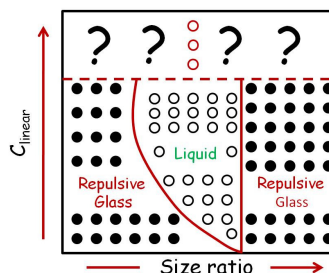


FIG. 1. A sketch of the current star/linear polymer phase diagram

they start to strongly dominate the fastest modes of the material. This concentration well fit with the "effective overlap concentration" of the star polymers being well reproduced by numerical calculations based on the 3D-osmotic theory [3]. We show how above this concentration in the case of high molecular weight of chains the complex modulus of the mixtures for high frequencies is well reproduced by simple concentrated polymer solutions having the same free volume as the mixtures.

Financial support of Marie Curie-Initial Training Network (ITN-COMPLOIDS) is gratefully acknowledged.

\* Corresponding author: truzzoli@iesl.forth.gr

- [1] C. N. Likos, H. Löwen, M. Watzlawek, B. Abbas, O. Jucknischke, J. Allgaier, and D. Richter, *Phys. Rev. Lett.* **80**, 4450–4453 (1998).
- [2] E. Stiakakis, D. Vlassopoulos, C. N. Likos, J. Roovers, and G. Meier, *Phys. Rev. Lett.*, **89** 20, 208302, (2002).
- [3] A. Wilk, S. Huißmann, E. Stiakakis, J. Kohlbrecher, D. Vlassopoulos, C.N. Likos, G. Meier, J.K.G. Dhont, G. Petekidis, R. Vavrin, *Eur. Phys. J. E* **32** 2, 127-134, (2010).
- [4] E. Zaccarelli, H. Löwen, P. P. F. Wessels, F. Sciortino, P. Tartaglia, and C. N. Likos, *Phys. Rev. Lett.*, **92** 22, 225703, (2004).

## Dynamics and elasticity of highly compressed microgel phases

Frank Scheffold,<sup>1,\*</sup> Pedro Díaz-Leyva,<sup>1</sup> Frederic Cardinaux,<sup>1</sup> Mathias Reufer,<sup>1</sup> Nasser Ben Braham,<sup>1</sup> Iseult Lynch,<sup>2</sup> and James L. Harden<sup>3</sup>

<sup>1</sup>Dep. of Physics and Fribourg Center for Nanomaterials,  
University of Fribourg, 1700 Fribourg, Switzerland

<sup>2</sup>School of Chemistry and Chemical Biology, University College Dublin, Belfield, Dublin 4, Ireland

<sup>3</sup>Department of Physics, University of Ottawa, Ottawa, Ontario K1N 6N5, Canada

Thermoresponsive microgel particles are a hybrid between a colloidal and a polymeric system with properties that can be tuned externally [1, 2]. Most of the previously studied stimuli responsive microgel systems are based on *poly(N-isopropyl-acrylamide)* (PNIPAM), a polymer which has a lower critical solution temperature (LCST) of approximately 33°C [1]. Above the LCST, the microgel particles expel water and are collapsed. The typical size of a collapsed microgel particle is in the range of 0.2-1 μm. Upon lowering the temperature the particles swell to about twice their original size. Responsive microgels thus provide the possibility to fabricate *smart* colloidal materials for applications as viscosity modifiers, carrier systems, bio-separators, optical switches or sensors. Due to their tuneability they are ideal model systems to study the phase behavior, glass transition and jamming in dense colloidal dispersions [3, 4].

Particles come into contact and form a viscoelastic paste below the LCST if the polymer density inside the swollen particles approaches the total polymer density. Since the particles consist of polymers and solvent in equilibrium they are elastically compliant, and thus elastic moduli do not diverge at the jamming transition, unlike the behavior of rigid colloidal particles. Several experimental studies show that in this regime the bulk modulus as a function of the effective volume fraction scales as a power law  $G_p \propto \phi_{eff}^{1+n/3}$  with values of  $n$  ranging from  $n = 9$  to  $n = 22$  [2]. Unfortunately a detailed model for the origin of these interactions has been missing until recently. This is due to the fact that modeling the interaction between swollen particles is complicated by the heterogeneous microstructure arising from the faster reaction rate of crosslinking compared to polymerization [5].

Here we show that interactions between thermosensitive microgel particles can be described by a polymer brush like corona decorating the dense core [6–8]. The softness of the potential is set by the relative thickness  $L_0$  of the compliant corona with respect to the overall size of the swollen particle  $R$ . The elastic modulus in quenched solid phases derived from the potential is found in excellent agreement with diffusing wave spectroscopy (DWS) data and mechanical rheometry. Moreover we analyze the local nanoscale thermal motion of the microgel particles in the dense phase and find that the short time dynamics is strongly affected by the compression. With increasing effective volume fraction the initial slope of the mean square displacement  $\langle \Delta r^2 \rangle \propto \tau^p$  drops from  $p = 1$  to  $p = 1/2$ . We

Microgel dynamics : elastic constant ( $\kappa$ ) and diffusion coefficient ( $D_s$ ) from DWS

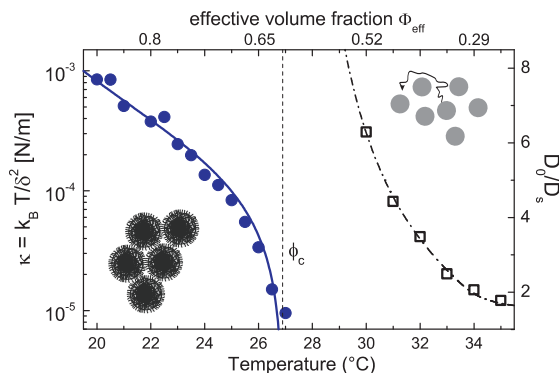


FIG. 1. Microgel liquid-solid transition as a function of temperature. The transition is driven by the change in effective particle volume due to swelling. The reciprocal short time diffusion coefficient  $D_0/D_s$  (open squares) increases strongly when approaching the transition. Solid circles: elastic spring constant  $\kappa = k_B T / \delta^2$  from DWS.

speculate that this qualitative change in the motion pattern can be directly linked to the polymer dynamics in the compressed corona.

\* Corresponding author: frank.scheffold@unifr.ch

- [1] S. Dai, P. Ravi and K. Chiu Tam, *Soft Matter* **5**, 2513 - 2533 (2009), C. Wu and X. Wang, *Phys. Rev. Lett.* **80**, 4092 (1998), S. Nayak and L.A. Lyon, *Angewandte Chemie Intl. Ed.* **44** (47), 7686-7708 (2005)
- [2] H. Senff and W. Richtering, *J. of Chem. Phys.* **111**, 1705, (1999); I. Deike, M. Ballauff, N. Willenbacher and A. Weiss, *J. Rheol.* **45**, 709-720 (2001).
- [3] A. N. St. John, V. Breedveld, and L. A., *J. Phys. Chem. B* **111**, 7796-7801 (2007)
- [4] C. Wu, B. Zhou and Z. Hu, *Phys. Rev. Lett.* **90**, 048304 (2003); A. M. Alsayed, M. F. Islam, J. Zhang, P.J. Collings and A.G. Yodh, *Science* **309** 1207 (2005); J. J. Crassous, M. Siebenbürger, M. Ballauff, M. Drechsler, O. Henrich and M. Fuchs, *J. Chem. Phys.* **125**, 204906 (2006); E.H. Purnomo, D. van den Ende, S.A. Vanapalli and F. Mugele, *Phys. Rev. Lett.* **101**, 238301 (2008)
- [5] X. Wu, R.H. Pelton, A.E. Hamielec, D.R. Woods, and W. McPhee, *Colloid Polym. Sci.* **272**, 467 (1994).
- [6] S. Milner, T. Witten and M. Cates, *Macromolecules* **21**, 2610 ( )
- [7] M. Reufer, P. Diaz-Leyva, I. Lynch and F. Scheffold, *Eur. Phys. J. E* **28**, 165–171 (2009).
- [8] F. Scheffold, P. Diaz-Leyva, M. Reufer, N. Ben Braham, I. Lynch, J.L. Harden, *Phys. Rev. Lett.* **104**, 128304 (2010)

## Dynamics of branch points in star polymers by computer simulations

Petra Bacova<sup>1,\*</sup> and Angel Moreno<sup>2</sup>

<sup>1</sup>University of the Basque Country (UPV/EHU), San Sebastián, Spain

<sup>2</sup>Centro de Física de Materiales (CSIC), San Sebastián, Spain

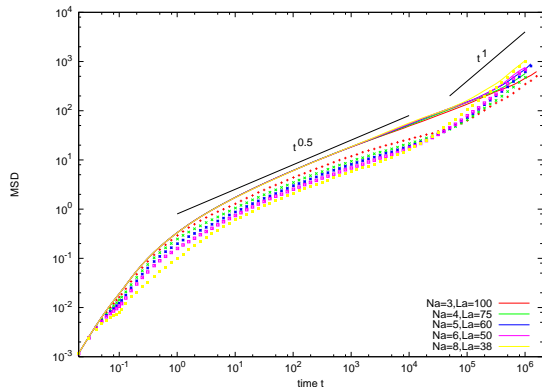


FIG. 1. Mean square displacement of star segments and branch point

We present extensive molecular dynamics simulations on the motion of the branch point in star polymers of different functionality and identical macromolecular

weight. A simple coarse-grained bead-spring model of stars is used, in order to cover a broad range of characteristic time and length scales.

We compute several dynamic correlators, including mean square displacements, van Hove functions and non-Gaussian parameters. No significant differences are found for the global dynamics (averaged over all monomers) between stars of different functionality but identical macromolecular weight.

However, it is found that the dynamics of the branch point is strongly slowed down in comparison to the motion of the rest monomers, and that this effect is enhanced by increasing the number of arms (see Fig. 1). It is also enhanced by increasing the arm length beyond the entanglement length.

\* Corresponding author: petra.bacova@ehu.es

## Effects of polydispersity on dynamic arrest properties of model colloidal systems

Luis F. Elizondo-Aguilera,<sup>1</sup> Alejandro Vizcarra-Rendón,<sup>2</sup> and Rigoberto Juárez-Maldonado<sup>3,\*</sup>

<sup>1</sup>Universidad Autónoma de San Luis Potosí

<sup>2</sup>Universidad Autónoma de Zacatecas

<sup>3</sup>Universidad Autónoma de Zacatecas, Universidad Autónoma de San Luis Potosí

The aim of this work is to study the effect that polydispersity has on dynamic arrest transition and other properties near and inside the dynamic arrest region of Hard Spheres model systems in bulk using the recent theory of dynamic arrest for colloidal mixtures (SCGLE)[1]. Polydispersity is modelled with a mixture of hard spheres, in which the standard deviation of the particle distribution will be basically the polydispersity parameter of the system. We show how the critical point of the dynamic arrest transition changes as we vary the polydispersity of the system and also show that this change is independent of the size distribution used. We will also show how the dynamic properties of the system vary with polydispersity. We conclude that the simple criteria for glass transition such as the Lindemann [2] and Hansen-Verlet[3] depend on the polydispersity of the system. Another very different and interesting results are obtained when we study the dynamic arrest threshold of a colloidal monodisperse hard sphere system moving through a polydispersity random porous medium modeled by a fixed matrix of hard sphere obstacles.

The SCGLE theory is summarized by a self-consistent system of equations [1] for the  $\nu \times \nu$  matrices  $F(k, t)$  and  $F^{(s)}(k, t)$  of collective and self (respectively) partial intermediate scattering functions. As illustrated in Ref. [1], the solution of the SCGLE theory provides the time and wave-vector dependence of the main dynamic properties. It also provides equations for their long-time asymptotic values, referred to as non-ergodicity parameters, which play the role of order parameters for the ergodic-non-ergodic transitions. The most fundamental of these results is the following equation for the asymptotic mean squared displacement  $\gamma_\alpha \equiv \lim_{t \rightarrow \infty} \langle (\Delta \mathbf{R}^{(\alpha)})^2 \rangle$ ,

$$\frac{1}{\gamma_\alpha} = \frac{1}{3(2\pi)^3} \int d^3k k^2 \{ \lambda[\lambda + k^2\gamma]^{-1} \}_{\alpha\alpha} \quad (1)$$

$$\times \{ c\sqrt{n}S\lambda[S\lambda + k^2\gamma]^{-1}\sqrt{n}h \}_{\alpha\alpha}$$

where  $S$  is the matrix of partial static structure factors,  $h$  and  $c$  are the Ornstein-Zernike matrices of total and direct correlation functions, respectively, related to  $S$  by  $S = I + \sqrt{n}h\sqrt{n} = [I - \sqrt{nc}\sqrt{n}]^{-1}$ , with the matrix  $\sqrt{n}$  defined as  $[\sqrt{n}]_{\alpha\beta} \equiv \delta_{\alpha\beta}\sqrt{n_\alpha}$ , and  $\lambda(k)$  is a diagonal matrix given by  $\lambda_{\alpha\beta}(k) = \delta_{\alpha\beta}[1 + (k/k_c^{(\alpha)})^2]^{-1}$ , where  $k_c^{(\alpha)}$  is the location of the first minimum following the main peak of  $S_{\alpha\alpha}(k)$ .

In our study we consider a  $\nu$ -component hard sphere mixture where the diameters of each component are

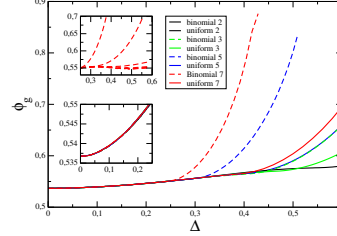


FIG. 1. Dependence of the full arrest transition point as a function of the polydispersity. For distributions and number of components indicated in the legend. The upper inset shows the line (bottom) of joint arrest of the components  $\sigma_4, \sigma_5, \sigma_6, \sigma_7$  and the lines (from bottom to top) of the sequential arrest of the species  $\sigma_3, \sigma_2$  and  $\sigma_1$ . The lower inset is a zoom of the full arrest transition point in the range from  $\Delta = 0$  to  $\Delta = 0.25$ .

$\sigma_1, \sigma_2, \dots, \sigma_\nu$ . Then we can think of this mixture as a polycomponent system of hard spheres with polydispersity in diameters and with a discrete distribution  $(x_1, x_2, \dots, x_\nu)$  of these, with  $x_\alpha$  being the molar fraction of the  $\alpha$ -component. The polydispersity will be defined by  $\Delta = \sqrt{\langle \sigma^2 \rangle - \langle \sigma \rangle^2} / \langle \sigma \rangle$  where  $\langle \sigma \rangle = \sum_\alpha x_\alpha \sigma_\alpha$  and  $\langle \sigma^2 \rangle = \sum_\alpha x_\alpha \sigma_\alpha^2$ . The distributions that we will use are the planar distribution defined by  $x_\alpha = 1/\nu$  and the binomial distribution defined by  $x_\alpha = \binom{\nu-1}{\alpha-1} / (\sum_\alpha \binom{\nu-1}{\alpha-1})$ . We define an effective structure factor of the polydisperse system in function of the partial structure factors  $S_{ij}$  of the multicomponent system of  $\nu$  species as follows:  $S_{eff} = \sum_{i,j=1}^\nu \sqrt{x_i x_j} S_{ij}$ . All dynamical properties can be defined in a similar way. The effective polydisperse intermediate scattering function is defined by  $F_{eff}(k, t) = \sum_{i,j=1}^\nu \sqrt{x_i x_j} F_{ij}(k, t)$ . The effective polydisperse non-ergodicity parameter is given by  $F_{eff}(k) = \lim_{t \rightarrow \infty} F_{eff}(k, t) = \sum_{i,j=1}^\nu \sqrt{x_i x_j} \lim_{t \rightarrow \infty} F_{ij}(k, t) = \sum_{i,j=1}^\nu \sqrt{x_i x_j} F_{ij}(k)$ . The effective polydisperse long-time mean square displacement is  $\gamma_{eff} = \sum_i x_i \gamma_i$ .

Some of our main results are shown in Fig. 1: polydispersity induces a series of various types of transitions, including simultaneous arrest of two or more species, as well as sequential arrest of several species (mixed states). We note that there are not significant changes in the transition up to moderate polydispersities.

\* Corresponding author: rigoxy@física.uaslp.mx

[1] R. Juárez-Maldonado and M. Medina-Noyola, Phys. Rev. E **77**, 051503 (2008).

[2] F. A. Lindemann, Phys. Z. **11**, 609 1911.

[3] J.P. Hansen and L. Verlet, Phys. Rev. **184**, 151 (1969)

## Colloidal Effective Interactions: the Role of Attraction in the Solvent

Nicoletta Gnan,\* Emanuela Zaccarelli, Piero Tartaglia, and Francesco Sciortino

*Dipartimento di Fisica and CNR-ISC, Università di Roma "La Sapienza", Piazzale A. Moro 2, 00185 Roma, Italy*

Describing the effective interactions between colloidal particles in the presence of macromolecular additives (e.g. surfactants, polymers, micelles, etc.) is crucial for understanding the behavior of soft-matter. Since the pioneering work of Asakura and Oosawa (AO) [1], it is known that the presence of co-solutes in solution gives rise to entropic forces that significantly modify the structure and the dynamics of colloidal systems [2]-[3]. These depletion forces arise from the entropy-driven exclusion of the cosolute from the volume between particles when their surface-to-surface relative distance is comparable to the cosolute size.[4].

Depletion forces can be strong enough to lead to colloidal aggregation. Increasing the size ratio between solute and co-solute gives rise to a fluid-fluid critical point at which colloids separate in a colloid-rich and a colloid-poor phase, in analogy with the gas-liquid separation in one-component systems. This aggregation process was found experimentally by Piazza's group [6] in the case of colloids dissolved in a micellar solution which is known to undergoes a gas-liquid phase separation on heating. Exploring the onset of colloidal aggregation as a function of temperature  $T$  and micelle concentration, the authors were able to show that a continuous line can be drawn in the  $(\phi_s, T)$  plane separating the region where the colloids are stable from the region where colloids aggregate.

Inspired by this work we have investigated numerically the general case of colloids immersed in a solution of interacting additives. For this purpose we have considered two different solvent models: an attractive square-well and a three-patch particle model. Both solvents are characterized by a gas-liquid critical point, thus recovering the experimental situation of ref. [6]. For a wide range of state points  $(\phi_s, T)$  we have evaluated the effective potentials for estimating the locus of points separating the stable from the unstable region (the "aggregation line") for a given ratio  $q$  between the solvent and the colloid sizes. Due to the short-range nature of the effective potential interactions, aggregation occurs roughly when the normalized second virial coefficient  $B_2^*$  is about  $-1.6$  which has been identified as the universal value for the onset of gas-liquid separation in short-range attractive potentials[7]. Moreover we have discussed the nature of the aggregation process close to the critical point for different  $q$  values since an important point in ref. [6] is that critical fluctuations are the driving forces for colloids aggregation close to the critical point. We find that critical fluctuations play a significant role only when the solvent size is not significantly smaller than the colloid size.

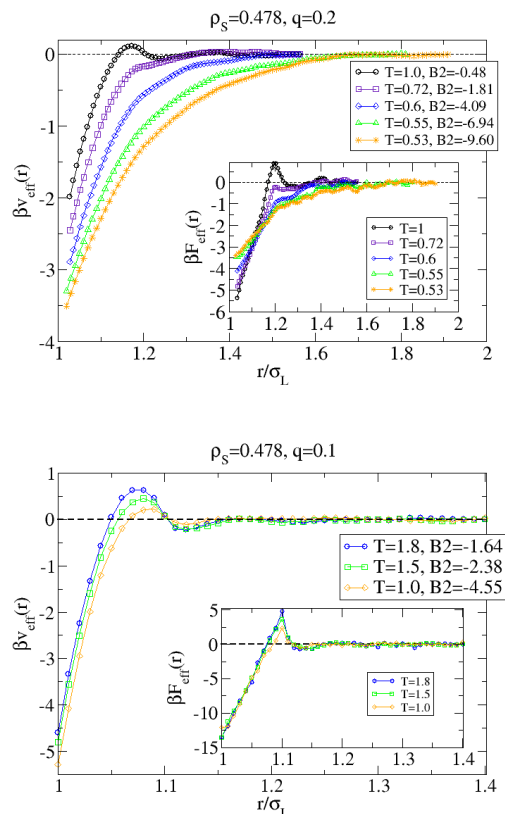


FIG. 1. Effective potentials along the solvent critical isochore for a solvent-solvent square-well attractive potential for two different size ratios:  $q = 0.2$  (top) and  $q = 0.1$  (bottom). At larger size ratios, the effective potential becomes fully attractive at low  $T$  and its range increases significantly, consistently with the increase of a static correlation length related to critical fluctuations. For smaller size ratios, the potential maintains a repulsive part and a shorter range also for very negative values of  $B_2^*$  (beyond the aggregation threshold). This implies that for smaller size ratios the temperature of colloidal aggregation will be higher, and consequently more far from the critical point. In these cases aggregation is mainly induced by entropic effects.

\* Corresponding author: nicoletta.gnan@roma1.infn.it

- [1] S. Asakura and F. Oosawa, *J. Polym. Sci.* **33**, 183 (1958).
- [2] Y. Mao, M.E. Cates, and H. Lekkerkerker, *physica A*, 10 (1995).
- [3] R. Roth, R. Evans, and S. Dietrich, *Phys. Rev. E* **62**, 5360 (2000).
- [4] C. Lykos, *Phys. Rep.* **248**, 267 (2001).
- [5] M. Dijkstra, R. van Roij, and R. Evans, *Phys. Rev. E* **59**, 5744 (1999).
- [6] S. Buzzaccaro, J. Colombo, A. Parola, and R. Piazza, *Phys. Rev. Lett.* **105**, 198301 (2010).
- [7] M. Noro and D. Frenkel, *J. Chem. Phys.* **113**, 2941 (2000).

## How do Self-Assembling Polymers and Gels Age Compared to Glasses?

John Russo and Francesco Sciortino\*

*Dipartimento di Fisica and CNR-ISC, Università di Roma "La Sapienza", Piazzale A. Moro 2, 00185 Roma, Italy*

Experiments on gels have provided contradictory results concerning the relation between correlation and response functions during aging. To clarify this puzzle, we numerically investigate the fluctuation-dissipation plot in equilibrium polymers and in network forming gels employing two distinct observables, (i) the density Fourier transform and (ii) the single-particle potential energy, to probe (i) diffusional processes and (ii) the development of a bond network. The plot behaves very differently for the two cases.

Violation from the equilibrium behavior is found only for the second observable. These results reflect the fact that the arrest mechanism in gels, differently from their high density counterparts (glasses), is not due to packing but to the formation of energy cages (bonds)[1].

\* Corresponding author: francesco.sciortino@uniroma1.it, john.russo@roma1.infn.it

[1] John Russo and Francesco Sciortino, Phys. Rev. Lett. **104**, 195701 (2010).

## Study of Transient Nuclei near Freezing

Masaharu Isobe<sup>1,\*</sup> and Berni J. Alder<sup>2</sup>

<sup>1</sup>*Graduate School of Engineering, Nagoya Institute of Technology, Nagoya, 466-8555, Japan*

<sup>2</sup>*Lawrence Livermore National Laboratory, P.O.Box 808, Livermore, CA 94551-9900, USA*

The long slow decaying potential part of the shear-stress autocorrelation function (SACF) has been called the “molasses tail” to differentiate it from the hydrodynamic origin of the long time tail in the velocity autocorrelation function [1, 2] and to emphasize its relation to the highly viscous glassy state [3]. From the numerical point of view, the long time tail of SACF has been computed by several molecular dynamics (MD) simulations in the early 80s. These studies seem to show that the long time tail of both the kinetic and potential parts have a power decay consistent with MCT, however, the amplitude of SACF in dense fluids was found to be orders of magnitude greater than predicted. Twenty years ago, Ladd and Alder have speculated that the long time tail of the SACF near the solid-fluid transition point in the hard sphere system is due to transient crystal nuclei formation [4]. They found that the potential part of the SACF and the angular orientational auto-correlation function (OACF) are identical in the long time limit and show non-algebraic decay in time. Since the evidence suggested that the reason for non-algebraic decay is slow structural relaxation around the peak of the structure factor rather than hydrodynamic flow, an attempt was made to understand this slow decaying mechanism by decomposing the OACFs into two-, three-, and four-body correlations, however, many of these correlation functions, especially the four-body correlations, have not been obtained accurately due to the computer limitation at that time.

Previously [5], we have investigated on a two dimensional system consisting of elastic hard disks at a single density near the solid-fluid transition point placed in a square box with periodic boundary conditions, using a modern fast algorithm based on event-driven MD simulation [6]. We confirmed that there exist three regimes in the relaxation of the pair orientational autocorrelation function, namely the kinetic, molasses (stretched exponential), and diffusional power decay. Then, we focus on the rapidly increasing time with increasing density for the decay of OACFs and are able to establish the length of time for which the biggest such nuclei exists at each density. It was expected that the non-algebraic decay (stretched exponential) at intermediate times presumably is due to the existence of various sized solid clusters at high densities decaying at different rates. The density dependence of both the molasses and diffusional power regimes are evaluated and the latter compares with theoretical predictions in three dimensions [7].

The cause of the stretched exponential relaxation in the molasses regime is considered to be due to the distribution of different life times of transient clusters

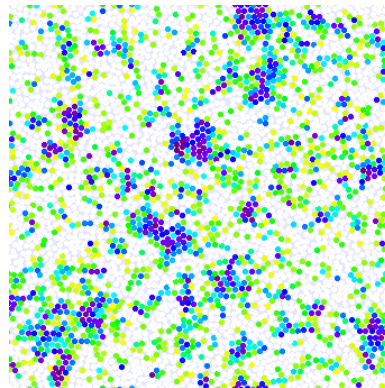


FIG. 1. The spatial distribution of  $\phi_6^i$  for 4096 particles system at a given time for packing fractions  $\nu = 0.69$ . The darker the region, the closer  $\phi_6$  is to unity.

of nuclei in dense fluid systems. Thus, there exist several exponential relaxation decays for each collision pair. To confirm the above speculation in 2D at the microscopic level, we calculated the bond orientational order,  $\phi_6$  as an alternative to two-body correlation, and furthermore, to visualize the distribution of crystal clusters in Fig. 1. We clearly observe the dramatic growth of several solid nuclei as the density nears solidification. The largest cluster at the freezing density of only a few sphere diameter in size persist for only about 30 picoseconds ( $\sim 2.8 \times 10^{-11}$ [s]) in the typical real liquids. The most striking observation through the bond orientational order parameter is the dramatic increase of the cluster size as the freezing density is approached [7]. To make the further quantitative progress, we are investigating an extension of  $\phi_6^i$  to a higher order orientational parameter involving further neighbors as the methodology of an alternative efficient calculation for quadruplet component, which will present at this workshop.

\* Corresponding author: isobe@nitech.ac.jp

- [1] B. J. Alder and T. E. Wainwright, Phys. Rev. Lett. **18**,988, (1967).; J. Phys. Soc. Jpn. Suppl.,**26**, 267, (1969).; Phys. Rev. A, **1**, 18, (1970).
- [2] M. Isobe, Phys. Rev. E, **77**, 021201, (2008).; Prog. Theor. Phys. Suppl., **178**, 72, (2009).
- [3] B. J. Alder, in *Molecular Dynamics Simulation of Statistical-mechanical Systems*, edited by G. Ciccotti and W. G. Hoover, (North-Holland, Amsterdam, 1986) p. 66.
- [4] A. J. C. Ladd and B. J. Alder, J. Stat. Phys., **57**, 473,(1989).
- [5] M. Isobe and B. J. Alder, Mol. Phys., **107**, 609, (2009).
- [6] M. Isobe, Int. J. Mod. Phys. C, **10**, 1281 (1999).
- [7] M. Isobe and B. J. Alder, Prog. Theor. Phys. Suppl., **184**, 437 (2010).

## Dynamical Signature at the Freezing Transition

V.A. Martinez,<sup>1,\*</sup> E. Zaccarelli,<sup>2</sup> C. Valeriani,<sup>1</sup> E. Sanz,<sup>1</sup> G. Bryant,<sup>3</sup> and W. van Meegen<sup>3</sup>

<sup>1</sup>*SUPA and COSMIC, School of Physics & Astronomy, The University of Edinburgh, UK*

<sup>2</sup>*Dipartimento di Fisica and CNR-ISC, Università di Roma La Sapienza, Roma, Italy*

<sup>3</sup>*Department of Applied Physics, Royal Melbourne Institute of Technology, Melbourne, Australia*

Suspensions of (nearly) identical spheres have turned out to be valuable experimental model systems for exploring dynamical properties of condensed matter, particularly the dynamics of the first order freezing-melting transition and the glass transition. The dynamics of concentrated suspensions are generally pictured in terms of the cage effect: the transient localization of particles by their neighbors. Another aspect of the dynamics, best exposed by the current-current correlation function (CCCF), is backflow: a particle current in one direction must, as dictated by conservation of number density, be compensated by a current in the opposite direction. However, this aspect of the cooperation among particles in dense fluids has been rarely considered.

Recently, we have investigated the CCCF for suspensions of particles with hard-spheres like interactions via Dynamic Light Scattering (DLS) experiments as function of both volume fraction  $\phi$  and scattering vector  $q$  [1]. The CCCF,  $C(q, \tau)$ , or autocorrelation function of the longitudinal current,  $j(q, \tau)$ , is defined as [2],

$$C(q, \tau) = q^2 \langle j(q, 0) j^*(q, \tau) \rangle = - \frac{d^2 f(q, \tau)}{d\tau^2} \quad (1)$$

Here  $\tau$  is the delay time,  $q$  is the scattering vector amplitude, and  $f(q, \tau)$  is the coherent intermediate scattering function (ISF) or normalised autocorrelation function of the  $q$ th spatial Fourier component,  $\Delta\rho(q, \tau)$  of the particle number density fluctuations,

$$f(q, \tau) = \frac{\langle \Delta\rho(q, 0) \Delta\rho^*(q, \tau) \rangle}{\langle |\Delta\rho(q)|^2 \rangle} \quad (2)$$

In [1], we have found a scaling of the space and time variables of the CCCF for suspensions in thermodynamic equilibrium, below the freezing point ( $\phi < \phi_f = 0.494$ ). However, in the metastable fluid, at volume fractions above freezing ( $\phi \geq \phi_f$ ), this scaling fails. Failure of the scaling is identified through the appearance of an inflection point in the CCCF and is best exposed by observing a minimum in the logarithmic derivative  $L(q, \tau) = d \log |C(q, \tau)| / d \log(\tau)$  (see Fig. 1). This dynamical singularity was first observed at  $\phi_f$  and in the vicinity of the peak of the structure factor, then expanding progressively to other  $q$ 's when the volume fraction is increased. At the glass point,  $\phi \approx 0.565$ , the CCCF at all experimentally accessible  $q$ 's display an inflection point.

We now perform Molecular Dynamic (MD) simulations to confirm and better understand our experimental findings. Preliminary results are presented in

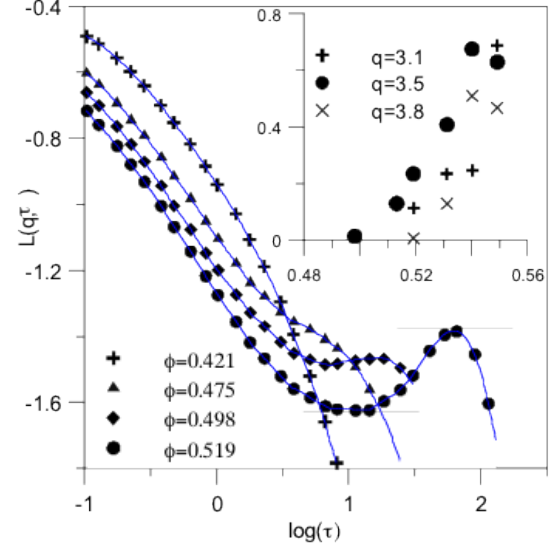


FIG. 1. Logarithmic derivative of the CCCF,  $L(q, \tau)$ , from DLS experiments, versus delay time  $\tau/\tau_B$ , normalised by the Brownian time ( $\tau_B = 0.013s$ ) in the vicinity of the peak of the structure factor for several volume fractions as indicated.

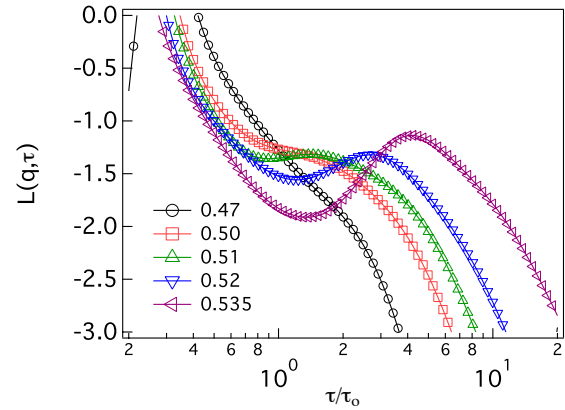


FIG. 2. Logarithmic derivative of the CCCF,  $L(q, \tau)$ , from MD simulation, versus delay time  $\tau/\tau_0$ , normalised by the thermal time ( $\tau_0$ ) in the vicinity of the peak of the structure factor for several volume fractions as indicated.

Fig. 2 and confirm the appearance of a minimum in  $L(q, \tau)$  around  $\phi_f$ . Both experimental and simulation data will be presented and discussed.

\* Corresponding author: vincent.martinez@ed.ac.uk

[1] W. van Meegen, V.A. Martinez and G. Bryant, Phys. Rev. Lett. **103**, 258302 (2009).

[2] J.-P. Hansen and I.R. McDonald *Theory of Simple Liquids* (Academic Press, London, 1986).

## Effective potential study of hard-spheres crystallization

L. A. Fernández,<sup>1</sup> V. Martín-Mayor,<sup>1,2</sup> B. Seoane,<sup>1,2,\*</sup> and P. Verrocchio<sup>1,2,3,2</sup>

<sup>1</sup>*Departamento de Física Teórica I, Universidad Complutense de Madrid, Av. Complutense, 28040 Madrid, Spain*

<sup>2</sup>*Instituto de Biocomputación y Física de Sistemas Complejos (BIFI), Spain*

<sup>3</sup>*Dipartimento di Fisica, Università di Trento, via Sommarive 14, 38050 Povo, Trento, Italy*

We present a new equilibrium approach to the study of crystallization of simple liquids [1]. We compute Helmholtz's potential for the crystalline order parameters. As a benchmark, we choose three-dimensional hard spheres, both for its simplicity, and for the availability of many previous results that we can compare with [2].

Up to now, equilibrium approaches to the hard-spheres crystallization have presented a terrible drawback: the exponential dynamical-slowness. In fact, they could only be applied to very small systems, (i.e.  $N \leq 256$  for the phase-switch Monte Carlo [3]). Because of that, in the last years, nonequilibrium methods, such as the coexistence method [2], based on the search of a steady state, have become very popular.

In this work, we recover the Helmholtz's potential from a thermodynamic integration of simulation data obtained in the Tethered Ensemble [5] (a constrained Monte Carlo method). This approach is a generalization of microcanonical simulations of first-order phase transitions (that have been applied both for magnetic systems [6] and for colloids [7]). Performing the Maxwell construction on Helmholtz's potential requires some technical modifications that we discuss. Thus, we gently accompany the system through the crystallization process by constraining its inner structure. This allows us to delay the apparition of exponential critical slowing down. Indeed, we are able to equilibrate systems up to 2048 particles.

In order to avoid metastabilities, we have found it crucial to constraint the values of two crystalline order parameters, namely  $Q_6$  and  $C$ .  $Q_6$  is the standard rotationally-invariant bond-ordering parameter.  $C$  is a variation of  $Q_6$  which is only invariant with respect to the cubic group, thus allowing us to orientate the crystalline planes in parallel with the walls of the simulation box.

A Maxwell construction yields accurate estimates of the surface tension, the densities of the coexisting

phases and the coexistence pressure. Specifically, we get  $11.573(4) k_B T / \sigma^3$ , to be compared with the phase-switch estimate,  $11.49(9) k_B T / \sigma^3$  [3], and the most precise steady state prediction,  $11.576(6) k_B T / \sigma^3$  [4].

In addition, for systems of  $N = 2916$  and 4000 particles, we observed the expected geometrical transitions, driven by surface-energy effects in a box with periodic boundary conditions. On melting, upon increasing the fraction of liquid phase, the initially bubble-shaped liquid nucleus becomes a cylinder, and then a slab (see Fig. 1).

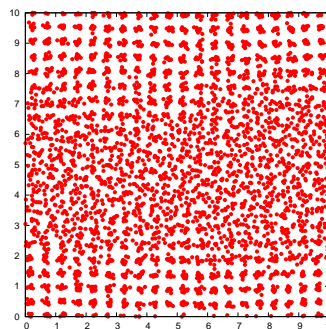


FIG. 1. Cylindrically shaped fluid region on a crystalline matrix for a 4000 particles system (the simulation box is endowed with periodic boundary conditions).

\* Corresponding author: seoane@lattice.fis.ucm.es

- [1] L. A. Fernández, V. Martín-Mayor, B. Seoane, and P. Verrocchio, manuscript in preparation.
- [2] C. Vega, E. Sanz, J. L. F. Abascal and E. G. Noya, *J. Phys.: Condens. Matter* **20** 153101 (2008).
- [3] N. B. Wilding and A. D. Bruce, *Phys. Rev. Lett.* **85**, 5138 (2000).
- [4] T. Zykova-Timan, J. Horbach, and K. Binder, *J. Chem. Phys.* **133**, 014705 (2010).
- [5] L. A. Fernández, V. Martín-Mayor, and D. Yllanes, *Nucl. Phys. B* **807**, 424 (2009).
- [6] V. Martín-Mayor, *Phys. Rev. Lett.* **98**, 137207 (2007).
- [7] L. A. Fernández, V. Martín-Mayor, B. Seoane, and P. Verrocchio, *Phys. Rev. E* **82**, 021501 (2010).

## The Crystallization of Hard-Sphere Glasses

Emanuela Zaccarelli,<sup>1</sup> Chantal Valeriani,<sup>2,\*</sup> Eduardo Sanz,<sup>2</sup> W. C. K. Poon,<sup>2</sup> M. E. Cates,<sup>2</sup> and P. N. Pusey<sup>2</sup>

<sup>1</sup>*Dipartimento di Fisica and CNR-INFM-SOFT, Università di Roma La Sapienza, Piazzale A. Moro 2, 00185, Roma, Italy*

<sup>2</sup>*SUPA, School of Physics and Astronomy, University of Edinburgh, Mayfield Road, Edinburgh, EH9 3JZ, Scotland*

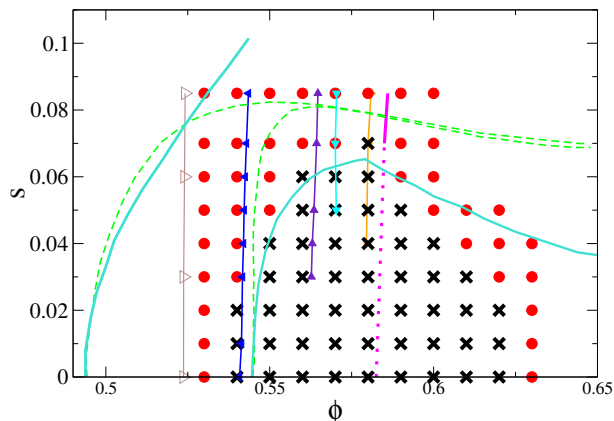


FIG. 1. Stability diagram in the  $(\phi, s)$  plane, reporting state points that crystallize (black crosses) in at least one of five runs, and state points where all runs remain disordered until  $t_M$  (red circles). We also show as triangles isodiffusivity lines (left to right:  $D = 5 \times 10^{-3}$  (blue),  $D = 10^{-3}$  (violet),  $D = 5 \times 10^{-4}$  (cyan),  $D = 5 \times 10^{-5}$  (orange)); to the right of these lie the MCT glass transition for a binary mixture of matched  $s$  (brown), and the extrapolated ideal glass line from our data (magenta), with a dotted continuation into the crystal as guide to the eye. The phase boundaries allowing [4] and not allowing [5] for fractionation are shown as solid (turquoise) and dashed (green) lines respectively.

In this work [1] we present molecular dynamics (MD) simulations that probe in detail the effects of polydispersity on the HS glass transition and on crystallization. We find almost no effect of polydispersity on the dynamics of diffusive rearrangement within the amorphous state near the glass transition, but confirm also that polydispersity strongly suppresses crystallization [2, 3].

For state-points in the plane of volume fraction ( $0.54 \leq \phi \leq 0.63$ ) and polydispersity ( $0 \leq s \leq 0.085$ ) (see fig.1), we delineate states that spontaneously crystallize from those that do not. For non-crystallising (or pre-crystallization) samples we find isodiffusivity lines consistent with an ideal glass transition at  $\phi_g \approx 0.585$ , independent of  $s$ .

Despite this, for  $s < 0.05$ , crystallization occurs at  $\phi > \phi_g$ . This happens on timescales for which the system is ageing, and a diffusive regime in the mean square displacement is not reached; by those criteria, the system is a glass (see fig.2). Hence, contrary to a widespread assumption in the colloid literature, occurrence of spontaneous crystallization within a bulk amorphous state does not prove that this state was an ergodic fluid rather than a glass.

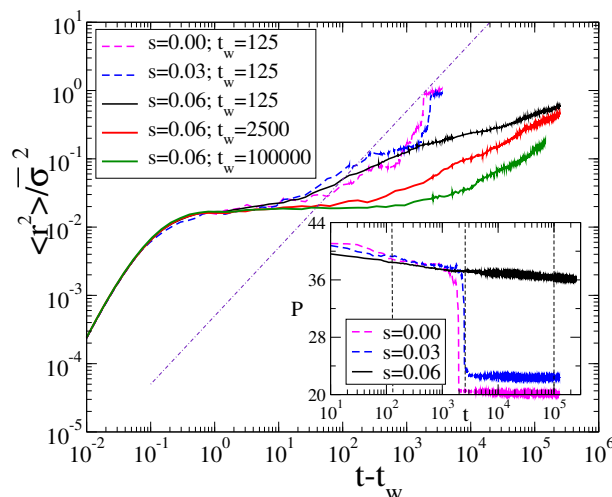


FIG. 2. MSD versus  $t - t_w$  for  $\phi = 0.60$  and  $s = 0.06$ , at various  $t_w$ , averaged over 9 different runs. The MSD for the same  $\phi$  and lower  $s$  ( $s = 0$  and  $0.03$ ) is also included. At these low  $s$  the system crystallizes, and averaging over different runs is no longer possible. As a consequence, the MSD is more noisy but, within the statistical error, identical to that of  $s = 0.06$  until crystallization takes place. The dashed-dotted line, with slope 1, has been included to stress the fact that the system is subdiffusive at the moment it crystallizes. Inset: Pressure versus time for the same state points. Vertical lines indicate the  $t_w$ -values employed in the MSD calculations.

We thank Giuseppe Foffi for his contributions to the early stages of this work. This work was funded by UK EPSRC (EP/E030173/1, EP/D071070/1), the EU MRTN-CT-2003-504712, and NMP3-CT-2004-502235 (SoftComp). ES and CV each acknowledge support from an Intra-European Marie Curie Fellowship. MEC is funded by the Royal Society. This work has made use of the resources provided by the Edinburgh Compute and Data Facility (ECDF), and was funded in part by EPSRC EO30173.

\* Corresponding author: cvaleria@ph.ed.ac.uk

- [1] E. Zaccarelli, C. Valeriani, E. Sanz, W. C. K. Poon, M. E. Cates and P. N. Pusey, Phys. Rev. Lett. **103**, 135704 (2009).
- [2] S. I. Henderson, T. C. Mortensen, S. M. Underwood and W. van Meegen, Physica A **233**, 102 (1996).
- [3] I. Moriguchi, K. Kawasaki and T. Kawakatsu, J. Phys. II (France) **5**, 143 (1995).
- [4] P. Bartlett and P. B. Warren, Phys. Rev. Lett. **82**, 1979 (1999).
- [5] M. Fasolo and P. Sollich, Phys. Rev. Lett. **91**, 68301 (2003).

# Crystallization and vitrification of a hard sphere like colloidal model system

Markus Franke and Hans Joachim Schöpe\*

*Institut für Physik, Johannes Gutenberg-Universität Mainz, Staudingerweg 7, 55128 Mainz*

Solidification of a meta stable melt by crystallization or vitrification is one of the most important non-equilibrium processes in physics. Colloidal model systems have been used for about 30 year studying this process and the achieved results increased our knowledge about solidification in an impressing way [1],[2]. It was shown by microscopic [3],[4] and spectroscopic experiments [5],[6] as well as by computer simulations [7] that the structure and the dynamics of the under cooled melt is not homogeneous as assumed by standard theories describing crystal nucleation and vitrification. New investigations suggest that crystal nucleation and vitrification are highly linked with the physical properties of the meta stable melt.

We investigated the solidification scenario in suspensions of gravity matched colloidal hard spheres using time resolved static light scattering (TRLS) as well as dynamic light scattering (DLS) techniques. Analysing the time evolution of the static structure factor of the solidifying sample by TRLS the solidification kinetics (Fig. 1, bottom) while by DLS the dynamic structure factor (Fig. 1, top) at the main structure factor peak is obtained. A detailed analysis of crystal nucleation path ways shows that crystallization is originated by transient precursors (structurally heterogeneous clusters) during the induction stage. Later these objects convert into highly ordered crystals in a fast, activated process [8],[9]. This scenario was verified by recent computer simulations and it was shown that the meta stable colloidal fluid relaxes the density first, by producing distorted crystalline structures and later the optimal crystal structure is achieved [10],[11]. Close to the glass transition the amount of these structural heterogeneities is still increasing with time, but crystal conversion is dramatically delayed or even frustrated. Following the same processes over a range of volume fractions from near freezing, to above the glass transition allows to systematically link the mechanisms involved in HS crystallization to those of the HS glass transition.

We thank Tanja Schilling, Bill van Meegen and Gary Bryant for fruitful discussions. We gratefully acknowledge the financial support of the DFG (SCHO1054/3-2).

\* Corresponding author: jschoepe@uni-mainz.de

- [1] U. Gasser, *J. Phys.: Condens. Matter* **21**, 203101 (2009).
- [2] P. N. Pusey, *J. Phys.: Condens. Matter* **20**, 494202 (2008).
- [3] W. K. Kegel and A. van Blaaderen, *Science* **287**, 290 (2000).
- [4] J. C. Conrad, F. W. Starr, D. A. Weitz, *J. Phys. Chem. B* **109**, 21235 (2005).

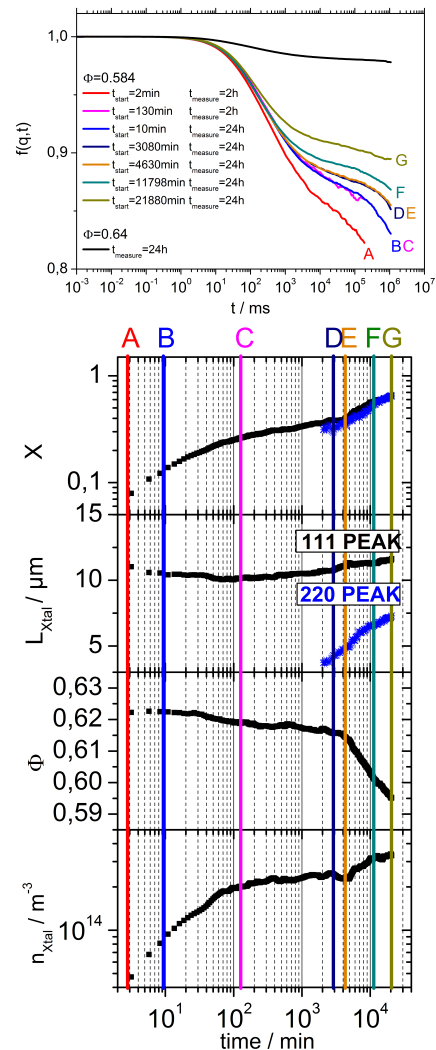


FIG. 1. Top: Dynamic structure factor at the the main structure factor peak as function of waiting time for a sample close to the glass transition (volume fraction  $\Phi = 0.584$ ). Bottom: Solidification kinetics of the same sample. X: precursor resp. crystal fraction, L - domaine size,  $\Phi$  - precursor resp. crystal volume fraction,  $n_{x(tal)}$  - precursor resp. crystal number density; black: precursor resp. (111)-peak; blue: (220)-peak.

- [5] W. van Meegen and G. Bryant, *Phys. Rev. E* **76**, 021402 (2007).
- [6] H. J. Schöpe, G. Bryant and W. van Meegen, *J. Chem. Phys.* **127**, 084505 (2007).
- [7] T. Kawasaki and H. Tanaka, *J. Phys.: Condens. Matter* **22**, 232102 (2010).
- [8] H. J. Schöpe, G. Bryant and W. van Meegen, *Phys. Rev. Lett.* **96**, 175701 (2006).
- [9] S. Iacopini, T. Palberg, H. J. Schöpe, *J. Chem. Phys.* **130**, 084502 (2009).
- [10] T. Schilling, H. J. Schöpe and M. Oettel, G. Opletal and I. Snook, *Phys. Rev. Lett.* **105**, 025701 (2010).
- [11] T. Kawasaki and H. Tanaka, *PNAS* **107**, 14036 (2010)

## Equilibrium dynamics of binary cluster crystals

Manuel Camargo,<sup>1,2,\*</sup> Angel J. Moreno,<sup>3</sup> and Christos N. Likos<sup>4</sup>

<sup>1</sup>*Institute for Theoretical Physics II, Heinrich-Heine University, Düsseldorf, Germany*

<sup>2</sup>*Dirección Nacional de Investigaciones, Universidad Antonio Nariño, Bogotá, Colombia*

<sup>3</sup>*Centro de Física de Materiales, CSIC-UPV/EHU, San Sebastián, Spain*

<sup>4</sup>*Faculty of Physics, University of Vienna, Vienna, Austria*

As result of the application of coarse-grained procedures to describe complex fluids, the study of systems consisting of particles interacting through bound, repulsive pair potentials has become of increasing interest in the last years. A well known example of this type of interaction potentials is the so-called Generalized Exponential Model (GEM- $m$ ), for which the interaction between particles is described by  $v(r) = \epsilon \exp[-(r/\sigma)^m]$ . Recently, the phase behavior of binary mixtures of such particles has been investigated [1, 2]. For the case of non-demixing mixtures, it was found evidence for formation of novel kind of alloys depending on the cross interactions between the two species. In this work we aim to study the dynamic behaviour of such binary mixtures by means of extensive Molecular Dynamics Simulations and to extend the findings displayed by one-component systems [3].

As a previous step, the stability limits for the fluid phase (coexistence and  $\lambda$  lines) were determined for representative examples of that class of mixtures by solving the Ornstein-Zernike (OZ) equation within the mean field approximation (MFA). Based on those results the specific systems to be simulated were determined. The parameters defining the mixture (relative sizes, relative compositions, temperature, self- and cross-interactions) were chosen in order to consider a non-demixing system [2] and, because of the high values of total densities, to be the less computationally demanding ones. In this way, the chosen system is a mixture of “big” GEM-8 particles and “small” Gaussian (GEM-2) ones, i.e. our system is composed by a cluster-forming component (GEM-8 specie) and a non-clustering component (GEM-2 specie) [4], at fixed temperature for a broad range of densities and relative compositions. The cross interaction was chosen to be a GEM-4 potential, which also displays cluster formation.

The obtained results show that as the total density increases at fixed composition, the GEM-8 species builds cluster crystals with a relatively high localization. As in the one-component system, the incoherent scattering functions indicate a localization transition for self-motions of the GEM-8 particles, which is avoided by incessant hopping motion between clusters. This transition seems to occur at lower densities than for out-of-lattice collective correlations, confirming in the mixture the dynamic decoupling observed in the one-component cluster crystal.

On the other hand, the Gaussian particles remain delocalized in the periodic potential induced by the

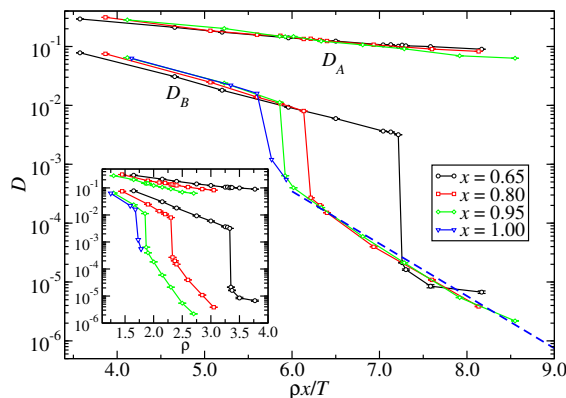


FIG. 1. Diffusivities of the GEM-2 ( $A$ ) and GEM-8 ( $B$ ) particles as a function of the total density  $\rho$  (inset) and of the combined variable  $\rho x/T$  (main panel) with  $x = \rho_B/\rho$  and  $T = 0.3$ . The solid lines are guides for the eyes. The dashed line in the main panel indicates approximate Arrhenius behavior  $D_B \sim \exp[-2.3\rho_B/T]$ .

GEM-8 clusters and display fast self-motions. However, slow collective dynamics is observed for specific wavevectors, namely those belonging to the reciprocal lattice. This feature reflects the preferential motion of the Gaussian particles over the interstitials, confirming the expectations from static correlations. A striking feature is revealed by the analysis of collective correlations of the GEM-8 particles, for wavevectors at the reciprocal lattice, a feature which we attribute to the stiffening of an acoustical mode at the edge of the Brillouin zone, caused by the presence of the Gaussian particles [5].

This work has been supported by the EU Network of Excellence “SoftComp”, DIPC (Spain) and the Training Network COMPROIDS. M.C. thanks DAAD (Germany)-ALECOL (Colombia) for a PhD Fellowship.

\* Corresponding author: camargo@thphy.uni-duesseldorf.de

- [1] S. Overduin and C.N. Likos, *Eur. Phys. Lett.* **85**, 26003 (2009)
- [2] S. Overduin and C.N. Likos, *Chem. Phys.* **131**, 034902 (2009)
- [3] A.J. Moreno and C.N. Likos, *Phys. Rev. Lett.* **99**, 107801 (2007)
- [4] C.N. Likos, B.M. Mladek, D. Gottwald and G. Kahl, *J. Chem. Phys.* **126**, 224502 (2007)
- [5] M. Camargo, A. J. Moreno, and C. N. Likos, *J. Stat. Mech.* P10015 (2010)

## Free Volume Distributions in Hard Sphere Fluid and Jammed Configurations

Srikanth Sastry<sup>1,\*</sup> and Moumita Maiti<sup>2</sup>

<sup>1</sup>*Jakkur Campus, Jawaharlal Nehru Centre for Advanced Scientific Research Bengaluru 560064 India*

<sup>2</sup>*Jakkur Campus, Jawaharlal Nehru Centre for Advanced Scientific Research, Bengaluru 560064 India*

The free volume is an important quantity characterizing hard sphere packings, as it relates directly to the equation of state in these systems, and is also invoked in some approaches to understanding the dynamics in hard sphere fluids. The free volume distribution can also be used to evaluate the distribution of cavity volumes, which in turn allows the calculation of the chemical potential. These distributions also characterize the geometry of these particle packings. Using an algorithm that allows the computation

of free volumes and the corresponding surface area for monodisperse and polydisperse sphere packings, we evaluate the free volume distribution, for fluid, crystal and nearly jammed configurations, and show how these distributions are different in these cases. We also describe the relationship between the free volume distributions we find to expectations concerning the geometry of jammed packings.

\* Corresponding author: sastry@jncasr.ac.in

# Spontaneous rotation and slow “breathing” in a vertically vibrated dense granular monolayer

Andrea Puglisi,<sup>1,2,\*</sup> Giacomo Gradenigo,<sup>1,2</sup> Alessandro Sarracino,<sup>1,2</sup> and Dario Villamaina<sup>1,2</sup>

<sup>1</sup>CNR-ISC Rome, Italy

<sup>2</sup>Dipartimento di Fisica, Università di Roma “La Sapienza”, Rome, Italy

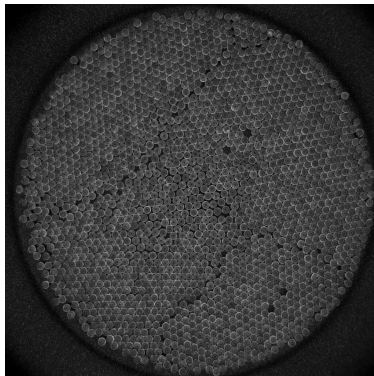


FIG. 1. An instantaneous configuration.

Granular materials are athermal systems, nevertheless they can be excited by periodic or stochastic macroscopic mechanical drivings, reaching very peculiar non-equilibrium steady states. A typical setup is constituted by one or more horizontal layers of spherical grains on a vertically vibrating surface: under periodical vibration this system displays a wide variety of ordering behaviors [1–4], sensitive to covering fraction, number of layers, vibration parameters, material properties, boundary conditions, etc.

In this communication we report about recent experiments on a quasi-2D monolayer made of  $\sim 2000$  glass beads,  $4\text{mm}$  of diameters, close to the hexagonal packing, as exemplified by Fig. 1. The vibrating container is made of a horizontal teflon-covered rigid aluminum circular plate, of diameter  $\sim 20\text{cm}$ , delimited by slowly rising boundaries to prevent highly dissipating frontal collisions between beads and borders. The teflon covering provides a finely rough surface which efficiently transfers vertical energy into horizontal motion. The energy input is provided by a shaker which vibrates the system vertically with a sinusoidal law at frequency  $f$ . We focus on the range of frequencies  $f \in [75, 200]$  and on amplitudes  $A$  such that  $\Gamma = A(2\pi f)^2/g \in [3, 5]$ . In this range a granular regime is observed, similar to a thermally vibrating crystal: most of the grains show rapidly fluctuating displacement with respect to an averagely stable hexagonal lattice, with few sparse fractures and defects due to the overall inconsistency of the boundary with the lattice. Superimposed to this thermal solid-like behavior, we observe a remarkably stable *rigid rotation* of the whole lattice at constant angular velocity  $\Omega$ . The period of rotation  $T = 2\pi/\Omega$  is several orders of magnitude larger than  $1/f$ . We find that  $\Omega$  increases with the amplitude of the vibration, but changes in a *non-monotonic* fashion when  $f$  is varied

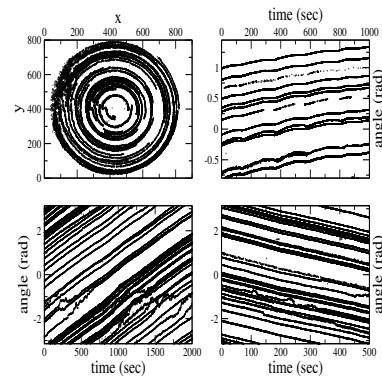


FIG. 2. From top-left, going anti-clockwise: 1) position  $x(t), y(t)$  of few particles during a 2000 seconds trajectory ( $f = 75\text{Hz}$ ,  $\Gamma = 3.5$ ); 2) angle  $\tan^{-1}(y/x)$  of the tracers as a function of time ( $f = 75\text{Hz}$ ,  $\Gamma = 3.5$ ); 3) the same for a different frequency ( $f = 100\text{Hz}$ ,  $\Gamma = 4$ ); 4) the same for  $f = 125\text{Hz}$  and  $\Gamma = 3$ , where the “breathing” mechanism can be identified.

from  $75\text{Hz}$  to  $200\text{Hz}$  [5]. In particular at least two inversions of the sign of  $\Omega$  are observed, increasing  $f$ . A careful study of the container reveals small imperfections which account for the rotational symmetry breaking. The comparison with known granular ratchet models is discussed [6]. At small amplitudes, i.e. at the onset of the vibrating crystal regime, we also observe a very slow *breathing* mechanism, where energy cyclically disappears and comes back into the system, while the rigid rotation slows down and accelerates: the breathing period is much larger than  $1/f$  but lower than  $T$ . This seems to be the cyclical reproduction of a front propagating “ignition” mechanism already observed in previous experiments [7].

This work is supported by the “Granular-Chaos” project, funded by the Italian MIUR under the FIRB-IDEAS grant number RBID08Z9JE.

\* Corresponding author: andrea.puglisi@roma1.infn.it

- [1] I. S. Aranson and L. S. Tsimring, Rev. Mod. Phys. **78**, 651 (2006).
- [2] P. B. Umbanhowar, F. Melo and H. L. Swinney, Nature **382**, 793 (1996).
- [3] A. Prevost, D. A. Egolf and J. S. Urbach, Phys. Rev. Lett. **89**, 084301 (2002).
- [4] F. V. Reyes and J. S. Urbach, Phys. Rev. E **78**, 051301 (2008).
- [5] R. Klages, I. F. Barna and L. Mátyás, Phys. Lett. A **333**, 79 (2004).
- [6] G. Costantini, A. Puglisi and U. Marini Bettolo Marconi, Phys. Rev. E **75** 061124 (2007).
- [7] W. Losert, D. G. W. Cooper and J. P. Gollub, Phys. Rev. E **59**, 5855 (1999).

## Growing time and length scales in the dissipative dynamics of a granular fluid

Giacomo Gradenigo,\* A. Sarracino, D. Villamaina, and A. Puglisi

CNR-ISC and Dipartimento di Fisica, Università di Roma “La Sapienza”, p.le A. Moro 2, 00185 Roma, Italy, EU

Violations of the equilibrium fluctuation-dissipation relation (FDR), together with the finding of time and length scales which grow at low temperature, is a well established scenario for glass-forming system. Recently it has been shown that also dissipative granular fluids exhibit, at high packing fractions, a dynamical arrest analogous to the glass transitions [1].

Here we characterize the slowing down of a dense granular fluid and the FDR violations occurring in this system: the dissipative dynamics of a massive intruder is studied at packing fractions lower than the threshold for dynamical arrest, where the system behaves as a dilute or dense fluid. The dynamics of such a probe particle is well captured by a generalized Langevin equation with an exponential memory kernel and a colored noise:

$$M\dot{V}(t) = - \int_{-\infty}^t dt' \Gamma(t-t')V(t') + \mathcal{E}'(t), \quad (1)$$

with  $\Gamma(t) = 2\gamma_0\delta(t) + \gamma_1/\tau e^{-t/\tau}$  and  $\gamma_0, \gamma_1$  two friction coefficients. We find that the time-scale  $\tau(\phi)/\tau_c(\phi)$ , with  $\tau_c(\phi)$  the mean collision time, is an increasing function of the packing fraction. Both the elastic and the dissipative dynamic can be modeled with eq. (1):  $\tau/\tau_c$  grows with the packing fraction in both situations. The decay of velocity autocorrelation for the massive probe is shown in fig. 1 as a function of  $t/\tau_c$ . Data are fitted with the analytical solution of eq. (1). Eq. (1) can be also mapped in a two variable Markovian model [2], exactly soluble [4], where the velocity of the probe  $V$  is coupled to another an auxiliary variable  $U$  understood as the value of a local velocity field present in the granular fluid. This picture suggests that, in the case of *dissipative* dynamics,  $\tau$  may be also regarded as the typical time over which is correlated the *local velocity field*  $U$  surrounding the tracer. Within this scheme the violations of the equilibrium

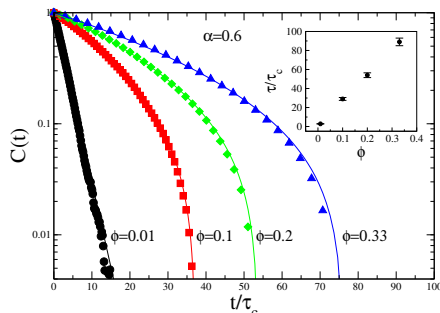


FIG. 1. Main: Velocity autocorrelation function of a massive intruder in a dense granular media at different values of  $\phi$ . Inset: Ratio  $\tau/\tau_c$  as function of  $\phi$ :  $\tau$  is the memory kernel characteristic time (eq. 1) and  $\tau_c$  the mean collision time.

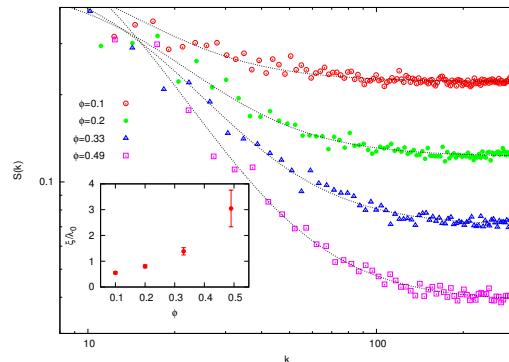


FIG. 2. Main: Low momentum behaviour of the velocity field structure factor  $S(k)$ . Inset: the ratio  $\xi/\lambda_0$  as function of packing fraction  $\phi$ , with the  $\lambda_0$  mean free path.

FDR come from the coupling between the massive tracer velocity and the local velocity field of the fluid. From the analysis above we learned that the velocities of particles surrounding the intruder appear to be correlated over increasing time-scales. This observation urged us to look also for a growing length scale in the velocity field of the dense granular fluid. We started this program by studying the low momentum behaviour of the static structure factor of the velocity field,  $S(k) = 1/N\langle U(k)U(-k) \rangle$ . Assuming that the low- $k$  behaviour of  $S(k)$  obeys a hydrodynamic approximation scheme [3],  $S(k) = (A + Bk^2)/(1 + \xi^2k^2)$ , numerical data, reported in fig. 2, can be fitted obtaining a correlation length  $\xi(\phi)$  (see inset of fig. 2). We find that the ratio  $\xi/\lambda_0$ , with  $\lambda_0$  the mean free path, grows as a function of  $\phi$ . At equilibrium (elastic collisions) we find  $S(k) = \text{const}$ : velocities are uncorrelated and equipartition between modes holds.

We have shown that in a dense granular system there are time and length scales, characterizing the velocity field, which are related to *dissipative* phenomena and which grow when the packing fraction is increased. This behaviour, observed at moderate packing fractions, appears as the prelude of the glass transition placed at higher packing fractions.

The work is supported by the “Granular-Chaos” project, funded by the Italian MIUR under the FIRB-IDEAS grant number RBID08Z9JE.

\* Corresponding author: ggradenigo@gmail.com

- [1] W. T. Kranz, M. Sperl, A. Zippelius. PRL **104**, 225701 (2010).
- [2] A. Sarracino, D. Villamaina, G. Gradenigo, A. Puglisi. EPL **90**, 34001 (2010).
- [3] T. P. C. van Noije, M. H. Ernst, E. Trizac, I. Pagonabarraga. PRE **59**, 4326 (1999).
- [4] Villamaina D., Baldassarri A., Puglisi A. Vulpiani A. J. Stat. Mech. P07024 (2009).

## A New Species of Active Brownian Particles

Ivo Buttinoni,<sup>1,\*</sup> Dominik Vogt,<sup>1</sup> Giovanni Volpe,<sup>1,2</sup> and Clemens Bechinger<sup>1,2</sup>

<sup>1</sup>*Physikalisches Institut, Stuttgart University,  
Pfaffenwaldring 57, 70550 Stuttgart, Germany*

<sup>2</sup>*Max-Planck-Institut für Metallforschung, Heisenbergstrasse 3, 70569 Stuttgart, Germany*

In recent years, active Brownian motion has attracted a lot of interest from the biological and physical communities [1]. Differently from simple Brownian motion, which is dominated by random fluctuations, active Brownian particles feature an interplay between random fluctuations and active swimming.

A paradigmatic example of active Brownian motion is the swimming behavior of bacteria such as *Escherichia Coli* [2]. Its strategy to look for nutrients can be described as a sequence of roughly straight trajectories, “runs”, and waiting times, “tumbles”. The presence of a nutrient gradient can influence the frequency of such tumbles and, thus, the bacterial motion can adapt to the ambient conditions [3]; furthermore, different behaviours may be observed under the same environmental conditions depending on the bacterial phenotype.

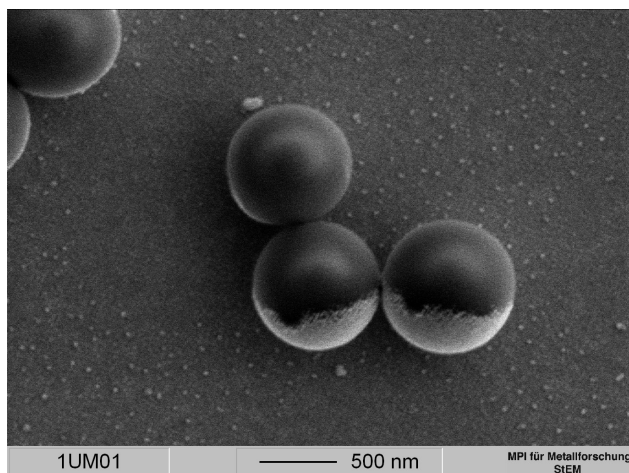


FIG. 1. Janus particles. SEM image of  $1\ \mu\text{m}$  diameter silica particles half-coated with a 50 nm layer of gold (lighter color).

Also artificial particles can perform active Brownian motion, provided that the symmetry of the suspension be broken towards a far from equilibrium status. This can be achieved by a periodic deformation of the Brownian swimmer [4]. It can be also be achieved using asymmetric particles, e.g., Janus particles [6] or microrods [5], immersed in an external gradient, e.g., a magnetic field gradient [7].

In this work, we present a novel technique to achieve and control active Brownian motion. As active Brownian particles, we use Janus particles, i.e. silica microparticles half-coated with a thin layer of gold (Fig.

1). These particles are immersed in a critical water-2,6-lutidine mixture stabilized just below the critical  $T_c = 34^\circ\text{C}$  [8]. Illumination of the particles leads to the heating of their golden side and therefore to a local demixing of the critical mixture, which eventually results in the propulsion of the particle.

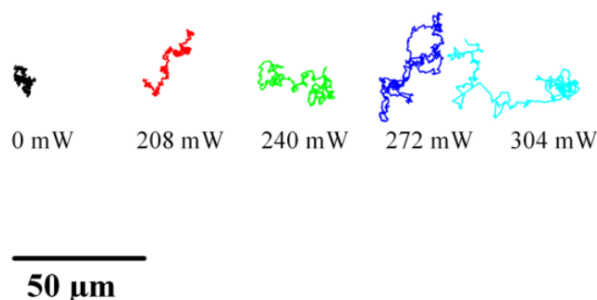


FIG. 2. Active Brownian trajectories. The particle is a  $1\ \mu\text{m}$  diameter Janus particle and the power of the illumination is indicated below each trajectory (60 s).

Some of the resulting trajectories are presented in Fig. 2. One of the main advantages of this new species of active Brownian particles is that the active Brownian motion can be tuned by the illumination power. In Fig. 2 one can see that the directed segments of the trajectories increase with increasing illumination. Thanks to this property, we can study for example the behaviour of active Brownian particles in a porous medium, which, for example, alters the statistical properties of the trajectories, e.g. their mean square displacement. Similar concepts can prove useful also in the study of biological active Brownian particles, e.g., *E. coli*.

This work is linked to ITN-COMPLOIDS project (<http://www.itn-complids.eu/>) and partially financed by Marie Curie Actions.

\* Corresponding author: [i.buttinoni@physik.uni-stuttgart.de](mailto:i.buttinoni@physik.uni-stuttgart.de)

- [1] S. J. Ebbens and J. R. Howse, *Soft Matter* **6**, 726 (2010).
- [2] Berg HC, *Nature* **254**, 389 (1975).
- [3] Berg HC, *E. coli in motion* (Springer-Verlag, New York, USA, 2004).
- [4] R. Dreyfus *et al.*, *Nature* **437**, 862 (2005).
- [5] W. F. Paxton *et al.*, *J. Am. Chem. Soc.* **126**, 13424 (2004).
- [6] J. R. Howse *et al.*, *Phys. Rev. Lett.* **99**, 048102 (2007).
- [7] A. Ghosh and P. Fisher, *Nano Lett.* **9**, 2243 (2009).
- [8] C. A. Grattoni *et al.*, *J. Chem. Eng. Data*, **38**, 516 (1993).

## Zero Reynolds number turbulent flow in active liquid crystals

H. H. Wensink\* and H. Löwen

*Institute for Theoretical Physics II: Soft Matter, Heinrich-Heine-University-Düsseldorf,  
Universitätsstrasse 1, D-40225, Düsseldorf, Germany*

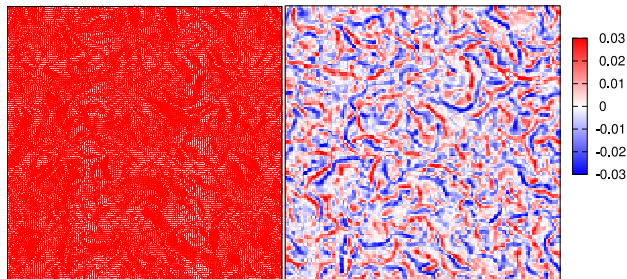


FIG. 1. Large-scale turbulent flow in 2D bulk systems of self-propelled colloidal rods (SPR). Shown is a map of the velocity field  $\mathbf{v}(t, \mathbf{r})$  (left) and vorticity field  $\nabla \times \mathbf{v}(t, \mathbf{r})$  (right) at time  $t$  for rods with aspect ratio  $\ell = 6$  and packing fraction  $\phi = 0.79$ . Results are obtained from simulating the overdamped deterministic motion of  $10^5$  SPRs.

Self-motile colloidal particles and microorganisms can generate fascinating macroscopic patterns ranging from complex swarms and vortices [1, 2] to compact hedgehog wall clusters [3]. A particularly interesting effect is the emergence of self-generated turbulent patterns in active bacterial suspensions due to the motility of the bacteria [1].

We have studied the collective dynamics of rigid self-propelled colloidal rods (SPR) with variable aspect ratio by means of computer simulation. Our focus is on dense suspensions where the dynamics is dominated by direct particle interactions rather than hydrodynamic forces mediated by the solvent.

Considering the regime relevant to microorganisms, we assume that motion of the SPRs is overdamped due to solvent friction ( $\text{Re} = 0$ ). In dense suspensions, thermal fluctuations are negligible for sufficiently large bacteria, implying that it is sufficient to study deterministic particle motions. With these assumptions only two relevant system parameters remain: the aspect ratio  $\ell$ , and the effective volume fraction  $\phi$  of the rods. The non-equilibrium phase diagram of active colloidal rods in the density versus aspect-ratio plane features a large region of complex turbulent flow patterns (see Fig. 1) which are generated solely by the steric interactions between rigid rods with short-ranged Yukawa interactions [3].

An analysis of the velocity structure functions and energy spectra reveals that the turbulent flow is distinctly different from regular 2D turbulence observed in simple fluids at high Reynolds numbers. The total

energy associated with local rotational (swirling) motion can be quantified in terms of the *enstrophy* per unit area which is defined as

$$\mathcal{E} = \frac{1}{2} \langle \langle |\boldsymbol{\omega}(t, \mathbf{r})|^2 \rangle \rangle_{t, \mathbf{r}}, \quad (1)$$

with  $\boldsymbol{\omega}(t, \mathbf{r}) = \nabla \times \mathbf{v}(t, \mathbf{r})$  denoting the vorticity of the flow field  $\mathbf{v}(t, \mathbf{r})$  at time  $t$ , and  $\langle \langle \cdot \rangle \rangle_{t, \mathbf{r}}$  denoting a space-time average. The enstrophy, when plotted against the volume fraction exhibits a maximum corresponding to an optimum density at which turbulent motion and, therefore, fluid mixing is maximized; this is shown in Fig. 2.

Variation of the rod aspect ratio leads to dramatic changes in the collective dynamics at high densities. Strongly elongated SP rods self-organize into laning patterns while very short rods tend to form jammed structures.

The authors gratefully acknowledge the SFB-TR6 for financial support.

\* Corresponding author: wensink@thphy.uni-duesseldorf.de

- [1] A. Sokolov, I. S. Aranson, J. O. Kessler, and R. E. Goldstein, *Phys. Rev. Lett.* **98**, 158102 (2007).
- [2] H. P. Zhang, A. Be'er, E.-L. Florin, and H. L. Swinney, *Proc. Natl. Acad. Sci. USA* **107**, 13626 (2010).
- [3] H. H. Wensink and H. Löwen, *Phys. Rev. E* **78**, 031409 (2008).

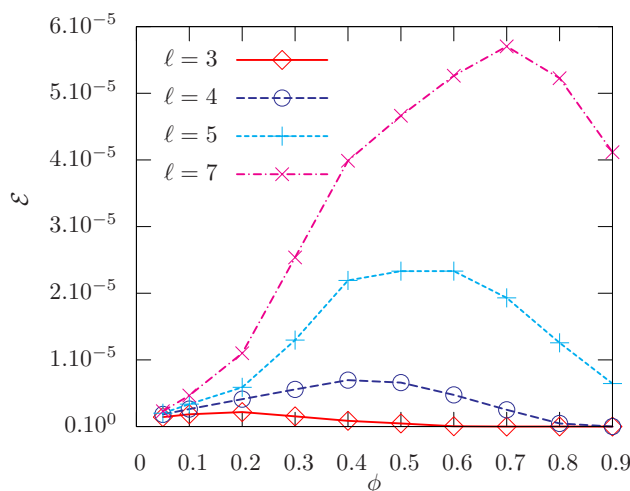


FIG. 2. Enstrophy  $\mathcal{E}$  (in arbitrary units) versus packing fraction  $\phi$  for a number of different aspect ratios  $\ell$ . The maxima indicate the existence of an optimal filling fraction for active turbulence at a given value of the aspect ratio  $\ell$ .

## Interplay of macroscopic and microscopic viscoelastic properties in spider silk

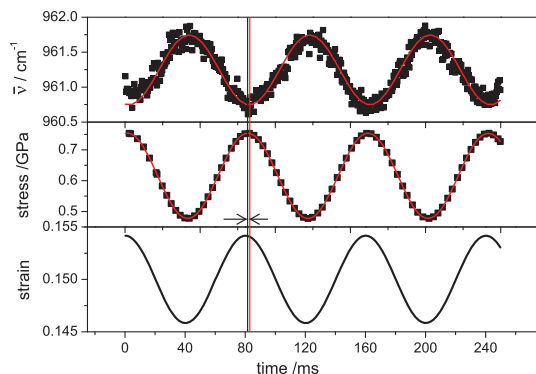
Periklis Papadopoulos,<sup>1,2,\*</sup> Roxana Ene,<sup>1</sup> and Friedrich Kremer<sup>1</sup><sup>1</sup>University of Leipzig, Institute for Experimental Physics I, Linnéstr. 5, 04103 Leipzig, Germany<sup>2</sup>Max Planck Institute for Polymer Research, Ackermannweg 10, 55128 Mainz, Germany

FIG. 1. The phase difference between nanocrystal stress and macroscopic stress and strain can be measured by time-resolved FTIR, while applying sinusoidal mechanical fields. Microscopic stress in dry spider silk is shifted by  $< 2^\circ$  with respect to the macroscopic one, in the entire strain range for frequencies from  $10^{-2}$  to  $10^2$  Hz.

Spider dragline silk is composed of two high molecular weight proteins, rich in alanine and glycine. It outperforms all other natural silks as well as synthetic polymers, with respect to toughness, but it has not yet been synthesized in the lab, despite significant recent progress[1]. It is known that its structure resembles phase-separated diblock copolymers; alanine forms nanocrystals, while the rest forms low persistence-length structures. In recent works, we have found that alanine nanocrystals are interconnected by pre-stained chains; the applied pre-stress can reach a few hundreds of MPa[2, 3]. The high pre-stress is directly linked to the macroscopic mechanical properties. However, the way pre-stress is created during a complicated process, involving extrusion of the protein solution, absorption of water and reduction of pH value, is currently only poorly understood. In this study we attempt to determine the interconnection of the nanocrystal and amorphous phases in two states of spider dragline silk, native, and “supercontracted” with water. Infrared spectroscopy is employed to measure crystal stress - by means of absorption band shifts - with a high time resolution, while varying mechanical fields are applied to the silk[2, 4, 5]. It is found that dry silk is almost elastic; the phase difference between crystal- and macroscopic stress is close to zero. These results show that in both states of silk a serial arrangement between the crystalline and amorphous phases dominates the nanostructure.

The determination of the molecular order parameter of different moieties after deuteration proves that amide hydrogen exchange is a selective process, taking

place at the surface of  $\beta$ -sheet nanocrystals, imply-

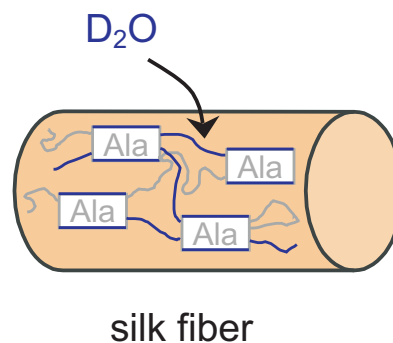


FIG. 2. Only the highly oriented parts of spider silk spidroins are accessible by water; these include the surface of the alanine nanocrystals and the pre-stained glycine-rich chains that interconnect them.

ing that only these regions are accessible by water[6]. The mechanical properties change dramatically when the fiber is wet, due to the fact that the pre-stress of the chains interconnecting the nanocrystals is irreversibly released. Water can break the hydrogen bonds of the amorphous chains, and, in combination with hydrophobic effects, it induces the formation of a physical network in the amorphous phase. After a stress limit is exceeded, the nanostructure of supercontracted silk is irreversibly transformed to one similar to native silk.

The results prove that the strong dependence of silk mechanical properties on hydration is due to the conformational changes that take place selectively in the chains with high pre-strain.

This work was supported by the Leipzig School of Natural Sciences, “Building with Molecules and Nano-Objects” (BuildMoNa).

\* Corresponding author: papadopoulos@physik.uni-leipzig.de

- [1] M. Heim, D. Keerl, T. Scheibel, *Angew. Chem. Intl. Ed.*, **48**, 3584 (2009).
- [2] P. Papadopoulos, J. Sölter and F. Kremer, *Eur. Phys. J. E: Soft Matter*, **24**, 193 (2007).
- [3] P. Papadopoulos, J. Sölter and F. Kremer, *Colloid Polym. Sci.*, **287**, 231 (2009).
- [4] R. Ene, P. Papadopoulos and F. Kremer, *Soft Matter*, **5**, 4568 (2009).
- [5] P. Papadopoulos, R. Ene, I. Weidner and F. Kremer, *Macromol. Rapid Commun.*, **30**, 851 (2009).
- [6] R. Ene, P. Papadopoulos and F. Kremer, *Polymer*, **51**, 4784 (2010).

## Effective Interactions between Colloids Suspended in a Bacterial Bath

Claudio Maggi,<sup>1,\*</sup> Luca Angelani,<sup>2</sup> and Roberto Di Leonardo<sup>2</sup>

<sup>1</sup>*Dipartimento di Fisica, Università di Roma "La Sapienza", I-00185, Roma, Italy*

<sup>2</sup>*Research Center SMC INFM-CNR, c/o Università di Roma "La Sapienza", I-00185, Roma, Italy*

Active suspensions, composed by self-propelled bacteria, represent an extremely interesting biophysical system where complex spatio-temporal behaviors may emerge [1]. When artificial micro-structures are suspended in those active baths an enhanced diffusive motion results from the collisions with swimming cells [2]. More interestingly, the off-equilibrium nature of bacterial suspension may give rise to surprising phenomena, like the conversion of chaotic bacterial motions into the *unidirectional* movement of micro-fabricated, asymmetric objects [3–5]. However, it still remains unknown if and how active baths can mediate effective interactions between suspended bodies.

We numerically and experimentally demonstrate that depletion of swimming cells in the gap between adjacent colloids induces a short-ranged *effective attraction*. This phenomenon is observed by studying the structure of diluted synthetic spheres suspended in a bacterial bath (see Fig. 1 (A) and (B)). The latter is composed by numerous *E. Coli* cells that are smaller than the passive spheres.

The radial distribution function  $g(r)$  of the micro-beads, measured by digital video-microscopy and by extensive computer-simulations, reveals a clear peak at short distances, signaling the presence of effective attractive forces (Fig. 1 (C)). Moreover the width of this peak is compatible with the average size of the bacteria, suggesting that bacteria-induced attractive forces may display additional analogies with equilibrium depletion-like interactions [6].

The phenomenon documented here represents a challenge for theories attempting a description based on non-equilibrium statistical-mechanics tools. Moreover it opens the way to further experimental investigations that aim to measure these forces *directly*, e.g. by optical-tweezers techniques. Finally new possibilities for applications arise, as assembling specially deigned micro-objects into large structures, by exploiting these bacterial-induced forces.

We acknowledge support from CINECA initiative for parallel computing, Italian Institute of Technology under the Seed project BACT-MOBIL and MIUR-FIRB project RBFR08WDBE.

\* Corresponding author: cmaggi@ruc.dk

[1] Hydrodynamic phenomena in suspensions of swimming micro-organisms, T. J. Pedley and J. O. Kessler, *Annu. Rev. Fluid Mech.* **24**,313 (1992).

- [2] Particle Diffusion in a Quasi-Two-Dimensional Bacterial Bath, Xiao-Lun Wu and Albert Libchaber, *Physical Review Letters*, **84**, 3017 (2007)
- [3] Self-starting micromotors in a bacterial bath, L. Angelani, R. Di Leonardo, Ruocco G., *Phys. Rev. Lett.*, **102**, 048104, (2009)
- [4] Bacterial ratchet motors, R. Di Leonardo al., *PNAS*, **107**, 9541, (2010)
- [5] Geometrically biased random walks in bacteria-driven micro-shuttles, Luca Angelani and Roberto Di Leonardo, *New Journal of Physics*, **12**, 113017, (2010)
- [6] Effective interactions in soft condensed matter physics C.N. Likos, *Physics Reports*, **348**, 267 (2001)

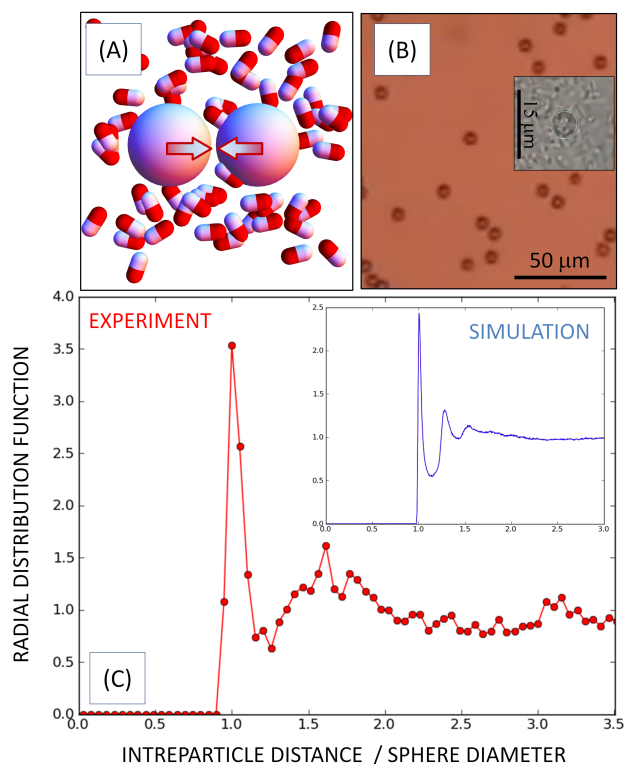


FIG. 1. (A) Pictorial representation of the system considered. Large passive micro-beads are immersed in a suspension of motile bacteria for studying the effective interaction acting between the micro-spheres. (B) Snapshot of the sample studied experimentally. Few silica spheres (5  $\mu\text{m}$  diameter) in a *E. Coli* bath (bacteria not visible at this magnification). In the inset a 100 $\times$  magnification image is shown, where the cells surrounding the sphere are clearly seen. (C) Radial distribution function measured in the experiment (the inset shows the  $g(r)$  obtained in the computer simulation). A clear peak is seen at short distance indicating the presence of effective attraction forces.

## Flow and Transport Properties of Microstructured Porous Media

Christian Scholz,<sup>1,\*</sup> Frank Wirner,<sup>1</sup> Yujie Li,<sup>1,2</sup> and Clemens Bechinger<sup>1,2</sup>

<sup>1</sup>*Physikalisches Institut, Universität Stuttgart,  
Pfaffenwaldring 57, 70569 Stuttgart, Germany*

<sup>2</sup>*Max-Planck-Institut für Metallforschung, Heisenbergstraße 3, 70569 Stuttgart, Germany*

Porous media are found extensively in nature from soils and rocks to biological tissues and foams. The corresponding transport properties for fluids, molecules and particles are of significant interest for biological drug delivery, environmental remediation, chemical reactors and oil recovery [1].

Despite the huge interest on this topic, relations between flow and transport properties of porous media and the corresponding microstructure are not fully understood. For many experimental systems transport processes at the pore scale cannot be visualized in real space. Here we present an experimental system which allows us to determine flow and transport properties of two-dimensional porous structures, with full knowledge of the microstructure and real space visualization of fluid flow and particle transport.

The transport processes are modeled and visualized by colloidal particles flowing through micro porous structures. Using soft lithography, any two-dimensional structure can be designed with full knowledge of the corresponding morphological properties, such as point statistics, correlation length, Minkowski functionals and pore size distributions [2].

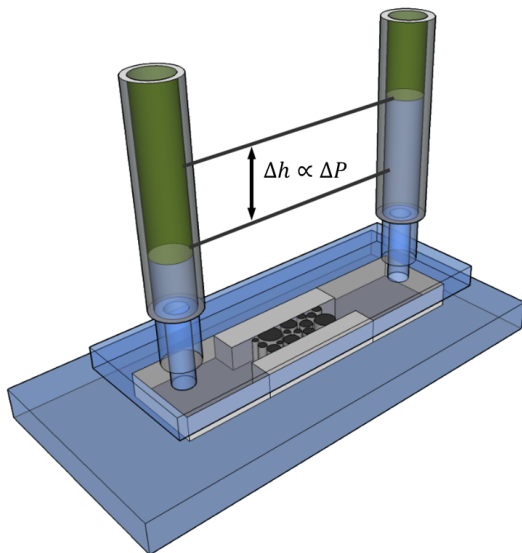


FIG. 1. A schematic of the experimental setup. The applied pressure is adjusted by the height of the two water columns connected to the porous structure.

Fig. 1 shows a schematic of the experimental setup. Pressure gradients can be accurately adjusted by the height of two water columns connected to the sample. By varying the applied pressure and spatial properties

of the sample structures the flow rate and thus the Reynolds number ( $Re$ ) and Péclet number ( $Pe$ ) can be varied to cover a large range of transport regimes. Using a fast and high-resolution camera system a detailed reconstruction of the particle trajectories inside the porous media can be performed with a temporal resolution of 2 ms and spatial resolution of  $0.3 \mu\text{m}$ . Fig. 2 shows a characteristic measurement of particle trajectories inside a random porous structure consisting of polydisperse overlapping circles.

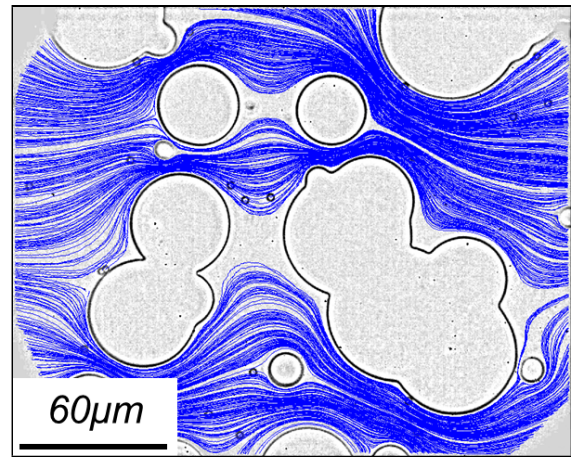


FIG. 2. Trajectories of colloidal particles flowing through a random porous structure.

Further analysis of the trajectories allows the reconstruction of the velocity field and the visualization of different dispersion mechanisms, such as molecular diffusion, bifurcation of the fluid streamlines and trapping of particles in stagnant parts.

Macroscopic quantifiers of flow and transport properties such as permeability and dispersion coefficients are studied in accordance with the morphological properties of different random porous structures. We are particularly interested in universal and non-universal relationships between the permeability and morphological properties of the random porous structures, such as transport exponents close to and far away from the percolation threshold [3].

\* Corresponding author: c.scholz@physik.uni-stuttgart.de

[1] Sahimi, M., *Rev. Mod. Phys.* **65**, 1393 (1993).

[2] Mickel, W. et al., *Biophys. J.* **95**, 6072 (2008).

[3] Halperin, B.I. et al., *Phys. Rev. Lett.* **54**, 22 (1985).

# Lorentz-like power-law decay of velocity anti-correlations in a supercooled liquid

Felix Höfling<sup>1,\*</sup> and Peter H. Colberg<sup>2,3</sup>

<sup>1</sup>Max-Planck-Institut für Metallforschung, Stuttgart,  
and Institut für Theoretische und Angewandte Physik, Universität Stuttgart, Germany

<sup>2</sup>Chemical Physics Theory Group, Department of Chemistry, University of Toronto, Canada

<sup>3</sup>Institut für Materialphysik im Weltraum, Deutsches Zentrum für Luft- und Raumfahrt (DLR), Köln, Germany

In the past few years, subdiffusive motion was discovered in several computer simulations for glass-forming mixtures of, e.g., strongly size-disparate particles. These findings are supported by theory, which predicts a continuous localisation transition being fundamentally different from the discontinuous ideal glass transition. The reference for this localisation transition is provided by the Lorentz model (tracer transport in a disordered matrix of hard obstacles), where the localisation transition is intimately connected to subdiffusion, an underlying percolation transition, and a divergent length scale [1].

Another link between supercooled liquids and the Lorentz model was recently provided by the observation that the velocity autocorrelation function (VACF) of a hard sphere liquid develops a power-law decay with negative prefactor,  $Z(t) \simeq -At^{-5/2}$ , upon undercooling [2]. Such a decay is reminiscent of the well-known long-time tail in the Lorentz model with the same exponent and sign; it is not specific to the localisation transition, it is universal and present at all densities [3]. For the supercooled liquid, it was speculated that the power law originates in the confined motion of mobile particles in a matrix of immobile regions as provided by the dynamic heterogeneities.

We have harnessed the compute power of recent graphics processors [4] to measure the VACF in the supercooled Kob-Andersen (KA) mixture for large systems sizes of 50,000 particles and low temperatures, providing data with an excellent signal-to-noise ratio. As the system is supercooled, the emergence of glassy

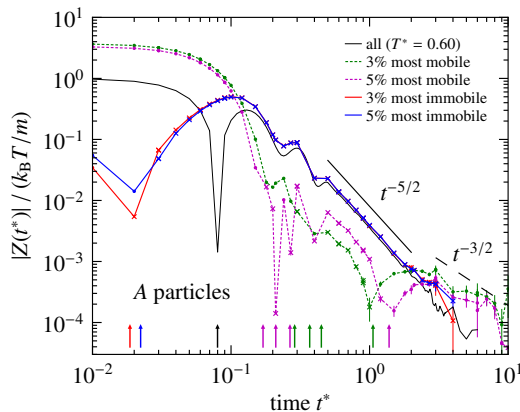


FIG. 1. VACFs of A particles at  $T^* = 0.60$  restricted to the most mobile (dotted) or immobile (dashed) particles using thresholds of 3% and 5%. The thin, black line shows the VACF of all A particles for comparison. Arrows at the bottom point at the zero crossings of the data.

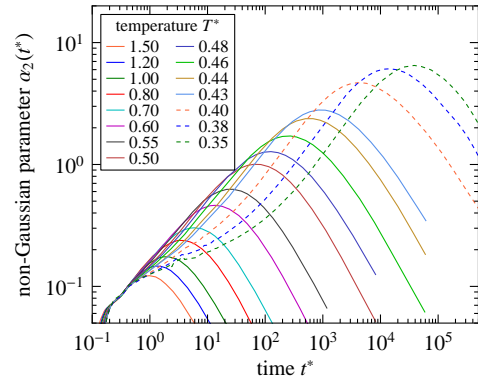


FIG. 2. The non-Gaussian parameter of A particles in a KA mixture for a wide range of temperatures. Dashed lines refer to smaller systems of merely 5,000 particles.

dynamics is systematically accompanied by a power-law decay of the VACF at intermediate times with exponent  $5/2$  and negative prefactor, similarly as for the hard sphere liquid. The role of dynamic heterogeneities for this power-law decay is addressed by considering correlation functions that are restricted to the most mobile or immobile particles (Fig. 1). We find that the Lorentz-like decay is absent in the VACF of the most mobile particles and conclude that the power law is *not* a manifestation of dynamic heterogeneities. For the most *immobile* particles, on the other hand, the Lorentz-like decay is well pronounced. Combining with recent analytical progress on the overdamped Lorentz model [5], we propose that the relevant mechanism for the power law is given by repeated encounters with the same particles due to the localised motion in quasi-arrested, microscopic particle cages.

The power law deteriorates at very low temperatures ( $T^* \lesssim 0.5$ ), which hints at additional relaxation processes beyond the slow rearrangement of cages. This view is supported by inspection of the non-Gaussian parameter (NGP) at very low temperatures, where scaling of the NGP breaks down and where its rising edge is delayed to increasingly longer times (Fig. 2).

\* Corresponding author: hoefling@mf.mpg.de

- [1] F. Höfling, T. Franosch, and E. Frey, Phys. Rev. Lett. **96**, 165901 (2006).
- [2] S. R. Williams, G. Bryant, I. K. Snook, and W. van Meegen, Phys. Rev. Lett. **96**, 087801 (2006).
- [3] F. Höfling and T. Franosch, PRL **98**, 140601 (2007).
- [4] P. H. Colberg and F. Höfling, arXiv:0912.3824.
- [5] T. Franosch, F. Höfling, T. Bauer, and E. Frey, Chem. Phys. **375**, 540 (2010).

## Aspects of subdiffusive transport in the Lorentz Model

Markus Spanner\* and Thomas Franosch

*Institut für Theoretische Physik, Universität Erlangen-Nürnberg, Staudtstraße 7, 91058, Erlangen, Germany*

The Lorentz model is a simple model for transport in porous materials, where a point-like tracer moves through an array of quenched spherical obstacles. Introduced by H. A. Lorentz in 1905 to describe electron conductance in metals, it is nowadays also used as a model e.g. for ion transport in glassforming liquids. Extensive computer simulations on the Lorentz model were performed recently [1] and it was shown that a window of subdiffusive transport  $\delta r_\infty^2(t) \sim t^{2/z}$ ,  $z = 6.25$  opens up at obstacle densities near the void-space percolation transition. The configuration space is known to decompose into a hierarchy of void space clusters and the motion has now been well characterized in terms of all-cluster averages.

In this work, we have performed simulations of particles confined to the ‘infinite’ cluster, i.e. the fraction of void space that percolates through the system of obstacles. The computational challenge is to identify the percolating cluster by a suitable Voronoi tessellation before the trajectories are calculated by molecular dynamics simulations. We find that the motion is still subdiffusive  $\delta r_\infty^2(t) \sim t^{2/d_w}$  with a new exponent  $d_w = 4.81$  known as the walk dimension in the context of random walks in lattice percolation (see Fig. 1). Besides measuring the volume of the remaining infinite cluster as a function of the obstacle density for systems of random overlapping spheres, a detailed analysis of transport on this infinite cluster was carried out, including the vanishing of the diffusion coefficient as the transition point is approached, the non-gaussian parameter, the influence of finite system sizes and extrapolation of the critical density.

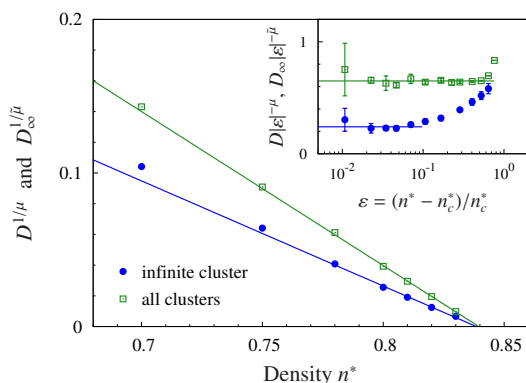


FIG. 1. Transport on the infinite cluster of the 3D Lorentz model displays mean-square displacement  $\delta r_\infty^2(t) \sim t^{2/d_w}$  with  $d_w = 4.81$ .

Second, since in all realistic systems the host structure displays short-range correlations, it is important to investigate the possible influence of obstacle corre-

lations on the subdiffusive exponent. In the Lorentz model the statistics of the narrow gaps enter explicitly into the dynamic exponent and it is unclear whether the universality class is affected by changing the local properties of the disordered system. Therefore, we have replaced the randomly distributed spheres by snapshots of equilibrated hard-sphere fluids. Due to the divergent length scale, large system sizes have to be considered and we achieved equilibrated samples comprising of up to 400,000 particles. The critical point is reached by gradually increasing the tracer radius up to the point where the infinite cluster ceases to exist. We corroborate for the first time, that indeed the Lorentz model is representative for the universal aspects of tracer motion in disordered solids and that the values of the exponents are robust (see Fig. 2). In particular, we find that the long-time behavior in the immediate vicinity of the localization transition is identical to the Lorentz model. For densities off the critical point, differences become manifest and we conclude that to compare with realistic molecular dynamics simulations for ion conductors the local structural properties need to be modeled properly.

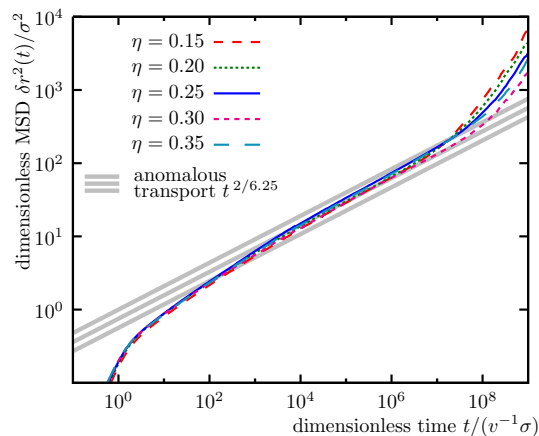


FIG. 2. Mean-square displacement  $\delta r_\infty^2(t) \sim t^{2/z}$  at the percolation transition at different hard-sphere packing fractions  $\eta$ . The long-time exponent  $z$  is compatible with the value of the Lorentz model, in particular it is independent of  $\eta$ .

M. S. and T. F. gratefully acknowledge support via the DFG research unit FOR-1394.

\* Corresponding author: markus.spanner@physik.uni-erlangen.de

- [1] F. Höfling, T. Franosch, and E. Frey, Phys. Rev. Lett. **96**, 165901 (2006).
- [2] T. Franosch, M. Spanner, T. Bauer, G. E. Schröder-Turk, F. Höfling, J. Non-Cryst. Solids (2010) doi:10.1016/j.jnoncrysol.2010.06.051

## Dynamic arrest of colloids in porous environments: disentangling crowding and confinement

Jan Kurzidim,<sup>1,\*</sup> Daniele Coslovich,<sup>2</sup> and Gerhard Kahl<sup>1</sup>

<sup>1</sup>*Institut für Theoretische Physik and CMS, Technische Universität Wien,  
Wiedner Hauptstraße 8-10, 1040 Wien, Austria*

<sup>2</sup>*Laboratoire des Colloïdes, Verres et Nanomatériaux, Université Montpellier 2,  
Place Eugène Bataillon, 34095 Montpellier cedex 5, France*

Using molecular dynamics simulations we have studied the slow dynamics of a dense hard-sphere fluid moving in a disordered configuration of hard-sphere obstacles. The high density and the quenched disorder lead to two distinct dynamic arrest mechanisms—crowding and confinement—that can also be observed for instance in the movement of proteins in cytoplasm.

We have investigated the particular case of “quenched-annealed” (QA) systems in which the obstacles are quenched from equilibrium fluid, and the fluid particles are subsequently inserted at random positions [1, 2]. Upon varying the volume fraction of the fluid ( $\phi_f$ ) and of the obstacles ( $\phi_m$ ) we discovered scenarios of both discontinuous and continuous dynamic arrest, anomalous diffusion, as well as a decoupling of the time scales for the relaxation of the single-particle and the collective correlators. Our observations are consistent with many predictions by a recent extension of mode-coupling theory to systems with quenched disorder [3, 4].

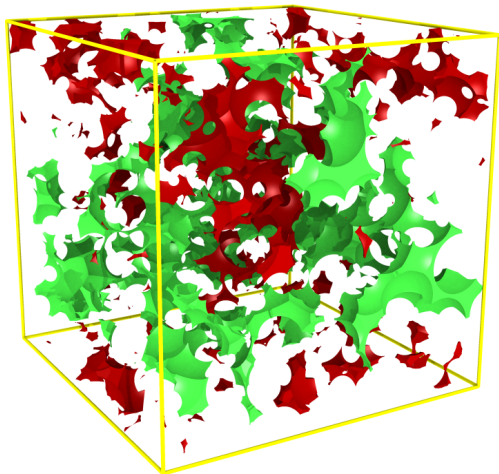


FIG. 1. Graphical representation of the volume accessible to the center of a fluid particle in a QA system. The light green void percolates across the simulation cell (taking into account periodic boundary conditions) whereas the dark red voids are of finite size. The volume fraction of the 714 obstacle particles (blanked out) is 25%, which is close to the percolation threshold.

In order to elucidate in more detail the microscopic origin of the observed dynamic arrest scenarios, we performed a Delaunay decomposition of the pore structure (similar to, yet more elaborate than those done in [5] and [6]). We were thus able to distinguish between particles that are “free” (located in the void percolating through space) and “trapped” (confined in

a void of finite volume) (Fig. 1). For these two classes of fluid particles we then separately calculated the same set of dynamic correlators as in [2]: the single-particle intermediate scattering function  $F_s(k, t)$ , the mean-squared displacement  $\delta r^2(t)$  and its logarithmic derivative  $z(t) = d[\log \delta r^2(t)]/d[\log t]$ , as well as the self part of the van Hove function.

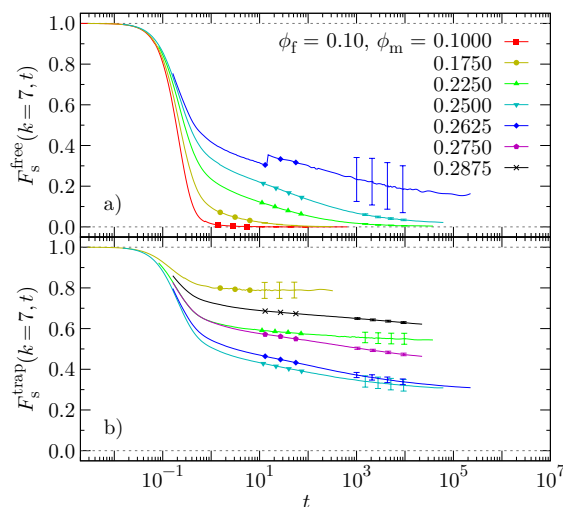


FIG. 2. Single-particle intermediate scattering function  $F_s(k^*, t)$  for constant fluid volume fraction  $\phi_f = 0.1$  and various obstacle volume fractions  $\phi_m$ . (a) “free” fluid particles, (b) “trapped” fluid particles. The wave vector  $k^* = 7$  is near the first peak in the static structure factor.

Among our key findings are: (1) as expected,  $F_s^{\text{trap}}(k, t)$  never completely relaxes whereas  $F_s^{\text{free}}(k, t)$  always does (see Fig. 2), (2) since the long-time values of  $F_s^{\text{trap}}(k, t)$  and  $\delta r_{\text{trap}}^2(t)$  reflect the trap sizes, they attain an extremum at the percolation transition when varying  $\phi_m$  (3) the exponent of subdiffusion of the free fluid particles is virtually the same as that of the free and trapped particles combined, and (4) for suitable  $\phi_f$  and  $\phi_m$ , dynamic heterogeneity is present among the free and the trapped particles.

\* Corresponding author: kurzidim@cmt.tuwien.ac.at

- [1] J. Kurzidim, D. Coslovich, and G. Kahl, *Phys. Rev. Lett.* **103**, 138303 (2009).
- [2] J. Kurzidim, D. Coslovich, and G. Kahl, *Phys. Rev. E* **82**, 041505 (2010).
- [3] V. Krakoviack, *Phys. Rev. E* **75**, 031503 (2007).
- [4] V. Krakoviack, *Phys. Rev. E* **79**, 061501 (2009).
- [5] B. J. Sung and A. Yethiraj, *J. Chem. Phys.* **128**, 054702 (2008).
- [6] S. Babu, J. C. Gimel, and T. Nicolai, *J. Phys. Chem. B* **112**, 743 (2008).

# Influence of Matrix Dynamics on Anomalous Diffusion in Strongly Heterogeneous Binary Mixtures

Simon Schnyder,<sup>1,\*</sup> Thomas Voigtmann,<sup>1,2</sup> and Jürgen Horbach<sup>1</sup>

<sup>1</sup>*Institut für Materialphysik im Weltraum, Deutsches Zentrum für Luft- und Raumfahrt (DLR), 51170 Köln, Germany*

<sup>2</sup>*Zukunftskolleg and Fachbereich Physik, Universität Konstanz, 78457 Konstanz, Germany*

Mass transport in disordered and heterogeneous systems, and in porous media is an important topic in fields ranging from physics to engineering to biology.

A property of such systems is that they consist of at least two components. One component serves as a slow matrix, in which the other, faster component moves. The slow matrix is heterogeneous and is either frozen or relaxes on time scales that are orders of magnitude larger than the ones of the faster component. The smaller component then can show anomalous diffusion, i.e. subdiffusive growth of its mean-squared displacement (MSD).

The origin of anomalous diffusion is debated, but it has been shown, that geometric confinement of the tracer, e.g. in fractal environments, is enough to trigger subdiffusive motion. One of the simplest models showing this is the Lorentz model (LM), a single particle in a potential of randomly placed, overlapping obstacles. There, the approach to a localisation transition is responsible for anomalous diffusion [1]. The connection between anomalous diffusion and a localisation transition has also been made in work on quenched annealed systems [2, 3].

The LM neglects two main features of heterogeneous media, the relaxation of the matrix and the interactions of many small particles. Two-component mixtures of colloids have these features. It has been shown, under high size ratios of the two species, that such mixtures go into a collective glassy state dominated by the big particles, while the small particles stay mobile, eg in [4] or our figure. The large particles follow the standard glass-transition scenario. On increasing particle density, their MSD exhibits a plateau over increasingly longer time scales, with a cross over to diffusion at increasingly larger times. The small particles' MSD shows no sign of glassy dynamics, but instead exhibits subdiffusive growth in increasing time spans as one goes to higher densities. Strong preasymptotic corrections make it difficult to identify power laws or asymptotic scaling near the localisation transition density. A connection to the LM couldn't be satisfactorily accomplished, even with small particle interactions turned off.

Therefore, it remains a challenge to understand the complex interplay of the glass and the localisation transition, especially the influence of the matrix dynamics and small particle interactions on anomalous diffusion.

Here, the same binary mixture of purely repulsive soft spheres with a large size ratio as in [4] is used in

molecular dynamics simulations to identify the effects of the large particle dynamics on the small particle anomalous diffusion. At densities, where the species' relaxation times are highly separated, the system was quenched from a low density and then equilibrated for a range of times. The large particle MSD then shows ageing: The plateau, that arises at intermediate times when the system has been fully equilibrated is disturbed by additional relaxation processes. Nonetheless, the long time dynamics of the small particles are nearly completely undisturbed by this.

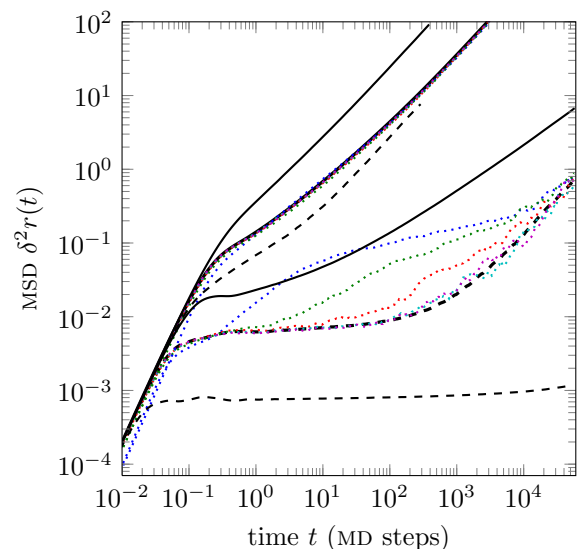


FIG. 1. Mean squared displacements for small particles (solid) and large particles (dashed) at densities  $\rho\sigma_{ll}^3 = 2.0, 2.8, 4.2$ . Dotted colored lines for both species at density  $\rho\sigma_{ll}^3 = 2.8$  for different equilibration times.  $\sigma_{ll}$  is large particle diameter.

Furthermore, we study the small particle dynamics, when the large particles are held fixed. Thus we are able to identify which contributions to the small particle relaxation come from the dynamics of the matrix. The asymptotic dynamics is discussed in terms of anomalous diffusion power laws.

This work was funded by DFG FOR1394 P8.

\* Corresponding author: simon.schnyder@dlr.de

- [1] F Höfling, Th Franosch, and E Frey, Phys. Rev. Lett. **96**, 165901 (2006)
- [2] J Kurzydum, D Coslovich, and G Kahl, Phys. Rev. E. **82**, 041505 (2010).
- [3] K Kim, K Miyazaki, and S Saito, EPL **88**, 36002 (2009)
- [4] Th Voigtmann and J Horbach, Phys. Rev. Lett. **103**, 205901 (2009).

## Anomalous diffusion and long-time tails in quenched-disordered systems

W. Schirmacher,<sup>1,2,\*</sup> C. Ganter,<sup>3</sup> and S. Köhler<sup>1</sup>

<sup>1</sup>*Institut für Physik, Johannes-Gutenberg-Universität Mainz, Staudinger Weg 7, D-55099 Mainz*

<sup>2</sup>*Physik-Department E13, Technische Universität München, James-Frank-Strasse 1, D-85747 Garching*

<sup>3</sup>*Institut für Röntgendiagnostik, Technische Universität München, Ismaninger Str. 22, D-81675 München*

We address the diffusive motion of a single particle in a quenched-disordered environment. We model the disorder by means of the assumption of a spatially fluctuating diffusion coefficient. By replacing the first with the second time derivative in the equation of motion this model can be mathematically mapped to a problem of wave propagation in a quenched disordered system.

We show that the velocity autocorrelation function (VAF) of the diffusion model exhibits a long-time tail of the form  $Z(t) \propto t^{-(d+2)/2}$ , where  $d$  is the dimensionality. In the analogous wave model this corresponds to the presence of Rayleigh scattering  $\ell(\omega) \propto \omega^{-(d+1)}$ , where  $\ell$  is the mean free path [1]. If the diffusing particles are charged, the long-time tail of the VAF leads to an anomalous low-frequency behavior of the loss function of the form  $(\sigma'(\omega) - \sigma(0))/\omega \propto \omega^{(d-2)/2}$ , where  $\sigma'(\omega)$  is the AC conductivity.

The mean square displacement in the diffusion model exhibits a crossover from anomalous diffusion, i.e.  $d \ln \langle r^2(t) \rangle / d \ln t < 1$  to normal diffusion with  $d \ln \langle r^2(t) \rangle / d \ln t = 1$ . In the frequency domain this crossover corresponds to a crossover from a frequency-independent to a frequency dependent AC conductivity. The presence of anomalous diffusion is shown to be related to the fact that the diffusion spectrum obeys random matrix statistics and to be generic for any quenched-disordered diffusion system.

An off-lattice version of the coherent-potential approximation (CPA) is derived [2] using functional-integral techniques.

The CPA equation for calculating the frequency-dependent diffusivity is

$$D(\omega) = \left\langle \frac{\hat{D}(\mathbf{r})}{1 - \frac{1}{2} \Lambda(\omega) [D(\omega) - \hat{D}(\mathbf{r})]} \right\rangle \quad (1)$$

where  $\langle \dots \rangle$  is an average over the fluctuating diffusivity  $\hat{D}(\mathbf{r})$ . The auxiliary function  $\Lambda(\omega)$  is given by

$$\Lambda(\omega) = \sum_{|\mathbf{k}| < k_c} \frac{k^2}{i\omega - D(\omega)k^2} \quad (2)$$

The cutoff  $k_c$  is inversely proportional to the size of the coarse-graining volume used to transform a microscopic transport equation into a diffusion equation

with fluctuating  $\hat{D}(\mathbf{r})$  [1]. The frequency-dependent diffusivity  $D(\omega)$  is just the Laplace transform (with  $p = i\omega + \epsilon$ ) of the VAF, and  $D(p)/p^2$  is the Laplace transform of the mean-square displacement. Via the Einstein relation  $\sigma(\omega) = (Nq^2/Vk_B T)D(\omega) = \sigma' + \sigma''$  the AC conductivity is obtained from the real part of  $D(\omega)$ . The form (2) of  $\Lambda(\omega)$  guarantees the presence of the non-analyticity in  $D(\omega)$  leading to the long-time tail in the VAF. If  $\Lambda$  is taken to have a simpler form (without diffusion pole) earlier effective-medium theories for diffusion in disordered media are obtained [3–6], which do *not* contain the non-analyticity.

If  $\hat{D}(\mathbf{r})$  is assumed to exponentially depend on another fluctuating quantity, e.g. an activation energy

$$\hat{D}(\mathbf{r}) = D_0 e^{-\epsilon(\mathbf{r})/k_B T} \quad (3)$$

the AC conductivity is shown to be approximately of the form

$$\sigma'(\omega) \propto \omega^s \quad (4)$$

with  $s \approx 0.8$ , a behavior frequently found in glassy fast-ion conductors. The DC conductivity and diffusivity of such a model can be shown to universally obey an Arrhenius law, independently of the distribution [6]. These features are also contained in the old theories ([3–5]).

As the CPA allows for the treatment of any distribution of local diffusivities, including alloy disorder, the CPA is also a mean-field theory of a percolation model, i.e. a schematic version of a Lorentz model. Near the percolation threshold the off-lattice CPA predicts the same critical exponents as the lattice CPA, namely  $D(p) \propto (p - p_c)^1$  and  $D(\omega) \propto \omega^{1/2}$  in the critical regime.

\* Corresponding author: wschirma@ph.tum.de

[1] C. Ganter and W. Schirmacher Phys. Rev. B **82**, 094205 (2010)

[2] S. Köhler, C. Ganter and W. Schirmacher, to be published

[3] C. R. Gochanour, H. C. Andersen and M. D. Fayer, J. Chem. Phys. **70**, 4254 (1979)

[4] B. Movaghar and W. Schirmacher, J.Phys., C **14**, 859 (1981)

[5] P. N. Butcher and S. Summerfield, J.Phys., C **L1099**, 859 (1981)

[6] W. Schirmacher, Sol. State Ionics, **28–30**, 129 (1988)

## On anomalous diffusion and fluctuation-dissipation relations

Alessandro Sarracino,\* Dario Villamaina, Giacomo Gradeingo, Andrea Puglisi, and Angelo Vulpiani

CNR-ISC and Dipartimento di Fisica, Università di Roma “La Sapienza”, Roma, Italy

In his seminal paper on the Brownian Motion, Einstein found the first example of fluctuation-dissipation relation. In the absence of external forcing one has

$$\langle x(t) \rangle = 0 \quad , \quad \langle x^2(t) \rangle \simeq 2Dt \quad , \quad (1)$$

where  $x$  is the position of the Brownian particle and  $D$  the diffusion coefficient. Once a small constant external force  $F$  is applied one has a linear drift  $\overline{\delta x(t)} \simeq \mu Ft$  which is proportional to  $\langle x^2(t) \rangle$  and the Einstein relation holds:  $\mu = \beta D$ .

However, it is now well established that in many systems the mean square displacement of a tagged particle does not grow linearly with time and anomalous diffusion can be observed, i.e.

$$\langle x^2(t) \rangle \sim t^{2\nu} \quad \text{with } \nu \neq 1/2, \quad (2)$$

see for instance [1].

Here we consider a couple of one-dimensional models, showing subdiffusive behaviour, and focus on the study of the relation between the response to an external driving force and unperturbed correlations. In particular, we study the dynamics of a single particle making a random walk on a “comb” lattice and the single-file model, i.e. a gas of hard rods coupled to an external thermal bath. In both systems we observe that the equilibrium fluctuation-dissipation theorem in the form of the Einstein relation is satisfied also in the subdiffusive regime, i.e. the response to an external force and spontaneous fluctuations are proportional. On the other hand, introducing “non equilibrium” conditions through a stationary current, in the form of unbalanced transition probabilities for the comb or with dissipative interactions for the single-file, we find in both cases strong violations of the Einstein relation (see figure 1 and reference [2]).

For the comb model, where the transition rates  $W[(x, y) \rightarrow (x', y')]$  of the process are explicitly known, we are able to write down an out of equilibrium fluctuation-dissipation relation [3–5]

$$\overline{\delta x(t)} = \frac{1}{2} [\langle x(t)x(t) \rangle - \langle x(t)x(0) \rangle - \langle x(t)A(t, 0) \rangle], \quad (3)$$

where  $A(t, 0) = \sum_{t'=0}^t B(t')$  and

$$B[(x, y)] = \sum_{(x', y')} (x' - x)W[(x, y) \rightarrow (x', y')], \quad (4)$$

which allows us to recover an exact relation between response function and unperturbed correlation func-

tions (see figure 1). The observable  $B$  gives an effective measure of the propensity of the system to leave a certain state  $(x, y)$ . Relation (3) is quite general and holds for all kinds of non-equilibrium states, stationary or not. It has been used to build very efficient field-free algorithms for the measure of the response function in the framework of aging systems [6].

In conclusion, we find that the Einstein formula holds also for models showing anomalous diffusion, provided that no currents are present in the system. On the contrary, when non equilibrium conditions are considered, strong violations occur, and a generalized non-equilibrium relation has to be taken into account.

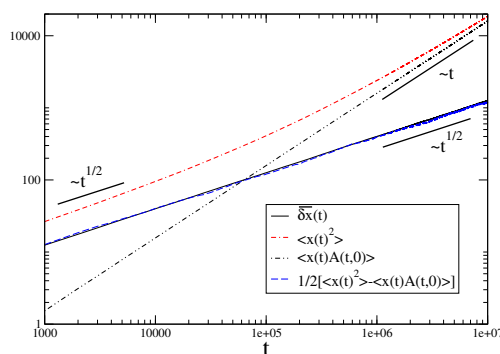


FIG. 1. Response function (black line) and m.s.d. (red dotted line) measured in the comb model. The correlation function  $\langle x(t)A(t, 0) \rangle$  (black dotted line) yields the right correction to recover the full response function (blue dotted line), in agreement with the FDR (3).

The work of GG, AS, DV and AP is supported by the “Granular-Chaos” project, funded by Italian MIUR under the grant number RBID08Z9JE.

\* Corresponding author: alessandro.sarracino@roma1.infn.it

- [1] R. Metzler and J. Klafter, Phys. Rep. **339**, 1 (2000).
- [2] D. Villamaina, A. Puglisi and A. Vulpiani, J. Stat. Mech. L10001 (2008).
- [3] E. Lippiello, F. Corberi and M. Zannetti, Phys. Rev. E **71**, 036104 (2005).
- [4] E. Lippiello, F. Corberi, A. Sarracino and M. Zannetti, Phys. Rev. E **78**, 041120 (2008).
- [5] M. Baiesi, C. Maes and B. Wynants, Phys. Rev. Lett. **103**, 010602 (2009).
- [6] E. Lippiello, F. Corberi and M. Zannetti, J. Stat. Mech. P07002 (2007).



## 4 Author Index

Page numbers in **bold face** indicate corresponding authors of oral contributions. Page numbers in *italic type* indicate coauthors.

- K. Adrjanowicz, 85, 87  
B. J. Alder, 140  
M. Amirkhani, 113, 114  
L. Angelani, 152  
R. Angelini, 57  
C. A. Angell, **70**, 74, 110  
A. Arbe, **65**  
L. Assoud, 116  
K. E. Avila, 76  
P. Bacova, 136  
N. P. Bailey, 30, 90, 93, 95  
M. Ballauff, 40, 41  
P. Ballesta, 45  
C. Barentin, 125, 128  
M. Barrio, 86  
J. K Basu, 83  
C. Bechinger, 149, 153  
A.L. Bel'tyukov, 108, 109  
J. Bergenholtz, 113, 114  
M. Bernabei, 80  
L. Berthier, 22, 44, 56, **60**, 62, 67  
R. Besseling, **45**  
K. Binder, 77, 121  
G. Biroli, 48  
L. Bocquet, 44, 128  
L. Bøhling, 92  
D. Bonn, 105  
V. Bořan, 54  
J.M. Brader, **40**, 42  
J. F. Brady, 122  
N. B. Braham, 135  
G. Brambilla, 56  
A. Bronsch, 132  
H. Bruus, 78  
G. Bryant, 141  
U. Buchenau, 96  
R. Busch, 110, 111  
S. Busch, 79  
I. Buttinoni, 149  
S. Buzzaccaro, **56**  
F. Caltagirone, 102  
M. Camargo, 145  
C. Cammarota, **25**, 48  
A. de Candia, 103  
S. Capaccioli, 86  
F. Cardinaux, **51**, 135  
C. Caroli, 127  
R. Casalini, 90  
H. E. Castillo, 76  
M. E. Cates, 45, 69, 143  
A. Cavagna, 25, 47  
D. Chandler, 66  
S. Chandran, 83  
B. Charbonneau, 63  
P. Charbonneau, 27, **63**  
D. Charkaborty, 34  
J. Chatteraj, 127  
P. Chaudhuri, **44**  
S.-H. Chen, 71  
V. K. Chikkadi, 105  
T. Christensen, 89, 90, 97  
F. Cichos, 34  
S. Ciliberto, 58  
L. Cipelletti, 56  
P. H. Colberg, 154  
A. Colin, 44  
J. Colmenero, 65, 80, 82  
J. Colombani, 128  
A. Coniglio, 103  
C. Corsaro, 71  
D. Coslovich, **55**, 156  
A. Crisanti, 101  
P. J. Daivis, 78  
C. Dalle-Ferrier, **53**  
C. Dasgupta, **23**  
E. Del Gado, 24, 115  
G. Diezemann, 99  
T. Divoux, 125  
J. C. Dyre, **30**, 35, 89, 90, 91, 93, 94, 95  
P. Díaz-Leyva, 135  
F. Ebert, 52, 129  
S. U. Egelhaaf, 38, 53  
L. F. Elizondo-Aguilera, 137  
I. Elyukhina, 106  
R. Ene, 151  
Z. Evenson, 111  
L. A. Fernández, 142  
U. Ferrari, 102  
L. Foini, 29  
D. Fragiadakis, 90  
M. Franke, 144  
T. Franosch, 54, 155  
S. Franz, **49**, 102  
S.J. Frey, 40  
M. Fuchs, 40, 42, 43  
A. Furukawa, 75  
I. Gallino, 110  
P. Gallo, **32**  
C. Ganter, 158  
J. P. Garrahan, 66  
M. Gauthier, 134  
I. Giardina, 25  
S. C. Glotzer, 66  
N. Gnan, 30, **35**, 95, 138  
M. V. Gnann, 43  
J. R. Gomez-Solano, **58**  
G. Gradeingo, 159  
G. Gradenigo, 25, 37, 147, 148  
S. Gradmann, 81  
A. Gray-Weale, 133  
T. S. Grigera, 25, 37, 47  
K. Grzybowska, 84

- A. Grzybowski, 84  
 D. Gundermann, 90  
 D. Hajnal, 42, 54  
 R. D.L. Hanes, 53  
 J. S. Hansen, 78  
 J. L. Harden, 135  
 Ch. J. Harrer, 43  
 M. Hassaine, 98  
 T. K. Haxton, 104  
 T. Hecksher, 89, 90  
 L. O. Hedges, 66  
 O. Herbst, 123  
 A. Heuer, 46, 99, 100, 120  
 F. Höfling, 154  
 M. Hofmann, 81  
 J. Horbach, 31, 39, 121, 157  
 M. Hussainov, 126  
 A. Ikeda, 27  
 P. Ilg, 24, 115  
 T. S. Ingebrigtsen, 94  
 L. Isa, 45  
 M. Isobe, 140  
 A. Ivlev, 131  
 S. Jabbari-Farouji, 112  
 A. Jacob, 133  
 H. Jacquin, 62  
 B. Jakobsen, 89, 90  
 M. C. Jenkins, 53  
 Y. Jin, 63  
 P. Jop, 44  
 R. Juárez-Maldonado, 36, 137  
 B. Kabtoul, 98  
 G. Kahl, 55, 156  
 L.V. Kamaeva, 107, 108  
 K. Kaminski, 85, 87  
 A. K. Kandar, 83  
 V. Kapko, 70  
 S. Karmakar, 23  
 T. Kawasaki, 68  
 P. Keim, 52, 129  
 G. Kelp, 126  
 A. S. Keys, 66  
 C. L. Klix, 129  
 W. Kob, 22  
 S. Köhler, 158  
 K. Koperwas, 84  
 N. Koumakis, 38, 122  
 F. Kremer, 151  
 K. Kroy, 34  
 M. Krüger, 42, 53  
 J. Kurzidim, 156  
 V.I. Lad'yanov, 107, 108, 109  
 S. Lang, 54  
 M. Laurati, 38  
 A. Lederer, 130  
 A. Lemaître, 127  
 M. Leocmach, 68  
 R. D. Leonardo, 152  
 L. Leuzzi, 101, 102  
 D. Levine, 50  
 Y. Li, 153  
 C. N. Likos, 145  
 A. J. Liu, 104  
 H. Löwen, 116, 150  
 I. Lynch, 135  
 C. Maggi, 35, 152  
 M. Maiti, 146  
 F. Mallamace, 71  
 S. Manneville, 125  
 G. Maret, 52, 129  
 O. Marti, 113, 114  
 V.A. Martinez, 141  
 V. Martín-Mayor, 142  
 V. V. Maslov, 109  
 T. G. Mason, 51  
 P. J. Masset, 132, 133  
 D. V. Matyushov, 70  
 S. Mazoyer, 52  
 M. Medina-Noyola, 36, 117  
 J. A. van Meel, 27  
 W. van Meegen, 141  
 S. G. Menshikova, 109  
 R. Messina, 116  
 A. Meyer, 31  
 K. Miyazaki, 27  
 G. Monaco, 64  
 A. Moreno, 55, 65, 80, 82, 136, 145  
 G. E. Morfill, 131  
 H. Morhem, 79  
 M. Mosayebi, 24  
 A. Moussaid, 57  
 A. N. Murugan, 86  
 K. Mutch, 38  
 S. R. Nagel, 104  
 T. Narayanan, 57  
 B. Nienhuis, 105  
 K. Niss, 89, 90, 91  
 V. Nosenko, 131  
 M. Oettel, 54  
 N. B. Olsen, 89, 91  
 H. C. Öttinger, 24  
 M. Paluch, 84, 85, 87  
 M. Paoluzzi, 101  
 P. Papadopoulos, 151  
 S. Papenkort, 124  
 J. Papini, 97  
 L.C. Pardo, 86  
 G. Parisi, 25, 49, 102  
 A. Parsaeian, 76  
 R. Pastore, 103  
 W. Paul, 77  
 U. R. Pedersen, 30, 90, 95  
 G. Pérez-Ángel, 36  
 G. Petekidis, 38, 45, 122  
 L. Petit, 128  
 A. Petrosyan, 58  
 R. Piazza, 56  
 M. Pica Ciamarra, 103  
 W. C. K. Poon, 45, 69, 143  
 A. Puglisi, 37, 147, 148, 159  
 P. N. Pusey, 69, 143  
 P. E. Ramírez-González, 36, 117

- M. A. Ramos, 98  
R. Rand, 126  
C. Rehwald, 46, 100  
K. Reinheimer, 40  
M. Reufer, 135  
F. Ricci-Tersenghi, 49, 102  
R. Rice, 59  
D. Rings, 34  
T. Rizzo, 49, 102  
M. Roland, 90  
S. Roldán-Vargas, 22  
M. Romanini, 86  
E. A. Rössler, 81  
R. Roth, 59  
C. P. Royall, 59  
O. Rubner, 46  
J. Russo, 139  
B. Ruzicka, 57  
L. E. Sánchez-Díaz, 36  
E. Sanz, 69, 141, 143  
C. K. Sarika, 83  
A. Sarracino, 37, 147, 148, 159  
S. Sastry, 23, 146  
F. Sausset, 50  
P. Schall, 105  
F. Scheffold, 51, 135  
R. Schilling, 28, 42, 54  
W. Schirmacher, 158  
B. Schmid, 28  
M. Schmiedeberg, 104  
S. Schnyder, 157  
C. Scholz, 153  
H. J. Schöpe, 130, 144  
T. B. Schröder, 30, 35, 90, 92, 93, 94, 95  
C. Schroer, 46, 120  
F. Sciortino, 57, 80, 138, 139  
T. Scopigno, 88  
M. Selmke, 34  
G. Semerjian, 29  
B. Seoane, 142  
S. Sharifi, 113, 114  
M. Siebenbürger, 40, 41  
M. Z. Slimani, 82  
M. Spanner, 155  
M. Sperl, 61  
S. Srivastava, 83  
H. E. Stanley, 71  
I.V. Sterkhova, 107  
L. Strauss, 55  
A. Swietly, 84  
G. Szamel, 26  
M. Sztucki, 57  
J. Ll.Tamarit, 86  
H. Tanaka, 68, 75  
G. Tarjus, 48, 67  
P. Tartaglia, 138  
M. Tarzia, 48  
T. Tätte, 126  
B.D. Todd, 78  
S. Toxvaerd, 94  
E. Trizac, 112  
D. Truzzolillo, 134  
K. Ueno, 74  
T. Unruh, 79  
C. Valeriani, 69, 141, 143  
M. G. Vasin, 109  
P. Verrocchio, 25, 47, 142  
D. Villamaina, 37, 147, 148, 159  
P. Virnau, 77, 121  
A. Vizcarra-Rendón, 36, 137  
D. Vlassopoulos, 134  
D. Vogt, 149  
Th. Voigtmann, 31, 41, 42, 43, 123, 124, 157  
G. Volpe, 149  
A. Vulpiani, 159  
S. Walta, 53  
S. Wei, 110  
J.-J. Weis, 112  
H. H. Wensink, 150  
F. Weysser, 40, 42  
M. Wilhelm, 40  
D. Winter, 121  
F. Wirner, 153  
P. Wlodarczyk, 85, 87  
Z. Wojnarowska, 85, 87  
J. Wuttke, 33  
C. Ybert, 128  
L. Yelash, 77  
E. Zaccarelli, 57, 69, 80, 138, 141, 143  
F. Zamponi, 29, 62, 63  
R. Zargar, 105  
J. Zausch, 39  
L. Zulian, 57